ANALYSIS OF CROSS-POLARIZATION DISCRIMINATION STATISTICS FOR MILLIMETRIC WAVES PROPAGATING THROUGH RAIN

by

JOHN KANELLOPOULOS

A Thesis submitted for the Degree of Doctor of Philosophy in the Faculty of Engineering, University of London

Department of Electrical Engineering
Imperial College of Science and Technology
University of London

February, 1979

ABSTRACT

This thesis reports on the results of a general investigation into the depolarization statistics of a microwave signal after propagation through a rain medium, and their application to the design of a microwave communication system.

Prediction of the long-term statistics for rain depolarization is presented for both spatially uniform and non-uniform rain and for any type of linear polarization (horizontal, vertical and at 45^0 inclination to the horizontal). Assuming a log-normal form for the rainrate statistics an approximate Gaussian model is deduced for the final cross-polarization isolation (XPI) or discrimination (XPD) distribution in decibels. The parameters of this normal distribution are related to the parameters of the radio link and the rainrate distributions. Applications of this conclusion to the estimation of radio outage time due to co-channel interference are also presented for various cross-polarization levels.

A theoretical formula is then derived for the joint statistics of cross-polarization discrimination (XPD) or isolation (XPI) and rain attenuation for a microwave link. This formula is then applied to the prediction of the distribution of XPD conditional on the co-polar rain attenuation, and also to the prediction of the distribution of XPD during a rain fade. Application is also made to the estimation of outage time of a dual-polarization communication system. Theoretical results are compared with experimental data from the Eastern USA and Southern England, and the agreement is found to be good.

ACKNOWLEDGEMENTS

The author would like to thank the people who have helped him during the project and in the preparation of this thesis.

Firstly, he acknowledges his debt to his supervisor, Dr. R. H. Clarke, who guided his efforts and shared his enthusiasm in this project, for his valuable suggestions, constant encouragement and kindly criticism.

The author wishes to thank Drs. J. A. Lane, J. R. Norbury and W. J. K. White of the Appleton Laboratory for providing the experimental data and making valuable suggestions.

He is very grateful to Mrs. Helen Bastin for her skilful work in typing the thesis.

The work described in this thesis was carried out while the author was supported by the Greek Foundation of Scholarships (I.K.Y.). This organisation is also gratefully acknowledged.

To my Wife and our parents

TABLE OF CONTENTS

Page

LIST OF FIGURES

LIST OF TABLES

CHAPTER 1
INTRODUCTION

The problem of the depolarization of electromagnetic waves passing through a rain medium is of crucial importance for the design of the new dual-polarization microwave communication systems, for frequency "re-use". A number of models has been proposed for predicting the cross-polarization of the received signal in terms of the parameters of the link and the rain medium. But, in general, these models are deterministic and predict only mean levels of depolarization. In this thesis, the problem is considered from a stochastic point of view. The results of the analysis give a complete description of the cross-polarization in terms of its probability density and also in terms of its joint density with the co-polar attenuation, both in the short and long term. Application of these results to experimental situations demonstrate their validity.

1.1 General Considerations

The need to make the most effective use of the limited radio spectrum allocated for microwave communication systems has already led to dual polarization transmission. This enables adjacent channels of opposite polarization to be positioned closer together by utilising the inherent polarization isolation of the system. The continuing pressure on bandwidth may force future terrestrial and satellite systems into a modification of the latter technique called "frequency re-use" in which information is transmitted on orthogonal polarizations at the same frequency. The implementation of these new systems depends entirely on the amount of isolation obtainable, which in turn depends on the amount of cross-coupling (or cross-polarization discrimination) likely to occur between the orthogonal polarizations. Cross-polarization discrimination (XPD) is the noise in the horizontal polarised channels caused by signals in the vertical polarised channels and vice versa. However, cross-coupling between orthogonal polarizations of the propagating wave can occur in the transmitter or in the receiver, or in the medium in between. Many causes of depolarization exist, including misalignment of antennas or waveguides, twisting of antenna towers (causing misalignment) atmospheric turbulence and rain. At frequencies above 10 GHz, the principal agent causing cross-polarization in the medium is rain. At these frequencies, when attenuation due to rain becomes significant, cross-polarization effects due to the non-spherical nature of the raindrops also become important.

A general consideration of the influence of precipitation on the propagation of microwaves through it, reveals the following. Precipitation scatters radiation in all directions from a passing wave; and if the particle size and concentration are sufficiently large, this scattering results in an appreciable rate of attenuation of the primary wave. In addition, as the precipitation particles comprise a lossy dielectric, they absorb energy from the wave and convert it into heat. Both phenomena are entirely negligible at wavelengths greater than about 10 cm; but as the wavelength decreases, the scattering and absorption become important, until at wavelengths around 1 cm they place a limitation on transmission over appreciable distances through rain.

Theoretical predictions of rain attenuation can be traced back to Ryde and Ryde (Ryde and Ryde, 1941; 1944; 1945). They carried out calculations of microwave rain attenuation, based on single scattering and Mie's (1909) scattering solution of a plane wave incident on a dielectric sphere. These calculations have since been extended by others (Medhurst, 1965) with the aid of modern computers. Recently both attenuation and phase shift through rain have been calculated for centimetre and millimetre wavelengths (Setzer, 1970) as a function of rainfall rate.

But the assumption of spherical raindrop shape used in the Mie calculation is only true to a first order of approximation. Close examination by photography reveals that many of the larger drops are better represented by oblate spheroids. The ratio of minor to major axes, of the oblate spheroidal raindrop, as determined from the experimental data (Pruppacher and Pitter, 1971), is approximately $a/b = 1 - \bar{a}$ where $\bar{a}$ is the radius (in centimetres) of an equi-volumic spherical drop. Oguchi (1960; 1964) first investigated the effect of oblate raindrops on microwave propagation using perturbation calculations. Point matching procedures (Oguchi, 1973; Morrison, Cross and Chu, 1973; Morrison and Cross, 1974) and improved perturbation techniques (Morrison and Cross, 1974) now provide extensive numerical results for the scattering of plane electromagnetic waves by oblate spheroidal raindrops. The differential rain-induced attenuation and phase shift have also been derived for vertical and horizontal incident polarization as a function of the rainfall rate.

Calculations of cross-polarization effects have also been made (Thomas, 1971; Saunders, 1976; Watson and Arbabi, 1973; Evans and Troughton, 1973a; Chu, 1974) using the previous differential attenuation and phase shift results. Due to the fact that raindrops usually have a finite canting angle, or departure from strictly vertical or horizontal alignment, the differential attenuation and phase shift lead to a rotation of the plane of polarization of the initially horizontally or vertically polarised radiation, thus producing unwanted signals in the cross-polar channel. A simplified analysis is adopted in all the previous calculations, that all raindrops (a) fall at the same canting angle and (b) that drops are tilted in a plane perpendicular to the direction of propagation. These assumptions correspond to the worst case of depolarization. Evans and Troughton (1973a) have calculated a more general case of depolarization and more recently, Attisani et al (1974) have discussed the problem of scatterers with arbitrary orientations using the Van de Hulst (1957) method of single scattering. Finally, Oguchi (1977) has put the whole problem of depolarization in a more concise form.

All these rain depolarization models are deterministic and predict mean levels of the cross-polarization discrimination on a short-term basis, that is, at a constant rainfall rate in time. From the statistical point of view, Hogler et al (1975) discuss the problem of statistical variations of XPD due to fluctuations in rain medium parameters (more specifically to drop-size fluctuations). Similarly, Evans and Troughton (1973b) give some statistical parameters (mean and variance) of the XPD concerning a medium which consists of aligned raindrops with random cosine-square distributed canting angle in time. These previous studies are concerned with the analysis of short-term statistics of XPD. Recent studies of polarization effects have been directed towards providing long-term distribution functions for predicting the occurrence of cross-polarised signals. Nowland et al (1977) have presented an approximate method to predict the rain depolarization statistics from attenuation statistics available for other frequencies, polarizations and elevation angles. This method can also predict the depolarization statistics from point rainrate statistics available for the location of the path. But, this model is more appropriate for earth space paths and uses the empirical meaning of equivalent path length through rain to take into account the effect of observed spatial non-uniformity of rainrate. The influence of the short-term statistics of XPD on its long-term statistical behaviour is not included. So, the general problem of predicting the depolarization statistics for a specific terrestrial microwave link is still a problem worthy of investigation. The purpose of this thesis is to propose a model for the solution of this problem using the statistics of point rainfall rate. This model will be quite general, and will include the effects of spatial non-uniformity of rain and short-term behaviour of XPD. Another aim of the thesis, will be the investigation of the joint statistics of the two propagation phenomena (XPD and attenuation) on a long-term basis. This problem is of crucial importance to the system planners and for this reason a theoretical analysis of the joint statistics of these two random processes, with applications to radio link performance, will also be given.

1.2 Outline of the Thesis

The following chapter is an introductory one for the whole work, where some generalities of radio wave propagation through rain, which are useful for the following analysis, are presented. More analytically, a configuration of the radio path and the elements of the rain medium are given. Special attention is drawn to the rainrate statistics and a log-normal model for it, as has been suggested by Lin (1975). The statistics of the rainfall rate is of crucial importance for the later analysis and dominates the long-term behaviour of the rain depolarization. In the last part of Chapter 2, a brief description of the propagation characteristics of a rain filled medium is given and a list of formulae for the calculation of the short-term mean levels of cross-polarization discrimination and attenuation.

Chapter 3 is devoted to a consideration of the long-term statistics of rain cross-polarization discrimination for spatially uniform rain. This assumption for rain is a sufficient approximation for path lengths up to 4 km. The technique adopted here is to find first the short-term statistics of XPD and then the long-term one using the theorem of total probability. A normal model for the XPD statistics in db is derived, based upon the observed log-normality of the rainrate statistics. Hence, this work can be considered as an extension to Lin's (1975) calculations of rain attenuation statistics. Numerical results for the cumulative depolarization statistics and the outage time due to co-channel interference are given for microwave links located in the USA and in Southern England. Comparison with experimental results from Martlesham Heath (Ipswich) is also included.

The more general case for a spatially non-uniform rain is given in Chapter 4. This is, in other words, an extension of the previous one, using the idea of spatially averaged rainfall rate. The non-uniform medium can be simulated by a uniform medium with an equivalent rainrate equal to the space-averaged rainrate. Hence, the statistics of XPD can be calculated, using the previous results and evaluating the statistics of space-averaged rainrate in terms of the parameters of the point rainrate. A normal model is thereby concluded with different statistical parameters (mean and variance). The two methods are compared and the conditions in which they are identical are also investigated. Similar results, as in the previous chapter, are given for the cumulative statistics and outage time of microwave links but without any restriction on the length of the path.

A study of the joint statistics of rain depolarization and attenuation is considered in Chapter 5 based on the previous statistical model for the XPD, and the one proposed by Lin (1975) for rain attenuation statistics. In the first instance, a theoretical formula for the joint statistics of these two random variables is derived, using the properties of the Jacobian transformation, and then applied to a number of practical cases such as (a) the prediction of the distribution of XPD conditional on a co-polar rain attenuation, (b) the prediction of the distribution of depolarization conditional on a rain fade, and finally (c) the estimation of the total outage time of a dual polarization communication system, taking into account the co-channel interference as well. For most of these applications a comparison is made with experimental results obtained in the USA and Southern England.

CHAPTER 2

GENERAL ASPECTS OF RADIO WAVE PROPAGATION THROUGH RAIN

Introduction

In this chapter some generalities concerning the propagation of microwaves through rain are discussed. First, the meaning of radio path between the transmitter and receiver stations is established using Ruthroff's definition (1970). Then, a more analytic configuration of the rain medium is given. The constituent elements of this medium such as the raindrops have a specific shape and size. The oblate spheroidal model proposed by Pruppacher and Pitter (1971) for the shape of raindrops is presented here and also the Laws-Parsons (1943) and Marshall-Palmer (1948) drop size distribution. The canting angle of falling raindrops is another important problem for depolarization studies. The distribution of canting angle especially under high wind conditions has not yet been completely investigated, so many authors propose different simulation models for it. In this thesis, the most recent one, proposed by Oguchi (1977) and Nowland et al (1977) is presented.

As will be shown in the later chapters, the dominant factor influencing the long-term behaviour of cross-polarization discrimination and attenuation statistics of a microwave link is the rainfall rate of the rain medium. Lin (1973; 1975; 1976; 1978), taking into account many sets of experimental data from all over the world, has proposed a log normal model for the long-term statistics of point rainfall rate. An analytical method has also been proposed by him (1976; 1978) for the evaluation of the parameters of this distribution in terms of existing experimental meteorological data for an arbitrary place. A brief review of this important theory is presented here, with a view to its application in the analysis of depolarization statistics.

The next step is the evaluation of the scattering of a plane electromagnetic wave by an oblate spheroidal raindrop. A description of this theory is presented in this chapter, for different frequencies from 4 - 50 GHz, raindrop sizes and elevation angles, so the results are applicable to both terrestrial and earth-space communication links. These basic results are summed over the drop size distribution to calculate the differential attenuation and differential phase shift caused by rain, which are of importance in the investigation of cross-polarization in radio communication systems.

Finally, taking into account the previous results, a list of formulae for the mean value of cross-polarization discrimination and attenuation at a constant rainfall rate, is given and is valid for both terrestrial and earth-space links.

2.1 Definition of the Radio Path

The radio link consists of two narrow-beam antennas pointing directly at each other over a distance of a few hundred to a few thousand metres. The space, or volume, of the path is taken to be the first Fresnel zone (Slater and Frank, 1933). This means that only the energy confined to that volume contributes significantly to the total energy collected by the receiving aperture. The first Fresnel zone is a long, thin, prolate ellipsoid of revolution. For a path of length L at wavelength λ, it has a major axis L and equal minor axes $(\lambda L)^{1/2}$ and is terminated at the ends by the antennas. The radius h(z) and the circular cross section Q(z) (see Fig. 2.1) of the radio beam at a distance z from the transmitter are:-

$$h(z) = \left[\frac{\lambda \cdot z(L - z)}{L}\right]^{1/2} \qquad (2.1.1)$$

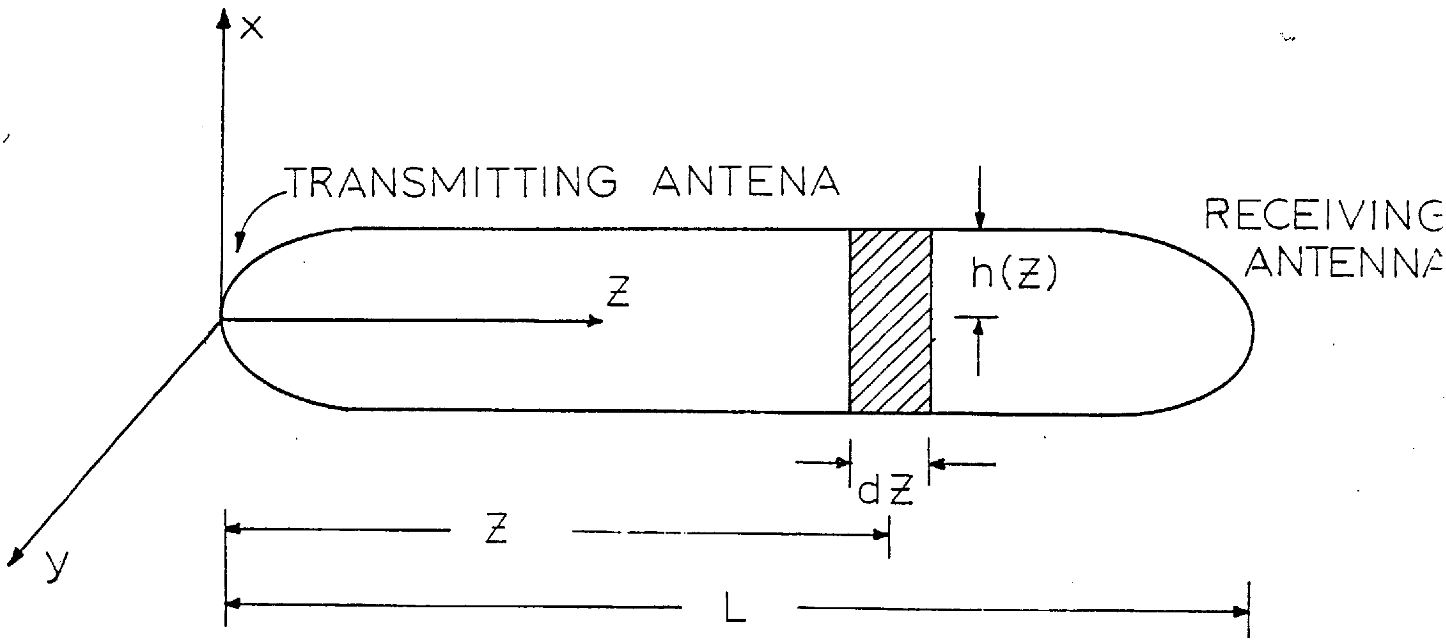

Fig. 2.1 Definition of the radio path

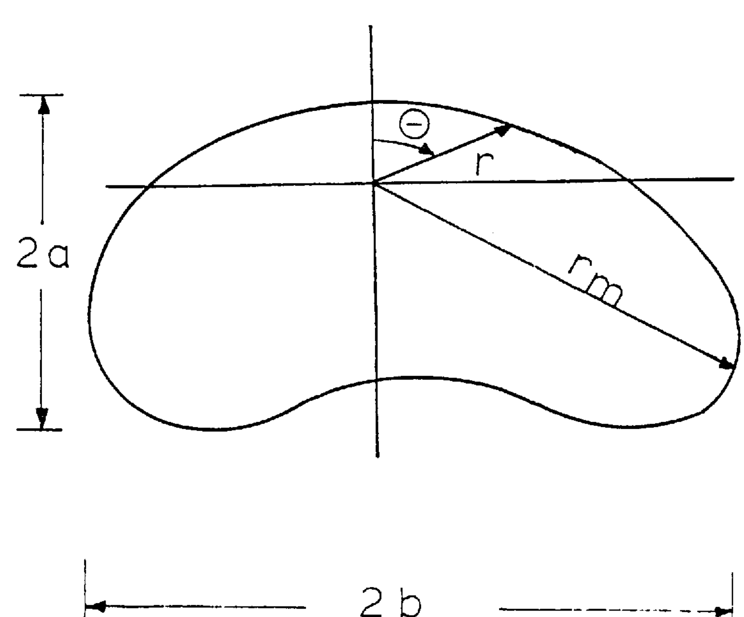

Fig. 2.2 Shape of a falling raindrop

and:-

$$Q(z) = \pi h^2(z) \tag{2.1.2}$$

The radio path is defined as the volume enclosed by the first Fresnel zone and the two antennas. When we speak of rain falling on the path we mean rain falling through this volume.

2.2 Description of the Rain Medium

2.2.1 Shape and Permittivity of the Raindrops

The rain medium will be assumed to consist of a large number of raindrops whose positions, sizes and orientations are random and independent of each other. The particles are also sufficiently far from each other (greater than three times the radius). The last property, combined with the fact that the wavelength of the incident wave is of the same order as their size, ensures that we will be concerned only with independent scattering.

It is well known that raindrops are usually non-spherical (Magono, 1954; Jones, 1959; Pruppacher and Pitter, 1971). The most commonly accepted model for a falling raindrop is that of a flattened spheroid which may present a canting angle to the horizontal at any instant. An instantaneous sample of falling raindrops (Jones, 1959) has shown that oblate and prolate spheroids can occur with almost equal probability. This might suggest that, in certain circumstances raindrops will vibrate. However, other authors have suggested that there is a predominance of oblate spheroids. Although drop shapes other than flattened spheroids are known to occur, which may lead to drop instability and break-up, the slightly flattened oblate spheroid model would seem to apply for the majority of drops and we will, therefore, use it in this study. The relation between the deformation (from a sphere) and the drop size is approximated by a linear relation. Recent investigations (Pruppacher and Pitter, 1972) give a physical model which predicts the shape of water drops falling at terminal velocity in air. The model is based on a balance of the forces which act on a drop falling under gravity in a viscous medium. The model was evaluated by numerical techniques and the shape of waterdrops of radii between 170 and 4000 μm (equivalent to Reynolds numbers between 30 and 4900) was determined. The results of these investigations show that the drop shapes predicted by the model agree well with those experimentally observed in the wind tunnel (Beard and Pruppacher, 1969; Pruppacher and Beard, 1970). Both theory and experiment demonstrate that (1) drops with radii $\leqq$ 170 μ are very slightly deformed and can be considered spherical, (2) the shape of drops between about 170 and 500 μ can be closely approximated by an oblate spheroid, (3) drops between about 500 and 2000 μ are deformed into an asymmetric oblate spheroid with an increasingly pronounced flat base, and, (4) drops $\geqq$ 2000 μ develop a concave depression in the base which is more pronounced for larger drop sizes. The polar equation describing such a shape is (see Fig. 2.2):-

$$r = r_m \sin (e^{-b \cos \theta}) \qquad (2.2.1)$$

where r_m is the radius of the enscribing sphere of the shape described by the above equation, b is a parameter depending on the drop size. For b = 0 the raindrop is a sphere; for small b's the shape described by Equation (2.2.1) is nearly an oblate spheroid. For large b's, Equation (2.2.1) describes a kidney shape.

The complex permittivity of raindrops is assumed to be constant throughout the raindrop volume and values for it can be found in Ray (1972) for various temperatures. Ray (1972) sets an empirical model of the complex refractive index for liquid water. This model is applicable from - $20^{o}C$ to $50^{o}C$. The spectral interval for which the model applies extends from 2 μm to several hundred metres in wavelength.

2.2.2 Drop Size Distribution

The knowledge of the drop size distribution in rain of given intensity is of major importance in the evaluation of attenuation and cross-polarization of a microwave signal due to an actual rainstorm. This distribution will vary according to wind temperature, and other conditions (Grunow, 1961). Representative distributions have been obtained by Laws and Parsons (1943), Marshall and Palmer (1948), and most recently by Joss et al (1968).

Laws and Parsons (1943) derived their distribution from a series of measurements during 1938 and 1939 in Washington DC. Table 2.1 is abridged from their Table 3, with the addition of a distribution for a precipitation rate of 5 mm/hr, which has been derived from their Fig. 1.

On the other hand, measurements of raindrop records on dyed filter papers were made (Marshall and Palmer, 1948) and have been analysed to give the distribution of drops with size. The distribution is in fair agreement with those of Laws and Parsons (1943). Except at small diameters, the experimental observations can be fitted by a general relation:-

$$n(D) = N_o \, e^{-\Lambda D} \qquad (2.2.2)$$

where D is the diameter of the equivolumic sphere, $n(D)\ \delta D$ is the number

TABLE 2.1 DROP SIZE DISTRIBUTIONS FOR VARIOUS PRECIPITATION RATES

Drop size (cm) (mean interval) Diameters \ Precipitation rate (mm/hour)	Percentage of Total Volume								
	0.25	1.25	2.5	5	12.5	25	50	100	150
0.05	28.0	10.9	7.3	4.7	2.6	1.7	1.2	1.0	1.0
0.1	50.1	37.1	27.8	20.3	11.5	7.6	5.4	4.6	4.1
0.15	18.2	31.3	32.8	31.0	24.5	18.4	12.5	8.8	7.6
0.2	3.0	13.5	19.0	22.2	25.4	23.9	19.9	13.9	11.7
0.25	0.7	4.9	7.9	11.8	17.3	19.9	20.9	17.1	13.9
0.3		1.5	3.3	5.7	10.1	12.8	15.6	18.4	17.7
0.35		0.6	1.1	2.5	4.3	8.2	10.9	15.0	16.1
0.4		0.2	0.6	1.0	2.3	3.5	6.7	9.0	11.9
0.45			0.2	0.5	1.2	2.1	3.3	5.8	7.7
0.5				0.3	0.6	1.1	1.8	3.0	3.6
0.55					0.2	0.5	1.1	1.7	2.2
0.6						0.3	0.5	1.0	1.2
0.65							0.2	0.7	1.0
0.7									0.3

of drops of diameter between D and D + δD in unit volume of space, and N_0 is the value of n(D) for D = 0. It is found that:-

$$\left.\begin{aligned} N_0 &= 0.08 \text{ cm}^{-4} \\ \Lambda &= 41.R^{-0.21} \text{ cm}^{-1} \end{aligned}\right\} \qquad (2.2.3)$$

where R is the rate of rainfall in mm hr^{-1}.

Finally, Joss et al (1968) for a place at Lucarno, Switzerland, give three raindrop size-distributions referring to a drizzle-rain (Joss-drizzle distribution), wide-spread rain (Joss-wide-spread distribution) and a thunderstorm (Joss-thunderstorm distribution).

2.2.3 Canting Angle Distribution

As noted previously, the most commonly accepted model for a falling raindrop is that of an oblate flattened spheroid which may present a canting angle to the horizontal. The analysis of this canting angle is of great importance in the study of rain induced cross-polarization. Saunders (1971) has shown from measurements the form of the distribution of raindrop canting angles and Brussaard (1976) has presented a meteorological model which relates the canting angles to wind conditions. But the influence of wind velocity and direction on the distribution of canting angles is not yet clear. In the absence of other information it has been usual to adopt a deterministic model in which the raindrops are all aligned, usually at a mean-path canting angle which has been determined from experimental measurements (Watson and Arbabi, 1975).

In this thesis, the most recent model proposed by Oguchi (1977) and Nowland et al (1977) will be presented for this distribution, which is valid for both terrestrial and earth-space communication links. So, let us consider a raindrop whose symmetry axis OA is in the YZ plane making an angle γ with an axis Oy, Oy being the projection of the symmetry axis on the HV plane and inclined at an angle θ from the vertical axis OV (see Fig. 2.3). We consider the case in which the raindrop-canting-angle is independent of the drop size. Furthermore, it is assumed that the two canting-angle distributions for θ and γ respectively are independent of each other. In particular, the transverse component θ and the longitudinal component γ of the canting angle are Gaussian distributed with parameters $\langle\theta\rangle = \theta_0$ and $\sigma_\theta = \sigma$, $\langle\gamma\rangle = \gamma_0$ and $\sigma_\gamma = \sigma'$. For all practical calculations of the cross-polarization discrimination it is assumed that the axes of all drops are in the plane normal to the propagation direction. Consequently, we set $\gamma_0 = \sigma' = 0$. This means, in other words, that the effect of the canting angle γ on cross-polarization is less significant than the canting angle θ.

2.3 Analysis of Long-Term Point Rainfall Rate Statistics

2.3.1 Generalities

One factor which is dominant for the evaluation of cross-polarization discrimination and attenuation of the microwave signal propagated through a rain medium, is the rainfall rate, that is the volume of water reaching the ground per unit time. So, if R represents the rainfall rate in mm/hr, then:-

$$R = 15.1 \int_0^\infty n(r)\, v(r)\, r^3\, dr \qquad (2.3.1)$$

where r is the equivolumic radius of the raindrop, and $v(r)$ is the terminal velocity of the drops in metres per second (Kerr, 1964).

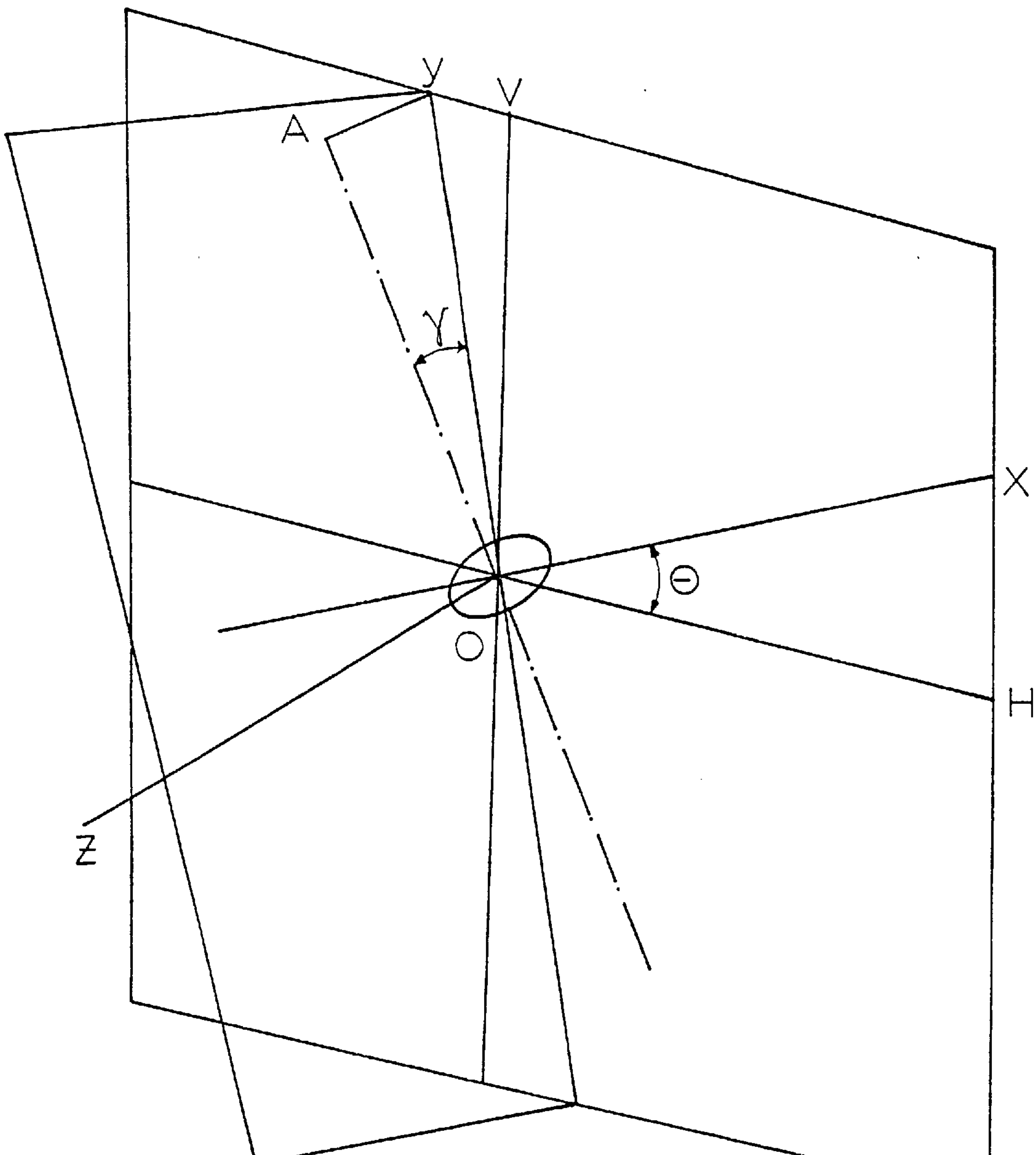

Fig. 2.3 Canting angles of falling raindrop

During rainfall, the rainfall rate R fluctuates in space and time. Most available data on rainrate statistics are measured by a single raingauge at a given geographic location. The results of raingauge network measurements indicate, however, that the measured short-term distributions of point rainrate vary significantly from gauge to gauge. For example, at Holmdel, New Jersey, there was considerable variation among the measured point rainrate distributions obtained from 96 raingauges located in a grid with 1.3 km spacing over a six-month period. Among these 96 distributions, the incidence of 100 mm/hr rains is higher by a factor of 5 for the upper quartile gauges than for the lowest quartile. Data from a raingauge network in England indicate that even with a four-year time base and averaging over observations by four gauges with 1 km gauge spacing, the four-gauge average rainrate incidence can differ by a factor of 3 for rainrates above 80 mm/hr depending on which four gauges are chosen for averaging. This means that knowledge of the long-term statistical behaviour of point rainrate is essential for radio path design.

The available experimental rainrate data (Lin, 1973; Lin, 1975) indicate that the long-term distribution of point rainrate R is approximately log-normal within the range of interest to designers of radio paths using frequencies above 10 GHz. It can be seen from these distributions that these are very close to the log-normal approximation in the range below 100 mm/hr. The rainrates beyond 100 mm/hr are generally separated more than 3 sigma from the median and constitute the tail of the log-normal distribution. A very long observation time (e.g. more than twenty years) is necessary to obtain stable statistics of extreme rainrates beyond 100 mm/hr (Seamon and Bartlett, 1956; Cole et al, 1969). Since the time bases of the data in these references are much less than twenty years, the departure of the data from the log-normal distribution in the tails is not unexpected. Lin (1978) taking into account rainrate data measured in Illinois (Mueller and Sims, 1966), New Jersey, Canada (Drufuca and Zawadzki, 1973) and Palmetto, Georgia has concluded that the rainfall process must be log-normal, by the following argument. He proved that the environmental parameters that influence the rainfall process affect the rainrate in a proportional fashion, so as it is known (Lin, 1973; Aitchison and Brown, 1957; Hald, 1952) the proportionality leads to a log-normal distribution whereas an additive fashion leads to a normal distribution. This is a strong theoretical argument completely supporting the log-normal hypothesis for the long-term statistics of rainfall rate.

Another important problem is the effect on the rainrate distribution of the raingauge integration time (Lin, 1976). When we refer to a "τ-minute" rainrate this corresponds to the average value of the randomly varying rainrate in a τ-minute interval. This is calculated as $\Delta H/\tau$ where ΔH is the τ-minute accumulated depth of rainfall and τ is the raingauge integration time. The most appropriate raingauge integration time which can be used in the following analysis may be calculated as follows. The division of the radio path into incremental slabs has been adopted for the analysis as will be seen in the following chapters. So if ΔV is the volume of each slab, A_g is the area of the collecting aperture of a raingauge and V_R the average descent velocity of rainfall, then the appropriate raingauge integration time will be:-

$$T = \frac{\Delta V}{A_g V_R} \tag{2.3.2}$$

For example, representative values for these parameters are $\Delta V \cong 1\ m^3$, $A_g \cong 0.073\ m^3$ and $V_R \cong 7$ m/s, so T is about 2 s. The integration times of most available point rainfall rate data are longer than the T = 2 s required by this formulation. The dependence of point rainrate distribution on the raingauge integration time in the range 1.5 s $\leq$ T $\leq$ 120 s has been determined by Bodtmann and Ruthroff (1974) for a two year (1971 - 1972) measurement at Holmdel, New Jersey. By using this experimental result and interpolation, we convert the available point rainrate distribution with T in the above range into a 2 s point rainrate distribution.

In this way the representation of point rainrate distribution is:-

$$P\left[R \geq r\right] = P_o(0) \cdot \frac{1}{2} \operatorname{erfc}\left(\frac{\ln r - \ln R_m}{\sqrt{2}\, S_R}\right) \qquad (2.3.3)$$

where erfc ( ) denotes the complementary error function, S_R the standard deviation of ln R during the raining time, R_m the median value of R, during the raining time. $P_o(0)$ is the probability that rain will fall at the point where the rainrate is measured.

In principle, the probability of raining, $P_o(0)$ is obtained:-

$$P\left[R \geq r_{min}\right] \equiv P_o(0) \qquad (2.3.4)$$

An instant t is considered to be during the raining time if the condition $R(t) > r_{min}$ is satisfied. The lower cutoff threshold in most presently available rainrate data is about 0.25 mm/hr. Therefore, in practice, we approximate r_{min} in previous definitions by 0.25 mm/hr. The rationale for this approximation is twofold:-

(a) Rainrates below 0.25 mm/hr have practically no significant effects on radio communication links at frequencies below 60 GHz.

(b) Rainrates below 0.25 mm/hr cannot be measured accurately by most existing raingauges with standard recording strip charts. At the present time, the probability $P\left[R \geq 0.25 \text{ mm/hr} \mid T \leq 1 \text{ min}\right]$ is available at only a few locations. For most locations, we can obtain $P\left[R \geq 0.25 \text{ mm/hr}\right]$ with 1 hour integration time from the Weather Station hourly precipitation data. The experimental results on the effect of raingauge integration time T on $P_0(0)$ in Florida (Jones and Sims, 1971; Sims and Jones, 1973) and Japan (Funakawa and Kato, 1962) indicate that:-

$$P\left[R \geq 0.25 \text{ mm/hr} \mid T \leq 1 \text{ min}\right] = 0.5\ P\left[R \geq 0.25 \text{ mm/hr} \mid T = 1 \text{ h}\right] \qquad (2.3.5)$$

Therefore, we can use Weather Station data and this approximation to estimate $P_0(0)$ at several locations of interest where direct measurement of $P_0(0)$ with 1 min integration time is not available.

The log-normal parameters R_m and S_R of the 2 s point rainrate distribution (Equation (2.3.3)) are estimated by a least-squares approximation. This step is carried out by a computer iteration process to obtain the (R_m, S_R) pair that minimises the differences (i.e. the sum of squares of errors), between the data points and the log-normal approximation (Lin, 1975). Table 2.2 is abridged from his Table III and gives some experimental data on point rainrate distribution at different locations in the USA and in Southern England.

The main problem in the estimation of these parameters is that many point rainrate measurements report only the heavy rain (e.g. $\geq$ 30 mm/hr) portion of the distribution, neglecting the light rain

TABLE 2.2 EXPERIMENTAL DATA ON POINT RAINRATE DISTRIBUTION

No.	Authors	Location	Time Base	Rain Gauge Integration Time	Rain Gauge	Estimated Log-normal Parameters		
						R_m mm/hr	S_R	$P_o(0)$
1	Ruthroff, Bodtmann	Miami, Fla.	1966 - 1970	1 min	Weighing gauge	2.48	1.54	0.026
2	Jones, Sims	Miami, Fla.	8/57 - 8/58	1 min	Weighing gauge	2.48	1.54	0.026
3	Jones, Sims	Urbana, Ill.	5/69 - 4/72	1 min	Weighing gauge	1.10	1.47	0.033
4	Ruthroff, Bodtmann Osborne	Atlanta, Ga.	1966 - 1970, 1973	1 min	Weighing gauge	3.23	1.15	0.026
5	Lin	Palmetto, Ga.	11/70 - 10/71 8/73 - 7/74	1 min	Tipping bucket	3.10	1.18	0.031

.... Continued

TABLE 2.2 (CONTINUED)

No.	Authors	Location	Time Base	Rain Gauge Integration Time	Rain Gauge	Estimated Log-normal Parameters		
						R_m mm/hr	S_R	$P_o(0)$
6	Lin	Palmetto, Ga.	8/73 - 7/74	1 min	Tipping bucket	3.85	1.11	0.030
7	Lentz	Merrimack Valley, Mass.	1971 - 1973	10 - 90 s	-	1.23	1.34	0.033
8	-	Holmdel, NJ	1968 - 1969	2 s	Flow-capacitance gauge	1.53	1.38	0.026
9	Norbury, White	Slough, England	1970 - 1971	10 s to 1 h	Special dropper gauge	0.42	1.40	0.044
10	Easterbrook, Turner	Southern England	5/61 - 5/62, 1963	2 - 60 min	-	0.42	1.40	0.044

statistics completely. Table 2.2 indicates that the median rainrates R_m at many locations are less than 4 mm/hr. In other words, the major portion ($\cong$ 98%) of the distribution is missing, and accurate estimation of the statistical parameters R_m and S_R from the tail region ($\leq$ 2%) is difficult. Furthermore, high rain rates (e.g. > 140 mm/h) require a long observation time to yield representative long-term statistics. The time bases of most available data may not be sufficient to yield stable statistics for these extreme rainrates. The omission of light-rain statistics together with the inherent instability of the extreme rainrate statistics causes considerable uncertainty in the estimation of P_o, R_m and S_R.

An alternative analytic method to obtain these parameters in terms of known meteorological long-term quantities such as the yearly τ-minute maximum rain rate data and yearly accumulated rainfall data, is presented in the next section.

2.3.2 A Method for Evaluation of the Parameters of the Rainrate Distribution

The three parameters characterizing the log-normal distribution can be calculated by application of the theory of extreme value statistics (Gumbel, 1954; Gumbel, 1958). This work has been done by Lin (1978) and we now present briefly the results.

Let W denote the long-term average value of the yearly accumulated depth of rain I. The relationship between W and the parameters in Equation (2.3.3) is:-

$$
\begin{aligned}
W &= \langle R \rangle \times \text{total raining time/year} \\
&= \langle R \rangle \times P_o(0) \times (8760 \text{ hours/year}) \\
&= R_m \times e^{S_R^2/2} \times P_o(0) \times (8760 \text{ hours/year}) \qquad (2.3.6)
\end{aligned}
$$

where:-

$$\langle R\rangle = R_m \times e^{S_R^2/2} \tag{2.3.7}$$

is the mean value of rainfall rate R during the raining time (see Appendix A, Equation (A-2)). Long-term ($\geq$ 30 years) data on W for US locations can be found in Conway, May and Armstrong (1963).

Let R_1 denote the yearly maximum τ-minute rainrate which varies from year to year. The distribution of R_1 is (Lin, 1976):-

$$P\left[\{R_1 \geq r\}\right] = 1 - e^{-(e^{-y})} \tag{2.3.8}$$

where:-

$$y = a_L(\ln r - U) \tag{2.3.9}$$

is called the reduced variate, a_L and U are scale and position parameters respectively. Notice that the log-normal rainrate distribution (Equation (2.3.3)) is uniquely determined by the three parameters $P_o(0)$, R_m and S_R, whereas the distribution (Equation (2.3.8)) of the yearly maximum τ-minute rainrate R_1 is uniquely determined by the two parameters a_L and U. Gumbel (1954; 1958) has given the following approximate relationships between a_L, U and the distribution (Equation (2.3.3)):-

$$\Phi\left(\frac{U - \ln R_m}{S_R}\right) \cong 1 - \frac{1}{P_o(0)\,.\,N} \tag{2.3.10}$$

$$a_L = \frac{P_o(0)\,.\,N}{S_R}\,\phi\left(\frac{U - \ln R_m}{S_R}\right) \tag{2.3.11}$$

where:-

$$\Phi\left(\frac{U - \ln R_m}{S_R}\right) = 1 - \frac{1}{2}\,\mathrm{erfc}\left(\frac{U - \ln R_m}{\sqrt{2}\,S_R}\right) \qquad (2.3.12)$$

is the standard unit normal distribution function,

$$\phi(x) = \frac{d}{dx}\,\Phi(x) \qquad (2.3.13)$$

is the normal probability density function, and:-

N = total number of τ-minute intervals per year (2.3.14)

The meaning of parameters a_L and U is determined as follows. From Equations (2.3.8) and (2.3.9), it is easily shown (Gumbel, 1954; 1958) that U is the most probable value of $\ln R_1$ where R_1 is the randomly varying yearly maximum τ-minute rainrate. Let us define:-

$$R_u = e^U \qquad (2.3.15)$$

Equation (2.3.10) states on long-term average, the randomly varying rainrate R will exceed R_u by approximately τ minutes per year. Equation (2.3.11) further specifies the slope (i.e. the derivative or probability density) of the rainrate distribution at $R = R_u$. Solving Equations (2.3.10) and (2.3.11) yields:-

$$S_R = \frac{P_o(0)\,.\,N}{a_L}\,\phi\left[\Phi^{-1}\left(1 - \frac{1}{P_o(0)\,.\,N}\right)\right] \qquad (2.3.16)$$

and:-

$$R_m = \exp\left\{U - S_R \cdot \Phi^{-1}\left\{1 - \frac{1}{P_o(0) \cdot N}\right\}\right\} \qquad (2.3.17)$$

where $\Phi^{-1}(\ )$ denotes the inverse normal probability function. Lin (1976) has given a set of formulae for calculating the parameters a_L and U from the yearly maximum τ-minute rainrate data. Alternatively, the same author (Lin, 1976) has given another set of formulae relating these a_L and U with rainfall-intensity-duration-frequency curves where these long-term data ($\geq$ 50 years) are available. Knowing the values W, a_L and U allows us to solve numerically by a computer iteration process, the three Equations (2.3.6), (2.3.16) and (2.3.17) for the three unknowns $P_o(0)$, R_m and S_R. Substituting these three parameters into Equation (2.3.3) then yields the entire rainrate distribution.

2.4 Scattering Properties of Raindrops at Microwave Frequencies

The scattering of electromagnetic waves by spheroidal dielectric raindrops has been the subject of much theoretical study because of its importance in the theory of radio wave propagation. For frequencies above 10 GHz, accurate scattering amplitudes are required to enable reliable estimates of attenuation and cross-polarization to be made. In this section, the available theory for the evaluation of these scattering amplitudes is summarised and also, the propagation characteristics of a rain-filled medium are given in terms of the scattering properties of the individual raindrop.

2.4.1 Scattering of a Plane Wave by a Single Raindrop

We now consider the problem of scattering of a plane electromagnetic wave by a single raindrop. Suppressing the factor $e^{-i\omega t}$, where ω is the angular frequency, the divergenceless electric and magnetic fields $\vec{E}$ and $\vec{H}$ satisfy Maxwell's equations (Stratton, 1941):-

$$\left.\begin{aligned} \nabla \times \vec{E} &= i\omega\mu_o \vec{H} \\ \nabla \times \vec{H} &= (\sigma_c - i\omega\varepsilon) \vec{E} \end{aligned}\right\} \qquad (2.4.1)$$

where μ_o is the constant permeability, σ_c is the conductivity, and ε is the dielectric constant. Exterior to the raindrop $\sigma_c = 0$ and $\varepsilon = \varepsilon_o$, while interior to it $\sigma_c = \sigma_1$ and $\varepsilon = \varepsilon_1$. The appropriate boundary conditions (Stratton, 1941) are that the tangential components of the total electric and magnetic fields be continuous across the surface of the raindrop. Let:-

$$k'^2 = \omega\mu_o(\omega\varepsilon + i\sigma) \qquad (2.4.2)$$

with $\mathrm{Re}(k') > 0$. Then the free space wave number is $k_o = \omega\sqrt{\mu_o \varepsilon_o}$ and the wave number in the raindrop is:-

$$k_1 = N' k_o \qquad (2.4.3)$$

where N' is the complex index of refraction of water. We consider two polarizations of the incident wave depicted in Fig. 2.4. We choose Cartesian coordinates (x', y', z') with origin interior to the raindrop and z'-axis coinciding with the axis of symmetry of the raindrop. The direction of propagation of the incident wave is perpendicular to the y'-axis and inclined at an angle a_c to the z'-axis. In the first polarization, the magnetic field is assumed parallel to the y'-axis and

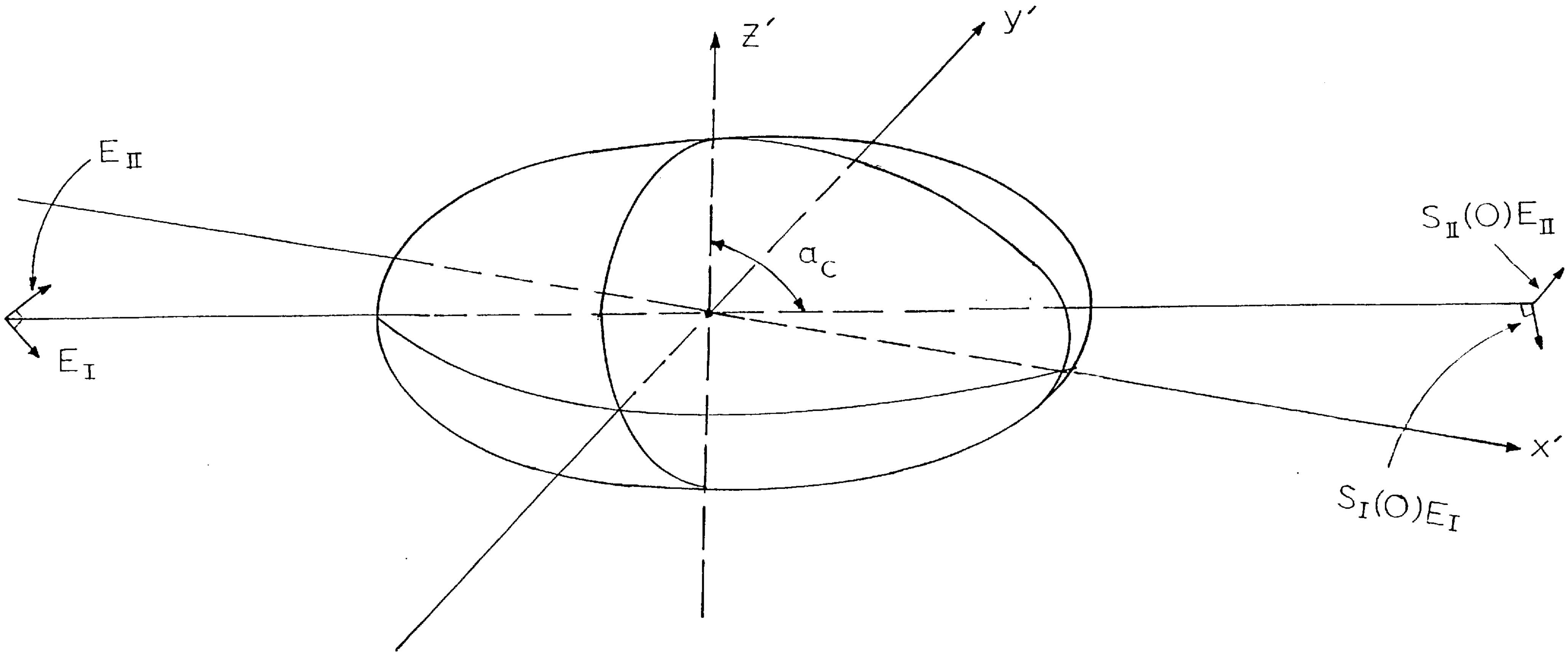

Fig. 2.4 Plane wave incident on a spheroidal raindrop

I polarization in the direction of minor axis

II polarization in the direction of major axis the incident fields are given by:-

$$\left.\begin{aligned} \vec{E}^i_I &= E_I(\cos a_c \, \vec{i} - \sin a_c \, \vec{k}) \exp\left[ik_o(x' \sin a_c + z' \cos a_c)\right] \\ \vec{H}^i_I &= \frac{k_o}{\omega\mu_o} E_I \, \vec{j} \exp\left[ik_o(x' \sin a_c + z' \cos a_c)\right] \end{aligned}\right\} \quad (2.4.4)$$

where $\vec{i}$, $\vec{j}$, $\vec{k}$ denote unit vectors parallel to the coordinate axes. In the second polarization, the electric field is assumed parallel to the y'-axis and the incident fields are given by:-

$$\vec{E}^i_{II} = E_{II} \, \vec{j} \exp\left[ik_o(x' \sin a_c + z' \cos a_c)\right]$$

and:- (2.4.5)

$$\vec{H}^i_{II} = -\frac{k_o}{\omega\mu_o} E_{II}(\cos a_c \vec{i} - \sin a_c \vec{k}) \exp\left[ik_o(x' \sin a_c + z' \cos a_c)\right]$$

We now consider the problem of representing the scattered and transmitted fields induced by the incident wave. It is convenient to introduce spherical coordinates $(r', \partial', \varphi')$ with corresponding unit vectors $\vec{i}_1$, $\vec{i}_2$, $\vec{i}_3$ as depicted in Fig. 2.5. Then the equations:-

$$\left.\begin{aligned} \nabla \times \vec{M} &= k' \, \vec{N} \\ \nabla \times \vec{N} &= k' \vec{M} \end{aligned}\right\} \quad (2.4.6)$$

are satisfied by the spherical vector wave functions (Stratton, 1941):-

$$\vec{M}_{mn}(k') = z_n(k'r')\, e^{im\varphi'} \left\{ \frac{im'}{\sin \partial'} P_n^{|m|}(\cos \partial')\, \vec{i}_2 - \right.$$

$$\left. - \frac{dP_n^{|m|}(\cos \partial')}{d\partial'} \vec{i}_3 \right\} \tag{2.4.7}$$

and:-

$$\vec{N}_{mn}(k') = e^{im\varphi'} \left\{ n(n+1) \frac{z_n(k'r')}{k'r'} P_n^{|m|}(\cos \partial')\, \vec{i}_1 + \right.$$

$$+ \left\{ \frac{z_n(k'r')}{k'r'} + z_n'(k'r') \right\} \times \left\{ \frac{dP_n^{|m|}(\cos \partial')}{d\partial'} \vec{i}_2 + \right.$$

$$\left. \left. + \frac{im}{\sin \partial'} P_n^{|m|}(\cos \partial')\, \vec{i}_3 \right\} \right\} \tag{2.4.8}$$

Here z_n denotes a spherical Bessel function (Stratton, 1941) of order n and $P_n^{|m|}$ denotes the associated Legendre function (Magnus et al, 1954) (of the first kind) of degree n and order $|m|$, where m is a positive or negative integer, and n is an integer with $n \geq |m|$ and $n \neq 0$. The prime denotes derivative with respect to the argument. As a matter of convenience, we have chosen to use complex linear combinations of the even and odd spherical vector wave functions (Stratton, 1941).

Outside the raindrop, the total electromagnetic field is the sum of the incident field of the plane wave and the scattered field. The scattered field must satisfy the radiation condition and, consequently, in view of Equations (2.4.1), (2.4.2) and (2.4.6), we assume expansions of the form:-

$$\vec{E}^s = - \sum_{m=-\infty}^{\infty} \sum_{\substack{n \geq |m| \\ n \neq 0}} \left[a_{mn} \vec{M}_{mn}^{(3)} (k_o) + b_{mn} \vec{N}_{mn}^{(3)} (k_o) \right] \tag{2.4.9}$$

and:-

$$\vec{H}^s = \frac{i k_o}{\omega \mu_o} \sum_{m=-\infty}^{\infty} \sum_{\substack{n \geq |m| \\ n \neq 0}} \left[a_{mn} \vec{N}_{mn}^{(3)} (k_o) + b_{mn} \vec{M}_{mn}^{(3)} (k_o) \right] \tag{2.4.10}$$

where the superscript 3 denotes that spherical Bessel functions of the third kind, i.e. spherical Hankel functions of the first kind, are used. Thus in Equations (2.4.7) and (2.4.8), $z_n(k_o\, r') = h_n^{(1)}\, (k_o\, r')$. For $k_o\, r' >> 1$:-

$$h_n^{(1)}\, (k_o\, r') \simeq \frac{(-\, i)^{n+1}}{k_o\, r'}\, e^{i k_o\, r'} \tag{2.4.11}$$

so that the expressions in Equations (2.4.9) and (2.4.10) involve outgoing waves.

Analogous expansions are assumed for the transmitted field inside the raindrop except that, since the origin of the coordinate system is interior to the raindrop, spherical Bessel functions of the first kind must be used so that the field remains finite at $r' = 0$. Also, the wave number inside the raindrop is k_1, as given by Equation (2.4.3). Thus, we assume expansions of the form:-

$$\vec{E}^t = - \sum_{m=-\infty}^{\infty} \sum_{\substack{n \geq |m| \\ n \neq 0}} \left[c_{mn} \vec{M}_{mn}^{(1)} (k_1) + d_{mn} \vec{N}_{mn}^{(1)} (k_1) \right] \tag{2.4.12}$$

and:-

$$\vec{H}^t = \frac{ik_1}{\omega\mu_o} \sum_{m=-\infty}^{\infty} \sum_{\substack{n\geq|m| \\ n\neq 0}} \left\{c_{mn} \vec{N}_{mn}^{(1)} (k_1) + d_{mn} \vec{M}_{mn}^{(1)} (k_1)\right\} \tag{2.4.13}$$

where the superscript 1 indicates that $z_n(k_1 r) = j_n(k_1 r)$ in Equations (2.4.7) and (2.4.8).

The unknown (complex) coefficients a_{mn}, b_{mn}, c_{mn}, d_{mn} in Equations (2.4.9), (2.4.10), (2.4.12) and (2.4.13) must be determined from the boundary conditions. The surface of the raindrop is given by:-

$$r' = R'(\partial') \quad , \quad 0 \leq \partial' \leq \pi \quad , \quad 0 \leq \varphi' \leq 2\pi \tag{2.4.14}$$

where it is assumed that $R'(\partial')$ is a single-valued, continuously differentiable function of ∂' (see Equation (2.1.1)). The continuity of the tangential components of the total electric and magnetic field, across the surface of the raindrop, implies that for $r' = R'(\partial')$:-

$$E_3^i + E_3^s = E_3^t \tag{2.4.15}$$

$$H_3^i + H_3^s = H_3^t \tag{2.4.16}$$

$$E_2^i + E_2^s + \frac{1}{R'}\frac{dR'}{d\partial'}(E_1^i + E_1^s) = E_2^t + \frac{1}{R'}\frac{dR'}{d\partial'}E_1^t \tag{2.4.17}$$

$$H_2^i + H_2^s + \frac{1}{R'}\frac{dR'}{d\partial'}(H_1^i + H_1^s) = H_2^t + \frac{1}{R'}\frac{dR'}{d\partial'}H_1^t \tag{2.4.18}$$

where $E_j = \vec{E} \cdot \vec{i}_j$ and $H_j = \vec{H} \cdot \vec{i}_j$ and the incident fields $\vec{E}^i$ and $\vec{H}^i$ are given by Equations (2.4.4) and (2.4.5).

Because of the axial symmetry of the raindrop, the following relationships between the coefficients, a_{mn}, b_{mn}, c_{mn}, d_{mn} are derived. For the first polarization of the incident wave:-

$$\left.\begin{aligned} a^{I}_{-mn} &= -\,a^{I}_{mn} \quad , \quad b^{I}_{-mn} = b^{I}_{mn} \\ c^{I}_{-mn} &= -\,c^{I}_{mn} \quad , \quad d^{I}_{-mn} = d^{I}_{mn} \end{aligned}\right\} \tag{2.4.19}$$

and for the second polarization:-

$$\left.\begin{aligned} a^{II}_{-mn} &= a^{II}_{mn} \quad , \quad b^{II}_{-mn} = -\,b^{II}_{mn} \\ c^{II}_{-mn} &= c^{II}_{mn} \quad , \quad d^{II}_{-mn} = -\,d^{II}_{mn} \end{aligned}\right\} \tag{2.4.20}$$

Thus, it is sufficient to consider only non-negative values of m.

The calculation of the aforementioned coefficients from the set of boundary conditions (2.4.15) - (2.4.18) follows two different approaches. Oguchi (1960) considered spheroidal raindrops with small eccentricity and carried out a perturbation expansion originally determining the first-order approximation and later the second-order one (Oguchi, 1964). He described the surface of the raindrop as:-

$$R'(\partial) = \bar{a}\left(1 + vR_1'(\partial') + \ldots\ldots\right) \ , \ |v| << 1 \tag{2.4.21}$$

where $\bar{a}$ is the radius of the equivolumic sphere. Corresponding to Equation (2.4.21) the coefficients in the expansions (2.4.9), (2.4.10), (2.4.12), (2.4.13) are expanded in the form:-

$$a_{mn} = a^{(0)}_{mn} + v\ a^{(1)}_{mn} \tag{2.4.22}$$

$$b_{mn} = b^{(0)}_{mn} + v\ b^{(1)}_{mn} \tag{2.4.23}$$

$$c_{mn} = c^{(0)}_{mn} + v\ c^{(1)}_{mn} \tag{2.4.24}$$

$$d_{mn} = d_{mn}^{(0)} + v\, d_{mn}^{(1)} \qquad (2.4.25)$$

The zero-order approximation, with $v = 0$ in Equation (2.4.21) corresponds to a spherical raindrop of radius $\bar{a}$. Thus the coefficients $a_{mn}^{(0)}$, $b_{mn}^{(0)}$, $c_{mn}^{(0)}$, $d_{mn}^{(0)}$ are determined from the well-known Mie solution (Mie, 1909). The first-order approximation $a_{mn}^{(1)}$, $b_{mn}^{(1)}$, $c_{mn}^{(1)}$, $d_{mn}^{(1)}$ are very complicated functions and are tabulated in Oguchi's paper (Oguchi, 1960).

An alternative non-perturbation solution of the scattering problem is also presented here. As mentioned previously, it is sufficient to determine the unknown coefficients for non-negative values of m and then to use the relationships in Equations (2.4.19) or (2.4.20). The boundary conditions in Equations (2.4.15) - (2.4.18) take the form:-

$$K_{mq}(\vartheta') - \sum_{\substack{n \geq m \\ n \neq 0}} \Big[a_{mn} A_{mnq}(\vartheta') + b_{mn} B_{mnq}(\vartheta') + $$

$$+ c_{mn} C_{mnq}(\vartheta') + d_{mn} D_{mnq}(\vartheta') \Big] = 0 \qquad (2.4.26)$$

for $q = 1, 2, 3, 4$ and $0 \leq \vartheta' \leq \pi$, where the functions $K_{mq}(\vartheta')$, $A_{mnq}(\vartheta')$, $B_{mnq}(\vartheta')$, $C_{mnq}(\vartheta')$, $D_{mnq}(\vartheta')$ involve the spherical Bessel functions of the first and third kind and the associated Legendre functions, and the derivatives of each of these functions (Morrison and Cross, 1974). In view of Equation (2.4.3), the argument of the spherical Bessel function of the first kind is complex.

For each m there are infinitely many unknown coefficients a_{mn}, b_{mn}, c_{mn}, d_{mn}. To obtain an approximate solution, only a finite number of coefficients is considered. One procedure is to truncate the sum in Equation (2.4.26) at $n = N_o$, say, and then to satisfy the boundary conditions at the points $\vartheta' = \vartheta'_{\ell m}$, $\ell = 1, \ldots, (N_o - m + 1 - \delta_{mo})$, which are appropriately selected, e.g. uniformly spaced in the interval 0 to π. This was the procedure adopted by Oguchi (1973) and it leads to a system of simultaneous linear equations for the coefficients. We refer to this procedure, in which the total number of fitting points is equal to the number of unknown coefficients, as collocation.

Another more effective method adopted by Mullin et al (1965) for the scalar scattering problem by a perfectly conducting cylinder of smooth contour, and Morrison and Cross (1974) for the raindrop problem, is the least-squares fitting procedure. According to this, the boundary conditions (Equation (2.4.26)) are satisfied in a least-squares sense at a larger number of points than the number of unknown coefficients in the truncated expansion of the scattered field. Morrison and Cross (1974) have found a significant improvement in the overall fit of the boundary conditions, although the far field quantities were not affected as significantly. This is because the higher-order coefficients are more significant at the boundary than in the far field. However, the accuracy of the lower-order coefficients is affected by the goodness of fit of the boundary condition. With collocation, there were much larger errors in the boundary condition (in between the fitting points) than with least-squares fitting with a sufficiently large number of points.

After this brief description of the methodology for the evaluation of the coefficients a_{mn}, b_{mn}, c_{mn}, d_{mn} we now turn to the quantities of physical interest.

2.4.2 Evaluation of the Far-Field Quantities

We consider only the far scattered field, so that $k_0 r' \gg 1$. Thus, we restrict our attention to the leading term in the asymptotic expansion of the spherical Bessel function of the third kind, as given by Equation (2.4.11). Also, it follows that:-

$$h_n^{(1)\prime}(k_o r') \underset{=}{\sim} \frac{(-i)^n}{k_o r'} e^{ik_o r'} \tag{2.4.27}$$

Then, from Equations (2.4.7) to (2.4.10), it is found that:-

$$k_o r' e^{-ik_o r'} \vec{E}^s \underset{=}{\sim} \sum_{m=-\infty}^{\infty} \sum_{\substack{n \geq |m| \\ n \neq 0}} (-i)^{n+1} \left\{ a_{mn} \left[\frac{dP_n^{|m|}(\cos \partial')}{d\partial'} \vec{i}_3 - \right. \right.$$

$$\left. - \frac{im}{\sin \partial'} P_n^{|m|} (\cos \partial') \vec{i}_2 \right] - ib_{mn} \left[\frac{dP_n^{|m|}(\cos \partial')}{d\partial'} \vec{i}_2 + \right.$$

$$\left. \left. + \frac{im}{\sin \partial'} P_n^{|m|} (\cos \partial') \vec{i}_3 \right] \right\} e^{im\varphi'} \tag{2.4.28}$$

and:-

$$\omega\mu_o \vec{H}^s \underset{=}{\sim} k_o \vec{i}_1 \times \vec{E}^s \tag{2.4.29}$$

Of particular interest are the scattered fields in the forward direction, corresponding to $\partial' = a_c$, $\varphi' = 0$. The unit vectors in Cartesian coordinates are given in terms of those in spherical coordinates by:-

$$\left. \begin{aligned} \vec{i} &= \sin \partial' \cos \varphi' \vec{i}_1 + \cos \partial' \cos \varphi' \vec{i}_2 - \sin \varphi' \vec{i}_3 \\ \vec{j} &= \sin \partial' \sin \varphi' \vec{i}_1 + \cos \partial' \cos \varphi' \vec{i}_2 + \cos \varphi' \vec{i}_3 \\ \vec{k} &= \cos \partial' \vec{i}_1 - \sin \partial' \vec{i}_2 \end{aligned} \right\} \tag{2.4.30}$$

Applying the forward condition to the Equations (2.4.30), we have that:-

$$\left.\begin{aligned}&(\cos a_c\,\vec{i} - \sin a_c\,\vec{k}) = \vec{i}_2\\&\vec{j} = \vec{i}_3\end{aligned}\right| \qquad (2.4.31)$$

From Equations (2.4.4), (2.4.5), (2.4.19), (2.4.20), (2.4.28), (2.4.29) and (2.4.30), it follows that the far scattered field in the forward direction has the same polarization as the incident wave for either polarization. The forward scattering amplitudes are (Van de Hulst, 1957):-

$$S_I(a_c, \bar{a}) = \frac{1}{E_I}(\cos a_c\,\vec{i} - \sin a_c\,\vec{k}) \lim_{r'\to\infty}\left(- ik_o r' e^{-ik_o r'} E_I^s/\partial' = a_c \atop \varphi' = 0\right) \qquad (2.4.32)$$

and:-

$$S_{II}(a_c, \bar{a}) = \frac{1}{E_{II}}\vec{j}\,.\lim_{r'\to\infty}\left(- ik_o r' e^{-ik_o r'} E_{II}^s/\partial' = a_c \atop \varphi' = 0\right) \qquad (2.4.33)$$

Thus, for the first polarization of the incident wave:-

$$E_I S_I(a_c, \bar{a}) = \sum_{m=-\infty}^{\infty} \sum_{\substack{n\geq|m|\\ n\neq 0}} (-i)^{n-1} \times$$

$$\times \left(a_{mn}^I \frac{m}{\sin a_c} P_n^{|m|}(\cos a_c) + b_{mn}^I \frac{dP_n^{|m|}(\cos a_c)}{d_{a_c}}\right) \qquad (2.4.34)$$

and for the second polarization:-

$$E_{II} S_{II}(a_c, \bar{a}) = \sum_{m=-\infty}^{\infty} \sum_{\substack{n \geq |m| \\ n \neq 0}} (-i)^{n+2} \times$$

$$\times \left[a_{mn}^{II} \frac{dP_n^{|m|} (\cos a_c)}{d_{a_c}} + b_{mn}^{II} \frac{m}{\sin a_c} P_n^{|m|} (\cos a_c) \right] \qquad (2.4.35)$$

The energy scattered by the raindrop is (Stratton, 1941):-

$$W_s = \frac{1}{2} \operatorname{Re} \int_0^{2\pi} \int_0^{\pi} \left[E_2^S (H_3^S)^* - (H_2^S)^* E_3^S \right] r'^2 \sin \partial' \, d\partial' \, d\varphi' \qquad (2.4.36)$$

where the asterisk denotes complex conjugate. The calculation of W_s using the asymptotic form of the scattered fields given by Equations (2.4.28) and (2.4.29) and letting $r' \to \infty$ is found in Morrison and Cross (1974) and the final result is:-

$$W_s = \frac{2\pi}{\omega\mu_o k_o} \sum_{m=-\infty}^{\infty} \sum_{n \geq |m|} \frac{n(n+1)(n+|m|)!}{(2n+1)(n-|m|)!} (|a_{mn}|^2 + |b_{mn}|^2) \qquad (2.4.37)$$

The scattering cross section Q_s is defined as the ratio of the scattered energy flow to the mean energy flow of the incident wave per unit area. Thus (Stratton, 1941):-

$$Q_s^I = \frac{2\omega\mu_o W_s^I}{k_o E_I E_I^*} \quad , \quad Q_s^{II} = \frac{2\omega\mu_o W_s^{II}}{k_o E_{II} E_{II}^*} \qquad (2.4.38)$$

The total extinction cross section is the sum of the scattering and absorption cross sections, so that:-

$$Q_t^I = Q_s^I + Q_a^I \quad , \quad Q_t^{II} = Q_s^{II} + Q_a^{II} \qquad (2.4.39)$$

It is known that (Van de Hulst, 1957):-

$$Q_t^I = \frac{4\pi}{k_o^2} \text{Re } S_I(a_c, \bar{a}) \quad , \quad Q_t^{II} = \frac{4\pi}{k_o^2} \text{Re } S_{II}(a_c, \bar{a}) \tag{2.4.40}$$

so that (2.4.39) may be used to determine the absorption cross-sections Q_a^I and Q_a^{II}. The relations (2.4.40) which are consistent with the optical theorem may be verified directly from the relations:-

$$Q_t^I = \frac{2\omega\mu_o \; W_t^I}{k_o \; E_I E_I^*} \quad , \quad Q_t^{II} = \frac{2\omega\mu_o \; W_t^{II}}{k_o E_{II} E_{II}^*} \tag{2.4.41}$$

and the expression for the total energy (Stratton, 1941):-

$$W_t = \frac{1}{2} \text{Re} \int_0^{2\pi} \int_0^{\pi} \left[E_3^i (H_2^s)^* + E_3^s (H_2^i)^* - E_2^i (H_3^s)^* - E_2^s (H_3^i)^* \right] r'^2 \sin \vartheta' \, d\vartheta' \, d\varphi' \tag{2.4.42}$$

2.4.3 Propagation Characteristics of a Rain-Filled Medium

The propagation of electromagnetic waves through a rain-filled medium consisting of an assemblage of scatterers will necessarily entail multiple-scattering considerations between the raindrops. However, to obtain results simply for a physical rain model using the discrete scatterer results, conventional analyses have assumed only single scattering with all drops to be aligned with their semimin or axis parallel to the z′-axis.* The propagation constants associated with the waves polarised in the directions of the raindrop minor (I) and major (II) axes are (Van de Hulst, 1957):-

$$\kappa_I(a_c) = k_o + \frac{2\pi}{k_o} \int_0^{\infty} f_I(a_c, \bar{a}) \; n(\bar{a}) \; d\bar{a} \tag{2.4.43}$$

$$\kappa_{II}(a_c) = k_o + \frac{2\pi}{k_o} \int_0^{\infty} f_{II}(a_c, \bar{a}) \; n(\bar{a}) \; d\bar{a} \tag{2.4.44}$$

where $n(\bar{a})\ d\bar{a}$ is the number of drops per unit volume (cm^3) having radius

* This is because multiple-scattering is not important in the frequency range of interest (Olsen, 1978)

in the region $\bar{a}$, $\bar{a} + d\bar{a}$. The complex quantities $f_{I,II}$ are given in terms of $S_{I,II}$ as:-

$$f_{I,II}(a_c, \bar{a}) = - ik_o \, S_{I,II}(a_c, \bar{a}) \tag{2.4.45}$$

Thus, using Equations (2.4.45), (2.4.34) and (2.4.35) for the $S_{I,II}$ and either the Laws-Parsons (1943) or Marshall and Palmer (1948) drop-size distribution the specific attenuation and phase rotation of the electromagnetic wave after passing through the medium may be calculated as:-

$$\left.\begin{aligned} A_I(a_c) &= 8.686 \; I_m\left[\kappa_I(a_c)\right] \times 10^5 \text{ db/km} \\ A_{II}(a_c) &= 8.686 \; I_m\left[\kappa_{II}(a_c)\right] \times 10^5 \text{ db/km} \end{aligned}\right\} \tag{2.4.46}$$

and correspondingly the phase rotation:-

$$\left.\begin{aligned} \Phi_I(a_c) &= \frac{180}{\pi} \, \mathrm{Re}\left[\kappa_I(a_c)\right] \times 10^5 \text{ deg/km} \\ \Phi_{II}(a_c) &= \frac{180}{\pi} \, \mathrm{Re}\left[\kappa_{II}(a_c)\right] \times 10^5 \text{ deg/km} \end{aligned}\right\} \tag{2.4.47}$$

These formulae will be used in the next section.

2.5 Cross-Polarization Discrimination and Attenuation at a Constant Rainrate

The rain medium produces attenuation and cross-polarization for a microwave signal propagating through it. The cross-polarization effect is a direct consequence of the oblate shape and the canting angle of falling raindrops. So, this depolarization in general must be calculated in terms of canting angle parameters, specific attenuation and phase shift of the rain medium, as they have been evaluated in the previous section. There are two terms used to describe the depolarization for a received signal, which are defined as follows:-

$$\text{Cross-polarization discrimination (XPD)} \equiv 20 \log_{10} \left|\frac{E_{CX}}{E_{CC}}\right| \tag{2.5.1}$$

and:-

$$\text{Cross-polarization isolation (XPI)} \equiv 20 \log_{10} \left|\frac{E_{XC}}{E_{CC}}\right| \tag{2.5.2}$$

where E_{XC} is the received field in the cross-polar direction to that transmitted, E_{CX} is the received field in the transmitted direction from interference caused by the cross-polar channel, where in both cases, E_{CC} is the co-polar received field to that transmitted. On the other hand, the attenuation of the co-polar received signal is defined as:-

$$\text{Co-polar attenuation (CPA)} \equiv 20 \log_{10} \left|\frac{E_0}{E_{CC}}\right| \tag{2.5.3}$$

where $|E_0|$ is the amplitude of the incident field.

For independent canting-angle and drop-size distribution and for raindrops which are axi-symmetric in shape, the XPD and XPI can be shown to be identical (Watson and Arbabi, 1973). So, in this thesis the whole analysis is made in terms of XPD, but the results will be the same for XPI. Many authors have reported on the approximate or exact expressions giving the cross-polarization discrimination for a rain medium with drop canting angle distribution (Attisani et al, 1974; Chu, 1974; McGormick, 1975; Brussaard, 1976; Östberg, 1976). Most recently Oguchi (1977) showed that all the calculations can be put in a concise form. The definitions and equations given here with slight changes of notation follow from there (Oguchi, 1977). In this way, the mean value of the XPD and CPA due to rain at a constant rainfall rate, are calculated. The following analysis is divided into two parts corresponding to terrestrial and earth-space links.

2.5.1 Terrestrial Links

In this case, we have:-

$$\langle XPD\rangle_s = -20\log_{10}\left|\frac{\Gamma_1(a_c)\cos^2\phi + \Gamma_2(a_c)\sin^2\phi}{\left(\Gamma_1(a_c) - \Gamma_2(a_c)\right)\sin\phi\cos\phi}\right| \tag{2.5.4}$$

and:-

$$\langle CPA\rangle_s = -20\log_{10}\left|\Gamma_1(a_c)\cos^2\phi + \Gamma_2(a_c)\sin^2\phi\right| \tag{2.5.5}$$

where the symbol $\langle\ \rangle_s$ means the short-term mean value (or equivalently, at a constant rainfall rate) for the XPD or CPA. In these equations, ϕ is the "effective canting angle" of the randomly oriented raindrops (Oguchi, 1977). As was mentioned previously (Section 2.2.3), we will consider the case in which the raindrop-canting angle is independent of the drop size. Also, it is assumed that the two canting angle distributions for the transverse component θ and the longitudinal component γ are independent of each other (Fig. 2.3), so the angle ϕ takes the simple form (Oguchi, 1977):-

$$\phi = (1/2)\tan^{-1}\left(\frac{\langle\sin 2\theta\rangle}{\langle\cos 2\theta\rangle}\right) \tag{2.5.6}$$

For a Gaussian distribution of θ with $<\theta> = \theta_o$ and $\sigma_\theta = \sigma$, we have finally (Oguchi, 1977):-

$$\phi \cong \theta_o \qquad (2.5.7)$$

Also, $\Gamma_1(a_c)$ and $\Gamma_2(a_c)$ are the average transmission coefficients of the characteristic polarizations for a medium of path length L (Oguchi, 1977), where these two characteristic polarizations are propagated without depolarization through a rain-filled medium. The transmission coefficients Γ_1, Γ_2 are defined as:-

$$\left.\begin{aligned} \Gamma_1(a_c) &= e^{-j\kappa_1(a_c)\,L} \\ \Gamma_2(a_c) &= e^{-j\kappa_2(a_c)\,L} \end{aligned}\right\} \qquad (2.5.8)$$

where the propagation constants $\kappa_1(a_c)$ and $\kappa_2(a_c)$ for an angle of incidence $a_c = \pi/2$ (terrestrial path) are related to the constants κ_I and κ_{II} along the minor and major raindrop axes for an "equi-oriented raindrop model" at $\pi/2$ angle of incidence by:-

$$\left.\begin{aligned} \kappa_1(\pi/2) &= \Phi_1(\pi/2) - iA_1(\pi/2) = (1+m_\theta m_\gamma)\,\kappa_{II}(\pi/2)/2 + (1-m_\theta m_\gamma)\,\kappa_I(\pi/2)/2 \\ \kappa_2(\pi/2) &= \Phi_2(\pi/2) - iA_2(\pi/2) = (1-m_\theta m_\gamma)\,\kappa_{II}(\pi/2)/2 + (1+m_\theta m_\gamma)\,\kappa_I(\pi/2)/2 \end{aligned}\right\} \qquad (2.5.9)$$

where $A_{1,2}$ and $\Phi_{1,2}$ are the specific attenuations (in neper/unit distance) and phase shifts (in radian/unit distance) correspondingly, for propagation along these characteristic polarizations, and:-

$$m_\theta = \left(<\cos 2\theta>^2 + <\sin 2\theta>^2\right)^{1/2} \qquad (2.5.10)$$

and:-

$$m_\gamma = \langle \cos^2 \gamma \rangle \tag{2.5.11}$$

The < > brackets indicate the ensemble average over the appropriate canting angle distribution. For terrestrial paths, the angle γ, that is the component of canting angle in the plane containing the propagation path and the raindrop axis of symmetry, can be neglected, so we can put:-

$$\left.\begin{array}{l} \langle\gamma\rangle = \gamma_0 = 0 \\ \text{and:-} \\ \sigma_\gamma = \sigma' = 0 \end{array}\right\} \tag{2.5.12}$$

so:-

$$m_\gamma \cong 1 \tag{2.5.13}$$

For a Gaussian distribution of θ, Oguchi (1977) has shown that:-

$$m_\theta = e^{-2\sigma_\theta^2} \tag{2.5.14}$$

The first step in simplifying the relations (2.5.4) and (2.5.5) for XPD and CPA is to make the small argument approximation (Nowland, 1977). From knowledge that $\kappa_1 \cong \kappa_2$, the CPA in Equation (2.5.5) can be accurately approximated as:-

$$<CPA>_s = -20 \log_{10} \left| e^{-i(\kappa_1 \cos^2 \phi + \kappa_2 \sin^2 \phi)L} \right| \cong$$

$$\cong -\frac{20\ L}{\ln(10)} I_m(\kappa_1 \cos^2 \phi + \kappa_2 \sin^2 \phi) \tag{2.5.15}$$

Rewriting Equation (2.5.15) in terms of the specific attenuations A_I and A_{II} (in db/unit distance) corresponding to κ_{II} and κ_I, as given in Equation (2.4.46), we have:-

$$<CPA>_s \cong \left[A_{II}(1 + m_\theta \cos 2\phi)/2 + A_I(1 - m_\theta \cos 2\phi)/2\right] L \tag{2.5.16}$$

Similarly, using the small argument approximation:-

$$e^{-i(\kappa_1 - \kappa_2)L} = 1 - i(\kappa_1 - \kappa_2)L \tag{2.5.17}$$

and the fact that the differential propagation constant $\Delta\kappa(\pi/2) = \kappa_1(\pi/2) - \kappa_2(\pi/2)$ is related as follows to the differential specific attenuation $\Delta a = a_{II} - a_I$ (in neper/unit distance) and the differential phase shift $\Delta\beta = \beta_{II} - \beta_I$ (in radians/unit distance) for "equi-oriented" raindrops with $\pi/2$ angle of incidence:-

$$\Delta\kappa(\pi/2) = m_\theta\left[\kappa_{II}(\pi/2) - \kappa_I(\pi/2)\right] = m_\theta\left[\Delta\beta(\pi/2) - i\Delta a(\pi/2)\right] \tag{2.5.18}$$

it follows that:-

$$<XPD>_s \cong -10 \log_{10}\left[\frac{4\{1 + 2m_\theta\ \Delta a.L \sin^2 \phi + \left[m_\theta(\Delta a^2 + \Delta\beta^2)^{1/2}.L \sin^2 \phi\right]^2\}}{m_\theta^2(\Delta a^2 + \Delta\beta^2)\ .\ L^2 \sin^2 2\phi}\right] \tag{2.5.19}$$

For frequencies in the 4 to 50 GHz range and for rainrates less than about 150 mm/hr, the expression in { } in the numerator of Equation (2.5.19) can be approximated with little error to unity. This yields a simplifed relation for XPD:-

$$\langle XPD \rangle_s = 20 \log_{10} \left[\frac{1}{2} m_\theta L(\Delta a^2 + \Delta\beta^2)^{1/2} \sin 2\phi\right] \tag{2.5.20}$$

Equations (2.5.16) and (2.5.20) provide a basis for readily relating both XPD and CPA to each other as well as to rainrate and path length. Moreover, the manner in which m_θ and ϕ appear in these equations indicates the simplicity with which the canting angle distribution and the incident polarization can be handled when the small argument approximations are applied. On the other hand, these equations are appropriate for horizontal incident polarization. In the case of vertical polarization the equations which are used are the same with the substitution of $(\pi/2 - \phi)$ as the new canting angle.

The second step in simplifying the problem is to approximate the specific attenuations and the magnitude of the differential propagation constant $|\kappa_{II}(\pi/2) - \kappa_I(\pi/2)| = (\Delta a^2 + \Delta\beta^2)^{1/2}$ by power law relations in terms of point rainrate (Olsen, Rogers and Hodge, 1978), i.e.:-

$$\left.\begin{aligned} A_I &= \alpha_I R^{b_I} \\ A_{II} &= \alpha_{II} R^{b_{II}} \\ (\Delta a^2 + \Delta\beta^2)^{1/2} &= cR^d \end{aligned}\right\} \tag{2.5.21}$$

Using Equations (2.5.16), (2.5.21) and the fact that $b_I \cong b_{II}$, it follows that:-

$$\langle CPA \rangle_s = \alpha\ R^b\ L \tag{2.5.22}$$

where:-

$$\left.\begin{aligned} \alpha &= \alpha_c\ J_\alpha \\ b &= b_c\ J_b \end{aligned}\right\} \tag{2.5.23}$$

$$\left.\begin{aligned} \alpha_c &= \frac{\alpha_I + \alpha_{II}}{2} \\ b_c &= \frac{\alpha_I b_I + \alpha_{II} b_{II}}{\alpha_I + \alpha_{II}} \end{aligned}\right\} \tag{2.5.24}$$

and:-

$$\left.\begin{aligned} J_a &= 1 + \left(\frac{\alpha_{II} - \alpha_I}{\alpha_I + \alpha_{II}}\right) m_\theta \cos 2\phi \\ J_b &= \frac{1}{J_a}\left[1 + \left(\frac{\alpha_{II} b_{II} - \alpha_I b_I}{\alpha_I b_I + \alpha_{II} b_{II}}\right) m_\theta \cos 2\phi\right] \end{aligned}\right\} \tag{2.5.25}$$

Similarly, from Equations (2.5.20) and (2.5.21):-

$$\langle XPD \rangle_s = 20 \log_{10} \left|\frac{1}{2}\, m_\theta\ c\ R^d\ L \sin 2\phi\right| \ * \tag{2.5.26}$$

The parameters A_I, A_{II} and $(\Delta a^2 + \Delta\beta^2)^{1/2}$ have been obtained for the drop-size distribution of Laws and Parsons (1943) using Oguchi's tabulations of forward-scattering amplitudes for oblate spheroidal (Oguchi and Hosoya, 1974) and Pruppacher-Pitter form raindrops (Oguchi,

* Experimental verification of this functional relationship would be desirable

1977). This work has been done by Nowland et al (1977) and regression coefficients for α_I, α_{II}, b_I, b_{II}, c, d are given in Table 2.3. These were obtained from regressions at the Laws-Parsons rainrates of 1.27, 2.54, 5.08, 12.7, 25.4 and 50.8 mm/hr, but are also valid for higher rainrates.

2.5.2 Earth-Space Links

For such links, the relations (2.5.4) and (2.5.5) for XPD and CPA, are modified as follows:-

$$\langle XPD\rangle_s = -20\log_{10}\left|\frac{\Gamma_1(a_c)\cos^2(\phi-\tau)+\Gamma_2(a_c)\sin^2(\phi-\tau)}{\left(\Gamma_1(a_c)-\Gamma_2(a_c)\sin(\phi-\tau)\cos(\phi-\tau)\right.}\right| \qquad (2.5.27)$$

and:-

$$\langle CPA\rangle_s = -20\log_{10}\left|\Gamma_1(a_c)\cos^2(\phi-\tau)+\Gamma_2(a_c)\sin^2(\phi-\tau)\right| \qquad (2.5.28)$$

In these equations, τ is the polarization tilt angle relative to the horizontal (Shkarofsky, 1977). The elevation angle ε which is defined as:-

$$\varepsilon = \pi/2 - a_c \qquad (2.5.29)$$

is always different from zero, so in this case, the component of the raindrop canting angle in the plane containing the propagation path and the raindrop axis of symmetry γ cannot be neglected. For earth-space paths, this γ is dependent on elevation angle and we can put (Nowland et al, 1977):-

$$\langle\gamma\rangle = \gamma_0 \cong \varepsilon \qquad (2.5.30)$$

TABLE 2.3 REGRESSION COEFFICIENTS FOR PRUPPACHER-PITTER-FORM RAINDROPS WITH LAWS-PARSONS DROPSIZE DISTRIBUTION; RAIN TEMPERATURE = 20^{o}C

Frequency	$\alpha_I \times 10^2$	b_I	$\alpha_{II} \times 10^2$	b_{II}	$c \times 10^4$	d
GHz	db/km		db/km		km^{-1}	
11.0	1.245	1.241	1.344	1.267	7.366	1.235
13.0	2.113	1.195	2.256	1.223	8.723	1.237
19.3	6.090	1.094	6.400	1.134	13.390	1.234
34.8	22.350	0.994	23.880	1.017	25.740	1.133

Following the same steps as in the previous case, we derive the following expressions for XPD and CPA:-

$$\langle XPD\rangle_s = 20 \log_{10} \left| \frac{1}{2} m_\theta m_\gamma \; c \; R^d \; \ell \; \sin 2 \left| \phi - T \right| \right| \tag{2.5.31}$$

and:-

$$\langle CPA\rangle_s = \alpha \; R^b \; \ell \tag{2.5.32}$$

where (Nowland et al, 1977):-

$$m_\gamma = \frac{1}{2} \left[1 + e^{-2\sigma_\gamma^2} \cos 2\langle\gamma\rangle \right] \tag{2.5.33}$$

and α, b are now given as:-

$$\left.\begin{aligned} \alpha &= \alpha_c \; J_a(a_c) \\ b &= b_c \; J_b(a_c) \end{aligned}\right\} \tag{2.5.34}$$

and α_c, b_c are the same as in Equation (2.5.24), but the $J_a(a_c)$, $J_b(a_c)$ are given as:-

$$\left.\begin{aligned} J_a(a_c) &= 1 + \left(\frac{\alpha_{II} - \alpha_I}{\alpha_I + \alpha_{II}} \right) m_\theta m_\gamma \cos 2(\phi - \tau) \\ J_b(a_c) &= \frac{1}{J_a(a_c)} \left[1 + \left(\frac{\alpha_{II}\, b_{II} - \alpha_I\, b_I}{\alpha_I\, b_I + \alpha_{II}\, b_{II}} \right) m_\theta m_\gamma \cos 2(\phi - \tau) \right] \end{aligned}\right\} \tag{2.5.35}$$

In Equations (2.5.31) and (2.5.32) the ℓ is the effective path length through rain as it is defined by Nowland et al (1977). This ℓ is a function of point rainfall rate R and the elevation angle ε. Experience has showed that this function can be approximated as (Nowland et al, 1977):-

$$\ell(R, \varepsilon) = \left[7.41 \times 10^{-3} R^{0.766} + (0.232 - 1.80 \times 10^{-4} R) \sin \varepsilon\right]^{-1} \qquad (2.5.36)$$

This result is applicable to at least north-western Europe and the north-eastern part of the USA. Making a regression analysis, we can obtain:-

$$\ell(R, \varepsilon) \cong u(\varepsilon) R^{v(\varepsilon)} \qquad (2.5.37)$$

Values of u and v as a function of elevation angle ε have been tabulated by Nowland et al (1977) and are given in Table 2.4.

In conclusion, the results of this section will be used as an estimation of the short-term mean value of XPD or rain co-polar attenuation in the following stochastic analysis.

TABLE 2.4 u AND v IN $\ell = uR^v$ AS FUNCTIONS OF ELEVATION ANGLE ε

1 - 50 mm/h RAINRATE RANGE

ε, deg.	10	20	30	40	50	60	70
u, km	24.9	13.3	9.11	7.06	5.91	5.21	4.79
v	- 0.364	- 0.252	- 0.196	- 0.164	- 0.143	- 0.129	- 0.121

CHAPTER 3

ANALYSIS OF THE LONG-TERM STATISTICS OF RAIN CROSS-POLARIZATION DISCRIMINATION FOR SPATIALLY UNIFORM RAIN

Introduction

In this chapter, calculations of the long-term statistics of the cross-polarised part of millimetric waves propagating through rain are considered. The work can be considered as an extension to Lin's (1975) calculations of rain attenuation statistics with a view to their application to radio path design. The analysis is limited to the case of propagation through regions in which the rainfall rate is uniform in space, but not necessarily uniform in time. The assumption of uniform rain throughout the entire length is a rather poor approximation for long paths, as it is well-known that rain cell sizes for heavy rains (> 100 mm/hr) rarely exceed 3 or 4 km (Freeny and Gabbe, 1969). This restricts applications of the results to path lengths of 2 km or so. For the higher frequencies of the microwave band (> 20 GHz) where the repeater spacing is usually designed to be less than 4 km, this assumption well approximates the real situation. However, this method can be developed into a long-path model, as will be shown in the next chapter, by dividing the propagation medium into a series of statistically uniform segments.

The technique adopted here is to divide the uniform region into thin slabs, each treated by the single-scatter method of Van de Hulst (1957). For these individual slabs the emerging waves have cross-polar components which are Rayleigh distributed, assuming temporal stationarity. The amplitude of the cross-polar signal that finally emerges from the spatially uniform region can then be shown using Nakagami's m-variable theory (1960), to be a Rayleigh distributed random variable. This is true for a rainfall rate R that is constant in time or, in other words, is the short-term distribution of the random variable.

Over a long period, when the whole region remains spatially uniform but the rainfall rate R is a random time process, the short-term mean square value of the fluctuating cross-polar received signal is shown to have a log-normal distribution. This is an exact result, assuming that the rainrate has a log-normal distribution (Section 2.3). Using the theorem of total probability, a numerical technique is used to show that the cross-polar signal itself is approximately log-normal.

An important application of this statistical distribution to the design of a radio communication path is also given in this chapter. This is the evaluation of radio outage time due to cross-channel interference. Tolerable interference levels of - 20 db, - 25 db and - 30 db are employed for the purposes of illustration.

3.1 General Theory of Depolarization

We will now present the idea of complex polarization factor and polarization coefficients which will be useful for our analysis (Beckmann, 1968).

Consider a plane electromagnetic wave propagating in the direction of the unit vector $\vec{k}$. Let $\vec{e}^{+}$ and $\vec{e}^{-}$ be mutually perpendicular unit vectors in the plane perpendicular to $\vec{k}$. These two unit vectors are usually oriented in privileged directions, e.g. vertical and horizontal, if the surface of the earth is relevant, or parallel and perpendicular to the plane of incidence in scattering problems. The superscripts + and - have been chosen with reference to vertical and horizontal polarizations since the corresponding reflection coefficients for a perfectly conducting plane are + 1 and - 1, respectively (Fig. 3.1).

Resolving the electric field strength $\vec{E}$ into its space components:-

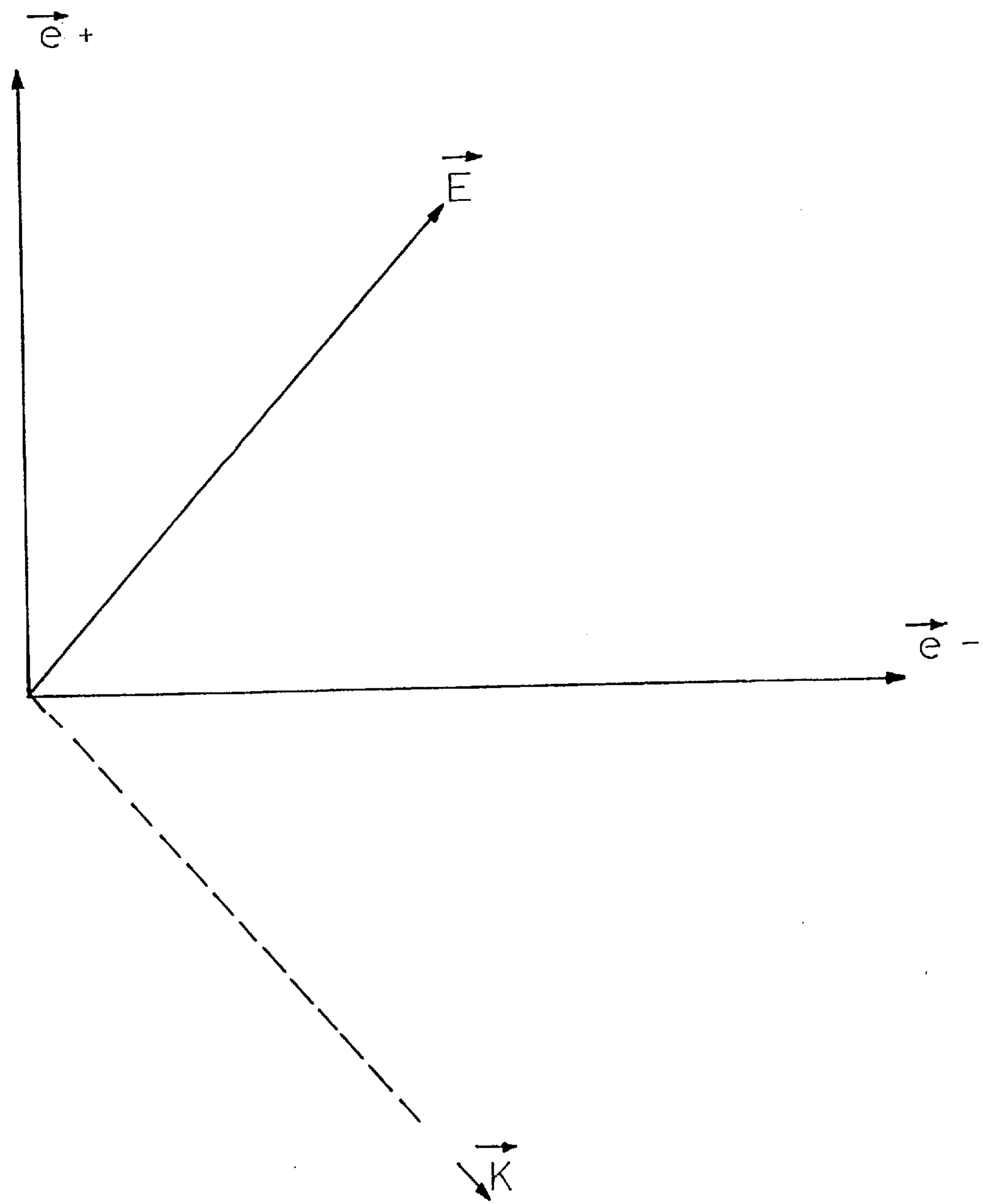

Fig. 3.1 General theory of depolarization

$$E^{+} = \vec{E} \cdot \vec{e}^{+} \quad , \qquad E^{-} = \vec{E} \cdot \vec{e}^{-} \tag{3.1.1}$$

we can write the vector-phasor $\vec{E}$ as:-

$$\vec{E} = E^{+}\,\vec{e}^{+} + E^{-}\,\vec{e}^{-} = E^{-}\left(\vec{e}^{-} + \frac{E^{+}}{E^{-}}\,\vec{e}^{+}\right) \tag{3.1.2}$$

or introducing the complex polarization factor $p = E^{+}/E^{-}$, we have:-

$$\vec{E} = E^{-}(\vec{e}^{-} + p\vec{e}^{+}) \tag{3.1.3}$$

In other words:-

$$p = |p| \exp\,(i\arg p) = |E^{+}/E^{-}| \exp\,(i\arg E^{+} - i\arg E^{-}) \tag{3.1.4}$$

It follows that $|p|$ is the ratio of the amplitudes of, and arg p the phase difference between, the two components of the wave. The complex polarization factor p uniquely describes the polarization of an electromagnetic wave. In particular, we have the following polarizations described by the corresponding values of p:-

$$\left.\begin{array}{ll}
\mathrm{Im}\,p = 0 & \text{Linear} \\
p = 0 & \text{Horizontal} \\
p = \infty & \text{Vertical} \\
\mathrm{Im}\,p > 0 & \text{Right elliptical} \\
\mathrm{Im}\,p < 0 & \text{Left elliptical} \\
p = i & \text{Right circular} \\
p = -\,i & \text{Left circular}
\end{array}\right\} \tag{3.1.5}$$

The complex polarization factor is particularly convenient for depolarization investigations. For example, if an incident wave with polarization factor p_1 is scattered, diffracted or otherwise subjected to an electromagnetic process so that it emerges with polarization p_2, the transformation may simply be described by:-

$$p_2 = qp_1 \tag{3.1.6}$$

where q is a depolarization factor, which, in many cases, is a constant determined only by the properties of the depolarizer, though in general it is a function of p_1.

We will now find the general solution of this problem in terms of four coefficients which have to be calculated (or measured) for each specific case for they depend on the input-output geometry and on the shape and electrical properties of the scatterer or other depolarizer. However, they do not depend (in linear media) on the input polarization p_1. If the incident (input field) is plus polarised, the scattered (output) field will generally be depolarised and will have both a plus and minus component. A similar statement holds if the incident field is minus polarised. Conversely, the plus component of the scattered field will consist of two terms - one due to the similarly polarised component of the incident field and one due to the cross-polarised component of the incident field. Thus:-

$$\left.\begin{array}{l} E_2^+ = E_{2s}^+ + E_{2x}^+ \\ E_2^- = E_{2s}^- + E_{2x}^- \end{array}\right\} \tag{3.1.7}$$

where the subscripts s and x indicate whether the field is produced, respectively, by the similarly polarised, or the cross-polarised, component of the input field.

Let us now introduce the "polarization coefficients":-

$$\left.\begin{aligned} \Gamma^{++} &= E^{+}_{2s}/E^{+}_{1} \quad , \quad & \Gamma^{+-} &= E^{+}_{2x}/E^{-}_{1} \\ \Gamma^{--} &= E^{-}_{2s}/E^{-}_{1} \quad , \quad & \Gamma^{-+} &= E^{-}_{2x}/E^{+}_{1} \end{aligned}\right\} \tag{3.1.8}$$

These four coefficients are easiest to calculate when one of the incident components vanishes. We then have:-

$$\left.\begin{aligned} \Gamma^{++} &= E^{+}_{2}/E^{+}_{1} \quad , \quad & \Gamma^{-+} &= E^{-}_{2}/E^{+}_{1} \quad & \text{for } E^{-}_{1} &= 0 \\ \Gamma^{--} &= E^{-}_{2}/E^{-}_{1} \quad , \quad & \Gamma^{+-} &= E^{+}_{2}/E^{-}_{1} \quad & \text{for } E^{+}_{1} &= 0 \end{aligned}\right\} \tag{3.1.9}$$

Substituting in the above equations, we have:-

$$\left.\begin{aligned} E^{+}_{2} &= \Gamma^{++}\, E^{+}_{1} + \Gamma^{+-}\, E^{-}_{1} \\ E^{-}_{2} &= \Gamma^{--}\, E^{-}_{1} + \Gamma^{-+}\, E^{+}_{1} \end{aligned}\right\} \tag{3.1.10}$$

Dividing the first of Equation (3.1.10) by the second and using the definition of the complex polarization factor, we find the basic general solution of the depolarization problem in the form:-

$$p_2 = \frac{\Gamma^{++}\, p_1 + \Gamma^{+-}}{\Gamma^{--} + \Gamma^{-+}\, p_1} \tag{3.1.11}$$

From the above formula, it is obvious that we are able to find the polarization factor p_2 for any input polarization p_1 in terms of the polarization coefficients Γ^{++}, Γ^{+-}, Γ^{-+}, Γ^{--} as defined in Equation (3.1.9).

3.2 Short-Term Statistics of the Cross-Polarised Signal

In this section, an analysis of the statistics of the XPD at a constant rainfall rate of the medium will be made. This is the first step for the evaluation of the total statistics for it.

3.2.1 Incident Linear, Horizontal or Vertical Polarization

The starting point of the method is to divide the radio path into successive incremental slabs in each of which we can use single scattering considerations (Van de Hulst, 1957). So, if for the j-slab (see Fig. 3.2) the components of the input field will be E_j^+ and E_j^- and the corresponding output are E_{j+1}^+ and E_{j+1}^- (+ and - referred to specified directions, usually vertical and horizontal), then using Equation (3.1.10), we have:-

$$\left.\begin{aligned} E_{j+1}^+ &= \Gamma_j^{++}\, E_j^+ + \Gamma_j^{+-}\, E_j^- \\ E_{j+1}^- &= \Gamma_j^{--}\, E_j^- + \Gamma_j^{-+}\, E_j^+ \end{aligned}\right\} \qquad (3.2.1)$$

The polarization coefficients, Γ_j^{++}, Γ_j^{+-}, Γ_j^{-+}, Γ_j^{--} can be evaluated from the above system by putting $E_j^+ = 1$, $E_j^- = 0$ (incident linear vertical polarization) and $E_j^- = 1$, $E_j^+ = 0$ (incident linear horizontal polarization). Generally (Beckmann, 1968; Van de Hulst, 1957) the cross-polar components Γ_j^{+-} and Γ_j^{-+} consist of the sum of many independent scattered waves (γ_j^{+-}, γ_j^{-+} from the i_{th} raindrop) so that for the j_{th} slab:-

$$\Gamma_j^{+-} = \sum_{i=1}^{n} \gamma_j^{+-} \qquad \text{and} \qquad \Gamma_j^{-+} = \sum_{i=1}^{n} \gamma_j^{-+} \qquad (3.2.2)$$

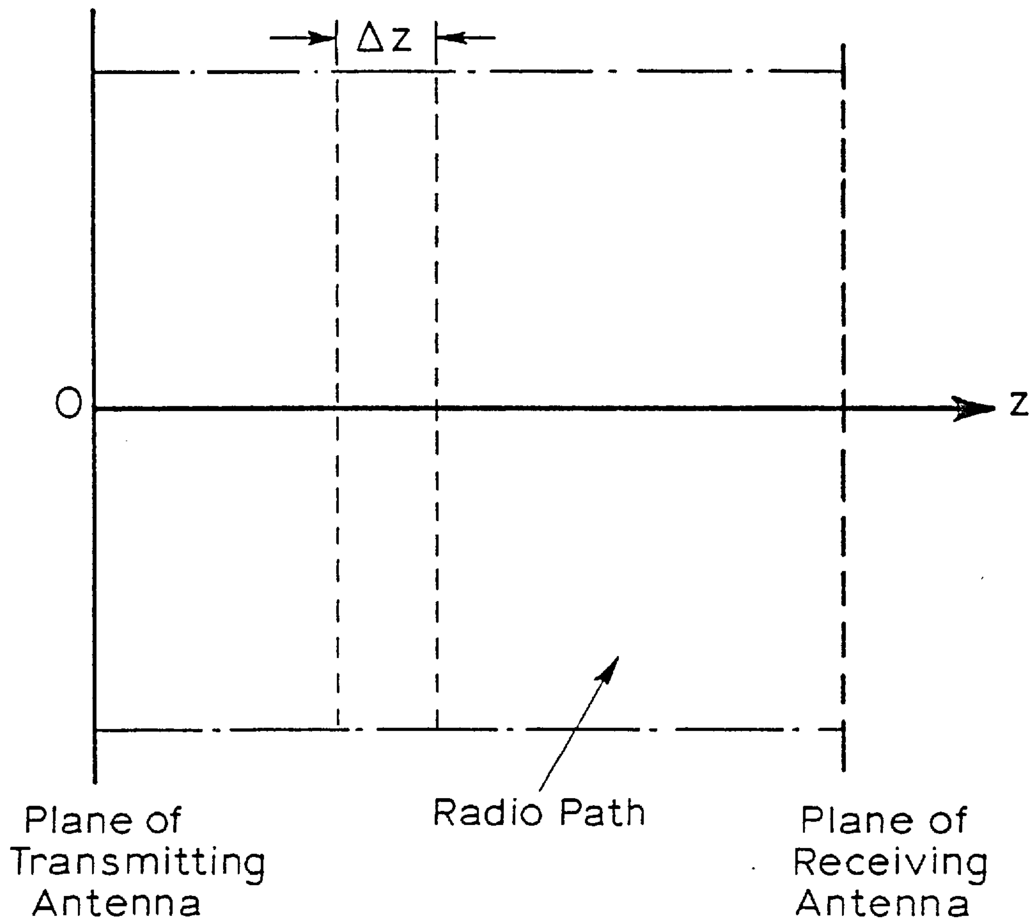

Fig. 3.2 Configuration of the radio path

assuming that single scattering has occurred. The assumption that the scattering from each raindrop is physically independent means that the γ_i are randomly phased uniformly throughout 0 to 2π and statistically independent. So, the terms in the sums (3.2.2) have phases which are independent and uniformly distributed and the $|\gamma_i|$ are all distributed identically. On the other hand, the number n of scattered waves is very large and approximately constant in time at a specified rainfall rate, depending only on the geographic location (Lin, 1975). In Appendix C, it is proved that these sums give Rayleigh phasors, or in other words, phasors whose amplitudes are Rayleigh distributed and whose phases are uniformly distributed. For the co-polar terms, Γ_j^{++} and Γ_j^{--}, we have in a similar manner:-

$$\Gamma_j^{++} = 1 + \sum_{i=1}^{n} \gamma_i^{++} \quad , \qquad \Gamma_j^{--} = 1 + \sum_{i=1}^{n} \gamma_i^{--} \tag{3.2.3}$$

where the scattered waves γ_i^{++} and γ_i^{--} have similar properties to γ_i^{+-} and γ_i^{-+}. According to Beckmann (1967), Norton and Vogler (1955) (see Appendix C) the Γ_j^{++}, Γ_j^{--} must be Rice-Nakagami phasors.

After the general theory, we will now analyse the case of horizontal incident linear polarization. The procedure for vertical polarization will be exactly the same.

The components of the incident wave will be:-

$$\left.\begin{aligned} E_o^+ &= 0 \\ E_o^- &= 1 \end{aligned}\right\} \tag{3.2.4}$$

(normalized wave)

Using Van de Hulst's (1957) approximation, the components at the output of the first slab will be:-

$$\begin{bmatrix} E_1^+ \\ E_1^- \end{bmatrix} = \begin{bmatrix} a_o^V & \beta_o \\ \beta_o & a_o^H \end{bmatrix} \begin{bmatrix} 0 \\ 1 \end{bmatrix} \tag{3.2.5}$$

where:-

$$\left.\begin{aligned} a_j^V &= \Gamma_j^{++} \\ a_j^H &= \Gamma_j^{--} \\ \beta_j &\equiv \Gamma_j^{+-} \equiv \Gamma_j^{-+} \end{aligned}\right\} \tag{3.2.6}$$

for j = 0, 1, 2, ... N_s where N_s is the total number of slabs, so:-

$$\left.\begin{aligned} E_1^+ &= \beta_o \\ E_1^- &= a_o^H \end{aligned}\right\} \tag{3.2.7}$$

These E_1^+, E_1^- are the input components of the second slab, so the output components will be:-

$$\left.\begin{bmatrix} E_2^+ \\ E_2^- \end{bmatrix} = \begin{bmatrix} a_1^V & \beta_1 \\ \beta_1 & a_1^H \end{bmatrix} \begin{bmatrix} \beta_o \\ a_o^H \end{bmatrix} \rightarrow \begin{aligned} E_2^+ &= a_1^V \beta_o + a_o^H \beta_1 \\ E_2^- &= a_o^H a_1^H + \beta_1 \beta_o \end{aligned}\right\} \tag{3.2.8}$$

For the third slab, we will have similarly:-

$$\begin{bmatrix} E_3^+ \\ E_3^- \end{bmatrix} = \begin{bmatrix} a_2^V & \beta_2 \\ \beta_2 & a_2^H \end{bmatrix} \begin{bmatrix} a_1^V \beta_o + a_o^H \beta_1 \\ a_o^H a_1^H + \beta_1 \beta_o \end{bmatrix} \tag{3.2.9}$$

or:-

$$\left.\begin{aligned} E_3^+ &= a_2^V\, a_1^V\, \beta_o + a_2^V\, a_o^H\, \beta_1 + \beta_2\, a_o^H\, a_1^H + \beta_2\, \beta_1\, \beta_o \\ E_3^- &= \beta_2\, \beta_o\, a_1^V + \beta_2\, \beta_1\, a_o^H + a_2^H\, a_1^H\, a_o^H + a_2^H\, \beta_1\, \beta_o \end{aligned}\right\} \qquad (3.2.10)$$

Considering the rain medium as a moderately depolarizing medium (Attisani et al, 1974), we can easily conclude that:-

$$E_3^- \cong a_o^H\, a_1^H\, a_2^H$$

$$(E_3^+/E_3^-) \cong (\beta_2/a_2^H) + (\beta_1/a_1^H)\,(a_2^V/a_2^H) + (\beta_o/a_o^H)\,(a_2^V/a_2^H)\,(a_1^V/a_1^H) \qquad (3.2.11)$$

When now we continue the process, the final result is:-

$$C_R^H \equiv (E_{N_s}^+/E_{N_s}^-) = (\beta_{N_s-1}/a_{N_s-1}^H) + (\beta_{N_s-2}/a_{N_s-2}^H)\,(a_{N_s-1}^V/a_{N_s-1}^H) +$$

$$+ (\beta_{N_s-3}/a_{N_s-3}^H)\,(a_{N_s-2}^V/a_{N_s-2}^H)\,(a_{N_s-1}^V/a_{N_s-1}^H) + \,.\,.\,.\,.\,.\,.\,.\,.\,.\,.\, +$$

$$+ (\beta_o/a_o^H)\,(a_{N_s-1}^V/a_{N_s-1}^H)\,(a_{N_s-2}^V/a_{N_s-2}^H)\,\ldots\ldots\,(a_2^V/a_2^H)\,(a_1^V/a_1^H) \qquad (3.2.12)$$

where C_R^H is the complex polarization factor at the output of the rain medium (as it is defined in Section 3.1).

If we define:-

$$\rho_j \equiv a_j^V/a_j^H \qquad (3.2.13)$$

then this complex random variable will have a negligible (almost zero) phase and amplitude (ratio of two correlated Rice-Nakagami variables) which will have a fluctuation with very small variance compared to the variance of the amplitude of β_j (Rayleigh variable). After that, it is reasonable to accept ρ_j as a constant term ρ, so the final result is:-

$$C_R^H = (\beta_{N_s-1}/a^H_{N_s-1}) + \rho(\beta_{N_s-2}/a^H_{N_s-2}) + \rho^2(\beta_{N_s-3}/a^H_{N_s-3}) + \ldots\ldots +$$

$$+ \rho^{N_s-1}(\beta_0/a_0^H) = \sum_{j=1}^{N_s} \rho^{N_s-j}(\beta_{j-1}/a^H_{j-1}) \qquad (3.2.14)$$

Again, the $|a_j^H|$ are almost constant terms nearly equal to 1, compared to the $|\beta_j|$ and we can put:-

$$<|a_0^H|>_s = <|a_1^H|>_s = \ldots\ldots = <|a_j^H|>_s = a_s \qquad (3.2.15)$$

where the vertical bars mean taking the modulus and the sharp brackets the expectation of the quantities within. So, C_R^H from Equation (3.2.14) is a complex variable which is the sum of many independent Rayleigh phasors (Beckmann, 1967). As explained analytically in Appendix C, we have that in this case the $|C_R^H|$ must follow a Rayleigh distribution with mean square value (m.s.):-

$$\Omega = \sum_{j=1}^{N_s} \Omega_j \qquad (3.2.16)$$

where:-

$$\Omega_j = <\beta_j^2>_s \rho^{2N_s-2j}/a_s^2 \qquad (3.2.17)$$

and:-

$$\Omega = \sum_{j=1}^{N_s} <\beta_j^2>_s \rho^{2N_s-2j} / a_s^2 = (1/a_s^2) \sum_{j=1}^{N_s} \rho^{2N_s-2j} <\beta_j^2>_s \tag{3.2.18}$$

The problem is now, to calculate the Ω in terms of the known parameters of the rain medium (such as the canting angle distribution, drop-size distribution, etc.). This is a very complicated task, but we can simplify it if we accept the following results. In the general theory of radio wave propagation through rain (Section 2.5), the short-term mean value of the amplitude of the complex cross-polarization factor, is given by (Expressions (2.5.4) and (2.5.20)):-

$$<|C_R^H|>_s \cong m_\theta \, L(\Delta a^2 + \Delta\beta^2)^{1/2} \sin 2\phi/2 \tag{3.2.19}$$

where L is the effective path length through rain, ϕ is the mean value of the canting angle distribution (Expression (2.5.7)) and m_θ the canting angle distribution factor (Expression (2.5.14)). $(\Delta a^2 + \Delta\beta^2)^{1/2}$ represents for an equioriented raindrop model the magnitude of the differential propagation constant for waves polarised in the directions of the raindrop major and minor axes. Using Expression (2.5.21), we have finally:-

$$<|C_R^H|>_s \cong m_\theta \, L \, cR^d \sin 2\phi/2 \tag{3.2.20}$$

R is the rainfall rate in mm/hr. The regression coefficients c and d for Pruppacher-Pitter raindrops having a Laws-Parsons drop-size distribution are given in Table 2.3 for various frequencies.

At this point, we need a general expression for the mean-square value of a Rayleigh variable R_1 and its mean value $<R_1>$. This expression is derived analytically in Appendix B for an m-distributed variable (Nakagami, 1960) and has the form of:-

$$<R_1> = \{\Gamma\left(m + \frac{1}{2}\right) / \left(\Gamma(m) \, . \, m^{1/2}\right)\} \surd \Omega^m \tag{3.2.21}$$

where $\Gamma(\ )$ is the gamma function (Abramovitz and Stegun, 1965). In our case, m = 1 (Rayleigh distribution) and so:-

$$\Omega = \{\Gamma^2(1)/\Gamma^2\left(1 + \frac{1}{2}\right)\} <R_1>^2 = (4/\pi) <R_1>^2 \tag{3.2.22}$$

Combination of formulae (3.2.20) and (3.2.22) gives us:-

$$\Omega \cong \left(m_\theta^2 \ L^2 \ c^2 \ \sin^2(2\phi)/\pi\right) R^{2d} = AR^B \tag{3.2.23}$$

with:-

$$\left.\begin{array}{l} A = m_\theta^2 \ L^2 \ c^2 \ \sin^2(2\phi)/\pi \\ B = 2d \end{array}\right\} \tag{3.2.24}$$

These constants must be functions of the wave-length λ, and the path length L. This is the situation for a constant rainfall rate R mm/hr at each time (short-term distribution).

3.2.2 Incident Linear 45^0 Polarization

The 45^0 linear polarization case can be considered approximately similar to circular polarization (Bostian, 1973). This can be done by rotating the principal axes of polarization (Beckmann, 1968) 45^0 relative to the vertical direction so the + and - directions are not now identical with the vertical and horizontal (see Fig. 3.3). The new canting angle θ' in this case will be:-

$$\theta' = \theta + (\pi/4) \tag{3.2.25}$$

The components of the incident wave will be:-

$$\left.\begin{aligned} E_o^+ &= 1 \\ E_o^- &= 0 \end{aligned}\right\} \tag{3.2.26}$$

The complex polarization factor C_R^+ will again be:-

$$C_R^+ = (E_{out}^-/E_{out}^+) = (\beta'_{N_s-1}/a^+_{N_s-1}) + (\beta'_{N_s-2}/a^+_{N_s-2})\ (a^-_{N_s-1}/a^+_{N_s-1}) +$$

$$+ (\beta'_{N_s-3}/a^+_{N_s-3})\ (a^-_{N_s-2}/a^+_{N_s-2})\ (a^-_{N_s-1}/a^+_{N_s-1}) + \ldots\ldots +$$

$$+ (\beta'_o/a^+_o)\ (a^-_1/a^+_1)\ (a^-_2/a^+_2)\ \ldots\ldots\ (a^-_{N_s-1}/a^+_{N_s-1}) \tag{3.2.27}$$

where:-

$$\left.\begin{aligned} a_j^+ &\equiv \Gamma_j'^{++} \\ a_j^- &\equiv \Gamma_j'^{--} \\ \beta_j' &\equiv \Gamma_j'^{+-} \equiv \Gamma_j'^{-+} \end{aligned}\right\} \tag{3.2.28}$$

and $\Gamma_j'^{++}$, $\Gamma_j'^{--}$, $\Gamma_j'^{+-}$, $\Gamma_j'^{-+}$ are the new polarization coefficients for the j-slab of the medium. Defining:-

$$\rho'_j \equiv a^-_j/a^+_j \tag{3.2.29}$$

then, again ρ'_j may be considered as a constant term ρ' and the final result is:-

$$C^+_R = \sum_{j=1}^{N_s} \rho'^{N-j} \, (\beta'_{j-1}/a^+_{j-1}) \tag{3.2.30}$$

We have also that:-

$$<|a^+_o|> = <|a^+_1|> = \, . \, . \, . \, . \, . \, . \, . = <|a^+_j|> = a'_s \tag{3.2.31}$$

The distribution for the variable $|C^+_R|$ will be Rayleigh with mean square value:-

$$\Omega' = \sum_{j=1}^{N_s} <\beta'^2_j> \, (\rho'^{2N-2j}/a'^2_s) \tag{3.2.32}$$

A simplified result for Ω' is derived, if we will consider that this case is equivalent to the previous one with new canting angle θ' given by Equation (3.2.25). So, using again the expressions of Nowland (1977), we have finally:-

$$\Omega' = A' \, R^{B'} \tag{3.2.33}$$

with:-

$$\left.\begin{aligned} A' &= m_\theta^2\, L^2\, c^2 \sin^2\left[2\left(\phi + (\pi/4)\right)\right]/\pi \\ B' &= 2d \end{aligned}\right\} \qquad (3.2.34)$$

3.3 Long-Term Statistics

For a long-term period, we must consider the fluctuations of the random variable R (rainfall rate). So, in this case we will use the log-normal model for the point rainrate statistics (Section 2.3):-

$$P\left[R \geq r\right] = P_o(0) \,.\, \left(\frac{1}{2}\right) \text{erfc}\left[(\ln r - \ln R_m)/(\sqrt{2}\, S_R)\right] \qquad (3.3.1)$$

The three parameters $P_o(0)$, R_m and S_R characterizing the log-normal distribution can be calculated by application of the theory of extreme value statistics, as explained analytically in Section 2.3.2.

3.3.1 Incident Linear Horizontal or Vertical Polarization

It then follows that the mean-square value Ω of the complex cross-polarization factor C_R^H, given by the formula (3.2.23) must follow a log-normal distribution (Aitchison and Brown, 1957; Lin, 1975):-

$$P\left[\Omega \geq \omega\right] = P_o(0) \,.\, \left(\frac{1}{2}\right) \text{erfc}\left[(\ln \omega - \ln \Omega_m)/(\sqrt{2}\, S_\Omega)\right] \qquad (3.3.2)$$

where S_Ω is the standard deviation of $\ln \Omega$ and Ω_m the median value of Ω during rain. The parameters S_Ω and Ω_m of the Ω-distribution are analytically related to the corresponding S_R and R_m of the R-distribution, by the following formulae:-

$$\left.\begin{aligned} \Omega_m &= A\, R_m^B \\ S_\Omega &= B\, S_R \end{aligned}\right\} \qquad (3.3.3)$$

These formulae have been derived by combining the relations (3.2.23), (3.3.1) and (3.3.2) and the well-known properties of the log-normal distribution (Aitchison and Brown, 1957). The density distribution function for the Ω-variable will be:-

$$P_{\Omega}(\omega) = (1/\sqrt{2\pi}) \left[1/(S_{\Omega} \,.\, \omega)\right] \exp\left[- (\ln \omega - \ln \Omega_m)^2/(2S_{\Omega}^2)\right] \tag{3.3.4}$$

If we define:-

$$X = 10 \log_{10} \Omega = 10\, M \ln \Omega \tag{3.3.5}$$

$$(M \equiv \log_{10} e)$$

then its density function will be (Papoulis, 1965):-

$$P_X(x) = (1/\sqrt{2\pi}) \left[1/(S_{\Omega}\, 10\, M)\right] \exp\left[- (x - 10\, M \ln \Omega_m)^2/(\sqrt{2}\, S_{\Omega}\, 10\, M)^2\right] \tag{3.3.6}$$

This is a normal variable with parameters:-

$$\left.\begin{aligned} \langle X\rangle &= 10\, M \ln \Omega_m \\ \sigma_X &= 10\, M\, S_{\Omega} \end{aligned}\right\} \tag{3.3.7}$$

The main point of this chapter is to find the statistics of the cross-polarization isolation (XPI) or discrimination (XPD) of the received signal after propagation through rain, which is defined as:-

$$Y = 20 \log_{10} |C_R^H| \tag{3.3.8}$$

where C_R^H is now the long-term complex polarization factor. From Papoulis (1965), we have that:-

$$P_Y(y) = \int_{-\infty}^{\infty} P_{YX}(y, x)\, dx \tag{3.3.9}$$

The function $P_{YX}(y, x)$ is the joint probability density function of the two variables Y and X and:-

$$P_{YX}(y, x) = P_Y(y|X = x)\, P_X(x) \tag{3.3.10}$$

where $P_Y(y|X = x)$ is the probability density function of the variable Y under the condition that the variable X has the value x. Hence:-

$$P_Y(y) = \int_{-\infty}^{\infty} P_Y(y|X = x)\, P_X(x)\, dx \tag{3.3.11}$$

The relation (3.3.11) is the theorem of "total probability". The $P_Y(y|X = x)$ is the short-term distribution of the random variable Y or equivalently the distribution at a constant rainfall rate R. At this point, the following fundamental theorem for the evaluation of the statistics of $Y = g(Z)$ in terms of the statistics of Z can be used (Papoulis, 1965).

If $z_1, z_2, z_3 \ldots z_n$ are all the real roots of the equation:-

$$y = g(z) \tag{3.3.12}$$

for a given y, then the density probability function $P_Y(y)$ can be expressed as:-

$$P_Y(y) = \frac{P_Z(z_1)}{|g'(z_1)|} + \ldots\ldots + \frac{P_Z(z_n)}{|g'(z_n)|} \tag{3.3.13}$$

where:-

$$g'(z) = \frac{dg(z)}{dz} \tag{3.3.14}$$

In our case, we have the following relation:-

$$Y = 20 \log_{10} |C_R^H| \tag{3.3.15}$$

and because we are referring to a constant rainfall rate, the random variable $|C_R^H|$ has a Rayleigh distribution with mean square value Ω given by Equation (3.2.23). Hence:-

$$P_Y(y|X = x) = (2/M') \exp\left\{\left[2(y - x)/M'\right] - \exp\left[2(y - x)/M'\right]\right\} \tag{3.3.16}$$

where:-

$$\left.\begin{aligned} M' &= 20\ M \\ x &= 10 \log \Omega \end{aligned}\right\} \tag{3.3.17}$$

The integral (3.3.11) can now be evaluated using Equations (3.3.6) and (3.3.16) as:-

$$P_Y(y) = \int_{-\infty}^{\infty} (2/M') \exp\left\{\left[2(y - x)/M'\right] - \exp\left[2(y - x)/M'\right]\right\} \cdot$$

$$\cdot \left[1/(\sqrt{2\pi}\ \sigma_X)\right] \exp\left[- (x - \langle X\rangle)^2/(2\sigma_X^2)\right] dx \tag{3.3.18}$$

If we now put:-

$$\omega_1 = 2(y - x)/M' \qquad (3.3.19)$$

then the integral becomes:-

$$I_1 = P_Y(y) = 1/(\sqrt{2\pi}\ \sigma_X)\ \exp\left\{-\left[1/(2\sigma_X^2)\right]\ (y - \langle X\rangle)^2\right\}$$

$$\int_{-\infty}^{\infty} \exp\left[-M^2\ \omega_1^2/(8\sigma_X^2)\right]\ \exp\left\{\omega_1 - e^{\omega_1} + \left[M'(y - \langle X\rangle)/(2\sigma_X^2)\right]\ \omega_1\right\}\ d\omega_1 \qquad (3.3.20)$$

With the new substitution:-

$$\omega_2 = M'\ \omega_1/(2\sqrt{2}\ \sigma_X) \qquad (3.3.21)$$

after an algebraic manipulation, we have:-

$$I_1 = \left[2/(\sqrt{\pi}\ M')\right]\ \exp\left\{-\left[1/(2\sigma_X^2)\right]\ (y - \langle X\rangle)^2\right\} \int_{-\infty}^{\infty} \exp\ (-\ \omega_2^2)$$

$$\exp\left\{\left[(2\sqrt{2}\ \sigma_X/M') + \left[\sqrt{2}\ (y - \langle X\rangle)/\sigma_X\right]\right]\ \omega_2 - \exp\left[2\sqrt{2}\ \sigma_X\ \omega_2/M\right]\right\}\ d\omega_2 \qquad (3.3.22)$$

This integral can be evaluated numerically by using Gauss-Hermite quadratures, as explained analytically in the following Section 3.4 of numerical analysis and results. It can be shown that it tends to follow a normal form more and more closely with increasing fluctuations in X. Nakagami (1960) has also been concerned with the calculation of the integral (3.3.18) and has established some approximate analytic formulae for the distribution of the variable Y. He also claims that with a root variance fluctuation of X greater than 7 db ($\sigma_X \geq 7$ db) then the distribution of Y may be taken as a normal. We believe that this limit for σ_X should be lower, based on the numerical integration of the distribution. A comparison of the two methods is given in Appendix B.

Equation (3.3.18) is the probability density function of cross-polarization isolation or discrimination during rain. The probability that cross-polarization isolation or discrimination exceeds a specified level y (in db) is given by:-

$$P\left[Y \geq y\right] = P_0(0) \int_y^{\infty} P_Y(y)\, dy \qquad (3.3.23)$$

3.3.2 Incident Linear 45° Polarization

The long-term statistics for the cross-polarization isolation or discrimination for incident linear 45° polarization can be predicted as follows. Defining:-

$$Y' = 20 \log_{10} |C_R^+| \qquad (3.3.24)$$

$$X' = 10 \log_{10} \Omega' \qquad (3.3.25)$$

where C_R^+ is now the long-term complex polarization factor, and the X'-variable is normal with parameters:-

$$\left.\begin{aligned} \langle X' \rangle &= 10\, M \ln \Omega'_m \\ \sigma_{X'} &= 10\, M\, S_{\Omega'} \end{aligned}\right\} \qquad (3.3.26)$$

where:-

$$\left.\begin{aligned} \Omega'_m &= A' R_m^{B'} \\ S_{\Omega'} &= B' S_R \end{aligned}\right\} \qquad (3.3.27)$$

and the constants A′ and B′ are given by formula (3.2.34).

The long-term distribution of the Y′-variable is again given by the theorem of total probability as:-

$$P_{Y'}(y') = \int_{-\infty}^{\infty} P_{Y'}(y'|X' = x')\ P_{X'}(x')\ dx' =$$

$$= \int_{-\infty}^{\infty} (2/M')\ \exp\left\{\left[2(y' - x')/M'\right] - \exp\left[2(y' - x')/M'\right]\right\}$$

$$\left[1/(\sqrt{2\pi}\ \sigma_{X'})\right]\ \exp\left[-\ (x' - \langle X'\rangle)^2/(2\sigma^2_{X'})\right]\ dx' \qquad (3.3.28)$$

Numerical integration of Equation (3.3.28) reveals to us that the density $P_{Y'}(y')$ is an approximately normal one. The tendency to the normal form depends entirely upon the value of the standard deviation $\sigma_{X'}$ (Section 3.5).

The probability that cross-polarization isolation or discrimination will exceed a specified level y′ (in db) will again be:-

$$P\left[Y' \geq y'\right] = P_o(0) \int_{y'}^{\infty} P_{Y'}(y')\ dy' \qquad (3.3.29)$$

3.3.3 Procedure for Calculating the Rain Cross-Polarization Isolation or Discrimination Distribution

A numerical method is developed in this chapter to calculate the cross-polarization isolation or discrimination distribution for a microwave link at each frequency (from 10 to 100 GHz) length, type of polarization and location. Note that the uniform rain condition restricts the method to short radio paths, less than 4 km. The following steps must be followed:-

(a) Evaluation of the parameters c and d for expression (2.5.21) by a regression analysis, at each frequency. These coefficients for Pruppacher-Pitter form raindrops having a Laws-Parsons drop-size distribution, have been tabulated for four frequencies and are presented in Table 2.3. A method of interpolation, as will be explained analytically in the following Section 3.4, will be used for the evaluation of parameters c and d for an intermediate frequency.

(b) Estimation of the log-normal parameters $P_o(0)$, R_m, S_R of the point rainrate distribution by a least squares approximation, or alternatively, using the Weather Bureau long term precipitation data, by application of the theory of extreme value statistics (Section 2.3.2).

(c) The parameters of the X or X′ distribution are evaluated by using formula (3.3.7) or (3.3.26).

(d) Evaluation of the density distribution function for Y or Y′ by performing the numerical integration (3.3.18) or (3.3.28) and finally estimation of the probabilities (3.3.23) or (3.3.29).

3.4 Numerical Analysis and Results

All the numerical techniques which are used for the evaluation of the rain cross-polarization discrimination or isolation distribution are described here. More analytically a method of interpolation, to find the parameters c and d at each frequency is analysed first, and then the Gauss-Hermite quadrature formula for the calculation of integrals of the same type as those in expressions (3.3.22) and (3.3.28). Finally, a brief presentation of the Chebyshev expansion method for the approximation of some special functions such as the complement of the cumulative normal distribution function and the error function complement, is given. These functions are used for the evaluation of the excess probabilities of cross-polarization discrimination or isolation and rainfall rate.

Numerical results for the two types of linear polarization at 34.8 GHz are presented in Figs. 3.4 - 3.15*. The rain parameters (R_m, S_R, $P_o(0)$) are taken from Lin (1975) and are suitable for a location in New Jersey (Figs. 3.3 - 3.8) and Southern England (Figs. 3.9 - 3.14). In Figs. 3.3, 3.4 and 3.9, 3.10, the active density function for the cross-polarization discrimination or isolation during rain and the best fitting approximate normal are shown for comparison. The excess probabilities for the rain cross-polarization isolation or discrimination at 34.8 GHz are also presented in Figs. 3.5 and 3.11. The differences between the two types of linear polarization are also shown and similarly the fact that the worst case for the XPD or XPI is the $\pi/4$ incident linear polarization which is similar to circular polarization (Bostian, 1973).

* These results are given in Sections 3.4.4 and 3.4.5.

An important application for radio designers is the estimation of radio outage time due to co-channel interference which is defined as the annual average time in which the radio system operates with a value of cross-polarization isolation greater than a specified level. In present 4 and 6 GHz radio relay systems, the minimum acceptable level is - 20 db. Future systems with increased numbers of circuits per channel will require less than - 30 db XPI. An increase in XPI levels results in increased crosstalk and noise levels and reduces the number of circuits per channel. Also, an increase in repeater station spacing will increase XPI levels. Hence, a trade-off exists between repeater station spacing and expected XPI levels and the optimal cost per circuit km must be chosen. Figs. 3.6, 3.7, 3.8 and 3.12, 3.13, 3.14 show the annual outage time per hop as a function of repeater spacing for a system operating at 34.8 GHz.

3.4.1 Analysis of Interpolation Technique

Given a set of function values $f(X_0)$, $f(X_1)$, ..., $f(X_n)$ the section is concerned with the estimation of $f(X)$ for some value X. When f is a function of one variable only (X_i scalar) and $X_0 < X_1 < \ldots\ldots < X_n$ the problem is one of interpolation if $X \varepsilon (X_0, X_n)$ and extrapolation if $X \notin (X_0, X_n)$. In general interpolation is more accurate than extrapolation. Indeed, it is desirable to have an equal amount of information about f either side of X. One basic idea employed in this section for the solution of this problem is to find a polynomial of degree n which takes the values $f(X_0)$, $f(X_1)$, ..., $f(X_n)$. This polynomial, the Lagrange interpolating polynomial is unique. By evaluation the polynomial at X an approximate value of f(X) may be obtained. There are many different ways of calculating the Lagrange interpolating polynomial evaluated at X. The two main methods are Aitken's successive linear approximation and

Everett's formula (Fröberg, C. E., 1965). This latter technique assumes that the X_i are equally spaced, with $X\varepsilon(X_{m-1}, X_m)$ or (X_m, X_{m+1}) where X_m is either the mid-point of the range, $\frac{1}{2}(X_o + X_n)$, if n is even, or one of the two tabular points either side if n is odd. Another idea is to pass piecewise cubic polynomials (cubic splines) through known data points. The first derivatives of the cubics are continuous at the matching points. The splines are then evaluated at the appropriate point to obtain an approximation to f(X). When f is a function of two variables the cubic spline technique is adopted.

In our case, the parameters c and d are given for four frequencies (Table 3.1). Aitken's method is adopted, and the subroutine EØ1AAF from the NAG (National Algorithmic Group) Library has been used. This routine interpolates at a given point X from a table of values X_i and Y_i (i = 1, 2, ..., N + 1) using Aitken's method. The intermediate values of linear interpolation are stored to enable an estimate of the accuracy of the result to be made. A full description of this routine can be found in Appendix F.

3.4.2 Analysis of Gauss-Hermite Quadrature Formula

This procedure estimates the value of an integral of the form:-

$$I_1 = \int_{-\infty}^{\infty} \exp(-X^2)\, f(X)\, dX \tag{3.4.1}$$

The integral is approximated by the formula:-

$$I_1 \cong \sum_{k=1}^{n} A_k f(X_k) \tag{3.4.2}$$

where A_k are the weights and X_k the pivots. The pivots are the zeros of the Hermite polynomials. This quadrature formula is exact if the function f(X) is a polynomial of degree not exceeding 2n - 1, where n is the number of pivots used. In the estimation of our integral, we use 48 points. The name of the subroutine which is taken from the NAG Library is DØ1AFF.

3.4.3 Analysis of Special Functions

The routines in this section have all been based on truncated Chebyshev expansions. This method of approximation was adopted as a compromise between the conflicting requirements of efficiency and ease of implementation on the many different machine ranges that are involved in the NAG Library project. For details of the reasons behind this choice and the production and testing procedures followed in constructing this section see (Schonfelder, 1976).

Basically, if the function to be approximated is f(X), then for $X\varepsilon(a, b)$ an approximation of the form:-

$$f(X) = g(X) \sum_{r=0} C_r T_r (t) \qquad (3.4.3)$$

is used, where g(X) is some suitable function which extracts any singularities, asymptotes and, if possible, zeros of the function in the range in question and t = t(X) is a mapping of the general range (a, b) to the specific range (- 1, + 1) required by the Chebyshev polynomials, T_r (t). For a detailed description of the properties of the Chebyshev polynomials see (Clenshaw, 1962; Fox and Parker, 1968).

The essential property of these polynomials for the purposes of function approximation is that $T_n(t)$ oscillates between ± 1 and it takes its extreme values n + 1 times in the interval (- 1, + 1).

Therefore, provided the coefficients C_r decrease in magnitude sufficiently rapidly the error made by truncating the Chebyshev expansion after N terms is approximately given by:-

$$E(t) \simeq C_N \; T_N(t) \qquad (3.4.4)$$

That is the error oscillates between $\pm$ C_N and takes its extreme values N + 1 times in the interval in question. Now this is just the condition that the approximation be a minimax representation, one which minimises the maximum error. By suitable choice of the interval (a, b), the auxiliary function, g(X), and the mapping of the independent variable, t(X), it is almost always possible to obtain a Chebyshev expansion with rapid convergence and hence truncations that provide near minimax polynomial approximations to the required function. The difference between the true minimax polynomial and the truncated Chebyshev expansion is seldom sufficiently great to be of significance.

The routine S15ADF is called from NAG Library and calculates an approximate value for the complement of the error function:-

$$\text{erfc }(X) = \frac{2}{\sqrt{\pi}} \int_X^{\infty} e^{-u^2} \, du = 1 - \text{erf}(X) \qquad (3.4.5)$$

For $X \geq 0$, it is based on the Chebyshev expansion:-

$$\text{erfc }(X) = e^{-X^2} \, . \, y(X) \qquad (3.4.6)$$

where:-

$$y(X) = \sum_{r=0} a_r \; T_r(t) \qquad (3.4.7)$$

and:-

$$t = (X - 3.75)/(X + 3.75) \quad , \quad -1 \leq + \leq +1 \tag{3.4.8}$$

For $X \geq X_{hi}$, where there is a danger of setting underflow, the result is returned as zero.

For $X < 0$:-

$$\mathrm{erfc}(X) = 2 - e^{-X^2}\, y(|X|) \tag{3.4.9}$$

For $X < X_{low} < 0$, the result is returned as 2 which is correct to within the rounding errors of the machine. The values of X_{hi} and X_{low} are given in the appropriate machine implementation document.

The routine S15ACF is called from the NAG Library and calculates an approximate value for the complement of the cumulative normal distribution function:-

$$\underset{\sim}{Q}\,(X) = \frac{1}{\sqrt{2\pi}} \int_X^{\infty} e^{-u^2/2}\, du \tag{3.4.10}$$

This routine is based on the fact that (Abramovitz and Stegun, 1965):-

$$\underset{\sim}{Q}\,(X) = \frac{1}{2}\,\mathrm{erfc}\,(X/\sqrt{2}) \tag{3.4.11}$$

and it calls the NAG routine S15ADF to obtain the necessary value of erfc, the complementary error function.

3.4.4 Numerical Results for the USA

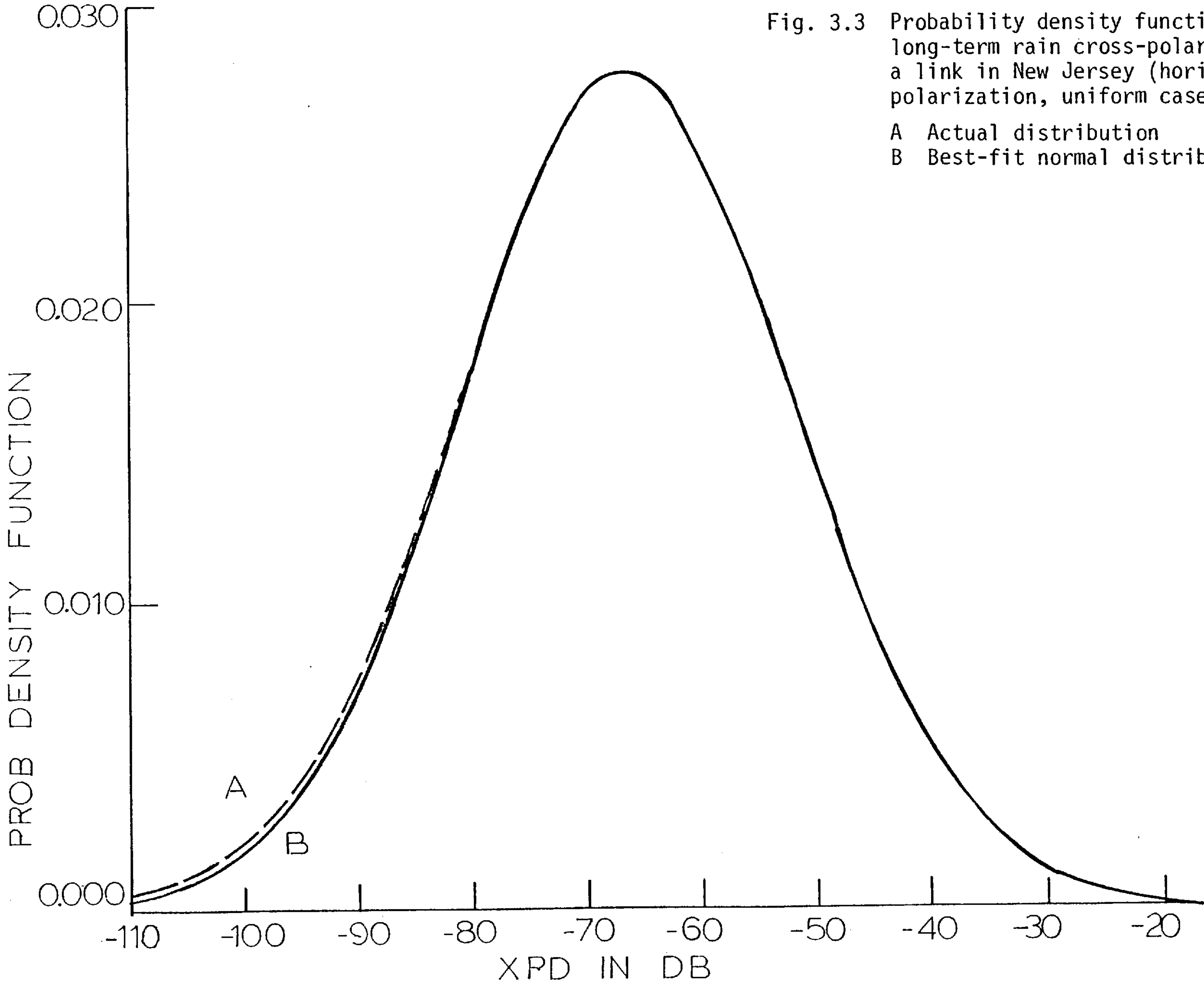

Fig. 3.3 Probability density function of the long-term rain cross-polarization for a link in New Jersey (horizontal polarization, uniform case)

A Actual distribution
B Best-fit normal distribution

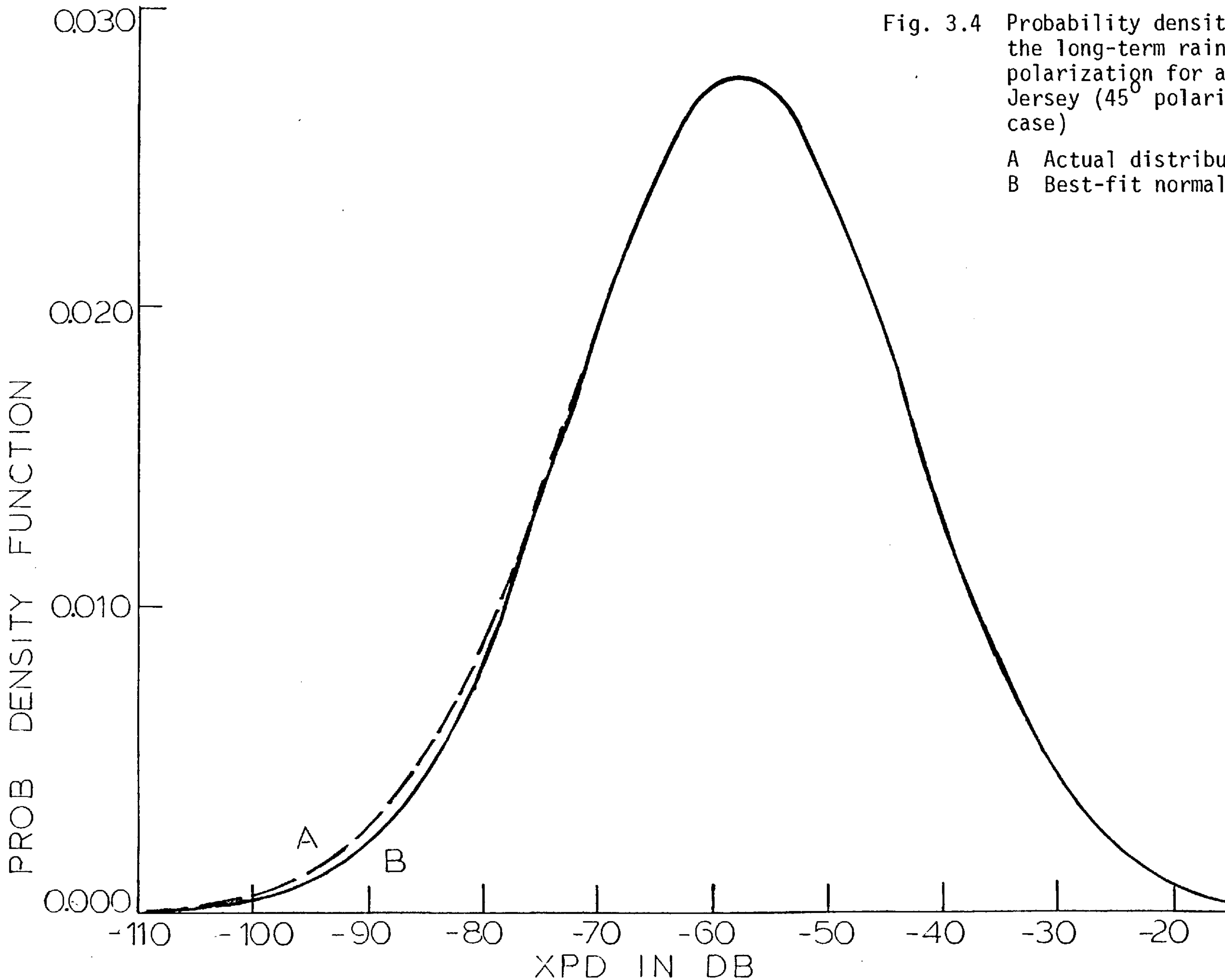

Fig. 3.4 Probability density function of the long-term rain cross-polarization for a link in New Jersey (45^{0} polarization, uniform case)

A Actual distribution
B Best-fit normal distribution

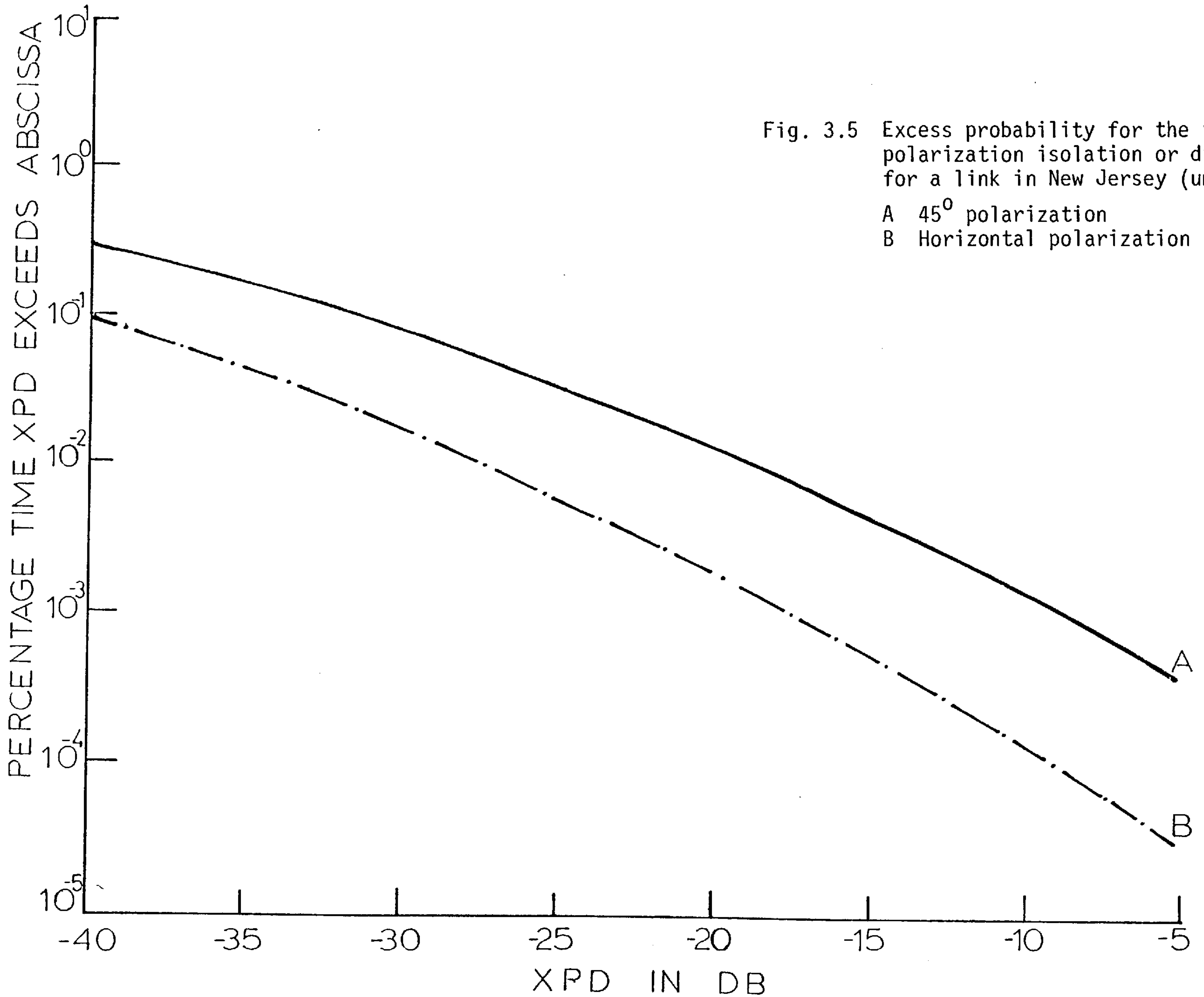

Fig. 3.5 Excess probability for the rain cross-polarization isolation or discrimination for a link in New Jersey (uniform case)

A 45^{0} polarization
B Horizontal polarization

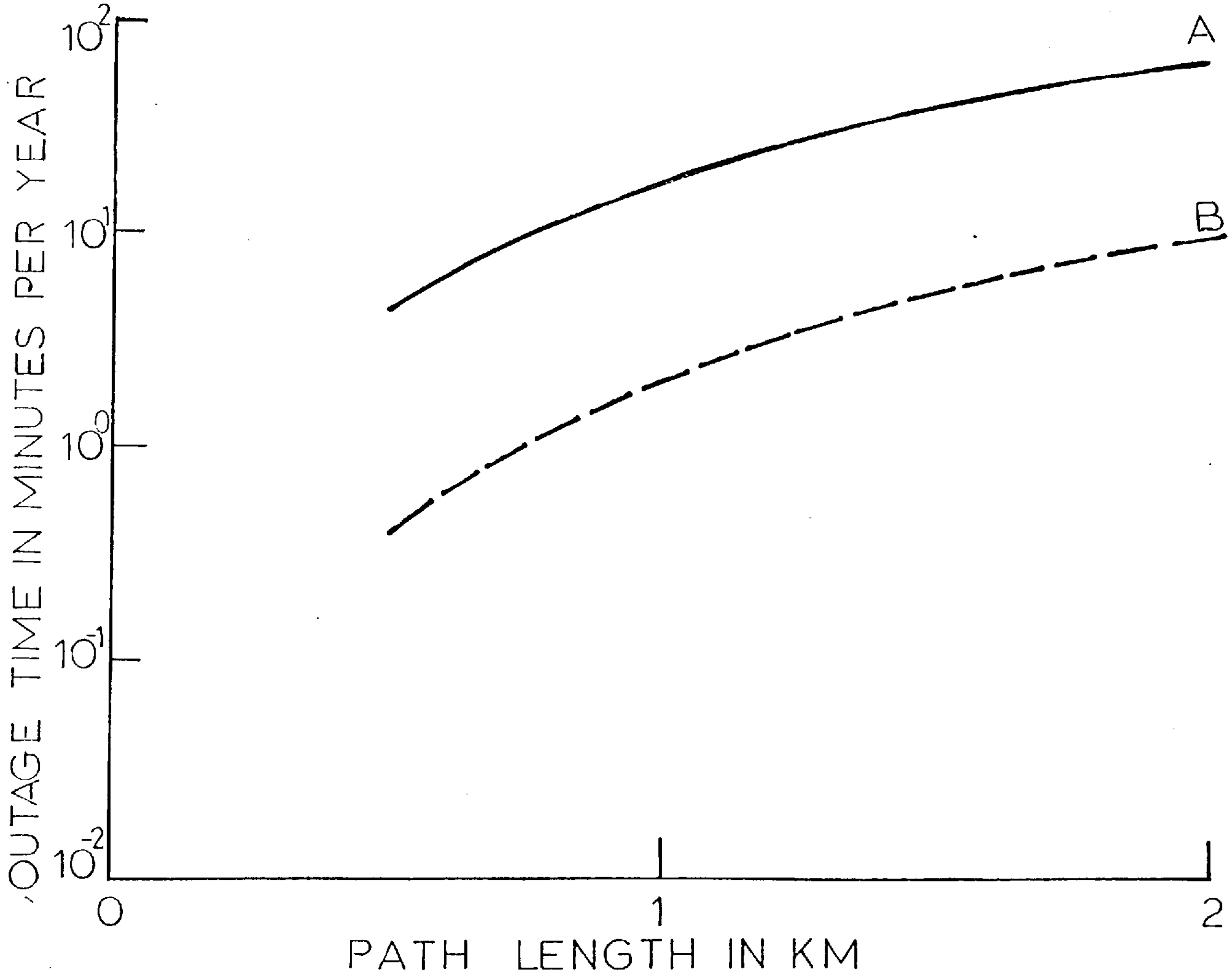

Fig. 3.6 Annual outage time due to channel interference for a communication link in New Jersey as a function of path length (minimum acceptable XPI threshold: - 20 db, uniform case)

A 45^{o} polarization
B Horizontal polarization

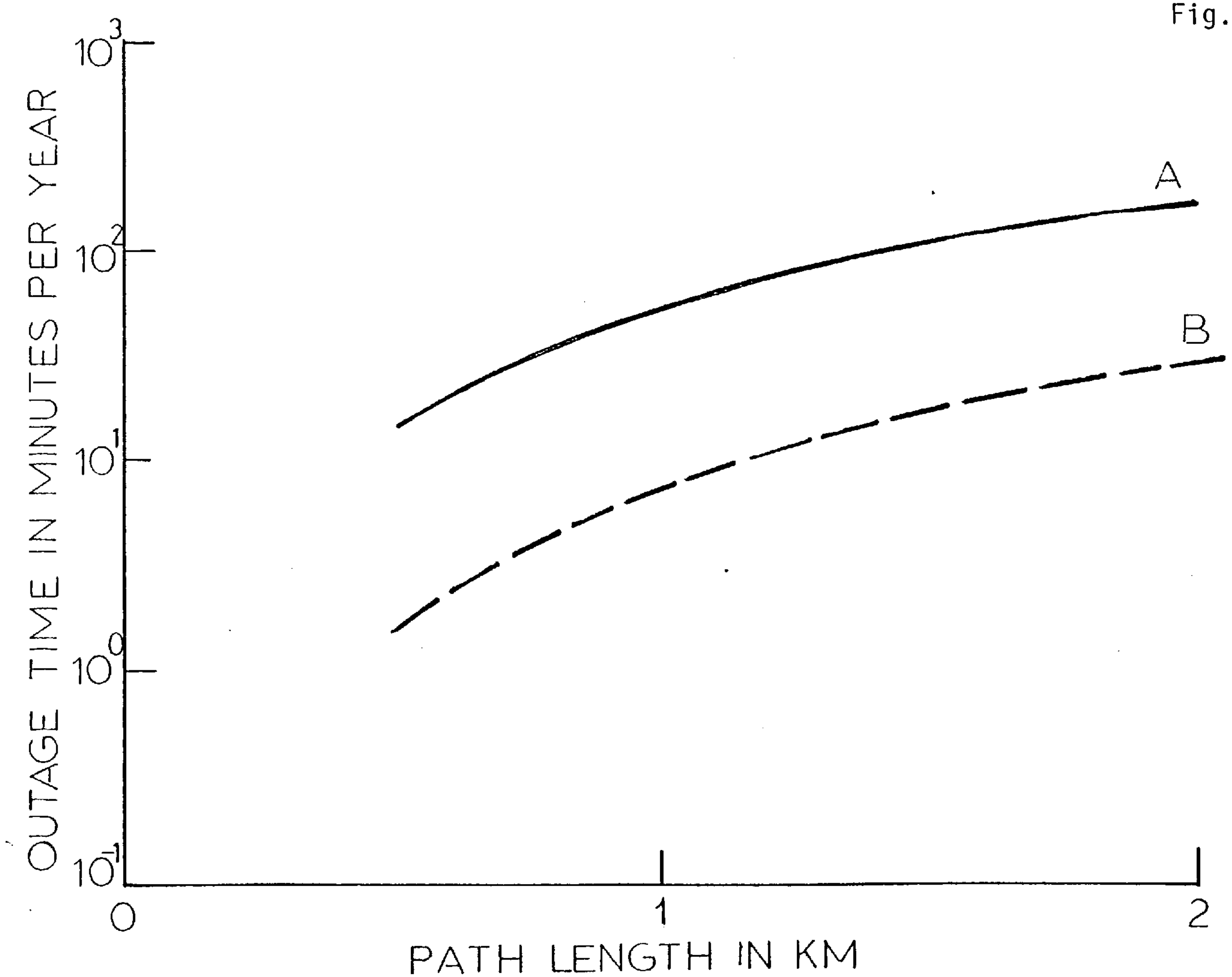

Fig. 3.7 Annual outage time due to channel interference for a communication link in New Jersey as a function of path length (minimum acceptable XPI threshold: - 25 db, uniform case)

A 45^o polarization
B Horizontal polarization

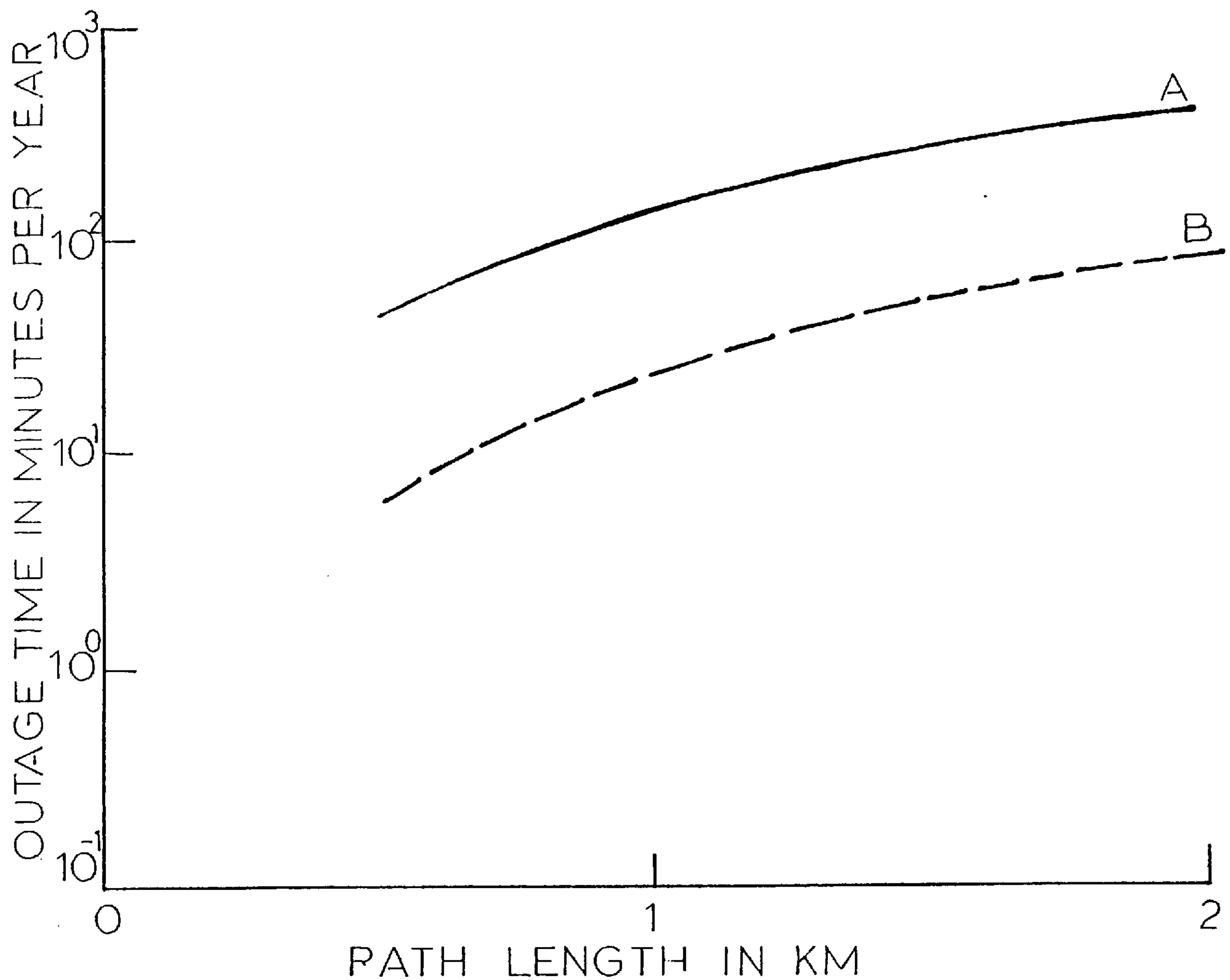

Fig. 3.8 Annual outage time due to channel interference for a communication link in New Jersey as a function of path length (minimum acceptable XPI threshold: - 30 db, uniform case)

A 45^o polarization
B Horizontal polarization

3.4.5 Numerical Results for Southern England

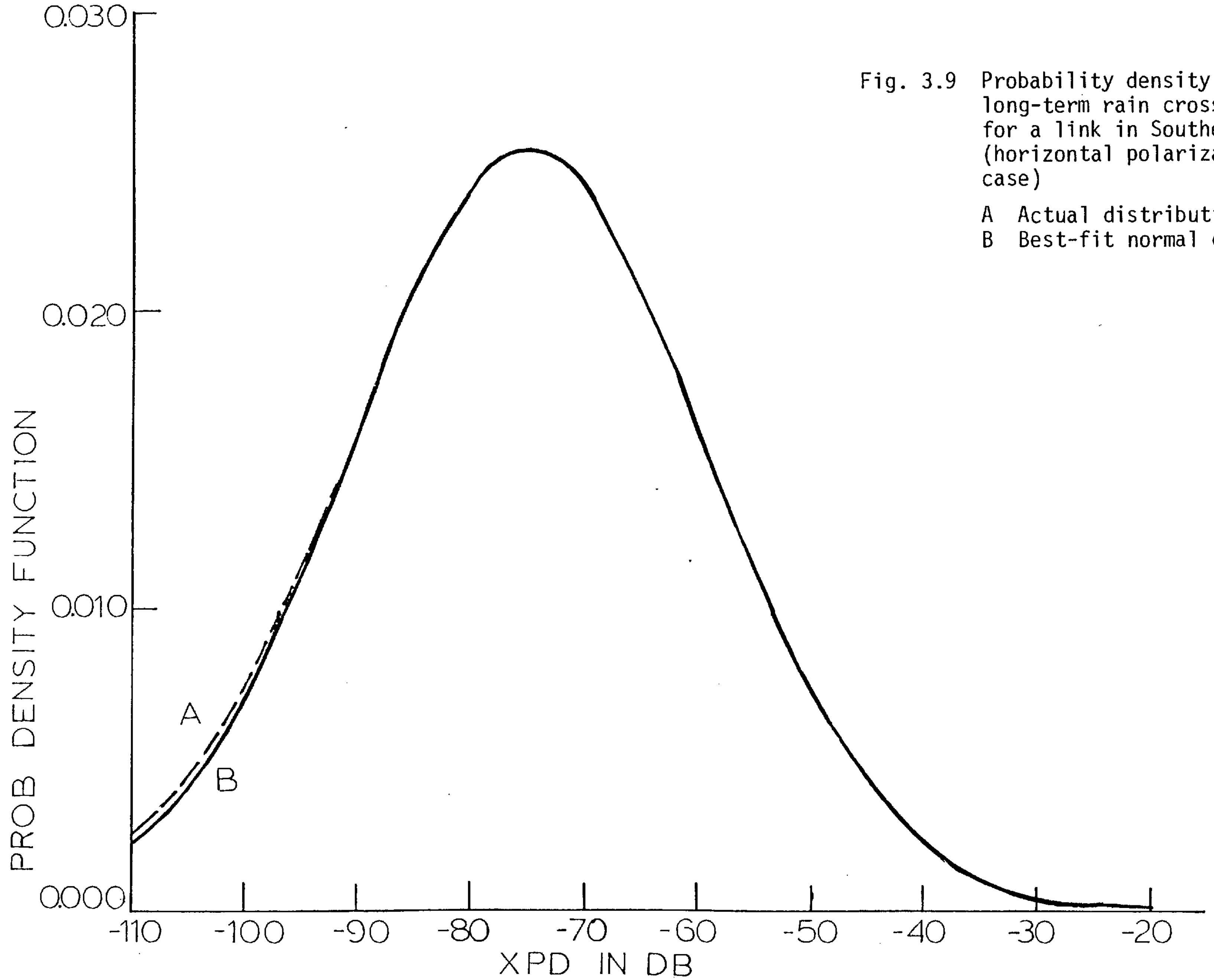

Fig. 3.9 Probability density function of the long-term rain cross-polarization for a link in Southern England (horizontal polarization, uniform case)

A Actual distribution
B Best-fit normal distribution

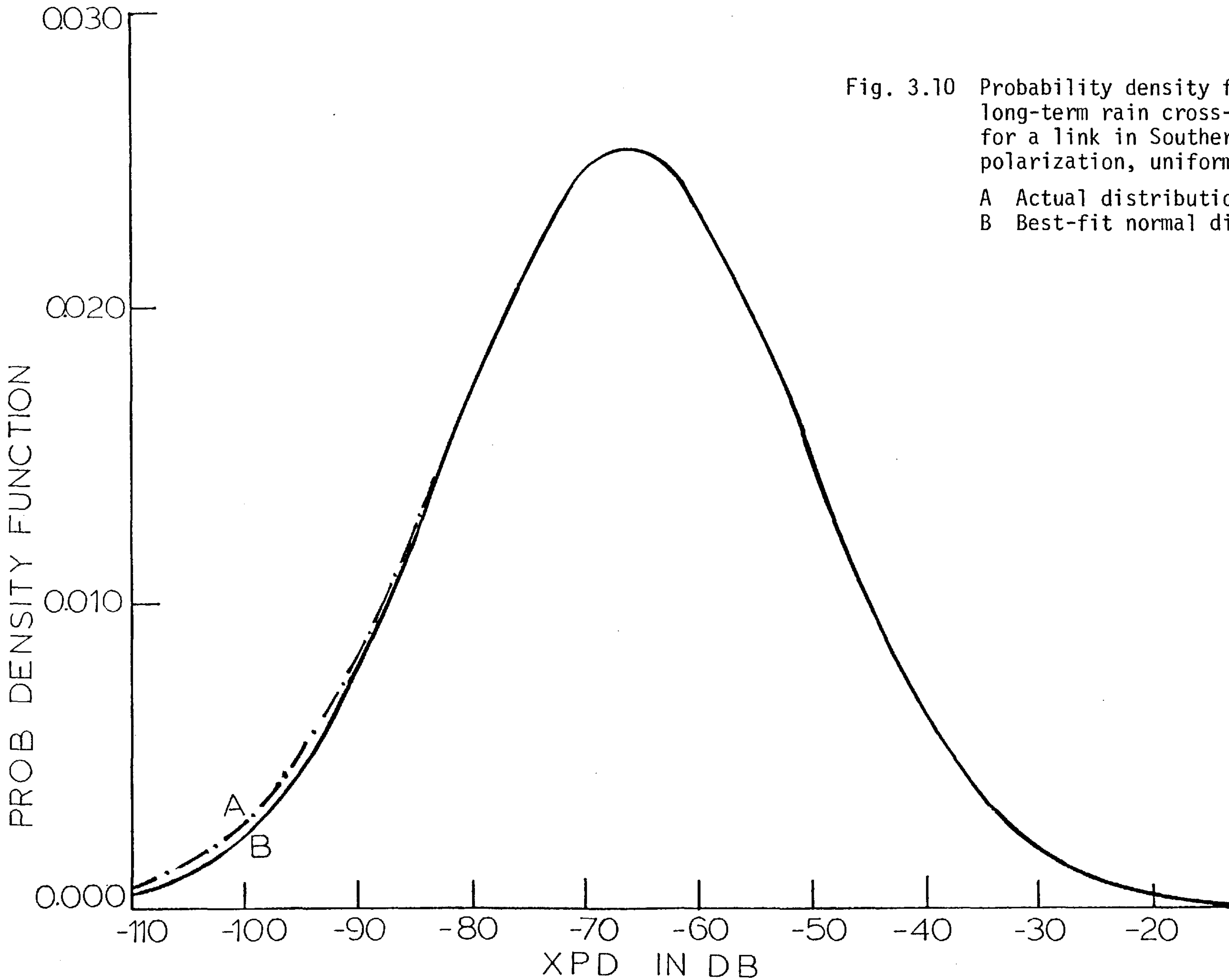

Fig. 3.10 Probability density function of the long-term rain cross-polarization for a link in Southern England (45^{o} polarization, uniform case)

A Actual distribution
B Best-fit normal distribution

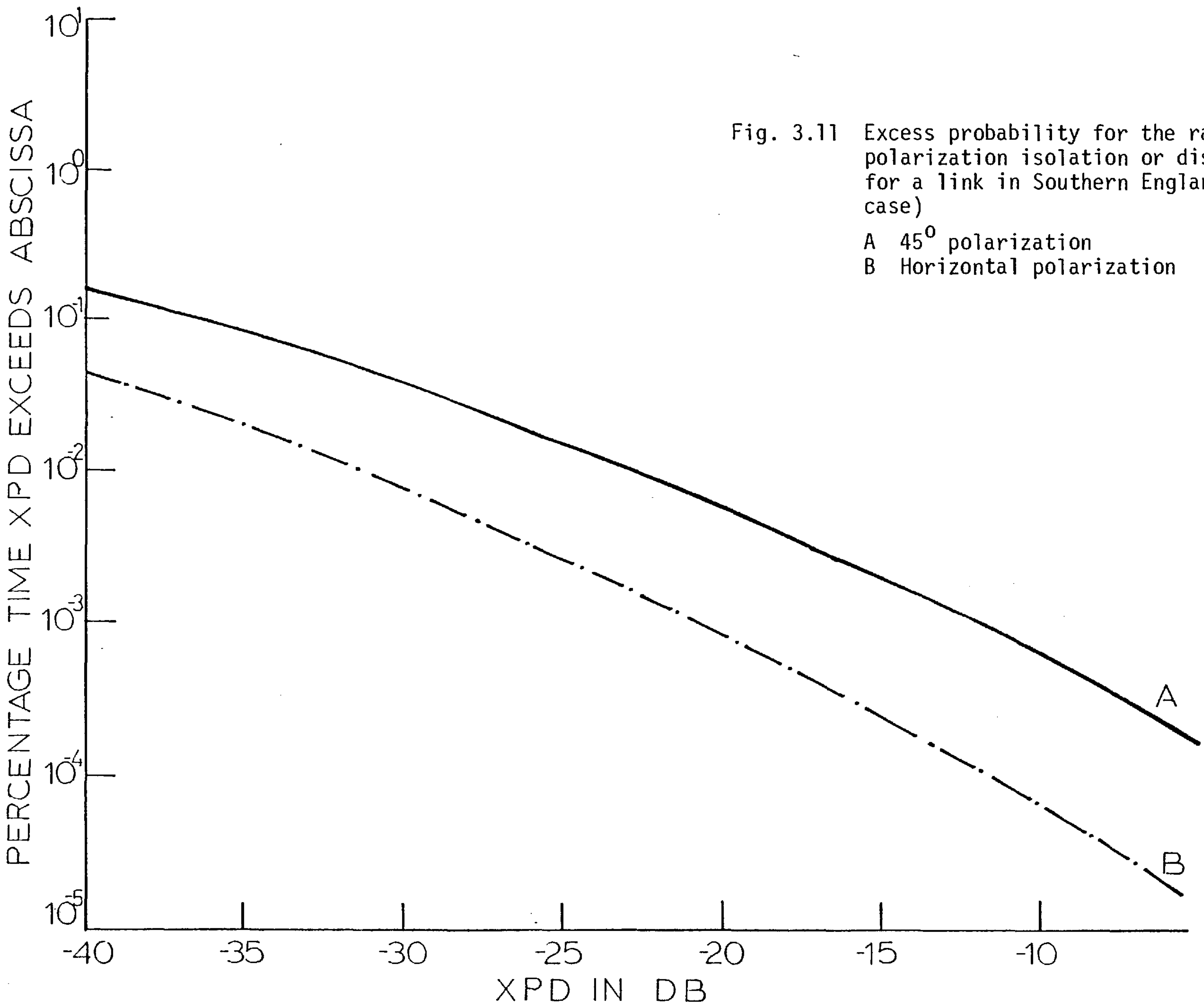

Fig. 3.11 Excess probability for the rain cross-polarization isolation or discrimination for a link in Southern England (uniform case)

A 45^{o} polarization
B Horizontal polarization

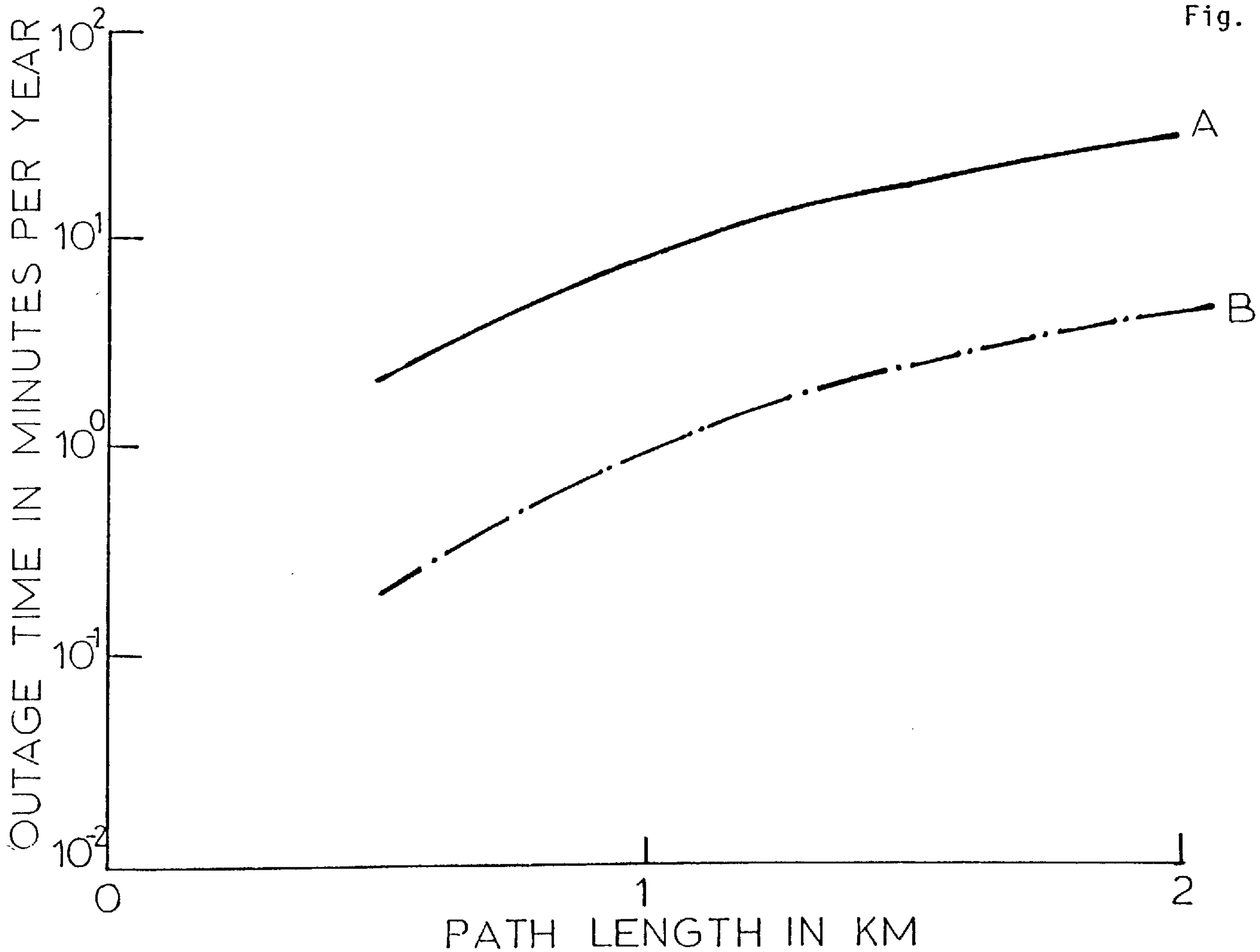

Fig. 3.12 Annual outage time due to channel interference for a communication link in Southern England as a function of path length (minimum acceptable XPI threshold: - 20 db, uniform case)

A 45^{0} polarization
B Horizontal polarization

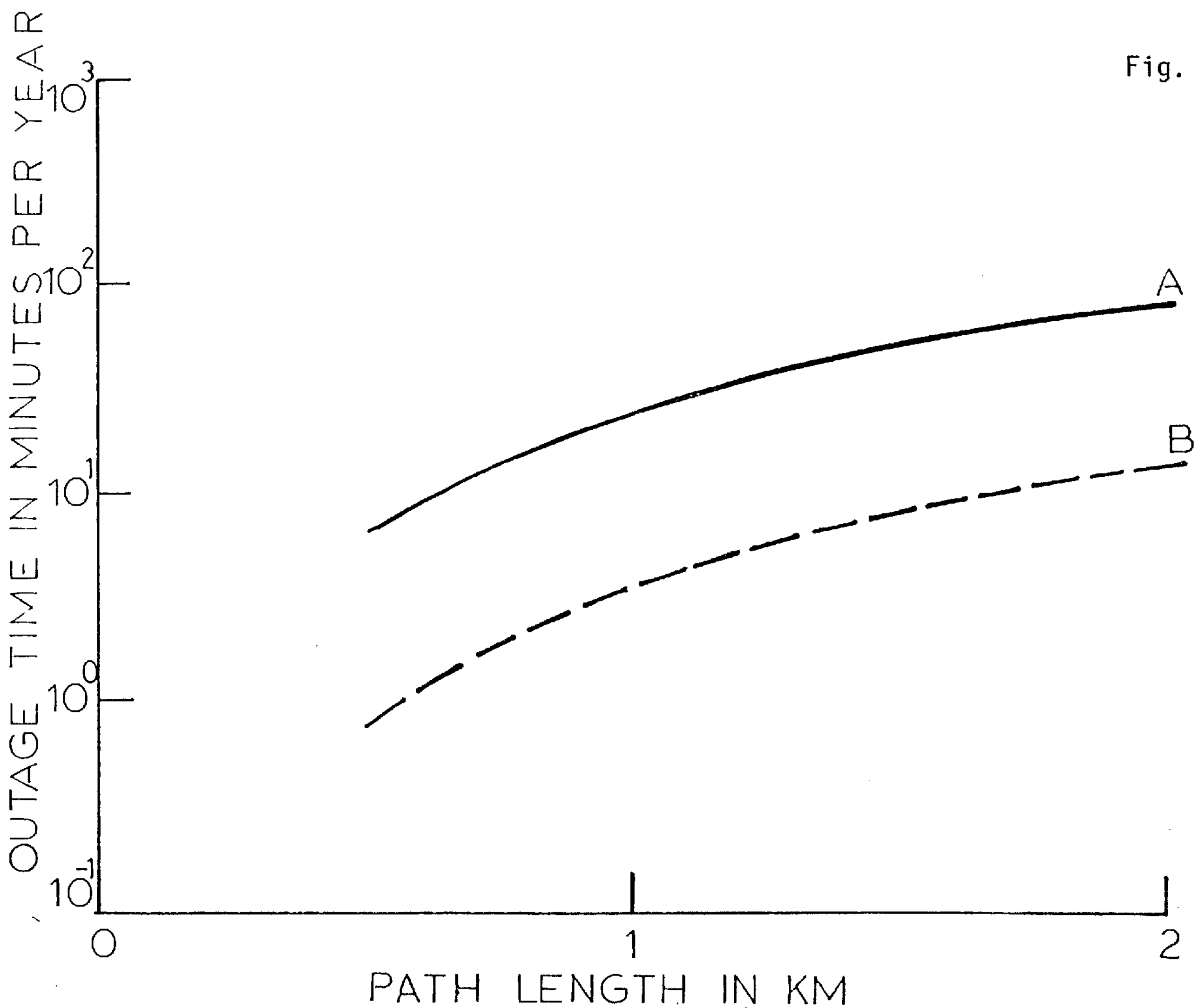

Fig. 3.13 Annual outage time due to channel interference for a communication link in Southern England as a function of path length (minimum acceptable XPI threshold: - 25 db, uniform case)

A 45^{o} polarization
B Horizontal polarization

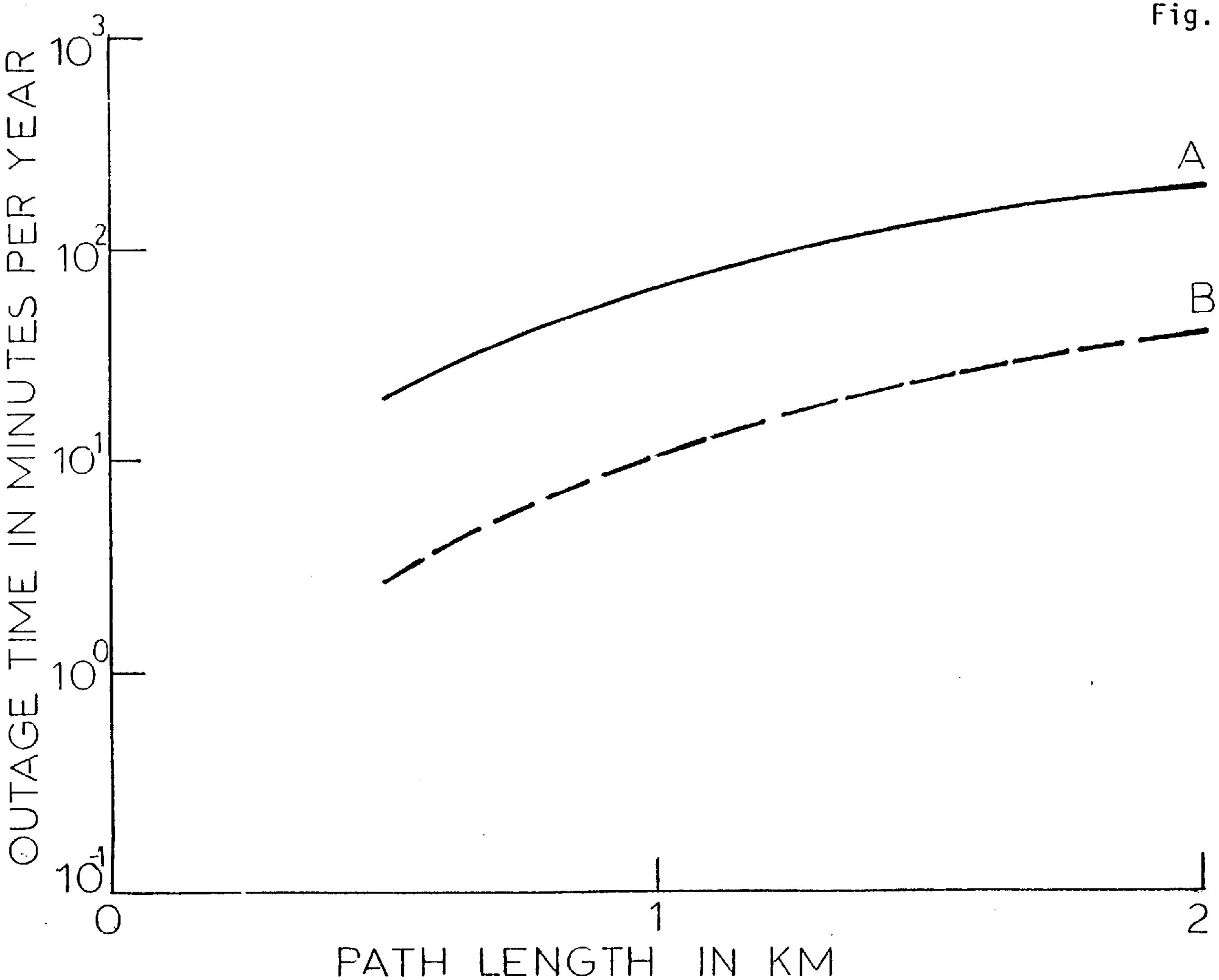

Fig. 3.14 Annual outage time for a communication link in Southern England as a function of path length (minimum acceptable XPI threshold: - 30 db, uniform case)

A 45^o polarization
B Horizontal polarization

3.4.6 Comparison with Experimental Results from Martlesham Heath (Ipswich)

In order to compare the predictions with experimental results, propagation data have been used from a 22 GHz, 4 km link at Martlesham Heath (Ipswich), operated jointly by the Post Office Research Department and the Appleton Laboratory. This communication system has been described elsewhere (Turner and Tattersall, 1977). Generally, the propagation data taken from this link are classified into four categories depending on which effect was dominant in the medium (rain, multipath, snow and fog), and are tabulated into attenuation and cross-polarization data. Four channels (two in the receiver station and the other two in the transmitter) have been used, in order to have results for the horizontal/vertical attenuation and horizontal/vertical cross-polarization discrimination. More specifically, rain cross-polarization data cover only the period of approximately twelve months (1974) and are given in terms of excess probability for each rain event. For all the rain events of the year ($\cong$ 80), a cumulative probability at each specified level of XPD has been constructed (see Table 3.1). It is worthwhile mentioning that this probability is under the condition that the XPD always exceeds the - 40 db level, where this value is estimated to be the clear-air weather XPD of the system (taking into account antennas imperfection, etc.). In mathematical terms, this distribution is the conditional probability:-

$$P\left[Y \geq y \mid Y \geq -40 \text{ db}\right] = \frac{P\left[Y \geq y\right]}{P\left[Y \geq -40 \text{ db}\right]} \tag{3.4.12}$$

where the two probabilities $P\left[Y \geq y\right]$ and $P\left[Y \geq -40 \text{ db}\right]$ are calculated by means of formula (3.3.29).

The rainrate parameters used in the theoretical prediction model are those which are calculated by a least-squares fitting procedure from an experimental rainrate distribution appropriate for Slough, Southern England (Norbury and White, 1973). Comparison of the theoretical curves with the experimental points reveals that the agreement is fairly good, especially for the model with standard deviation of the canting angle equal to zero (that is the "equi-oriented" one). For all the theoretical curves of Fig. 3.15 a mean value $\theta_m = 10^o$ has been used. A possible reason for the discrepancy of the theoretical and experimental results, particularly in the region of the higher values of XPD (- 20 db and higher), may be the shortness of the period over which the data was taken. The period, which was the year 1974, was also unusually dry. For both these reasons the experimental data are not too reliable, and the comparison, therefore, somewhat inconclusive. The ideal would be to have at least three years of data taken under "normal" conditions.

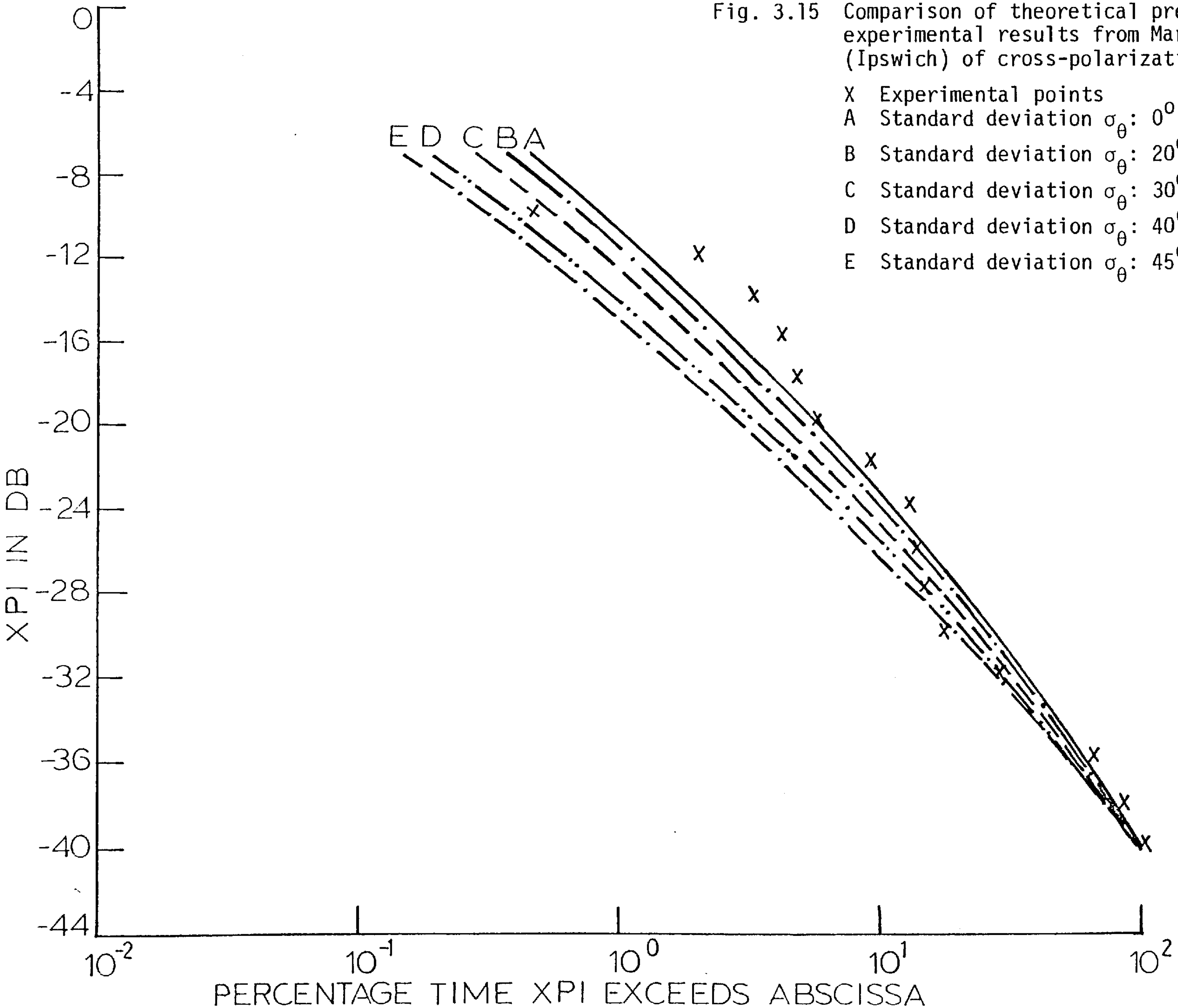

Fig. 3.15 Comparison of theoretical prediction with experimental results from Martlesham Heath (Ipswich) of cross-polarization isolation (XPI)

X Experimental points
A Standard deviation σ_θ: 0^o
B Standard deviation σ_θ: 20^o
C Standard deviation σ_θ: 30^o
D Standard deviation σ_θ: 40^o
E Standard deviation σ_θ: 45^o

TABLE 3.1

EXPERIMENTAL RESULTS FROM MARTLESHAM HEATH (IPSWICH)

REFERENCE LEVEL OF XPD (in db)	% probability that XPD is greater than ordinate value under the condition that XPD is greater than - 40 db
- 2	0
- 4	0
- 6	8.523×10^{-4}
- 8	2.73×10^{-1}
- 10	4.6×10^{-1}
- 12	2
- 14	3
- 16	4
- 18	5
- 20	6
- 22	9
- 24	13
- 26	14
- 28	14
- 30	18
- 32	28
- 34	45
- 36	65
- 38	85
- 40	100

3.4.7 Concluding Remarks

A numerical method for estimating the long-term first order statistics of cross-polarization isolation or discrimination of a signal after propagating through a rain medium has been presented here. The case of uniform rain has been considered and this restricts the method to short radio paths, less than 4 km.

A normal form for the long-term distribution function of XPI or XPD in db has been concluded after assuming a log-normal form for the rainrate statistics. The parameters of this distribution (mean and variance) are functionally related to the parameters of the rainrate statistics and those of the radio link (length, frequency, type of incident polarization).

This conclusion is then applied to the estimation of radio link reliability such as the evaluation of annual radio outage time because of channel interference. Various cross-polarization levels (- 20 db, - 25 db or - 30 db) are considered.

CHAPTER 4

ANALYSIS OF THE LONG-TERM STATISTICS OF RAIN CROSS-POLARIZATION FOR SPATIALLY NON-UNIFORM RAIN

Introduction

In this chapter, the long-term statistics of rain cross-polarization discrimination or isolation for an actual rain medium are considered. Actual rainfalls are usually not uniform over an entire radio path. The observations by a capacitor flow raingauge (Semplak and Turrin, 1969) and by a raindrop photographic method (Mueller and Sims, 1966) indicate that heavy rain has fine scale structure of the order of 1 m. So, we will consider that the rainfall rate is randomly varying over the path as well as in time: in other words, the rainfall rate is a random process in both space and time.

The radio path is again divided into successive incremental slabs in which the approximation of Van de Hulst (1957) for single scattering can be made and also the rainrate can be considered to be approximately uniform. For short-term statistics, the complex polarization factor at the output can be proved to be a Rayleigh phasor. By analogy with Bodtmann and Ruthroff's (1974) analysis for attenuation, we propose that the mean square value of the amplitude of this factor can be expressed in terms of the space-averaged rainfall rate $\overline{R}$, in the form $\Omega = A(\overline{R})^B$.

In order to determine the long-term statistics of cross-polarization discrimination or isolation, the rainfall rates in each slab (R_1, R_2, ...) must be treated as correlated random variables, their individual distributions being log-normal. First, it is shown that $\overline{R}$ is itself log-normal, and the dependence of the mean and standard deviation on the link parameters is derived. (The link parameters include the probabilities of rainfall along that particular path, the median and standard deviation of the point rainfall rate, the spatial correlation coefficient of the rainfall rate between slabs, radio frequency, path length and type of polarization). Then, as noted in the previous chapter, once the statistics of Ω are known, the long-term statistics of the cross-polarization discrimination or isolation are established, and being very closely a log-normal process (variable). Results are given for path lengths up to 4 km, the results being compared with calculations assuming spatially uniform rainfall rates.

4.1 Short-Term Statistics

4.1.1 General Considerations

We will examine in this chapter the case for a horizontally incident polarised wave. The procedure for obtaining the XPD or XPI distribution for a vertical polarization or a 45^{0} one is exactly similar. A configuration of the radio path is shown in Fig. 4.1. The division of the path into successive incremental slabs of width Δz is adopted here within which the rainfall rate (R_j for the j_{th} slab, $j = 1, \ldots. N_s$) is assumed to be uniform. In the short-term, these R_j can be considered as constants. Hence, for the first slab, the components of the incident wave will be:-

$$\left.\begin{aligned} E_o^+ &= 0 \\ E_o^- &= 1 \end{aligned}\right\} \qquad (4.1.1)$$

Then, the output components of the first slab will be:-

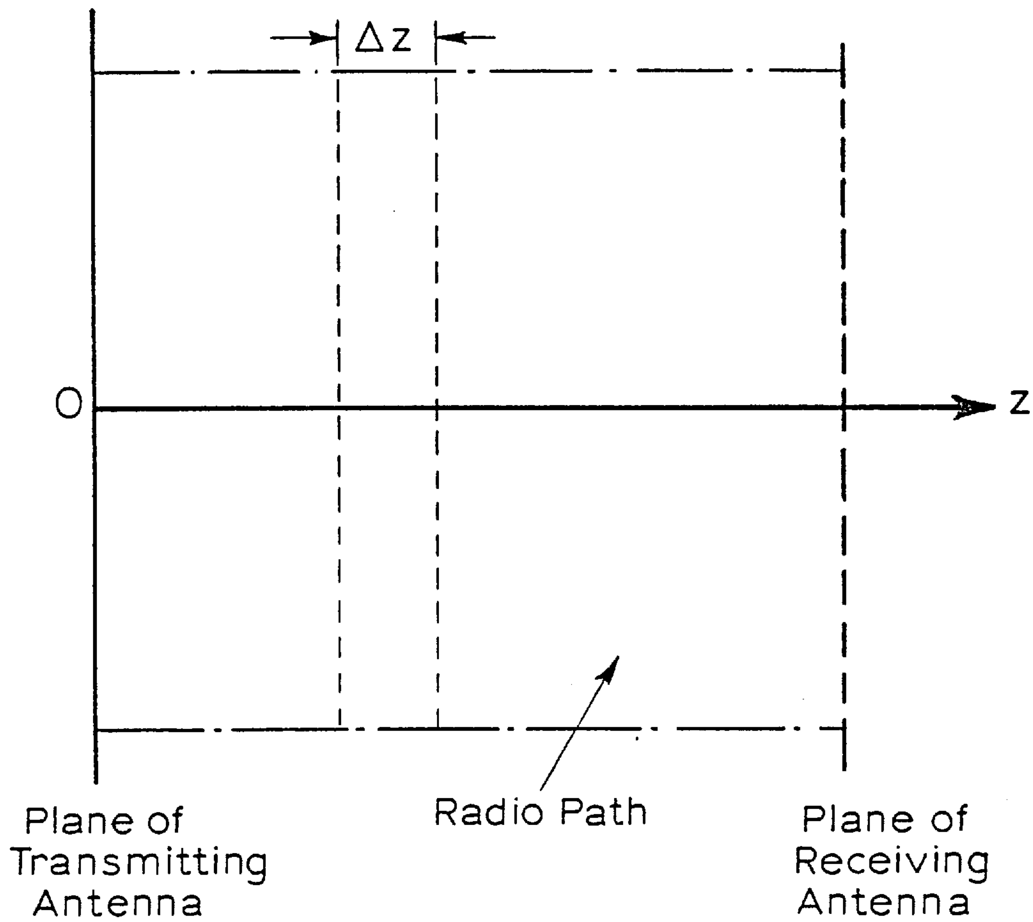

Fig. 4.1 Configuration of the radio path

$$\begin{bmatrix} E_1^+ \\ E_1^- \end{bmatrix} = \begin{bmatrix} \alpha_1^V & \beta_1 \\ \beta_1 & \alpha_1^H \end{bmatrix} \begin{bmatrix} 0 \\ 1 \end{bmatrix} \rightarrow \left.\begin{array}{l} E_1^+ = \beta_1 \\ E_1^- = \alpha_1^H \end{array}\right\} \tag{4.1.2}$$

where:-

$$\left.\begin{array}{l} \alpha_j^V \equiv \Gamma_j^{++} \\ \alpha_j^H \equiv \Gamma_j^{--} \\ \beta_j \equiv \Gamma_j^{+-} \equiv \Gamma_j^{-+} \end{array}\right\} \tag{4.1.3}$$

for the j_{th} slab.

The polarization coefficients Γ_j^{++}, Γ_j^{+-}, Γ_j^{-+}, Γ_j^{--} are defined by Beckmann (1968). The cross-polar coefficients Γ_j^{+-}, Γ_j^{-+} can be found to behave as Rayleigh phasors; on the other hand the amplitudes of the co-polar terms Γ_j^{++}, Γ_j^{--} obey a Rice-Nakagami distribution (Chapter 3). The input components of the second slab will, therefore, be:-

$$\left.\begin{array}{l} E_1^+ = \beta_1 \\ E_1^- = \alpha_1^H \end{array}\right\} \tag{4.1.4}$$

and the output components of the second slab will be:-

$$\begin{bmatrix} E_2^+ \\ E_2^- \end{bmatrix} = \begin{bmatrix} \alpha_2^V & \beta_2 \\ \beta_2 & \alpha_2^H \end{bmatrix} \begin{bmatrix} \beta_1 \\ \alpha_1^H \end{bmatrix} \rightarrow \left.\begin{array}{l} E_2^+ = \alpha_2^V \beta_1 + \beta_2 \alpha_1^H \\ E_2^- = \alpha_1^H \alpha_2^H + \beta_1 \beta_2 \end{array}\right\} \tag{4.1.5}$$

This process can be continued throughout the entire region to yield, finally, the complex cross-polarization factor C_R^H at the output of the

N_{th} slab, viz:-

$$C_R^H \equiv (E_{N_s}^+/E_{N_s}^-) = (\beta_{N_s}/\alpha_{N_s}^H) + (\beta_{N_s-1}/\alpha_{N_s-1}^H)\,(\alpha_{N_s}^V/\alpha_{N_s}^H) + (\beta_{N_s-2}/\alpha_{N_s-2}^H)\,\cdot$$

$$\cdot\,(\alpha_{N_s-1}^V/\alpha_{N_s-1}^H)\,(\alpha_{N_s}^V/\alpha_{N_s}^H) + \ldots\ldots + (\beta_1/\alpha_1^H)\,(\alpha_2^V/\alpha_2^H)\,(\alpha_3^V/\alpha_3^H)\,\cdot$$

$$\cdot\,\cdot\,(\alpha_{N_s}^V/\alpha_{N_s}^H) \tag{4.1.6}$$

Considering the complex random variable $\rho_j \equiv \alpha_j^V/\alpha_j^H$, this will have a negligible (almost zero) phase and amplitude which will have a fluctuation with very small variance compared to the variance of the amplitude of β_j. So, it is reasonable to take ρ_j as a constant term, whose value depends on the value of the corresponding R_j. So, we have:-

$$C_R^H = (\beta_{N_s}/\alpha_{N_s}^H) + (\beta_{N_s-1}/\alpha_{N_s-1}^H)\,\rho_{N_s} + (\beta_{N_s-2}/\alpha_{N_s-2}^H)\,\rho_{N_s-1}\,\rho_{N_s} + \ldots\ldots +$$

$$+ (\beta_1/\alpha_1^H)\,\rho_2\,\rho_3\,\ldots\ldots\,\rho_{N_s} \tag{4.1.7}$$

Again, the α_j^H are almost constant terms nearly equal to 1, so the C_R^H is a complex variable which is the sum of many independent Rayleigh phasors. As it is analytically explained in Appendix C, in this case, we have that the distribution of the amplitude of C_R^H will have a Rayleigh form, with:-

$$\Omega = \sum_{j=1}^{N_s} (\langle\beta_j^2\rangle_s/\alpha_j^2)\,\rho_{j+1}^2\,\rho_{j+2}^2\,\ldots\ldots\,\rho_{N_s}^2 \quad \text{(with } \rho_i \equiv 1\text{, for } i > N_s\text{)} \tag{4.1.8}$$

where Ω is the mean square value of the amplitude of C_R^H. The following analysis for the evaluation of the Ω can be simplified if we will adopt the concept of space-averaged rainfall rate $\overline{R}$ throughout the path (Bodtmann and Ruthroff, 1974). This theory is explained analytically in the following section.

4.1.2 The Concept of the Space-Averaged Rainfall Rate for a Spatially Non-Uniform Rain Medium

Ruthroff (1970), considering the problem of rain attenuation through a non-uniform rain medium, has made the following assumptions.

The attenuation in a radio path depends upon the number and size of the raindrops and not explicitly upon their speed or direction. But the quantity usually measured is rainrate and it does depend on the speed and direction of the raindrops. Since rainrate is the product of a density and a velocity, it can be interpreted as a vector.

Let there be a uniform distribution of N_D drops of water per cubic centimetre in the space between two antennas. The drops have equivolumic diameter D and velocity v_D. The fraction of volume occupied by water is defined as the density:-

$$p_D = (\pi/6)\, N_D\, D^3 \tag{4.1.9}$$

Rain density is a dimensionless, real, non-negative quantity. The rainrate for drops with diameter D and velocity v_D is:-

$$R_D = p_D\, v_D \tag{4.1.10}$$

The direction of the rainrate is the direction of the travel of the drops. The vector expression for rainrate is, therefore:-

$$\vec{R}_D = p_D \vec{v}_D \tag{4.1.11}$$

In general, a rain storm has drops of many diameters and the total rainrate is a summation over the drop diameters present:-

$$\vec{R} = \sum_D p_D \vec{v}_D \tag{4.1.12}$$

On the other hand, for a rain consisting of uniformly distributed drops with diameter D the attenuation of radio waves with wavelength λ is (Medhurst, 1965):-

$$\text{Attenuation} = 4.343 \frac{N_D \lambda^2}{2\pi} A_D \times 10^5 \qquad \text{db/km} \tag{4.1.13}$$

where A_D is a function of the drop diameter, the wavelength λ and the dielectric constant of water. Substituting from Equation (4.1.9), the attenuation is:-

$$a_D = k(\lambda, D)\ Lp_D \qquad \text{in db} \tag{4.1.14}$$

where:-

$$k(\lambda, D) = 3 \times 4.343 \times \frac{\lambda^2 A_D}{\pi^2 D^3} \times 10^5 \tag{4.1.15}$$

The result in Equation (4.1.14) is extended to the case of non-uniform spatial distribution of raindrops by replacing the uniform rain density in Equation (4.1.14) with the average rain density in the radio path. The path attenuation is, therefore, assumed to be:-

$$a_D(t) = k(\lambda, D) \frac{L}{V} \iiint\limits_V p_D(x, y, z, t)\, dV \tag{4.1.16}$$

The expression reduces to Equation (4.1.14) for uniform rain density. The optimum direction for rainfall rate is expected to be vertically downward in many regions, and if we will assume that the speed of raindrops does not change while in the radio path, the attenuation can be written in terms of rainrate. From Equation (4.1.16):-

$$a_D(t) = \frac{k(\lambda, D)}{v_D} \iiint\limits_V R_D(x, y, z, t)\, dV \tag{4.1.17}$$

Now let the radio path be divided into a large number N_s, of volume elements such that the rainrate is uniform in each element. The average rainrate on the path is:-

$$\overline{R}(t) = \frac{1}{N_s} \sum_{i=1}^{N_s} R(x_i, y_i, z_i, t) \tag{4.1.18}$$

In integral form, this is written:-

$$\overline{R}(t) = \frac{1}{V} \iiint\limits_V R(x, y, z, t)\, dV \tag{4.1.19}$$

Let also the rain have a Laws and Parsons distribution of diameters. Then:-

$$R_D(x, y, z, t) = R(x, y, z, t)\, p_D \tag{4.1.20}$$

where p_D is the fraction of water in the rain consisting of drops of diameter D. Substituting into Equation (4.1.17) and using the definition (4.1.19), the expression for attenuation becomes:-

$$a_D(t) = \frac{k(\lambda, D)}{v_D} L p_D \overline{R}(t) \tag{4.1.21}$$

The total attenuation is:-

$$a(t) = L\overline{R}(t) \sum_D \frac{k(\lambda, D)}{v_D} p_D \tag{4.1.22}$$

The quantity represented by the summation has been computed by Ryde and Ryde (1941) and by Medhurst (1965) for the Laws-Parsons drop diameter distribution and for the terminal velocities of waterdrops in still air.

On the other hand, the path attenuation for a uniform rainrate R_o is from Medhurst (1965):-

$$a_o(t) = LR_o \sum_D \frac{k(\lambda, D)}{v_D} p_D \tag{4.1.23}$$

As can be verified analytically, the expressions for a_o and $\langle CPA \rangle_s$ in Equations (4.1.23) and (2.5.5) must be equivalent. A comparison of Equations (4.1.22) and (4.1.23) shows that the attenuation for a non-uniform rain medium can be calculated as the corresponding one for a uniform path with the equivalent space-averaged rainrate $\overline{R}(t)$.

This concept can be extended in the case of cross-polarization discrimination to yield the mean square value Ω of the expression (4.1.8) as:-

$$\Omega = A\overline{R}^B \tag{4.1.24}$$

with:-

$$\left.\begin{aligned} A &= m_\theta^2 \, L^2 \, c^2 \, \sin^2(2\phi)/\pi \\ B &= 2d \end{aligned}\right\} \qquad (4.1.25)$$

The definition of parameters m_θ, c, d and ϕ has been established in the previous Chapters 2 and 3.

Finally, this space-averaged rainfall rate can be considered to be equivalent to the line rainfall rate (Bodtmann and Ruthroff, 1974; Harden, Norbury and White, 1977) throughout the path, or:-

$$\overline{R} \cong R_L = \frac{1}{L} \sum_{j=1}^{N_s} R_j \, \Delta z \qquad (4.1.26)$$

That is the situation which completes our consideration of the short-term statistics.

4.2 Long-Term Statistics

4.2.1 Analysis of Rain Probabilities

At this point, we will discuss two statistical parameters which are needed for the complete definition of raining time.

(a) $P_o(0)$: This is the probability that rain will fall at a specific location (point rain probability). This probability, $P_o(0)$, will be the same for all the points of the microwave path, and has been established in Chapter 2 (see expression (2.3.4) for the definition).

(b) $P_o(L)$: This is the probability that rain is falling somewhere on the path of length L (path-rain probability). This probability has been analysed both theoretically and experimentally by Bodtmann and Ruthroff (1974) and Lin (1975). Intuitively, it is expected that the probability $P_o(L)$ of rainfall on a radio path of length L is increased with L, since a longer path has a higher chance of intercepting rain of limited extent. An empirical formulation has been proposed which correlates the rain-path probability $P_o(L)$ with the point rain probability $P_o(0)$ (Lin, 1975):-

$$P_o(L) \cong 1 - \frac{1 - P_o(0)}{\left(1 + \frac{L^2}{21.5}\right)^{0.014}} \qquad (4.2.1)$$

where the path length L is in units of kilometres. As can be seen from this formula:-

$$\left.\begin{array}{l} P_o(L) \rightarrow P_o(0) \ (L \rightarrow 0) \\ P_o(L) \rightarrow 1 (L \rightarrow \infty) \end{array}\right\} \qquad (4.2.2)$$

This formulation is satisfactory for the USA, as has been verified with an experiment using a multiple raingauge network at Atlanta, Georgia (Lin, 1975). But further experimental work is needed before this formula can be considered as applicable everywhere.

4.2.2 Analysis of Space-Averaged Rainfall Rate Statistics

On a long-term basis, the point rainfall rates R_j (j = 1, 2, ... N_s) can be considered as correlated random variables with the same log-normal distribution during rain:-

$$p_{R_1}(r) = p_{R_2}(r) = p_{R_3}(r) = \ldots = p_{R_{N_s}}(r) = \Lambda \tag{4.2.3}$$

The space-averaged rainfall rate $\overline{R}$ can be shown to be a log-normal variable during rain, for the following reasons. Combining the results of Section 4.1.2 and the formula (2.5.22), the following expression for the attenuation of a non-uniform rain medium is obtained:-

$$\text{Attenuation} = \alpha \overline{R}^b L \tag{4.2.4}$$

From this formula, it is obvious that the space-averaged $\overline{R}$ can be expressed as:-

$$\ln \overline{R} = C_1 + \frac{1}{b} \ln (\text{Attenuation}) \tag{4.2.5}$$

But Lin (1973), analysing many sets of data from all over the world, has concluded that the long-term distribution for the rain attenuation must be log-normal. Hence, expression (4.2.5) shows that the $\overline{R}$ is also a log-normal variable during rain.

We turn now to the evaluation of the statistical parameters of the space-averaged rainrate $\overline{R}$ in terms of the corresponding ones of the point rainfall rate R_j. We have that:-

$$\overline{R} = \frac{1}{L} \sum_{j=1}^{N_s} R_j \, \Delta z = \frac{1}{L} \int_0^L R(z) \, dz \tag{4.2.6}$$

where now R(z) is a random variable which has the same statistical parameters as R_j. So:-

$$\left.\begin{aligned} &\langle R(z)\rangle = \langle R_j\rangle = \langle R\rangle \equiv E\left[R(z)\right] \\ &\text{var}\left[R(z)\right] = \text{var}\left[R_j\right] = \text{var}\left[R\right] \equiv E\left[(R_j - E\left[R_j\right])^2\right] \end{aligned}\right\} \quad (4.2.7)$$

and:-

$$\left.\begin{aligned} &\langle R(z)\rangle_u = \langle R_j\rangle_u = \langle R\rangle_u \equiv E_u\left[R(z)\right] \\ &\text{var}_u\left[R(z)\right] = \text{var}_u\left[R_j\right] = \text{var}_u\left[R\right] = E_u\left[(R_j - E_u\left[R_j\right])^2\right] \end{aligned}\right\} \quad (4.2.8)$$

Generally speaking, all probabilities and consequent expectations in this chapter are conditional on there being rain at <u>some</u> point on the path for variables which are referred to the total path such as $\overline{R}$ or Ω, and there being rain at a specific point of the radio path for variables such as the point rainfall rate R_j. Unconditional probabilities and derived quantities are indicated by the suffix u.

From the formulae (4.2.6) and (4.2.8), we have that:-

$$\langle\overline{R}\rangle_u = \frac{1}{L}\langle R\rangle_u L = \langle R\rangle_u \quad (4.2.9)$$

and:-

$$\text{var}_u\left[\overline{R}\right] = E_u\left[(\overline{R} - E_u\left[\overline{R}\right])^2\right] = E_u\left[\frac{1}{L^2}\int_0^L R(z)\,dz \int_0^L R(z')\,dz'\right] -$$

$$- \langle\overline{R}\rangle_u^2 = E_u\left[\frac{1}{L^2}\int_0^L\int_0^L R(z)\,R(z')\,dz\,dz'\right] - \langle\overline{R}\rangle_u^2 =$$

$$= \frac{1}{L^2} \int_0^L \int_0^L \left(E_u \left[R(z)\, R(z') - \langle R \rangle_u^2 \right] \right) dz\, dz' \qquad (4.2.10)$$

where in the last relation, we have used expression (4.2.9) for the $\langle \overline{R} \rangle_u$. By definition:-

$$C_R(z, z') = E_u \left[R(z)\, R(z') - \langle R \rangle_u^2 \right] \qquad (4.2.11)$$

is the spatial co-variance function for the correlated random variables $R(z)$ and $R(z')$ (point rainfall rates at the points z and z'). In other words:-

$$\psi_R(z, z') = \frac{C_R(z, z')}{\mathrm{var}_u \left[R \right]} \qquad (4.2.12)$$

is the spatial correlation coefficient between $R(z)$ and $R(z')$ (Papoulis, 1965), so:-

$$\mathrm{var}_u \left[\overline{R} \right] = \frac{1}{L^2}\, \mathrm{var}_u \left[R \right] \int_0^L \int_0^L \psi_R(z, z')\, dz\, dz' \qquad (4.2.13)$$

At this point, a general formula for the correlation coefficient $\psi_R(z, z')$ is needed, as a function of the distance d between the two points z and z'. The following postulation can be used, as analogously Lin (1975) did for the evaluation of the correlation coefficient $\psi_\beta(z, z')$ of the attenuation gradients $\beta(z)$ and $\beta(z')$ between two points z and z' of the path:-

$$\psi_R(z, z') = G/\left[G^2 + (z - z')^2\right]^{1/2} \tag{4.2.14}$$

where G is the characteristic distance in km at which ψ_R becomes $1/\sqrt{2}$. Lin (1975), for many parts of the US, Harden, Norbury and White (1974) for Southern England have suggested that this characteristic distance must be about 1.5 km. Substituting back to formula (4.2.13) for $\text{var}_u\left[\overline{R}\right]$, we will have:-

$$\text{var}_u\left[\overline{R}\right] = \frac{1}{L^2}\left\{\text{var}_u\left[R\right]\right\} H(L) \tag{4.2.15}$$

where:-

$$H(L) = \int_0^L \int_0^L \left[G/\left[G^2 + (z - z')^2\right]^{1/2}\right] dz\, dz' \tag{4.2.16}$$

This double integral is derived analytically in Appendix D and the final result is:-

$$H(L) = 2G^2\left\{L/G\left(\frac{\sinh^{-1}(L/G) - \sinh^{-1}(- L/G)}{2}\right) - \sqrt{1 + \frac{L^2}{G^2}} + 1\right\} \tag{4.2.17}$$

Plots of $H'(L) = H(L)/L^2$, for various values of the parameter G, are shown in Fig. 4.2.

We are now interested in the evaluation of the median value $\overline{R}_m$ and standard deviation $S_{\overline{R}}$ of the space-averaged $\overline{R}$, during rain. From Appendix A, the following relation is valid (the second of formulae A-7):-

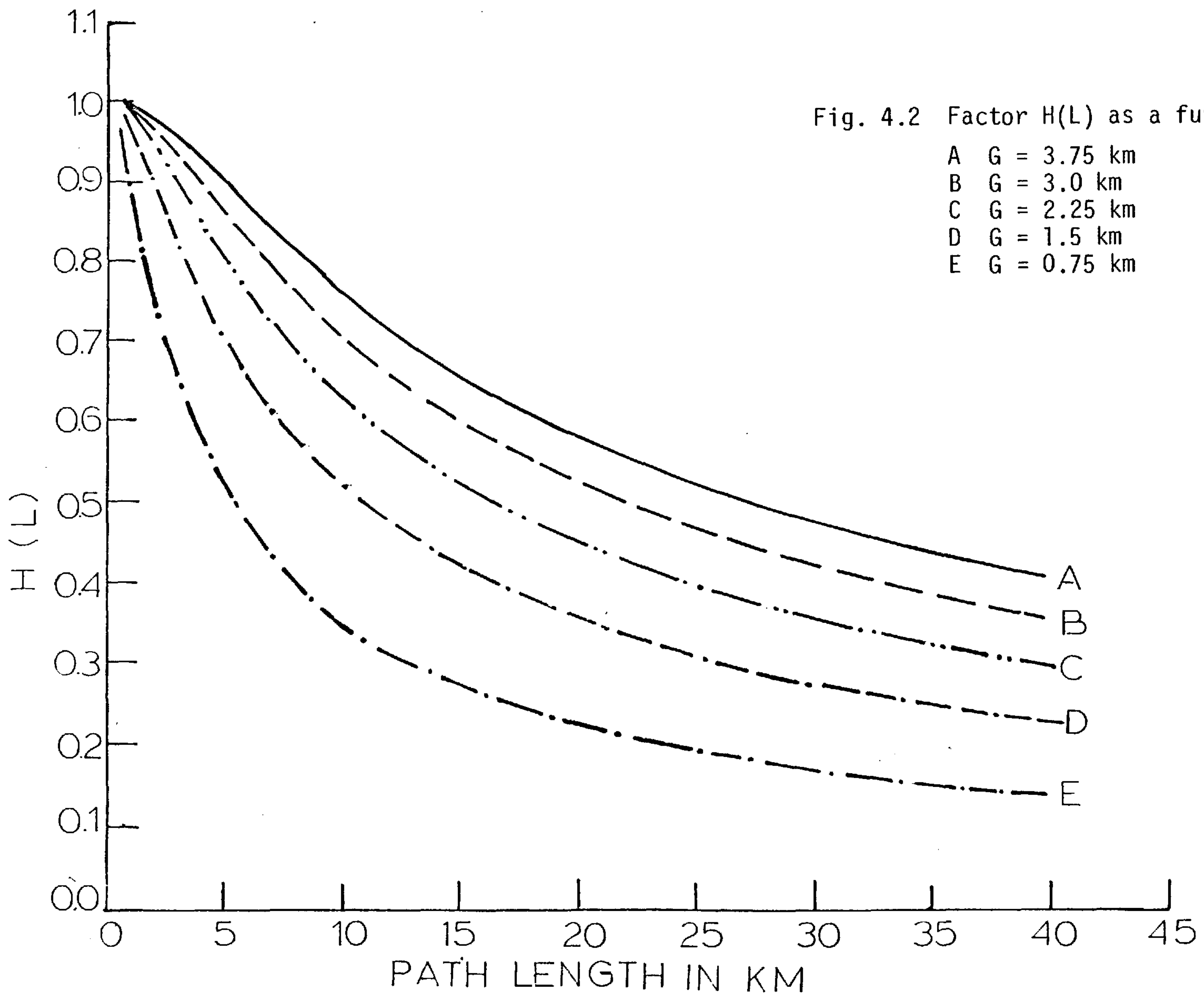

Fig. 4.2 Factor H(L) as a function of path length

A G = 3.75 km
B G = 3.0 km
C G = 2.25 km
D G = 1.5 km
E G = 0.75 km

$$S^2_{\overline{R}} = \ln \left[P_o(L) \left[1 + \left\{ \frac{\mathrm{var}_u \left[\overline{R} \right]^2}{\langle \overline{R} \rangle_u} \right\} \right] \right] \tag{4.2.18}$$

Using expressions (4.2.9), (4.2.15) and the first from relations (A-7) for the ratio ($\mathrm{var}_u \left[R \right] / \langle R \rangle_u$), we have finally:-

$$S^2_{\overline{R}} = \ln \left[P_o(L) \left[1 + \left\{ \left(e^{S^2_R} / P_o(0) \right) - 1 \right\} H'(L) \right] \right] \tag{4.2.19}$$

Using also the first of formulas (A-2) from Appendix A, we have for the median value R_m:-

$$\overline{R}_m = \langle \overline{R} \rangle \exp \left[- S^2_{\overline{R}} / 2 \right] \tag{4.2.20}$$

Using successively the second of formulas (A-6), (4.2.9) the first of (A-6), and finally the second of (A-2), the relation (4.2.20) becomes:-

$$\overline{R}_m = R_m \frac{P_o(0)}{P_o(L)} \exp \left[\frac{S^2_R - S^2_{\overline{R}}}{2} \right] \tag{4.2.21}$$

The relations (4.2.19) and (4.2.21) evaluate the parameters $\overline{R}_m$ and $S_{\overline{R}}$ for the log-normal distribution of $\overline{R}$ during rain, in terms of rain probabilities $P_o(0)$, $P_o(L)$, the statistical parameters R_m, S_R of the point rainfall distribution, the path length L and the characteristic distance G.

4.2.3 Analysis of Cross-Polarization Discrimination Statistics

The short-term mean square value of the amplitude of the complex cross-polarization factor Ω, as given by formula (4.1.24), is a random variable on a long-term basis, which has a log-normal distribution during rain and is identically zero during non-rain (other atmospheric effects causing cross-polarization such as multipath are not treated here). At this point, the median value Ω_m and standard deviation S_Ω of the log-normal distribution of Ω during rain can be evaluated in terms of $\overline{R}_m$ and $S_{\overline{R}}$ as (Aitchison and Brown, 1965):-

$$\left.\begin{aligned} \Omega_m &= A\overline{R}_m^B \\ S_\Omega &= BS_{\overline{R}} \end{aligned}\right\} \tag{4.2.22}$$

The distribution density function for the Ω-variable during rain will be (Papoulis, 1965):-

$$p_\Omega(\omega) = \frac{1}{\sqrt{2\pi}}\frac{1}{S_\Omega \cdot \omega} e^{-\left[\frac{\ln\omega - \ln\Omega_m}{\sqrt{2}\,S_\Omega}\right]^2} \tag{4.2.23}$$

Defining:-

$$X = 10\log\Omega = 10\,M\ln\Omega \tag{4.2.24}$$

then (Papoulis, 1965):-

$$p_X(x) = \frac{1}{\sqrt{2\pi}}\frac{1}{S_\Omega\,10\,M} e^{-\left[\frac{x - 10\,M\ln\Omega}{\sqrt{2}\,S_\Omega\,10\,M}\right]^2} \tag{4.2.25}$$

This is a normal distribution with parameters:-

$$\left.\begin{aligned} \langle X \rangle &= 10\ M\ \ln\ \Omega_m \\ \sigma_X &= 10\ M\ S_\Omega \end{aligned}\right\} \qquad (4.2.26)$$

The last step is the analysis of the long-term statistics of XPI or XPD which is defined as:-

$$Y = 20\ \log\ \left|C_R^H\right| \qquad (4.2.27)$$

The analysis follows the same steps as in the case of spatially uniform rainfall rate (Chapter 3) and the total probability of XPD or XPI is now given as:-

$$p_Y(y) = \int_{-\infty}^{\infty} \frac{2}{M'}\ \exp\ \left[\left(2(y - x)/M' - e^{2(y - x)/M'}\right)\right] \frac{1}{\sqrt{2\pi}\ \sigma_X} \ .$$

$$.\ e^{-\ (1/2\sigma_X^2)\ \left((x - \langle X \rangle)\right)^2}\ dx \qquad (4.2.28)$$

$$\text{with } M' = 20\ M = 20\ \log_{10}\ e \qquad (4.2.29)$$

This integral is again calculated numerically by means of Gauss-Hermite quadratures (Chapter 3), and it can be shown that it is a very close approximation to a normal form. Hence for engineering applications, the density $p_Y(y)$ can be taken as normal.

The excess probability for XPD or XPI will be:-

$$P\left[Y \geq y\right] = P_o(L) \int_y^{\infty} p_Y(y)\ dy \qquad (4.2.30)$$

where y is a specified level of XPI or XPD in db.

4.3 Numerical Analysis and Results

All the numerical techniques which are used for the evaluation of the rain cross-polarization discrimination or isolation distribution are the same as those described in Chapter 3. A special routine which calculates the value of the inverse hyperbolic sine, is described here analytically. This routine is used for the evaluation of the factor H(L) (expression (4.2.17)).

Numerical results are given for a microwave link on 34.8 GHz cited at a location in New Jersey and for another one working on 22 GHz cited at a location in Southern England (Figs. 4.3 - 4.26)*. In Figs. 4.3, 4.4 and 4.15, 4.16, the actual density function for the cross-polarization discrimination or isolation during rain and the best fitting approximate normal are shown for comparison. The excess probabilities for the rain cross-polarization discrimination have been calculated by the two methods (uniform and non-uniform one) for path lengths up to 4 km. The results for the USA are shown in Figs. 4.5 to 4.11 and the corresponding ones for Southern England in Figs. 4.17 to 4.23. From these figures, it is obvious that up to 2 km at least, the approximation of the spatially uniform rainfall rate gives an almost identical distribution to the actual non-uniform one. For longer paths, the discrepancy between the two curves becomes progressively greater. The approximate upper limit of 4 km across which it was assumed in previous chapters that the rainfall rate was uniform, is thereby confirmed.

Finally, the outage time, caused by co-channel interference, is shown as a function of hop length for the two locations for three different threshold levels of XPD (- 20 db, - 25 db and - 30 db) in

* These results are given in Sections 4.3.2 and 4.3.3.

Figs. 4.12 to 4.14 and 4.24 to 4.26. Two types of linear polarization are used (horizontal and 45^{0} inclination to horizontal) and the latter is shown to be the worst case for linear incident polarization.

4.3.1 Analysis of Special Function

The routine for the evaluation of inverse hyperbolic sine has been based on truncated Chebyshev expansions. This method of approximation has been explained analytically in the previous chapter (Section 3.4.3).

The routine S11ABF is called from NAG Library and calculates an approximate value for the arcsinh(x). For $|x| \leq 1$, it is based on the Chebyshev expansion:-

$$\operatorname{arcsinh}(x) = x \cdot y(t) = x \sum_{r=0} C_r\, T_r(t) \tag{4.3.1}$$

$$\text{where } t = 2x^2 - 1 \tag{4.3.2}$$

For $|x| > 1$, it uses the fact that:-

$$\operatorname{arcsinh}(x) = \operatorname{sign}(x) \,.\, \ln \left[|x| + \sqrt{x^2 + 1}\right] \tag{4.3.3}$$

This form is used directly for $1 < |x| < 10^{k}$, where k is related to the number of figures of precision of the machine representation as follows. If the machine works to n decimal figures then $k = n/2 + 1$. For $|x| \geq 10^{k}$, $\sqrt{x^2 + 1}$ is equal to $|x|$ to within the accuracy of the machine and hence we can guard against premature overflow and, without loss of accuracy, calculate:-

$$\operatorname{arcsinh}(h) = \operatorname{sign}(x) \left[\ln(2) + \ln(|x|)\right] \tag{4.3.4}$$

4.3.2 Numerical Results for the USA

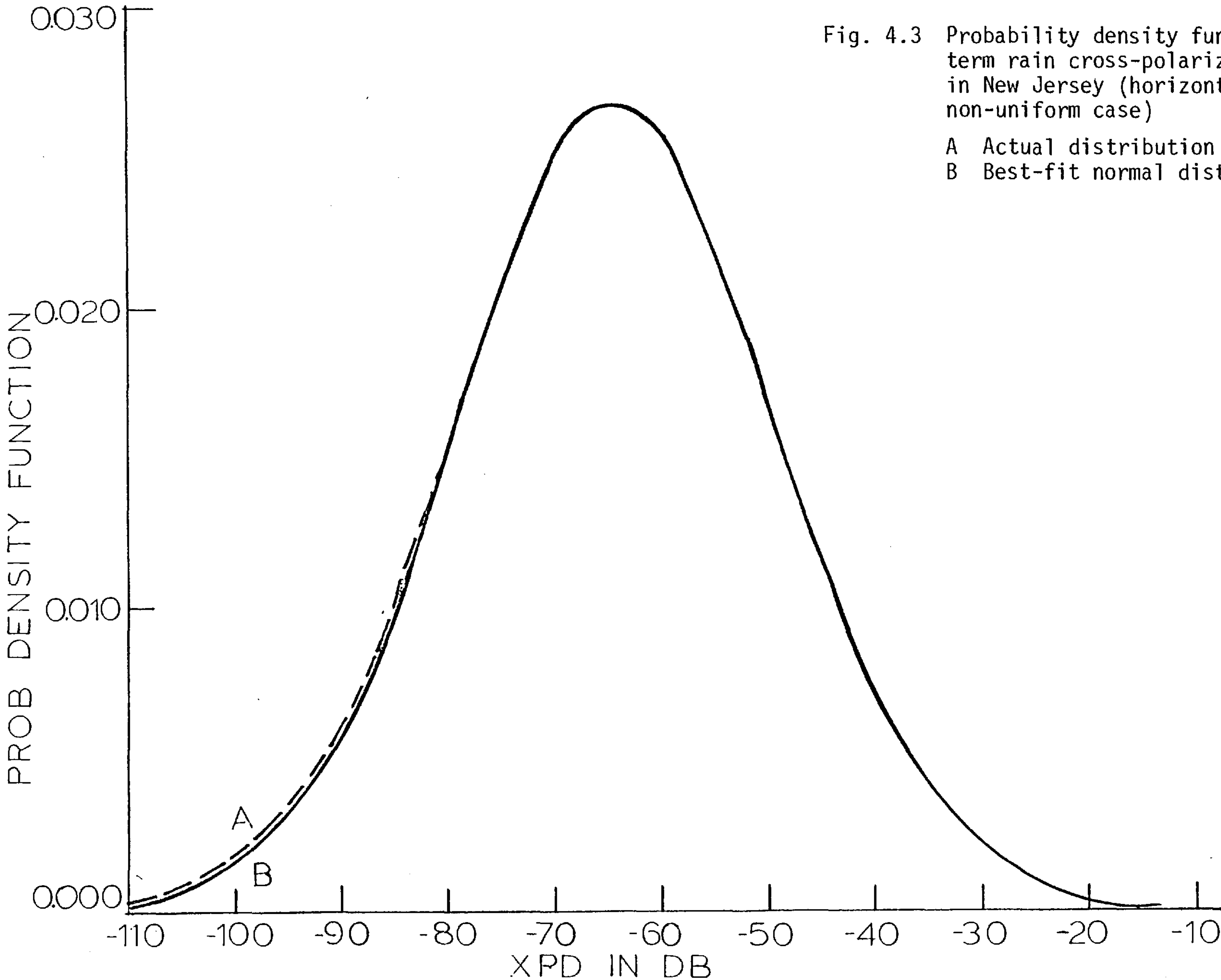

Fig. 4.3 Probability density function of the long-term rain cross-polarization for a link in New Jersey (horizontal polarization, non-uniform case)

A Actual distribution
B Best-fit normal distribution

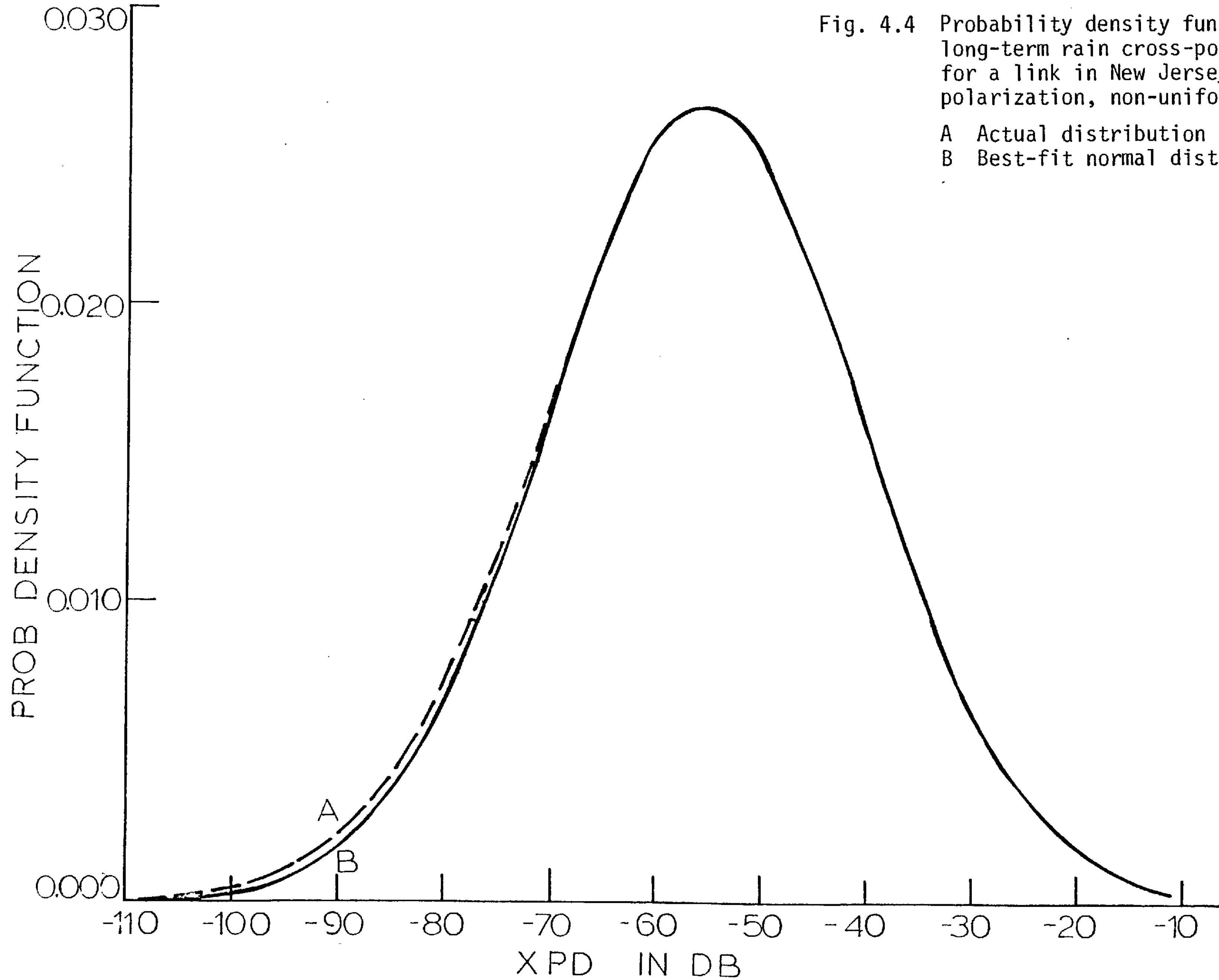

Fig. 4.4 Probability density function of the long-term rain cross-polarization for a link in New Jersey (45° polarization, non-uniform case)

A Actual distribution
B Best-fit normal distribution

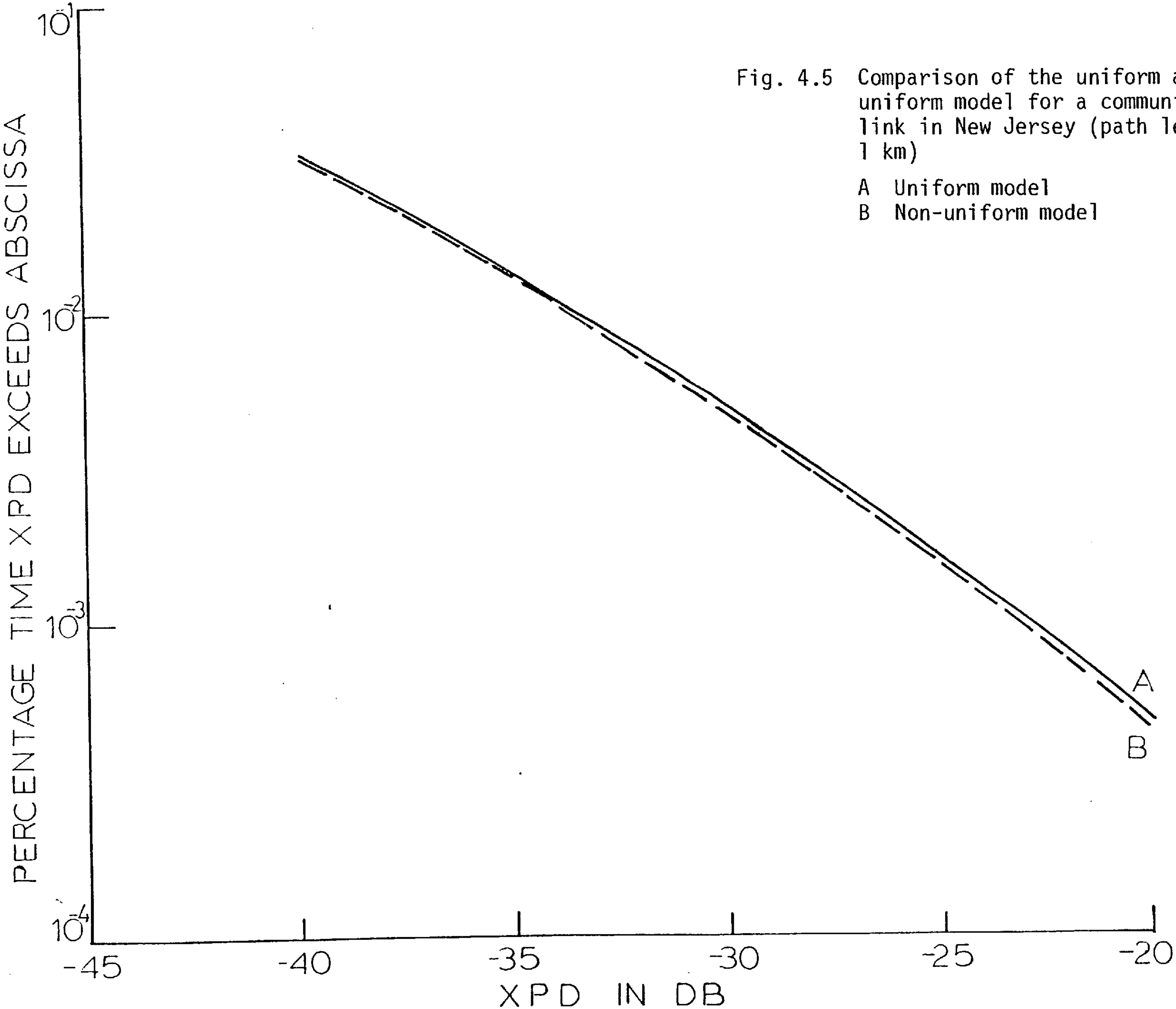

Fig. 4.5 Comparison of the uniform and non-uniform model for a communication link in New Jersey (path length: 1 km)

A Uniform model
B Non-uniform model

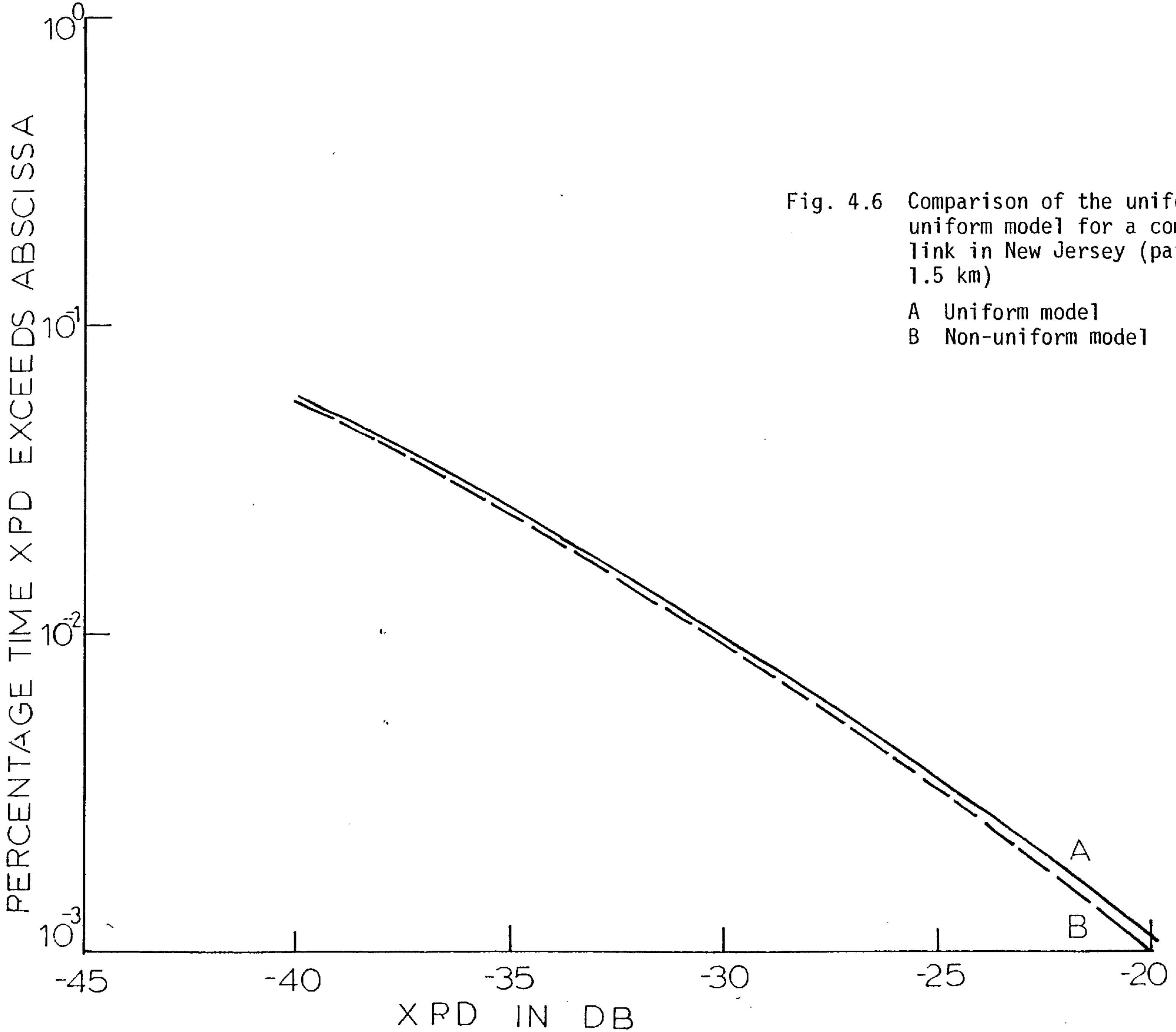

Fig. 4.6 Comparison of the uniform and non-uniform model for a communication link in New Jersey (path length: 1.5 km)

A Uniform model
B Non-uniform model

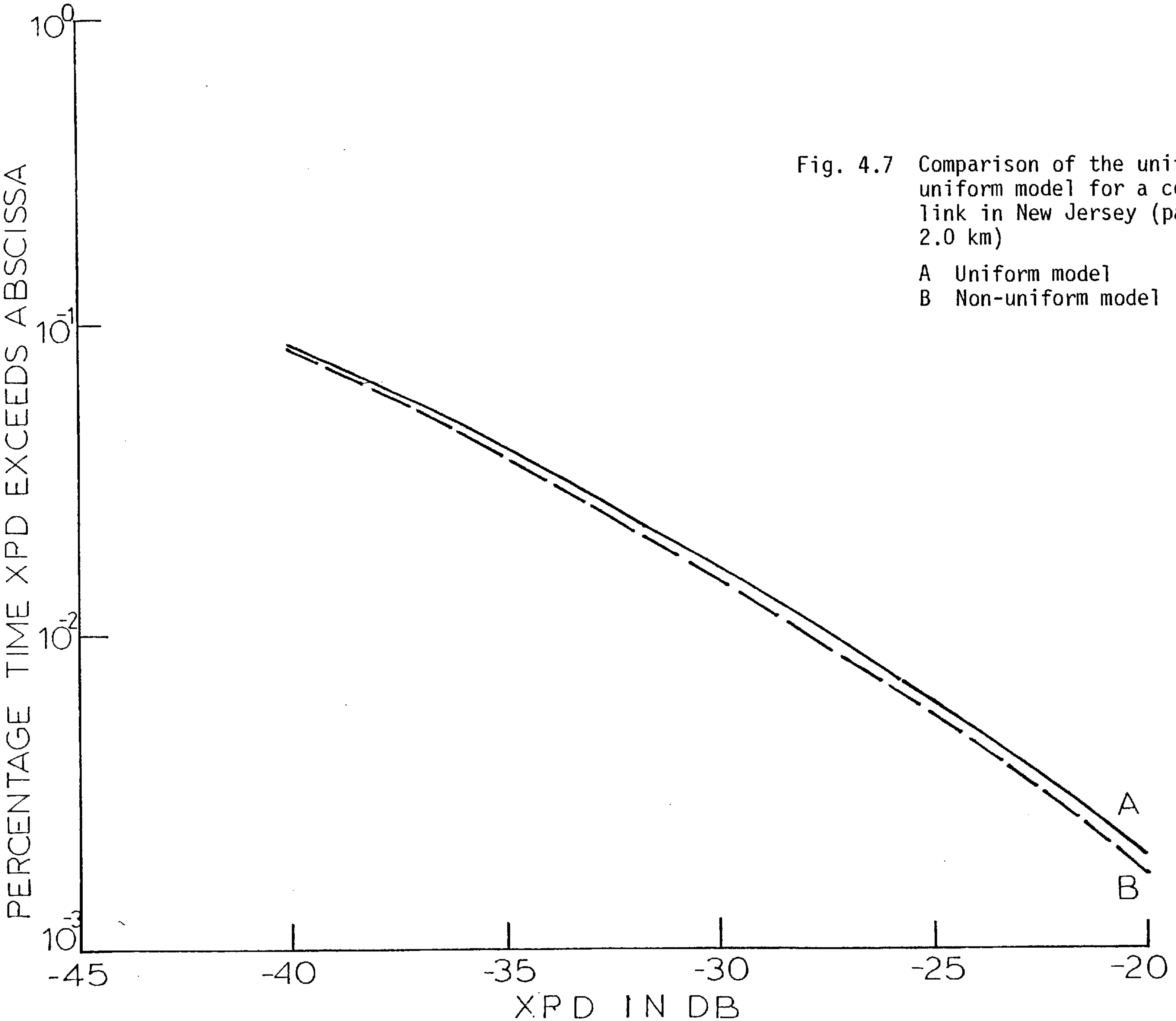

Fig. 4.7 Comparison of the uniform and non-uniform model for a communication link in New Jersey (path length: 2.0 km)

A Uniform model
B Non-uniform model

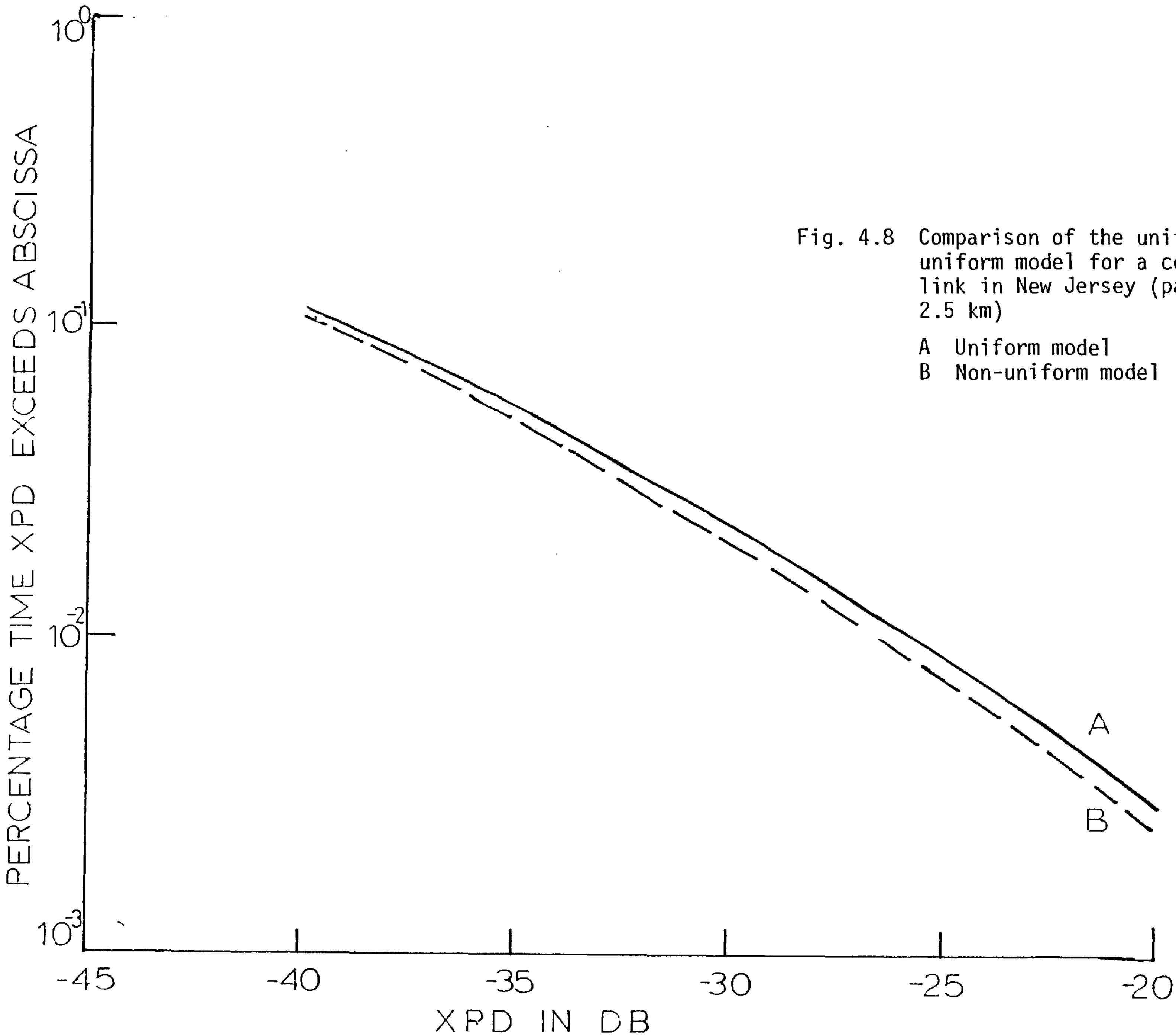

Fig. 4.8 Comparison of the uniform and non-uniform model for a communication link in New Jersey (path length: 2.5 km)

A Uniform model
B Non-uniform model

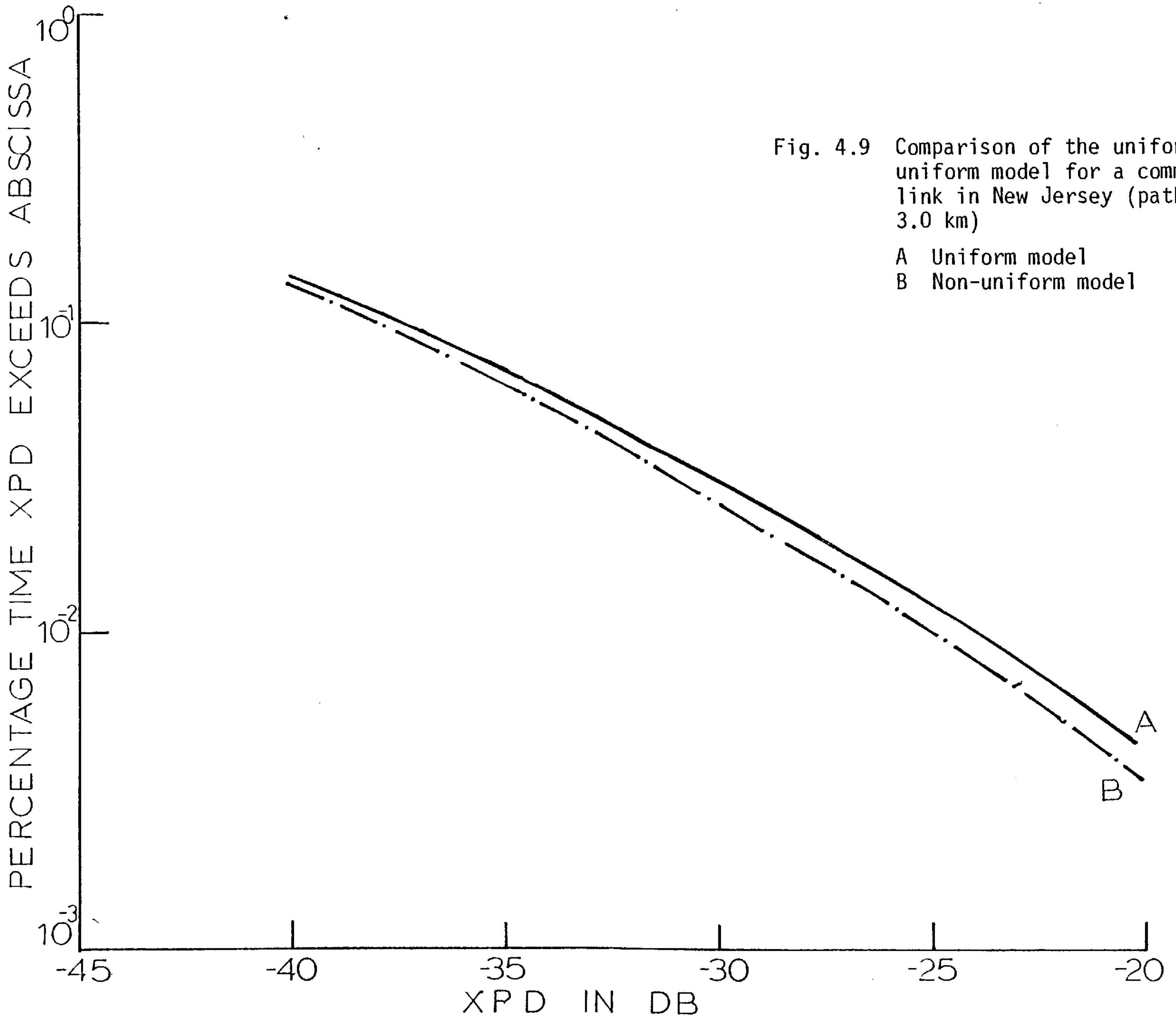

Fig. 4.9 Comparison of the uniform and non-uniform model for a communication link in New Jersey (path length: 3.0 km)

A Uniform model
B Non-uniform model

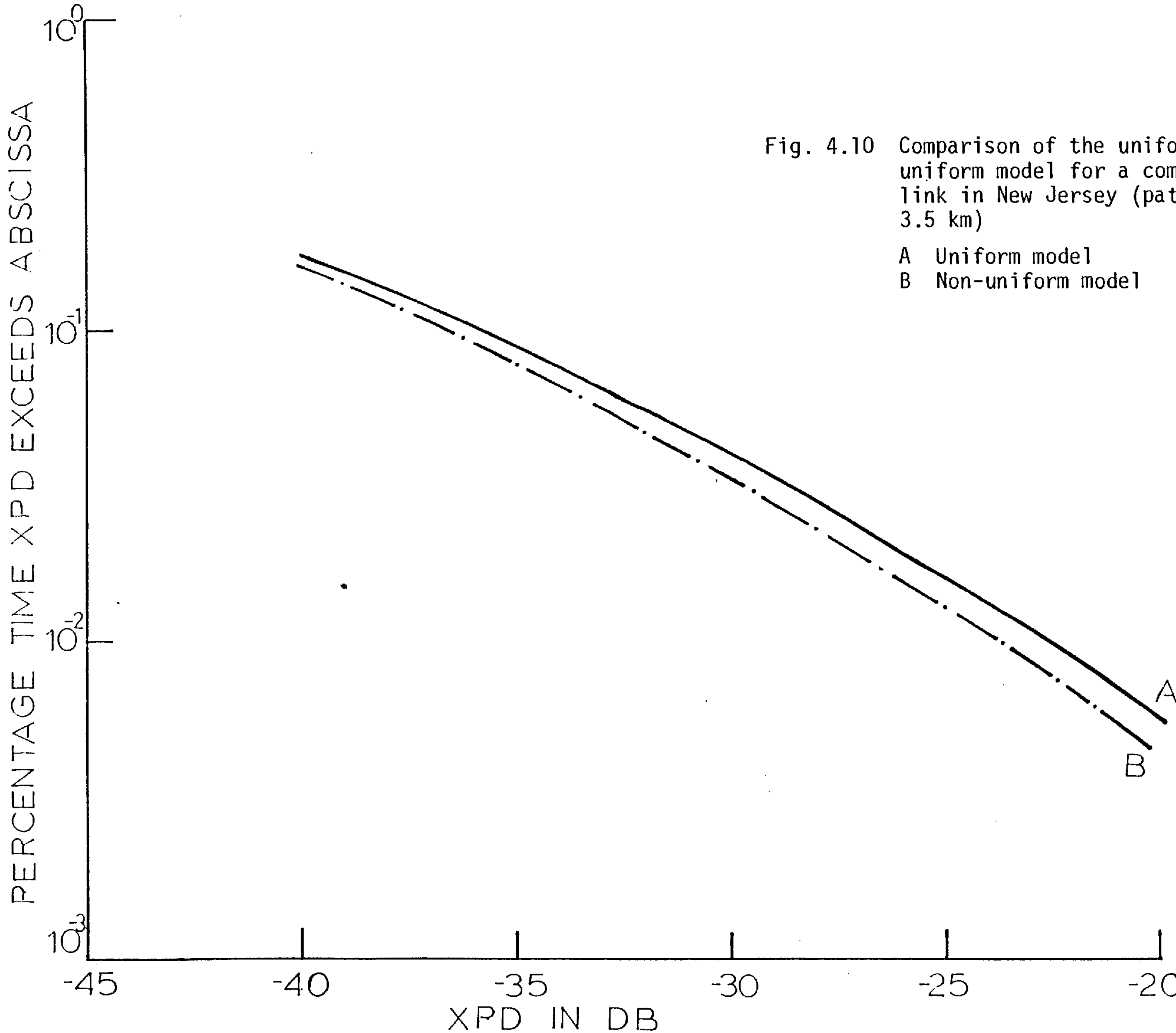

Fig. 4.10 Comparison of the uniform and non-uniform model for a communication link in New Jersey (path length: 3.5 km)

A Uniform model
B Non-uniform model

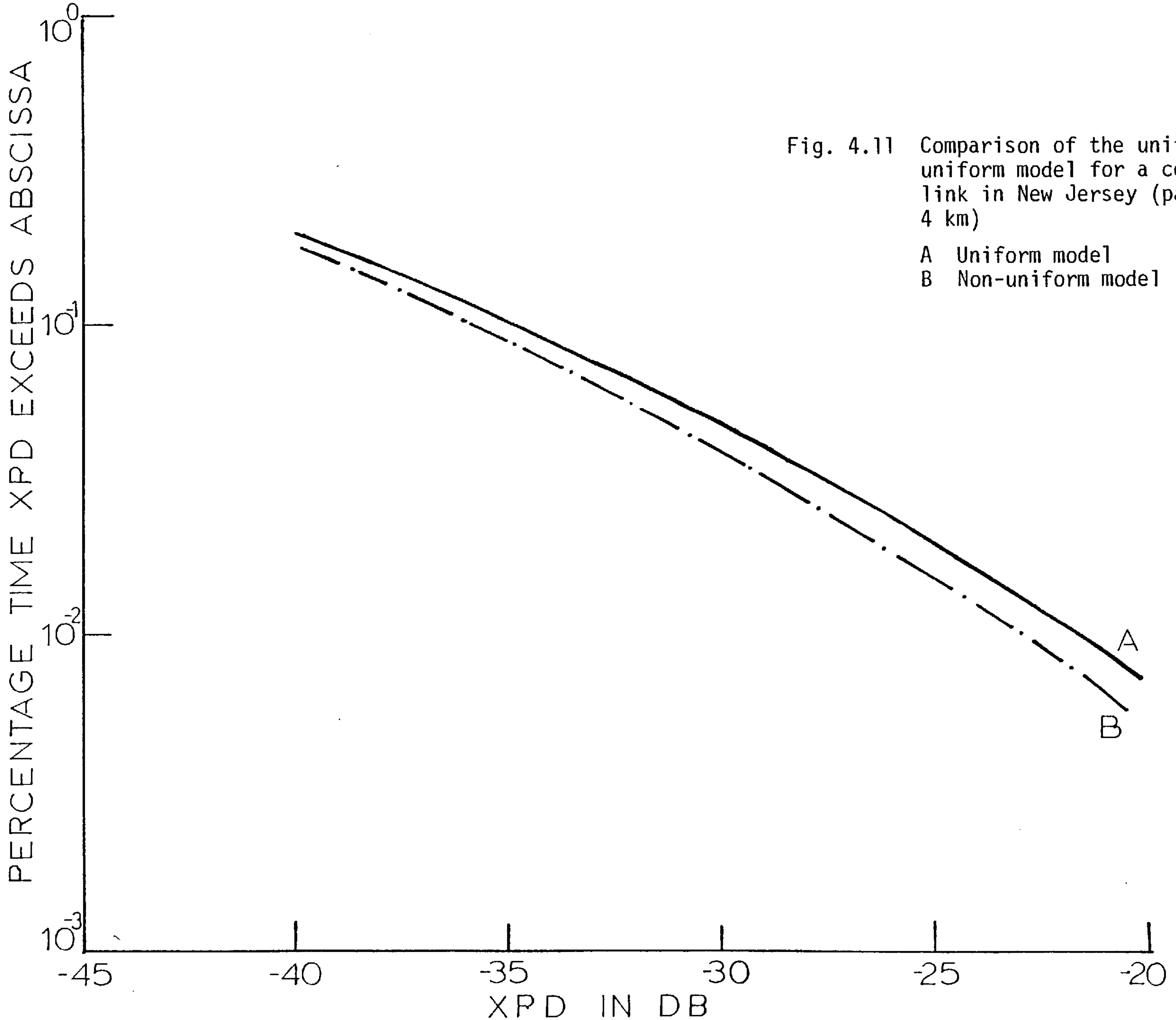

Fig. 4.11 Comparison of the uniform and non-uniform model for a communication link in New Jersey (path length: 4 km)

A Uniform model
B Non-uniform model

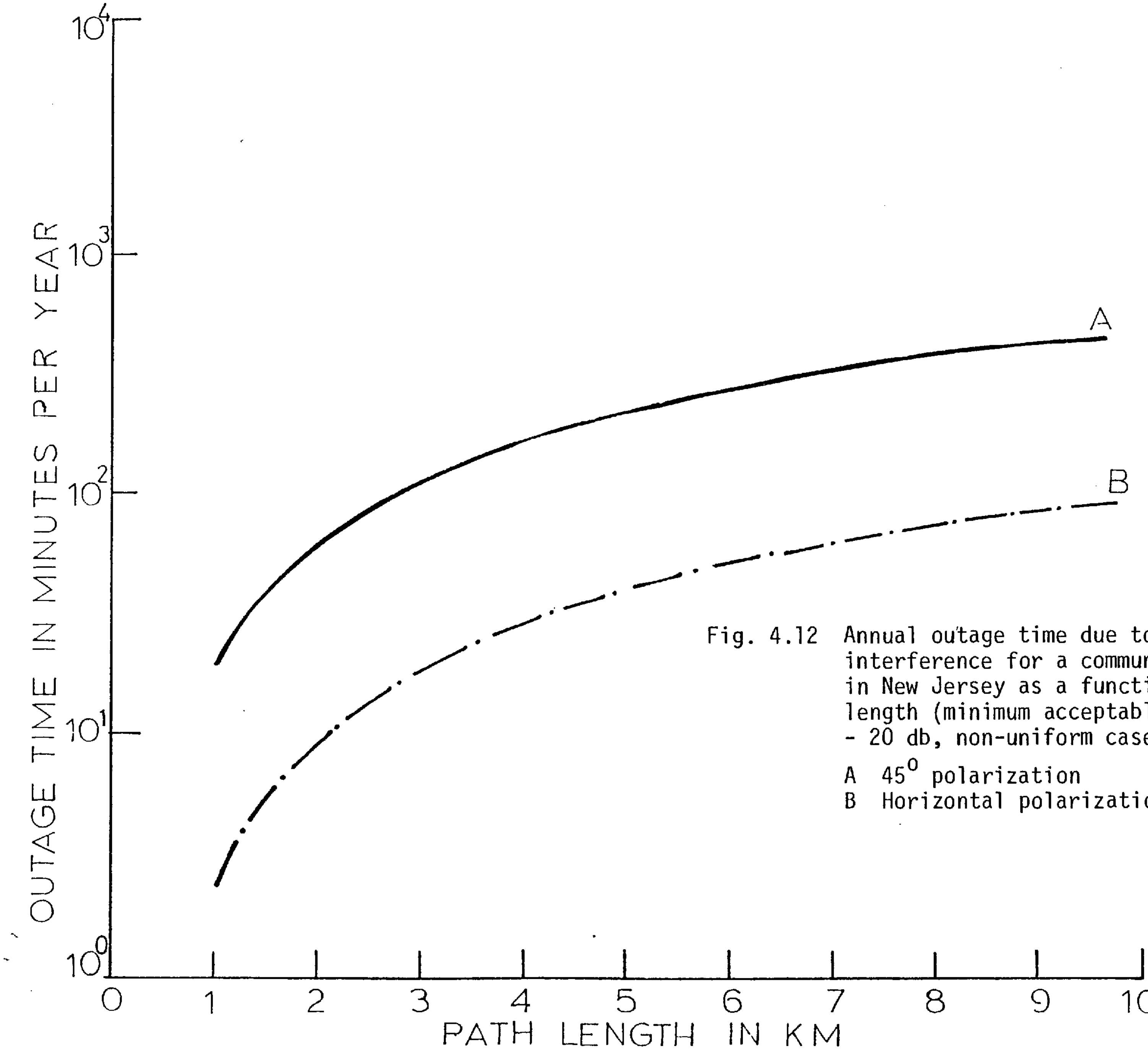

Fig. 4.12 Annual outage time due to channel interference for a communication link in New Jersey as a function of path length (minimum acceptable XPI threshold: - 20 db, non-uniform case)

A 45^0 polarization
B Horizontal polarization

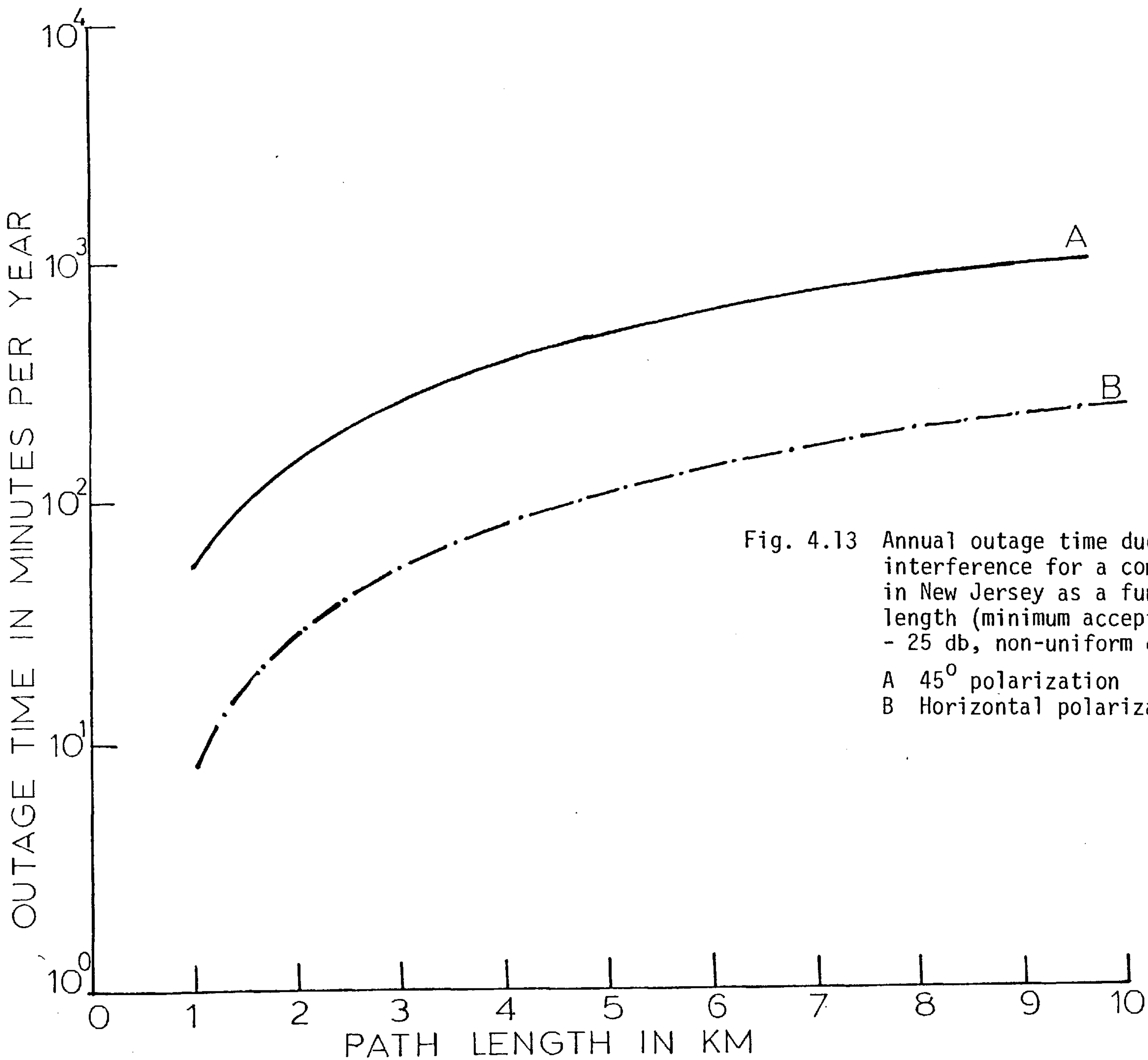

Fig. 4.13 Annual outage time due to channel interference for a communication link in New Jersey as a function of path length (minimum acceptable XPI threshold: - 25 db, non-uniform case)

A 45^0 polarization
B Horizontal polarization

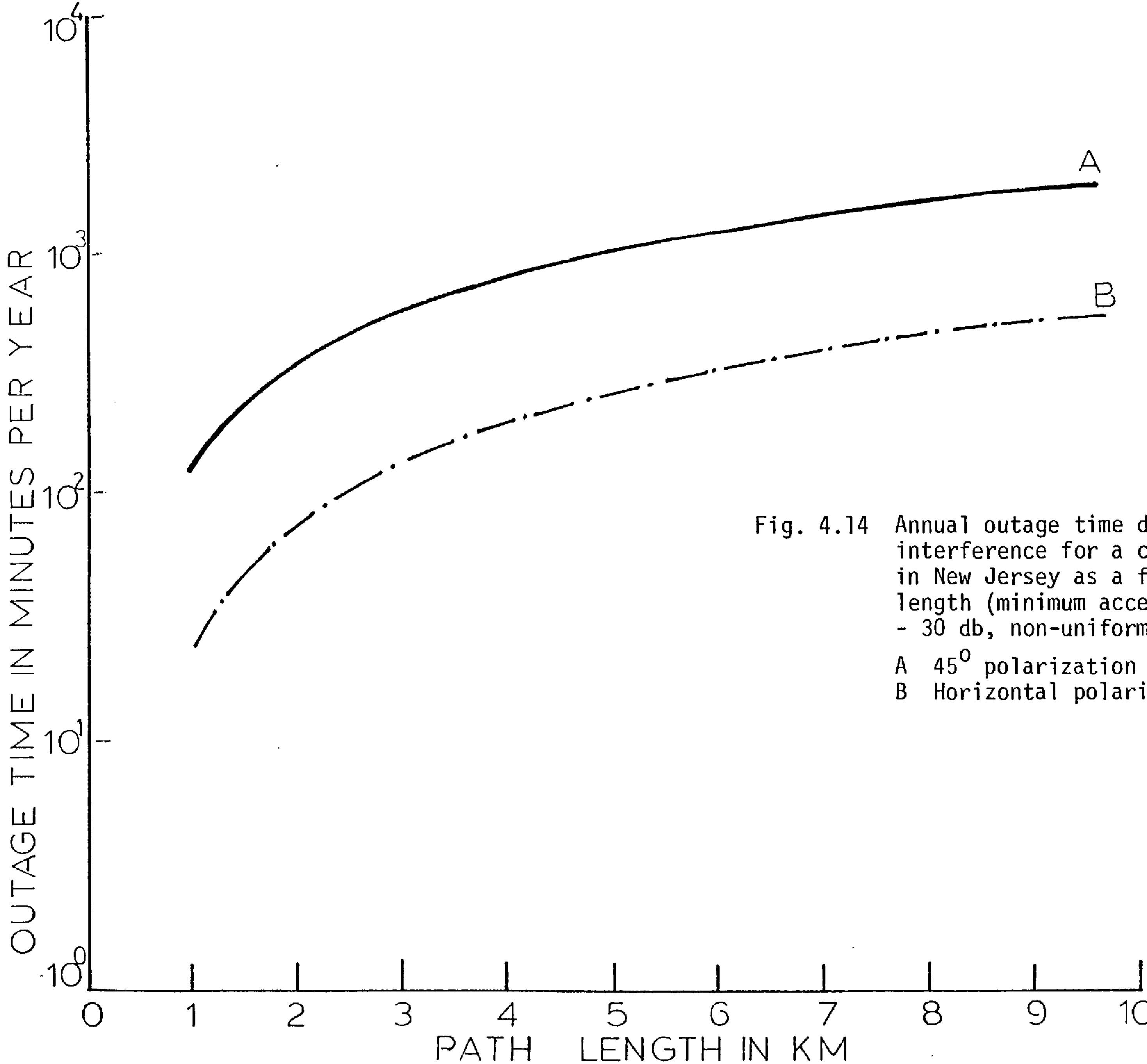

Fig. 4.14 Annual outage time due to channel interference for a communication link in New Jersey as a function of path length (minimum acceptable XPI threshold: - 30 db, non-uniform case)

A 45^0 polarization
B Horizontal polarization

4.3.3 Numerical Results for Southern England

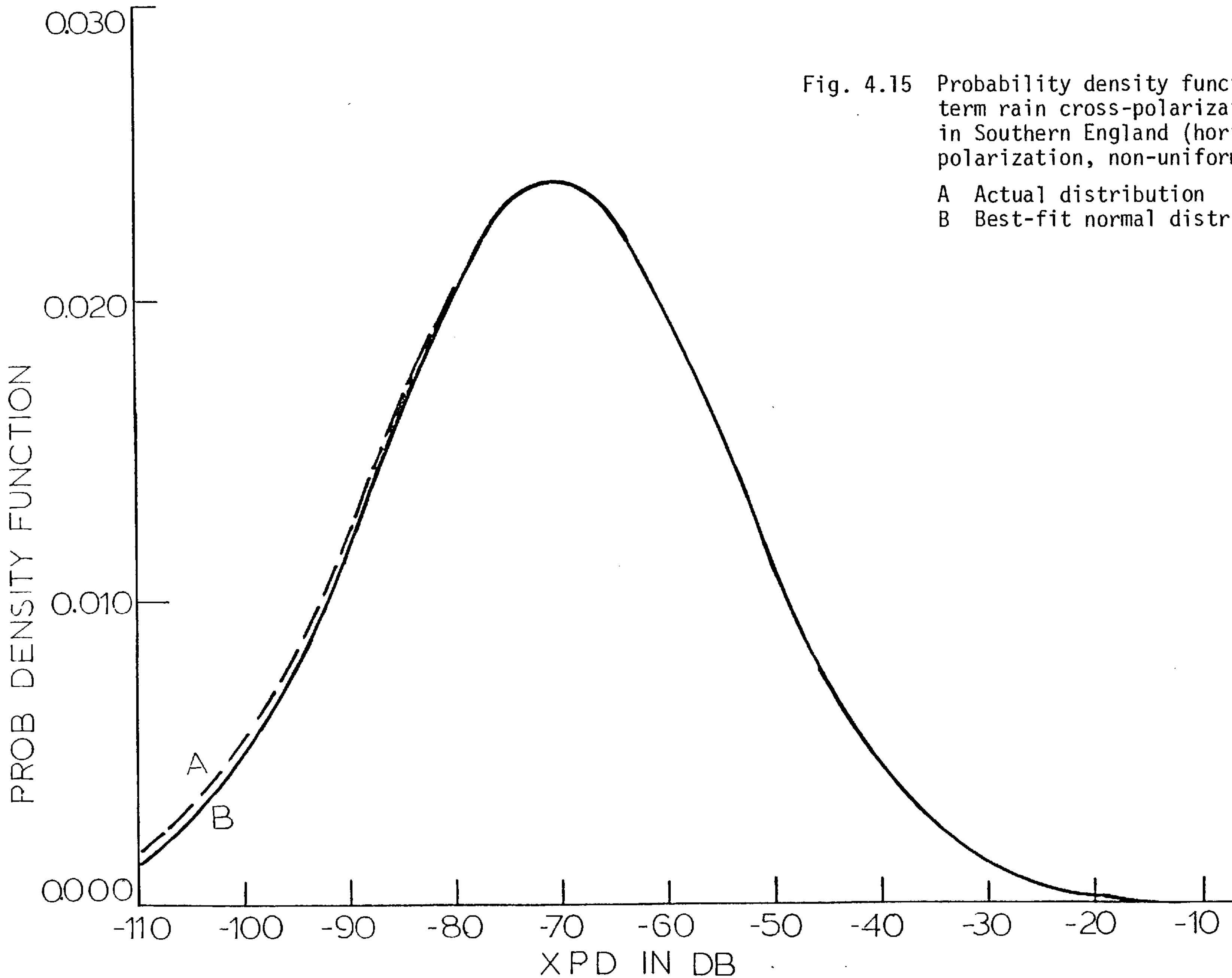

Fig. 4.15 Probability density function of the long-term rain cross-polarization for a link in Southern England (horizontal polarization, non-uniform case)

A Actual distribution
B Best-fit normal distribution

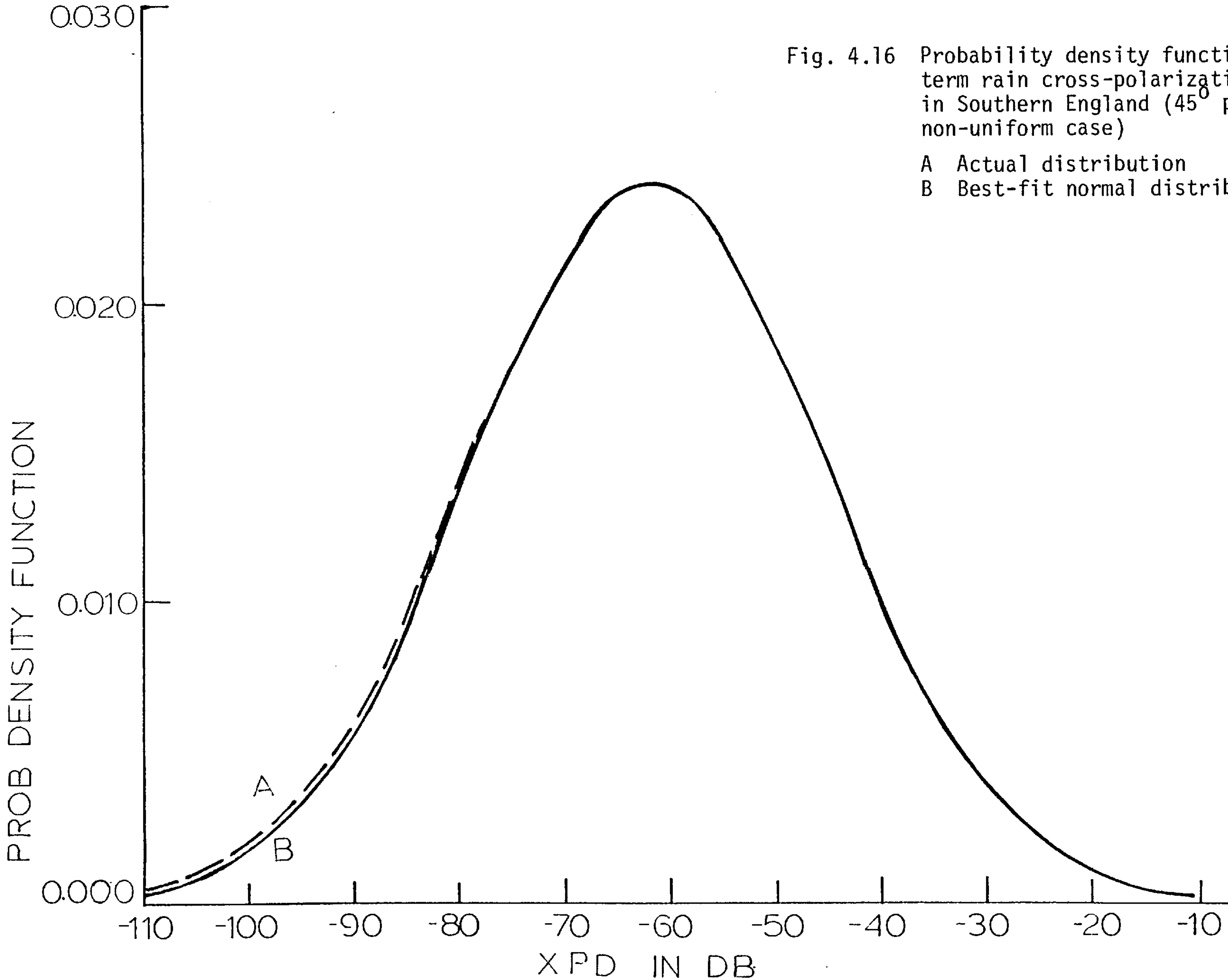

Fig. 4.16 Probability density function of the long-term rain cross-polarization for a link in Southern England (45^{0} polarization, non-uniform case)

A Actual distribution
B Best-fit normal distribution

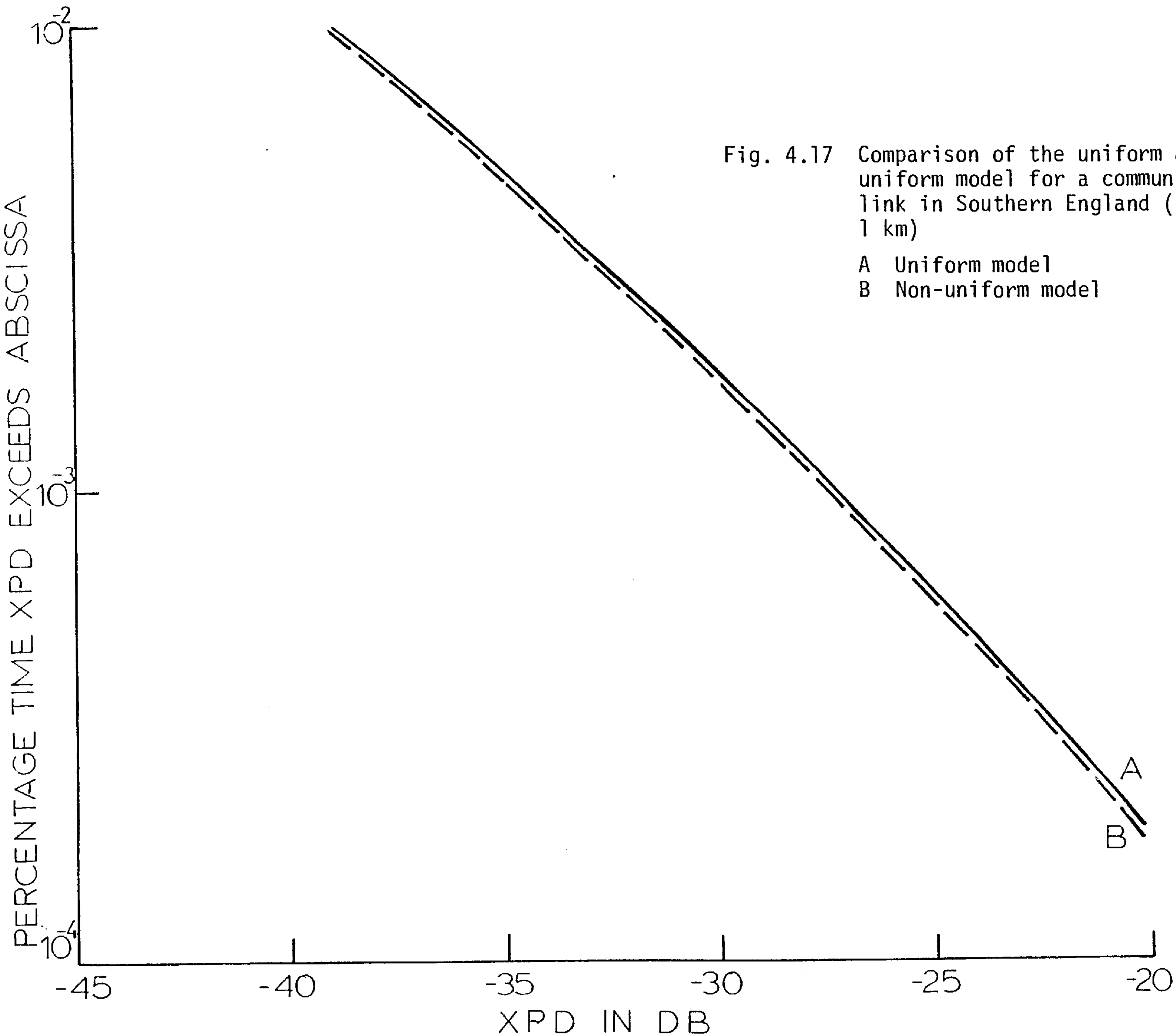

Fig. 4.17 Comparison of the uniform and non-uniform model for a communication link in Southern England (path length: 1 km)

A Uniform model
B Non-uniform model

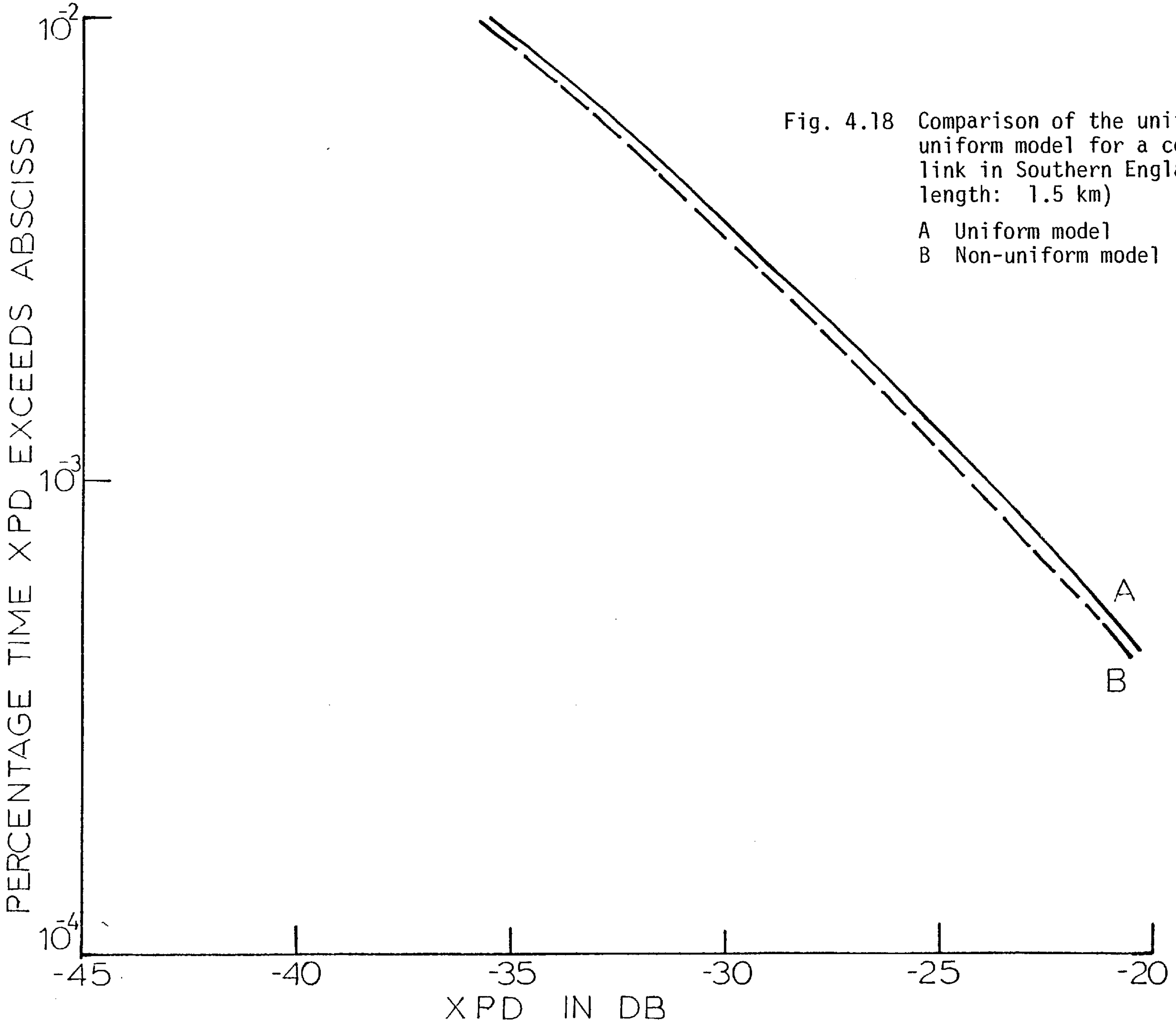

Fig. 4.18 Comparison of the uniform and non-uniform model for a communication link in Southern England (path length: 1.5 km)

A Uniform model
B Non-uniform model

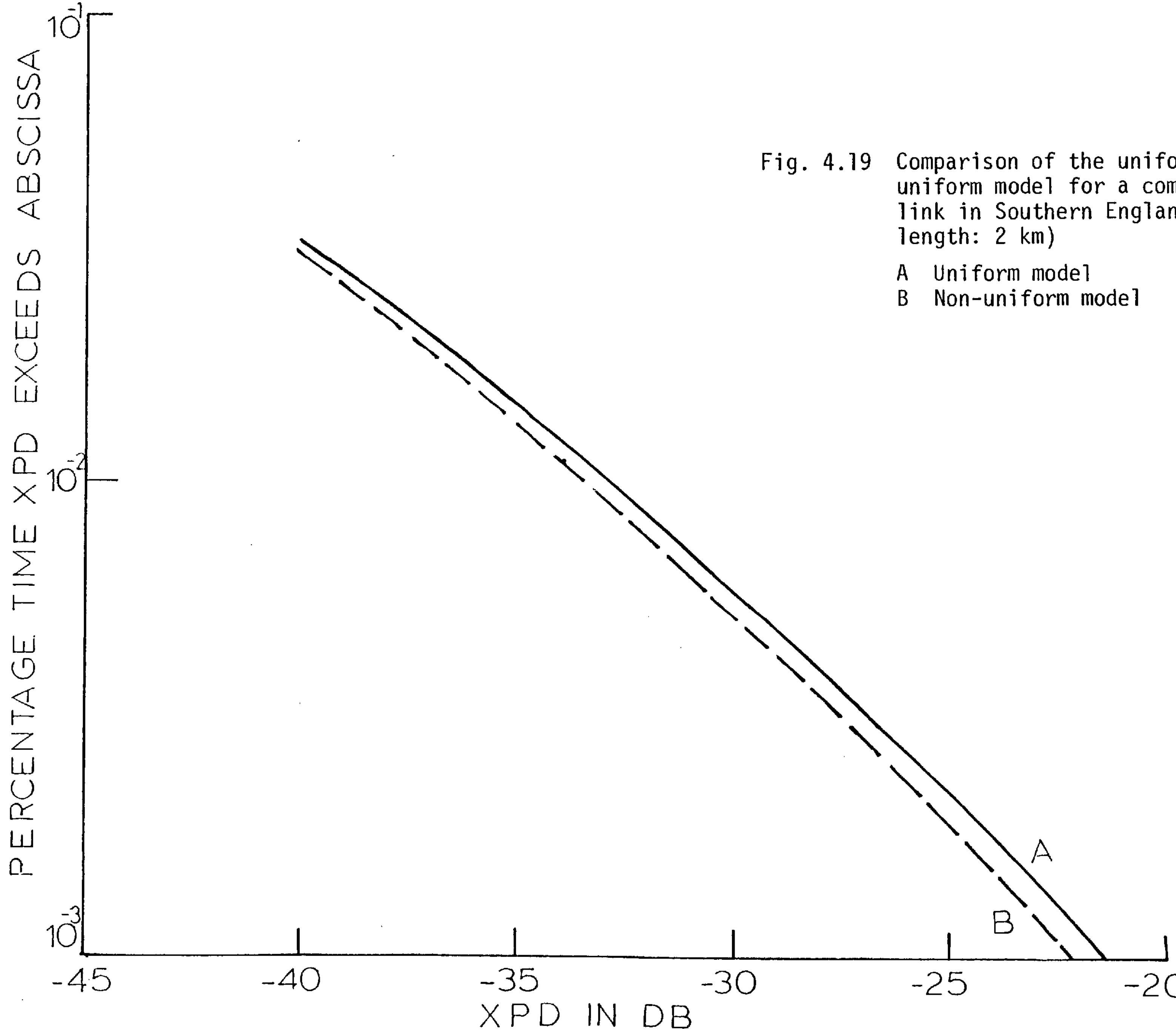

Fig. 4.19 Comparison of the uniform and non-uniform model for a communication link in Southern England (path length: 2 km)

A Uniform model

B Non-uniform model

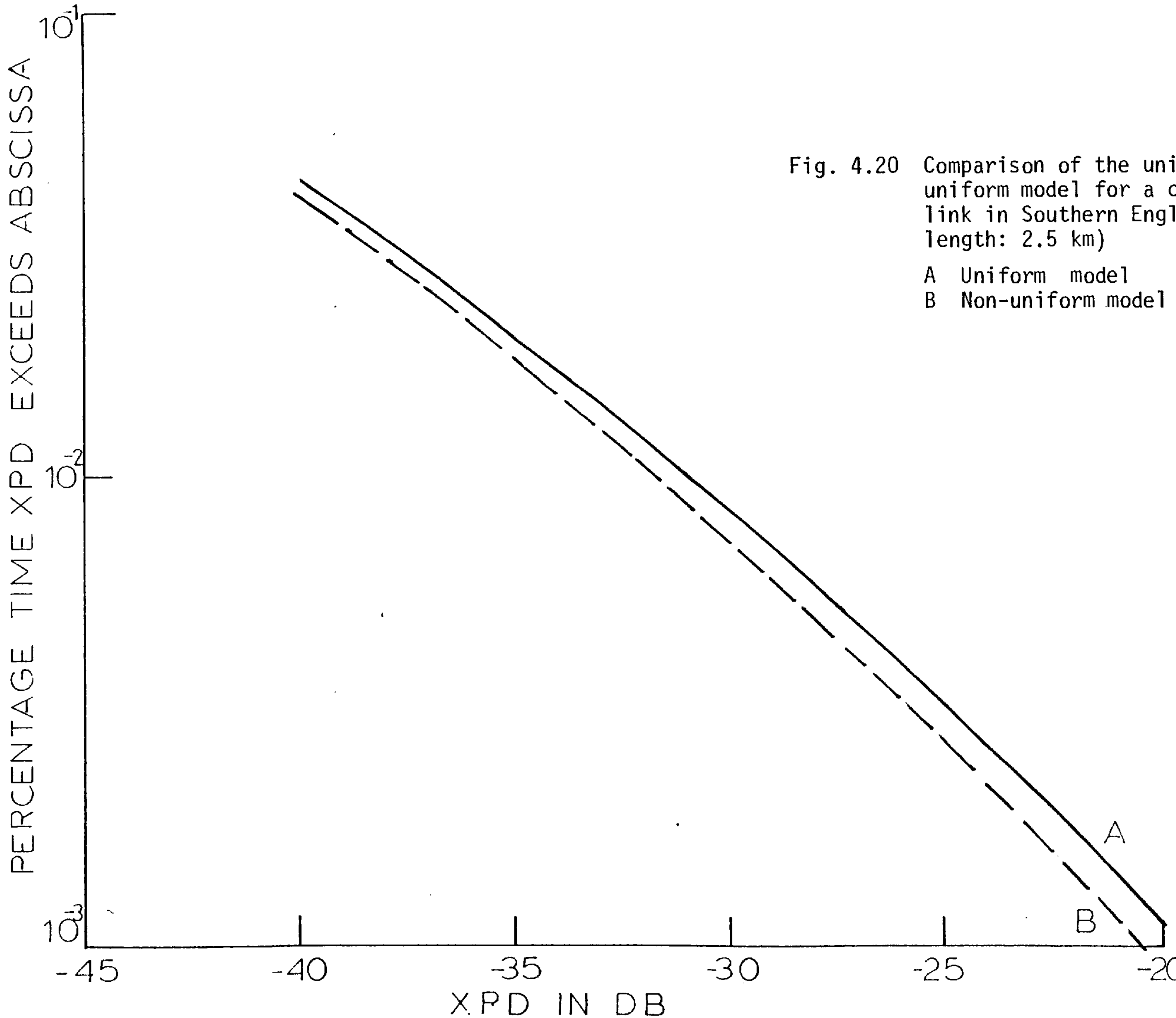

Fig. 4.20 Comparison of the uniform and non-uniform model for a communication link in Southern England (path length: 2.5 km)

A Uniform model
B Non-uniform model

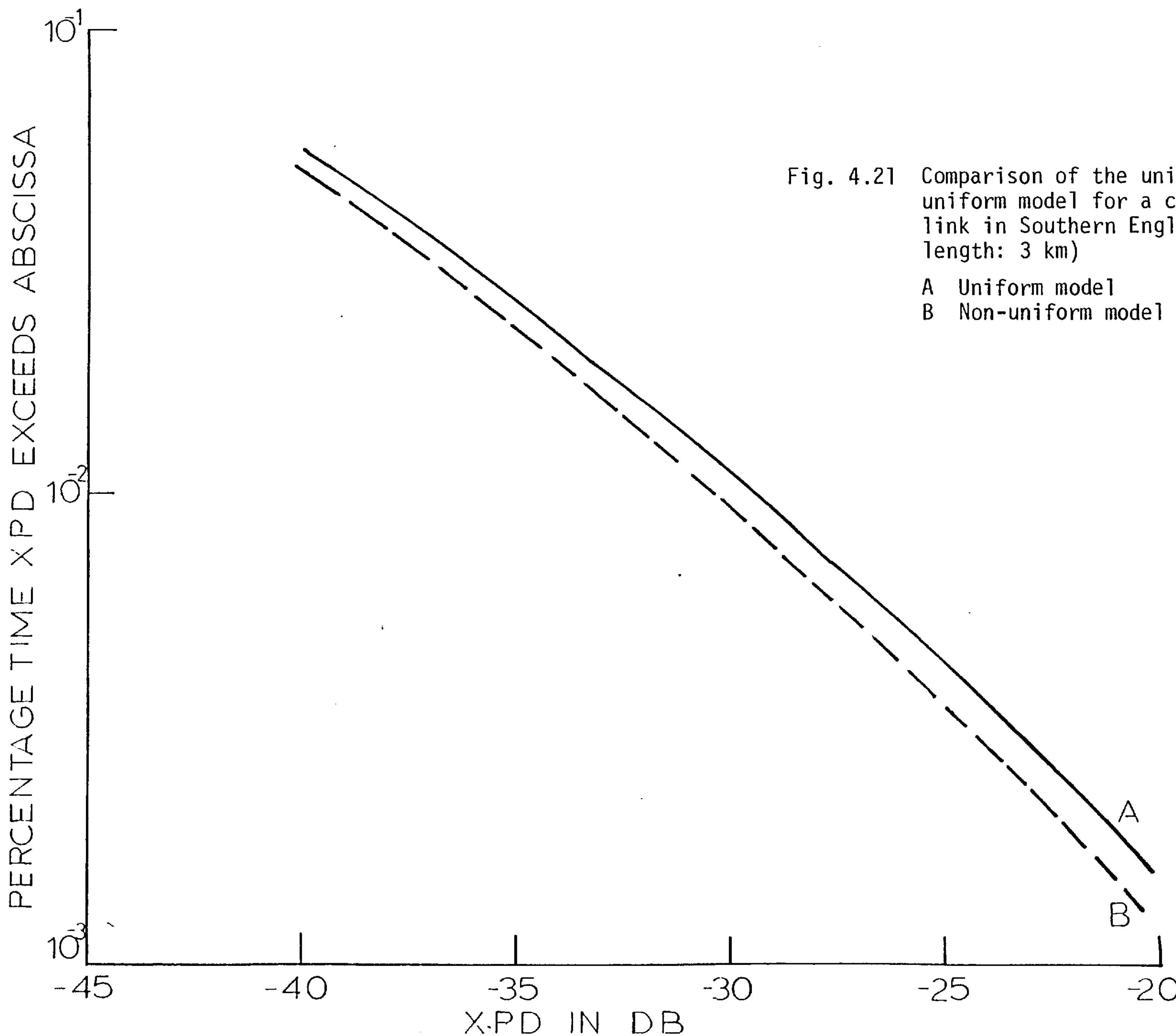

Fig. 4.21 Comparison of the uniform and non-uniform model for a communication link in Southern England (path length: 3 km)

A Uniform model
B Non-uniform model

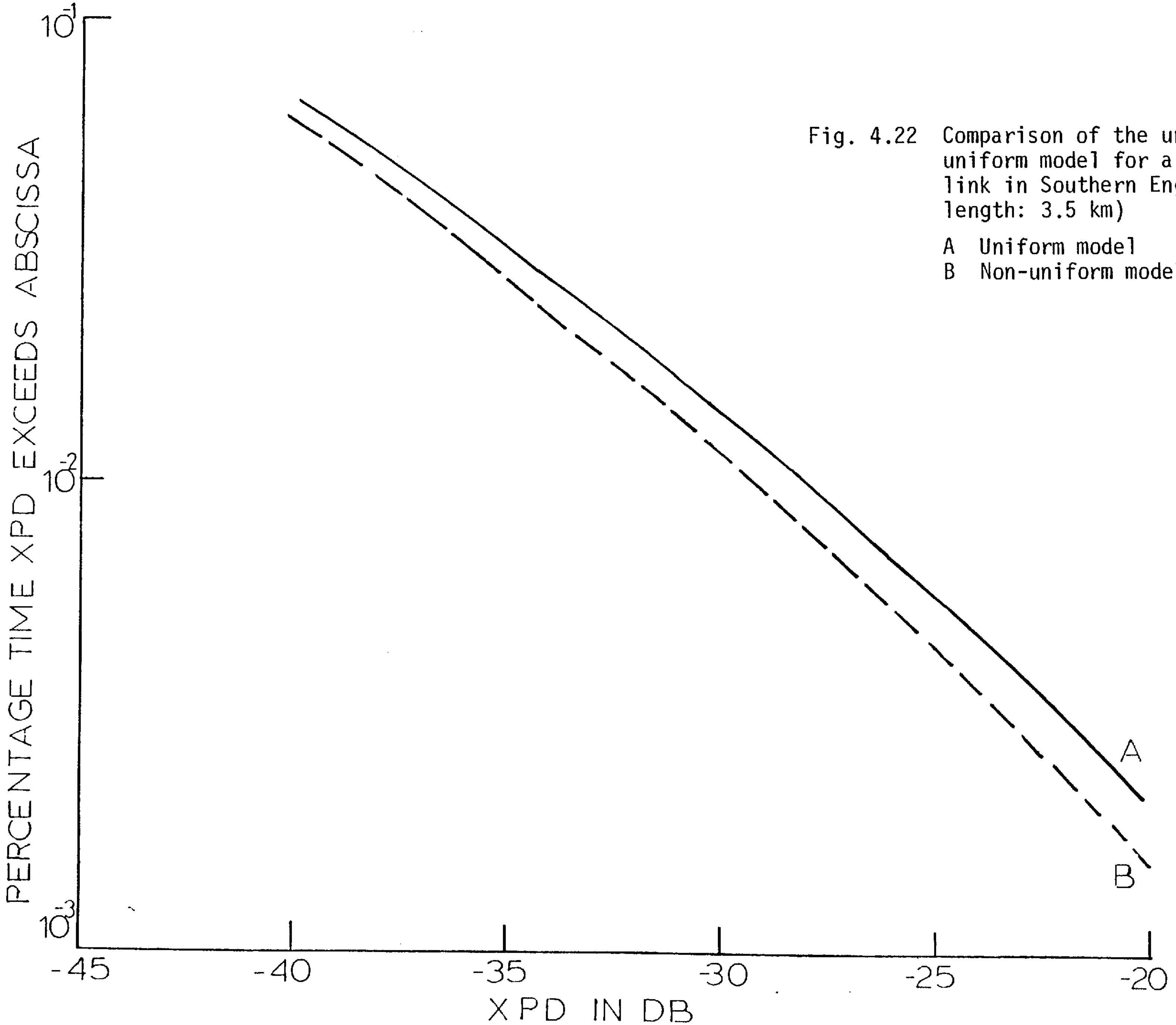

Fig. 4.22 Comparison of the uniform and non-uniform model for a communication link in Southern England (path length: 3.5 km)

A Uniform model
B Non-uniform model

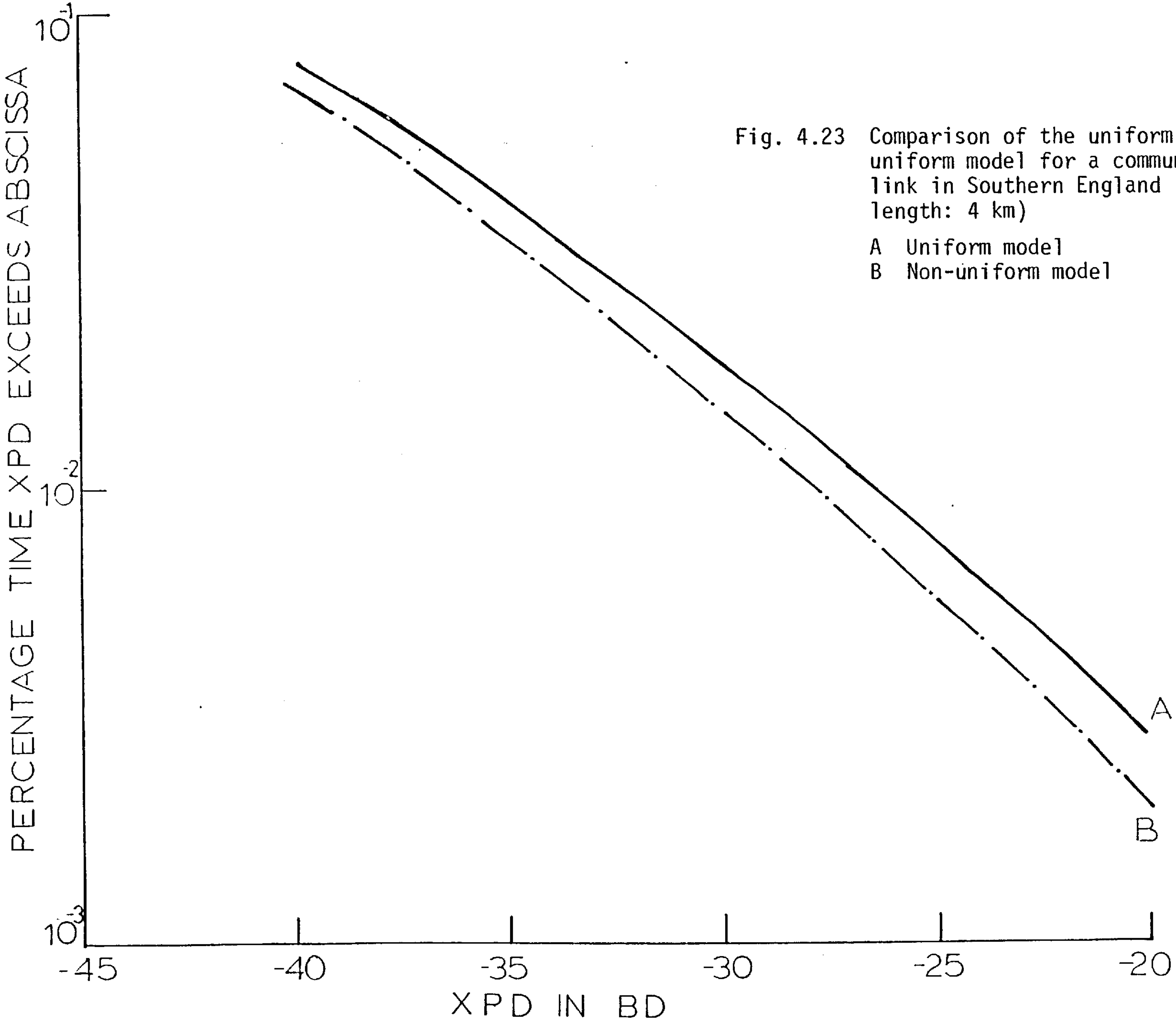

Fig. 4.23 Comparison of the uniform and non-uniform model for a communication link in Southern England (path length: 4 km)

A Uniform model
B Non-uniform model

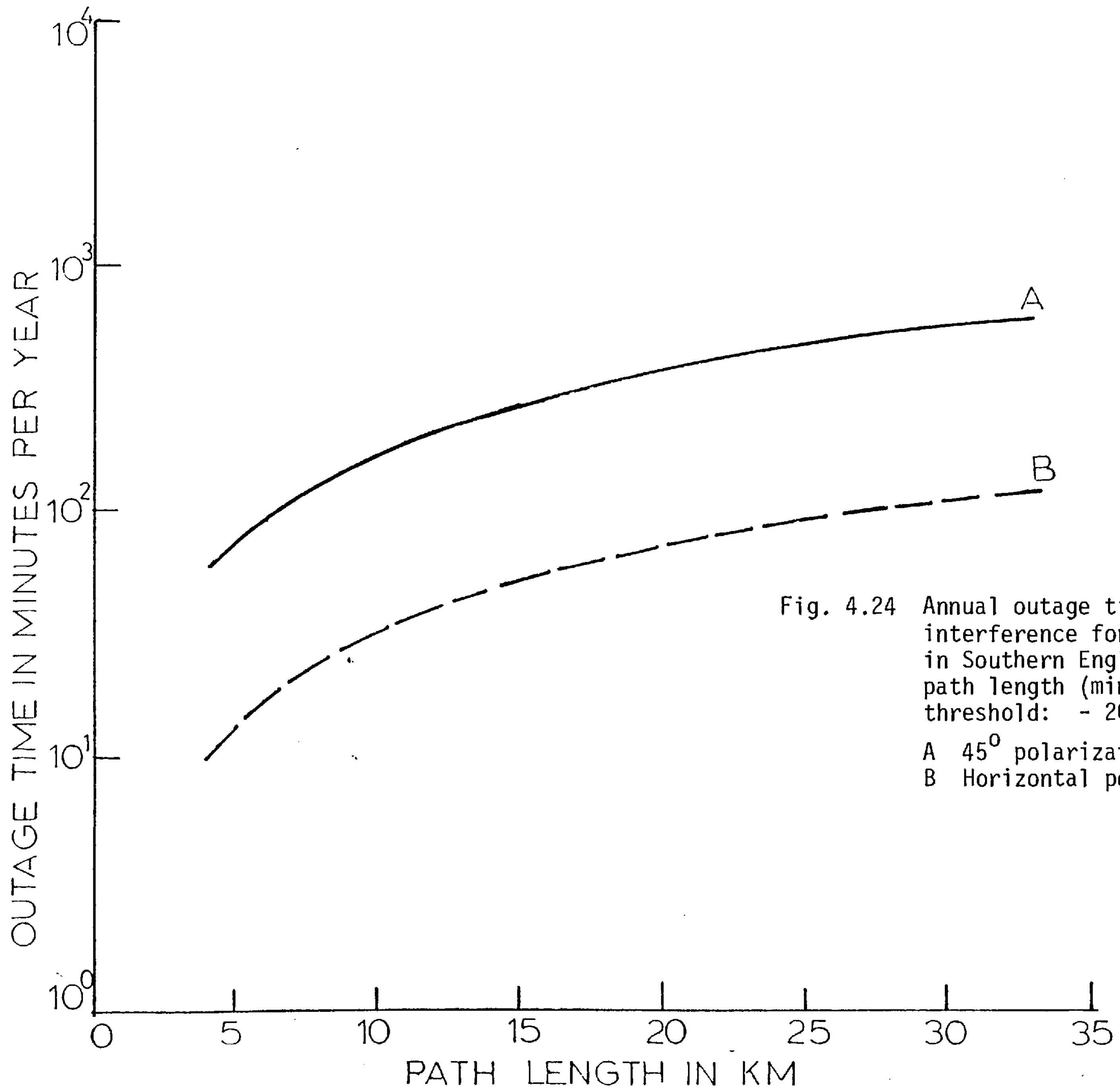

Fig. 4.24 Annual outage time due to channel interference for a communication link in Southern England as a function of path length (minimum acceptable XPI threshold: - 20 db, non-uniform case)

A 45° polarization
B Horizontal polarization

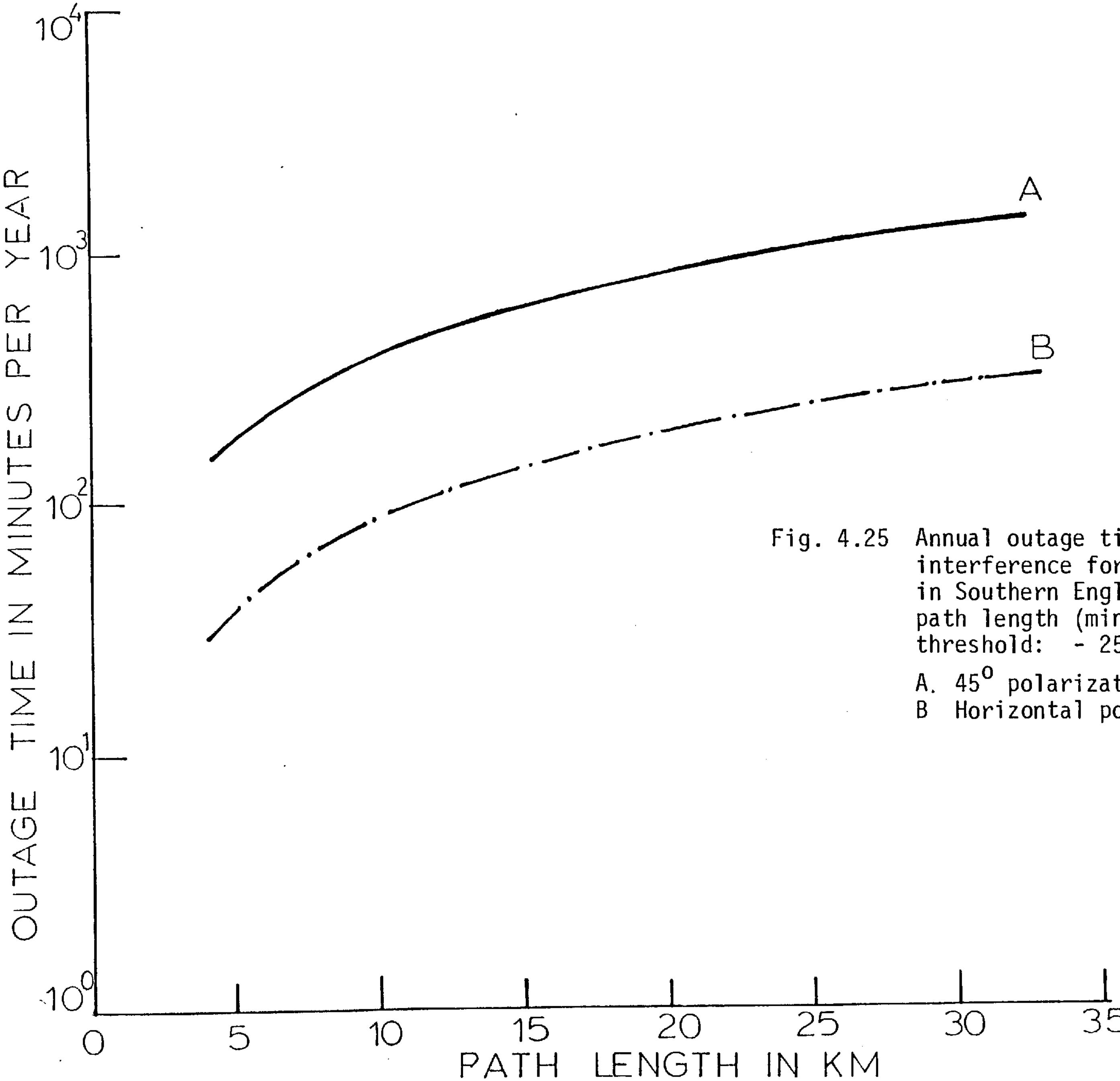

Fig. 4.25 Annual outage time due to channel interference for a communication link in Southern England as a function of path length (minimum acceptable XPI threshold: - 25 db, non-uniform case)

A. 45^{o} polarization
B Horizontal polarization

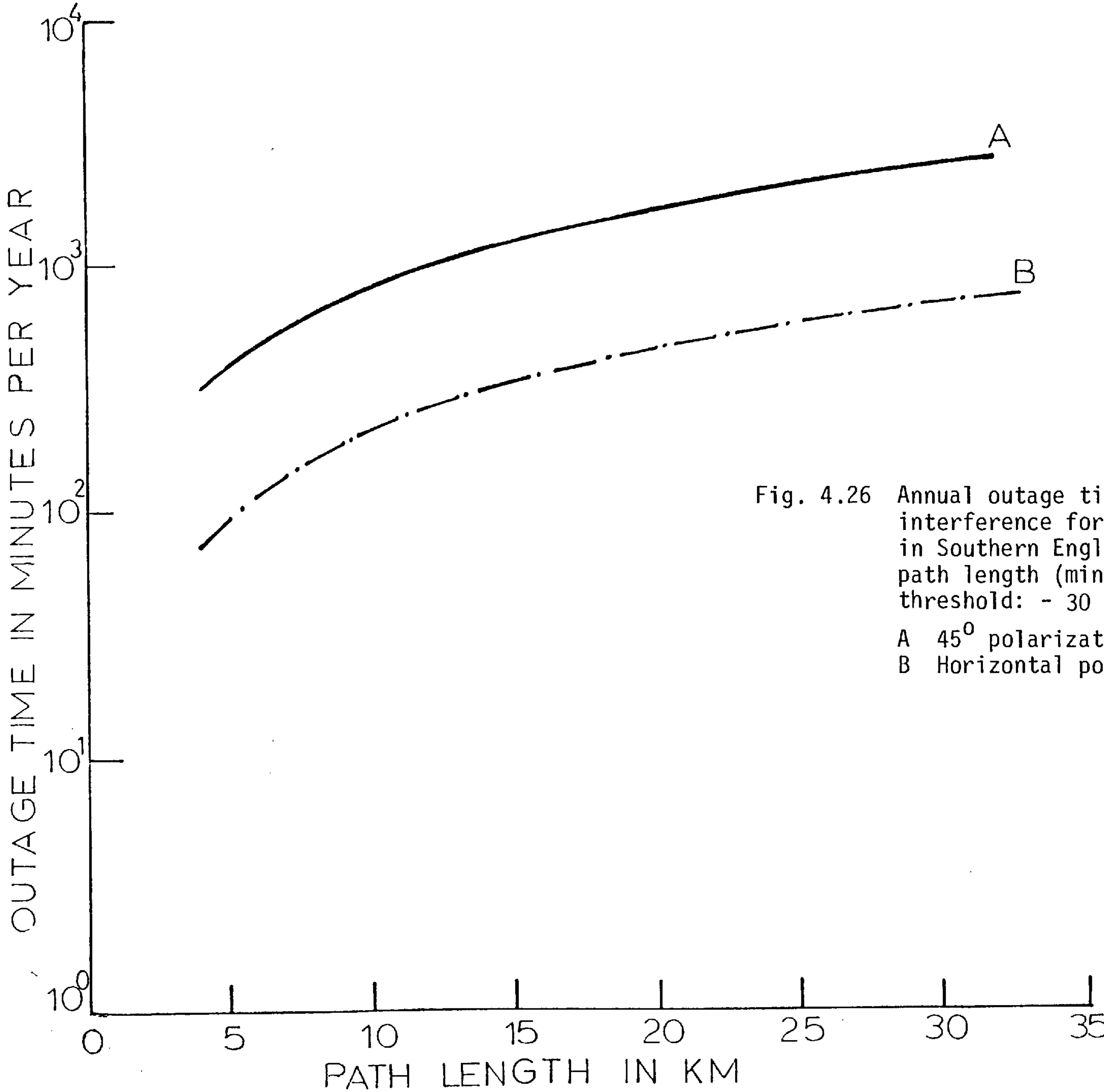

Fig. 4.26 Annual outage time due to channel interference for a communication link in Southern England as a function of path length (minimum acceptable XPI threshold: - 30 db, non-uniform case)

A 45^0 polarization
B Horizontal polarization

4.3.4 Concluding Remarks

A numerical method for estimating the long-term first-order statistics of cross-polarization isolation or discrimination of a signal after propagation through a rain medium has been presented here. This method uses a spatially non-uniform model for the rainfall rate and so it has applicability for all lengths of microwave links.

For reasons of comparison, the two methods (uniform and non-uniform) are used for the evaluation of the excess probability of XPI or XPD for a microwave link, and it is obvious that the results are almost identical for at least a path length up to 2 km, or with a small discrepancy, up to 4 km.

Estimations of annual radio outage time because of channel interference are also shown for various acceptable cross-polarization levels (- 20 db, - 25 db and - 30 db) as a function of path length in km.

CHAPTER 5

ANALYSIS OF THE JOINT STATISTICS OF RAIN DEPOLARIZATION AND ATTENUATION, APPLIED TO THE PREDICTION OF RADIO LINK PERFORMANCE

Introduction

In the previous chapters, a normal form for the long-term distribution of cross-polarization discrimination (XPD) or isolation (XPI) during rain has been established and methods to evaluate the parameters of this distribution have been considered. In the present chapter, an analysis of the joint statistics of rain depolarization and attenuation is derived, based on the previous results for the XPD and known results for the attenuation distribution. In the first section, a method of estimating the statistical parameters of the long-term rain attenuation distribution is described, which is equivalent to the one proposed by Lin (1975). A theoretical formula for the joint density function is then established, using the properties of Jacobian transformation of two-dimensional statistical distributions (Papoulis, 1965).

An important application of this formula is in the evaluation of the distribution of XPD conditional on the co-polar rain attenuation. Using Bayes' theorem, this distribution is shown to be normal. The mean value of this distribution gives us a best estimate of XPD at a given rain attenuation. Comparison of these results with data from Atlanta, Georgia and Southern England shows very good agreement.

Another important application is in the prediction of the distribution of XPD during a rain fade. By periods of rain fade, we mean that in all this time the XPD must be worse than the clear-air XPD of the system C and the rain attenuation less than the fade margin D.

This probability can be evaluated by calculating a double integral of the joint density function. This integration, which involves the treatment of some singularities, is calculated using Gauss-Laguerre polynomials. Experimental verification is also provided by data from a microwave link in Atlanta, Georgia.

Finally, the third application of this joint statistics analysis is in the precise prediction of the outage time of a microwave communication system for a location where the effects of rain are dominant. Lin (1975) has established a method of finding the outage time for a single polarization microwave system considering only the rain attenuation. In this chapter, the case of a dual-polarization system is analysed and the interference caused by the orthogonal channel is taken into account. The exact calculation requires the evaluation of a double integral of the joint density function of the same type as above, so we can use the previous results for this numerical integration. Curves of outage time as a function of path length are plotted for different minimum acceptable XPD thresholds (- 30, - 25 and - 20 db).

5.1 Calculation of Statistical Parameters of Rain Attenuation Distribution

We will consider here that the rain attenuation is a random process in time, which has not appreciable fluctuations on a short-term basis (in other words, at a constant space-averaged rainfall rate $\overline{R}$) (Oguchi, 1961). So, if a(L) is the path attenuation for a microwave link of length L, then we define:-

$$X_2 = a(L) \cong \langle CPA \rangle_s = \alpha \overline{R}^b L \qquad (5.1.1)$$

where the short-term mean value of the co-polar attenuation can be taken as given by expression (2.5.22).

The long-term statistics of X_2 can now be predicted from the statistics of the variable $\overline{R}$ as (Aitchison and Brown, 1965):-

$$\left.\begin{aligned} a_m &= \alpha \overline{R}_m^b L \\ S_a &= bS_{\overline{R}} \end{aligned}\right\} \tag{5.1.2}$$

where a_m is the median value of the log-normal distribution of X_2 during rain and S_a the standard deviation of $\ln X_2$. The parameters $\overline{R}_m$ and $S_{\overline{R}}$ can be taken from expressions (4.2.19) and (4.2.21) and the final result is:-

$$\left.\begin{aligned} a_m &= \alpha R_m^b L \left(\frac{P_o(0)}{P_o(L)}\right)^b \exp\left[\frac{bS_R^2 - bS_{\overline{R}}^2}{2}\right] \\ S_a &= bS_{\overline{R}} \end{aligned}\right\} \tag{5.1.3}$$

where the standard deviation $S_{\overline{R}}$ is given by:-

$$S_{\overline{R}}^2 = \ln\left[P_o(L)\left[1 + \left(\left(e^{S_R^2}/P_o(0)\right) - 1\right) H'(L)\right]\right] \tag{5.1.4}$$

The density distribution function for the variable X_2 will be:-

$$p_{X_2}(x_2) = \frac{1}{\sqrt{2\pi}\, S_a\, x_2} \exp\left(- \frac{(\ln x_2 - \ln a_m)^2}{2S_a^2}\right) \tag{5.1.5}$$

Lin (1975) has proposed for the evaluation of the same parameters a_m and S_a the following formulas:-

$$\left.\begin{aligned} S_a^2(L) &= \ln\left\{P_o(L)\left[1 + H_1(L)\left[\frac{\exp(S_b^2)}{P_o(0)} - 1\right]\right]\right\} \\ a_m(L) &= b_m L\,\frac{P_o(0)}{P_o(L)}\exp\left[\frac{S_b^2 - S_a^2}{2}\right] \end{aligned}\right\} \qquad (5.1.6)$$

where $H_1(L)$ is a function of path length L and is related to the spatial correlation coefficient between the rainfall rates at two points across the path (Lin, 1975). For radio links using frequencies above 10 GHz, the following approximate formula applies:-

$$H_i(L) \cong (2G^2/L^2)\left\{(L/G)\ln\left[(L/G) + \sqrt{1 + (L^2/G^2)}\right] - \sqrt{1 + (L^2/G^2)} + 1\right\} \qquad (5.1.7)$$

where G is a characteristic distance for the spatial correlation coefficient and empirically has the value G = 1.5 km (Chapter 4).

Coming back again to formula (5.1.6), the parameters b_m and S_b are expressed as follows:-

$$\left.\begin{aligned} b_m &= \alpha R_m^b \\ S_b &= b S_R \end{aligned}\right\} \qquad (5.1.8)$$

where the regression coefficients α and b are the same as those encountered in formulas (5.1.1) and (5.1.2).

A direct comparison of Equations (5.1.3) and (5.1.6) shows that these formulas are almost identical, because the regression parameter b in all cases takes values approximately equal to 1 (Chapter 2).

5.2 Theoretical Analysis of the Joint Statistics of XPD and Rain Attenuation

The cross-polarization discrimination (XPD) and attenuation due to rain for a microwave radio link are correlated random processes. In the previous section, the formulas for calculating the parameters of the rainfall rate (R) statistics, have been presented. In addition, a normal form for the distribution of XPD has been proposed and a numerical method to evaluate the parameters (mean and variance) of this distribution for any microwave link has been developed (Chapters 3 and 4). A theoretical formula is now proposed for the evaluation of the joint statistics of XPD and attenuation during rain. Defining:-

$$\left.\begin{aligned} X_1 &= XPD(L) \\ X_2 &= a(L) \\ X_3 &= \ln a(L) \end{aligned}\right\} \qquad (5.2.1)$$

then the density distribution functions for the random variables X_1 and X_2 will be:-

$$\left.\begin{aligned} p_{X_1}(x_1) &= (1/\sqrt{2\pi}\,\sigma_1)\exp\left[-\frac{(x_1 - \langle X_1\rangle)^2}{2\sigma_1^2}\right] \\ p_{X_2}(x_2) &= \frac{1}{\sqrt{2\pi}\,S_a\,x_2}\exp\left[-\frac{(\ln x_2 - \ln a_m)^2}{2S_a^2}\right] \end{aligned}\right\} \qquad (5.2.2)$$

where $\langle X_1\rangle$ is the mean value of XPD during rain, σ_1 is the standard deviation of this distribution.

The density function for the variable X_3 will now be:-

$$p_{X_3}(x_3) = \left(\frac{1}{\sqrt{2\pi}\,\sigma_3}\right) \exp\left(-\frac{(x_3 - \langle X_3\rangle)^2}{2\sigma_3^2}\right) \tag{5.2.3}$$

This is a normal form with parameters:-

$$\left.\begin{aligned} \langle X_3\rangle &= \ln a_m \\ \sigma_3 &= S_a \end{aligned}\right\} \tag{5.2.4}$$

Hence, the random variables X_1 and X_3 will be marginally normal. A reasonable assumption for their joint density function is that this must be a two-dimensional normal (Papoulis, 1965) and will have the form of:-

$$p_{X_1X_3}(x_1, x_3) = \frac{1}{2\pi\,\sigma_1\sigma_3\sqrt{1 - r^2_{X_1X_3}}} \exp\left(\left(-1/2\,(1 - r^2_{X_1X_3})\right)\right.\,.$$

$$\left.\cdot\left[\frac{(x_1 - \langle X_1\rangle)^2}{\sigma_1^2} - \frac{2r_{X_1X_3}(x_1 - \langle X_1\rangle)(x_3 - \langle X_3\rangle)}{\sigma_1\,\sigma_3} + \frac{(x_3 - \langle X_3\rangle)^2}{\sigma_3^2}\right]\right) \tag{5.2.5}$$

with $r_{X_1X_3}$ the correlation coefficient between the two random variables X_1 and X_3. A method for estimating this coefficient for any microwave link will be presented in the following section of this chapter. Intuitively, we believe that this coefficient must be related to the parameters of the radio link such as frequency, type of polarization, characteristics of rainfall rate (R_m, S_R) in the specified location of the radio link.

Our purpose is the calculation of the joint statistics of the variables X_1 and X_2, so at this point the following important theorem from statistics can be used (Papoulis, 1965). If the joint statistics of the random variables X and Y is known, and the variables Z and W are analytic functions of X and Y, such as:-

$$\left.\begin{aligned} Z &= g(X, Y) \\ W &= h(X, Y) \end{aligned}\right\} \tag{5.2.6}$$

then the joint density function $p_{ZW}(z, w)$ can be evaluated in terms of the known joint density function $p_{XY}(x, y)$ as follows:-

$$p_{ZW}(z, w) = \frac{p_{XY}(x_1, y_1)}{|J(x_1, y_1)|} + \; . \; . \; . \; . \; + \frac{p_{XY}(x_n, y_n)}{|J(x_n, y_n)|} \tag{5.2.7}$$

where:-

$$J(x, y) \equiv \begin{vmatrix} \partial g(x, y)/\partial x & \partial g(x, y)/\partial y \\ \partial h(x, y)/\partial x & \partial h(x, y)/\partial y \end{vmatrix} \tag{5.2.8}$$

is the Jacobian of the transformation and (x_1, y_1), (x_2, y_2) .... (x_n, y_n) are all the pairs of real solutions of the equations:-

$$\left.\begin{aligned} g(x, y) &= z \\ h(x, y) &= w \end{aligned}\right\} \tag{5.2.9}$$

In our case, the transformation is the following:-

$$\left.\begin{aligned} X_1 &= X_1 \\ X_2 &= \exp(X_3) \end{aligned}\right\} \tag{5.2.10}$$

and the joint density function of variables X_1 and X_3 is given by Equation (5.2.5). Applying relation (5.2.7), then the joint density function $p_{X_1X_2}(x_1, x_2)$ will be:-

$$p_{X_1X_2}(x_1, x_2) = \frac{p_{X_1X_3}(x_1', x_3')}{|J(x_1', x_3')|} \tag{5.2.11}$$

where (x_1', x_3') is the only real solution of the system:-

$$\left.\begin{aligned} x_1 &= x_1 \\ e^{x_3} &= x_2 \end{aligned}\right\} \tag{5.2.12}$$

or:-

$$\left.\begin{aligned} x_1' &= x_1 \\ x_3' &= \ln x_2 \end{aligned}\right\} \tag{5.2.13}$$

so:-

$$|J(x_1', x_3')| = x_2 \tag{5.2.14}$$

After that, substituting relations (5.2.5), (5.2.13), (5.2.14) to (5.2.11), we will have:-

$$p_{X_1X_2}(x_1, x_2) = \frac{1}{2\pi\,\sigma_1\,\sigma_3\sqrt{1 - r^2_{X_1X_3}}\;x_2} \exp\left[-\frac{1}{2(1 - r^2_{X_1X_3})}\right.\,.$$

$$\cdot \left[\frac{(x_1 - \langle X_1\rangle)^2}{\sigma_1^2} - \frac{2r_{X_1X_3}(x_1 - \langle X_1\rangle)(\ln x_2 - \langle X_3\rangle)}{\sigma_1\sigma_3} + \frac{(\ln x_2 - \langle X_3\rangle)^2}{\sigma_3^2}\right]\Bigg) \tag{5.2.15}$$

This theoretical formula has many applications in the prediction of the performance of a radio link as it will be shown in the next section.

5.3 Applications of the Analysis

5.3.1 Prediction of the Distribution of XPD Conditional on the Co-Polar Rain Attenuation

An important application of the formula (5.2.15) is in the precise prediction of cross-polarization discrimination XPD at a given rain attenuation. This factor must be kept in mind when median values of cross-polarization discrimination at given rain fades are used for the design of a dual-polarization radio communication system (Chu, 1974). This can be done by using the conditional density distribution function $p_{X_1}(x_1|X_2 = D)$ where D is a specified rain fade level in db. By Bayes' theorem in statistics (Papoulis, 1965), this conditional function can be evaluated as follows:-

$$p_{X_1}(x_1|X_2 = D) = p_{X_1X_2}(x_1, D)/p_{X_2}(D) \tag{5.3.1}$$

By substituting $p_{X_1X_2}$ and p_{X_2} from relations (5.2.2) and (5.2.15) we have that:-

$$p_{X_1}(x_1|X_2 = D) = \frac{1}{2\pi\,\sigma_1\,\sigma_3\sqrt{1 - r^2_{X_1X_3}}\;D} \exp\Bigg\{\left(- 1/2(1 - r^2_{X_1X_3})\right) \cdot$$

$$\cdot \left[\frac{(x_1 - \langle X_1\rangle)^2}{\sigma_1^2} - \frac{2r_{X_1X_3}(x_1 - \langle X_1\rangle)(\ln D - \langle X_3\rangle)}{\sigma_1\sigma_3} + \frac{(\ln D - \langle X_3\rangle)^2}{\sigma_3^2}\right]\Bigg) \Bigg/$$

$$\Bigg/ \left[\frac{1}{\sqrt{2\pi}\,\sigma_3\, D} \exp\left(-\frac{(\ln D - \langle X_3\rangle)^2}{2\sigma_3^2}\right)\right] = \frac{1}{\sqrt{2\pi}\,\sigma_1\sqrt{1 - r^2_{X_1X_3}}} \cdot$$

$$\cdot \exp\left(\left(-1\Big/\left[2\sigma_1^2(1 - r^2_{X_1X_3})\right]\right) \cdot \left[x_1 - \langle X_1\rangle - r_{X_1X_3}\left(\frac{\sigma_1}{\sigma_3}\right)(\ln D - \langle X_3\rangle)\right]^2\right) \tag{5.3.2}$$

This is a normal distribution with mean and variance given by:-

$$\left.\begin{aligned} E\left[X_1 | X_2 = D\right] &= \langle X_1\rangle + r_{X_1X_3}\left(\frac{\sigma_1}{\sigma_3}\right)(\ln D - \langle X_3\rangle) \\ \operatorname{var}\left[X_1 | X_2 = D\right] &= \sigma_1^2(1 - r^2_{X_1X_3}) \end{aligned}\right\} \tag{5.3.3}$$

At this point, we turn to the estimation of the correlation coefficient $r_{X_1X_3}$. If we consider that the rain attenuation is a random process in time which has no appreciable fluctuations in the short-term (as in Section 5.1), then:-

$$X_2 \cong \alpha \overline{R}^b L \tag{5.3.4}$$

and, for a constant value D of the variable X_2, we will have:-

$$\overline{R} = \exp\left(\frac{\ln\left(\frac{D}{\alpha L}\right)}{b}\right) = \text{constant} = C_1 \tag{5.3.5}$$

Hence, from formulas (4.1.24), (4.2.24):-

$$X = 10 \log \Omega = 10 \log (A\overline{R}^B) = C_2 = \text{constant} \tag{5.3.6}$$

So:-

$$p_{X_1}(x_1|X_2 = D) \cong p_{X_1}(x_1|X = C_2) \tag{5.3.7}$$

But the conditional density $p_{X_1}(x_1|X = C_2)$ is the log of a Rayleigh variable (expressions (4.2.30) and (4.2.31)). From Nakagami (1960), we have that such a distribution for $x_1 \leq M'$ approaches the form of a normal distribution:-

$$p_{X_1}(x_1|X = C_2) = \frac{1}{M'}\sqrt{\frac{2}{\pi}}\, e^{-2(C_2 - x_1)^2/M'^2} \tag{5.3.8}$$

with parameters:-

$$\left.\begin{aligned} E\left[X_1|X = C_2\right] &= C_2 \\ \text{var}\left[X_1|X = C_2\right] &= \frac{M'^2}{4} \end{aligned}\right\} \tag{5.3.9}$$

A direct comparison of formulas (5.3.3) and (5.3.9) gives us the correlation coefficient $r_{X_1X_3}$ as:-

$$r_{X_1X_3} = \sqrt{1 - \frac{M'^2}{4\sigma_1^2}} \tag{5.3.10}$$

where the standard deviation σ_1 can be calculated theoretically by means of the method which is presented analytically in the previous Chapters 3 and 4. From up-to-date results from the USA and Southern England, the range of values of r has been found to lie between 0.96 - 0.98. In other words, this result shows that there is strong correlation between the two random processes of cross-polarization and co-polar attenuation during rain.

The function $g(D) = E\left[X_1 | X_2 = D\right]$ is known as the regression curve and serves as a mean-square estimation of the random variable X_1 in terms of variable X_2. From Papoulis (1965), we have that this estimation of the random variable X_1 by a suitable function $g(X_2)$ of the variable X_2 is such that the mean-square estimation error:-

$$E\left[\left(X_1 - g(X_2)\right)^2\right] \equiv \int_{-\infty}^{\infty}\int_{-\infty}^{\infty} \left(x_1 - g(x_2)\right)^2 p_{X_1 X_2}(x_1, x_2)\, dx_1\, dx_2 \qquad (5.3.11)$$

is minimum. Regression curves of XPD against co-polar rain attenuation are drawn in the thesis for different paths in Southern England and the USA. A more analytic configuration of the results will be presented in the later Section 5.4.

5.3.2 Prediction of the Distribution of XPD During a Rain Fade

Another important application of the formula (5.2.15) is in the precise prediction of total XPD distribution during periods of rain fades. By this term "periods of rain fade", we mean that in all this time the XPD of the received signal is greater than a specified level C (this is approximately the clear air XPD of the system) and the path rain attenuation is always less than another specified level D. This level is approximately:-

$$D = \text{Fade Margin - Loss due to radomes} \tag{5.3.12}$$

where the loss caused by radomes can be taken to be a few db as Lin (1975) and many other authors have predicted it to be. This XPD can be expressed in mathematical terms as:-

$$P\left[\{X_1 \geq x_1\}/\{X_1 \geq C,\ X_2 \leq D\}\right] \tag{5.3.13}$$

By Bayes' theorem (Papoulis, 1965), this probability can be expressed as:-

$$P\left[\{X_1 \geq x_1\}/\{X_1 \geq C,\ X_2 \leq D\}\right] = P\left[\{X_1 \geq x_1,\ X_2 \leq D\}\right] /$$

$$/\ P\left[\{X_1 \geq C,\ X_2 \leq D\}\right] \tag{5.3.14}$$

where $x_1 \geq C$ and common values for C are - 40 db or - 35 db depending on the system design.

The crucial point at this moment is the calculation of the joint probabilities $P\left[\{X_1 \geq x_1,\ X_2 \leq D\}\right]$ and $P\left[\{X_1 \geq C,\ X_2 \leq D\}\right]$. We have that:-

$$P\left[\{X_1 \geq C,\ X_2 \leq D\}\right] \equiv \int_C^{\infty} \int_0^D p_{X_1 X_2}(x_1,\ x_2)\ dx_1\ dx_2 \tag{5.3.15}$$

The integral (5.3.15) can be evaluated as follows, using (5.2.15) as:-

$$I(C,\ D) \equiv \int_C^{\infty} \int_0^D p_{X_1 X_2}(x_1,\ x_2)\ dx_1\ dx_2 =$$

$$= \int_0^D \frac{1}{2\pi\, \sigma_1\, \sigma_3 \sqrt{1 - r^2_{X_1 X_3}}\; x_2} \exp\left(\left(- \frac{1}{2(1 - r^2_{X_1 X_3})}\right)\left[\frac{(\ln x_2 - \langle X_3\rangle)^2}{\sigma_3^2}\right]\right) .$$

$$. \left[\int_C^\infty \exp\left(\left(- \frac{1}{2(1 - r^2_{X_1 X_3})}\right) . \left[\frac{(x_1 - \langle X_1\rangle)^2}{\sigma_1^2} -\right.\right.\right.$$

$$\left.\left.\left. - \frac{2r_{X_1 X_3}(x_1 - \langle X_1\rangle)(\ln x_2 - \langle X_3\rangle)}{\sigma_1\, \sigma_3}\right]\right) dx_1\right] dx_2 \qquad (5.3.16)$$

The two parts of the integral (5.3.16) are treated analytically in Appendix E and the final result is (expression E-8):-

$$I(C, D) = \int_{-\ln D}^\infty e^{-Y} f(Y)\, dY \qquad (5.3.17)$$

where the function f(Y) is given by (expression E-9):-

$$f(Y) = \frac{1}{2\sqrt{2\pi}\, \sigma_3} \exp\left(- \frac{(Y + \langle X_3\rangle)^2}{2\sigma_3^2} + Y\right) .$$

$$. \operatorname{erfc}\left[\frac{(C - \langle X_1\rangle)}{\sqrt{2}\sqrt{1 - r^2_{X_1 X_3}}\;\sigma_1} + \frac{r_{X_1 X_3}(Y + \langle X_3\rangle)}{\sqrt{2}\sqrt{1 - r^2_{X_1 X_3}}\;\sigma_3}\right] \qquad (5.3.18)$$

The other joint density function:-

$$I(x_1, D) \equiv \int_{x_1}^{\infty} \int_{0}^{D} p_{X_1X_2}(x_1, x_2)\, dx_1\, dx_2 \tag{5.3.19}$$

is again given by:-

$$I(x_1, D) = \int_{-\ln D}^{\infty} e^{-Y} f_1(Y)\, dY \tag{5.3.20}$$

with:-

$$f_1(Y) = \frac{1}{2\sqrt{2\pi}\,\sigma_3} \exp\left[-\frac{(Y + \langle X_3 \rangle)^2}{2\sigma_3^2} + Y\right] .$$

$$. \operatorname{erfc}\left[\frac{(x_1 - \langle X_1 \rangle)}{\sqrt{2}\sqrt{1 - r^2_{X_1X_3}}\,\sigma_1} + \frac{r_{X_1X_3}(Y + \langle X_3 \rangle)}{\sqrt{2}\sqrt{1 - r^2_{X_1X_3}}\,\sigma_3}\right] \tag{5.3.21}$$

The two integrals (5.3.17) and (5.3.20) are evaluated numerically by using Gauss-Laguerre polynomials, as explained analytically in Appendix E. A presentation of the numerical results is given in the later Section 5.4.

5.3.3 Estimation of the Outage Time of a Dual-Polarization Microwave Communication System

For a working microwave communication system, various factors can generally cause outage such as rain, multipath interference, etc. In general, for the systems with frequency less than 10 GHz, the multipath interference is the most important factor for its design and performance. On the other hand, systems with $f > 10$ GHz are influenced mainly by the effects of the rain. For such systems, radio outage occurs when the path rain attenuation exceeds the clear day fade margin F_0. For a constant transmitter power, the dependence of fade margin $F_0(L)$ in db on the path length L is:-

$$F_0(L) = F_0(L_0) - 20 \log_{10}(L/L_0) \qquad \text{in db} \tag{5.3.22}$$

where L_0 is a reference repeater spacing and $F_0(L_0)$ is the corresponding reference fade margin. For 11 and 18 GHz radio systems, reasonable clear-day reference fade margins are:-

$$\left.\begin{aligned} F_0 &= 40 \text{ db for 18 GHz at } L_0 = 4 \text{ km} \\ F_0 &= 40 \text{ db for 11 GHz at } L_0 = 40 \text{ km} \end{aligned}\right\} \tag{5.3.23}$$

Lin (1975) has calculated the probability of radio outage time per hop as a function of repeater spacing L by substituting the fade margin $F_0(L)$ into the rain attenuation distribution as:-

$$P\left[X_2 \geq F_0(L)\right] = P_0(L) \;.\; P\left[\{X_2 \geq F_0(L)\}\right] \tag{5.3.24}$$

where:-

$$P\left[\{X_2 \geq F_0(L)\}\right] = \left(\frac{1}{2}\right) \operatorname{erfc}\left[\frac{(\ln F_0(L) - \langle X_3\rangle)}{\sqrt{2}\,\sigma_3}\right] \tag{5.3.25}$$

is the complementary of the distribution function of random variable X_2.

This is the situation for a single-polarization communication system. But for a dual-polarization system, we must consider the interference caused by the orthogonal channel too. So, the most convenient method is to use the joint distribution function of XPD and rain attenuation as given by formula (5.2.15). We can now evaluate the probability of radio outage by means of this joint distribution function. This probability can be given as:-

$$P\left[\text{outage of the system}\right] = P_0(L) \cdot \left[P\left[\{X_2 \geq F_0(L)\}\right] + \right.$$

$$\left. + P\left[\{X_1 \geq C_1, X_2 < F_0(L)\}\right]\right] \tag{5.3.26}$$

where $P\left[\{X_1 \geq C_1, X_2 < F_0(L)\}\right]$ is the joint probability during rain that the XPD will exceed a specified threshold C_1 in db and concurrently the rain attenuation is less than the fade margin $F_0(L)$. In present 4 and 6 GHz radio relay systems, the maximum acceptable XPD level C_1 is - 20 db. However, future systems with an increased number of circuits per channel will require C_1 to be less than - 30 db XPD.

Coming back to the formula for the outage probability of the system, we have that $P\left[\{X_2 \geq F_0(L)\}\right]$ is given by formula (5.3.25) and:-

$$P\left[\{X_1 \geq C_1, X_2 < F_0(L)\}\right] \equiv \int_{C_1}^{\infty} \int_{0}^{F_0(L)} p_{X_1 X_2}(x_1, x_2)\, dx_1\, dx_2 \equiv I\left(C_1, F_0(L)\right) \tag{5.3.27}$$

This integral is of the same type as those in Equations (5.3.15) and (5.3.20), so using the results of Appendix E, we have that:-

$$I\left(C_1, F_0(L)\right) = \int_{-\ln F_0(L)}^{\infty} e^{-Y} f_2(Y)\, dY \tag{5.3.28}$$

with:-

$$f_2(Y) = \frac{1}{2\sqrt{2\pi}\,\sigma_3} \exp\left[-\frac{(Y + \langle X_3\rangle)^2}{2\sigma_3^2} + Y\right] .$$

$$. \ \mathrm{erfc}\left[\frac{(C_1 - \langle X_1\rangle)}{\sqrt{2}\sqrt{1 - r^2_{X_1X_3}}\ \sigma_1} + \frac{r_{X_1X_3}(Y + \langle X_3\rangle)}{\sqrt{2}\sqrt{1 - r^2_{X_1X_3}}\ \sigma_3}\right] \qquad (5.3.29)$$

and again integral (5.3.28) is evaluated numerically using Gauss-Laguerre polynomials. A presentation of the numerical results is given in the following Section 5.4.

5.4 Numerical Analysis and Results

All the numerical techniques which are used in this chapter are the same as those described in previous chapters. A special routine which computes a definite integral over a semi-infinite range, using the Gauss-Laguerre quadrature formula, is described here analytically. This routine is used for the evaluation of the integrals (5.3.17), (5.3.19) and (5.3.28).

Numerical results are given for a microwave link on 18 GHz sited at a location in Palmetto, Georgia, USA and for another one working on 11 GHz sited at a location in Southern England (Figs. 5.1 to 5.19)* In Figs. 5.1 and 5.2 plots of the profile of the joint density function as given by Equation (5.2.15), are shown for 1.5 km, 18 GHz terrestrial link with horizontal incident polarization, at Palmetto, Georgia. Regression curves of XPD against co-polar rain attenuation are drawn for different paths in Figs. 5.3 and 5.13. In Fig. 5.3, cross-polarization discrimination against attenuation is shown for a 8 km, 18 GHz terrestrial link situated at Palmetto, Georgia. In Fig. 5.13, calculations of the theoretical model for an 11 GHz, 18 km link

* These results are given in Sections 5.4.2 and 5.4.3.

situated in Southern England are compared with experimental measurements from an 11.6 GHz link at the University of Essex (Table 5.1). These curves have been calculated with an approximate correlation coefficient which is estimated by means of the formula (5.3.10). The values of the other parameters correspond to a Laws-Parsons drop-size distribution (Laws-Parsons, 1943), Pruppacher-Pitter size of raindrops (Pruppacher-Pitter, 1971) and for a Gaussian model of canting angle with a mean value ϕ and standard deviation σ_ϕ (Oguchi, 1977; Nowland et al, 1977). Different values for the standard deviation σ_ϕ are considered in Figs. 5.3 and 5.15 from 0^o - 40^o with a mean value $\phi = 10^o$, as has been proposed by many authors such as Watson and Arbabi (1973), Chu (1974) and recently by Nowland et al (1977). From Fig. 5.13, it is obvious that the most appropriate model of canting angle distribution for this particular link, is the equi-oriented one with $\sigma_\phi = 0^o$, where good agreement between theoretical and experimental points has been found.* This is because the situation of the link is such that the wind direction is 90^o with respect to the propagation axis and so this effect produces the worst case of depolarization (Uzunoglu et al, 1977).

Distributions of XPD conditional on co-polar rain attenuation are drawn for linear horizontal polarization. Specified levels of 20, 25, 30, 35 db are selected for a 5 km link operating at 18 GHz and situated at a location in Palmetto, Georgia where the rain parameters are R_m = 3.10 mm/hr, S_R = 1.18 (Lin, 1975). Theoretical curves are compared with experimental ones for the same link taken from Barnett (1972). The results are shown in Figs. 5.4, 5.5, 5.6 and 5.7 and the agreement is fairly good, especially with the theoretical curve, using the canting angle model $\sigma_\theta = 45^o$. The slight deviations mainly in the case of Fig. 5.5, can be explained by the short-term statistics of the received data (they cover only a period of 10 months). Similar

* It must be emphasised here that this argument should be weakened because the data points cover only one single event.

results for an 18 km link operating at 11 GHz situated in Southern England are shown in Figs. 5.14, 5.15, 5.16 and 5.17.

Theoretical probability distributions of XPD during a rain fade, are produced for the same 5 km link at Palmetto, Georgia operating at 18 GHz with horizontal polarization. A value of - 35 db for the clear-air XPD threshold C of the system is selected, but with different values for the rain attenuation margin D, of 35 db and 42 db. These theoretical predictions are compared with experimental results for the same link taken by Barnett (1972) from November, 1970 to June, 1971 and are shown in Figs. 5.8 and 5.9. As can be seen, there is good agreement with the theoretical curve using the canting angle $\sigma_\theta = 45^0$ model. The slight deviation in the region of small values of XPD (- 35 to - 40 db) are mainly due to antenna effects. On the other hand, a possible explanation for the deviations in the region of higher values of XPD, can be found in the short-term statistics of the data. Similar results for an 18 km link operating at 11 GHz in Southern England are shown in Figs. 5.18 and 5.19.

Finally, for an 18 GHz system with horizontal polarization situated in Palmetto, Georgia, we plot curves of outage time as a function of repeater spacing L for three different acceptable threshold levels (- 20 db, - 25 db and - 30 db). The results are shown in Figs. 5.10, 5.11 and 5.12 where in each of which, the corresponding outage time due to rain attenuation is also drawn. The difference between the two outage times for the - 30 db threshold becomes appreciable.

5.4.1 Analysis of the Gauss-Laguerre Quadrature

The routine DØ1AEF is called from the NAG Library and computes a definite integral of the form:-

$$\int_a^\infty e^{-x} f(x)\,dx$$

using Gauss-Laguerre polynomials. If the lower limit is not zero, then the integral is written in the form:-

$$I_2 = e^{-a} \int_0^\infty e^{-x} f(x + a)\,dx \tag{5.4.1}$$

This is approximated by the Gauss-Laguerre quadrature formula:-

$$I_2 = \sum_{k=1}^{n} A_k f(X_k) \tag{5.4.2}$$

where A_k are the weights and X_k the abscissae. The abscissae are the zeros of the Laguerre polynomials (Froberg, 1965; Ralston, 1965). This quadrature formula is exact if the function f(x) is a polynomial of degree not exceeding 2n - 1, where n is the number of abscissae used.

In this routine, we may use 4, 8, 12, 16, 20, 32 and 48 points. If a different value of n is supplied to the routine, then the formula of next highest order is used unless $n > 48$ in which case, the 48-point formula is used.

5.4.2 Numerical Results for the USA

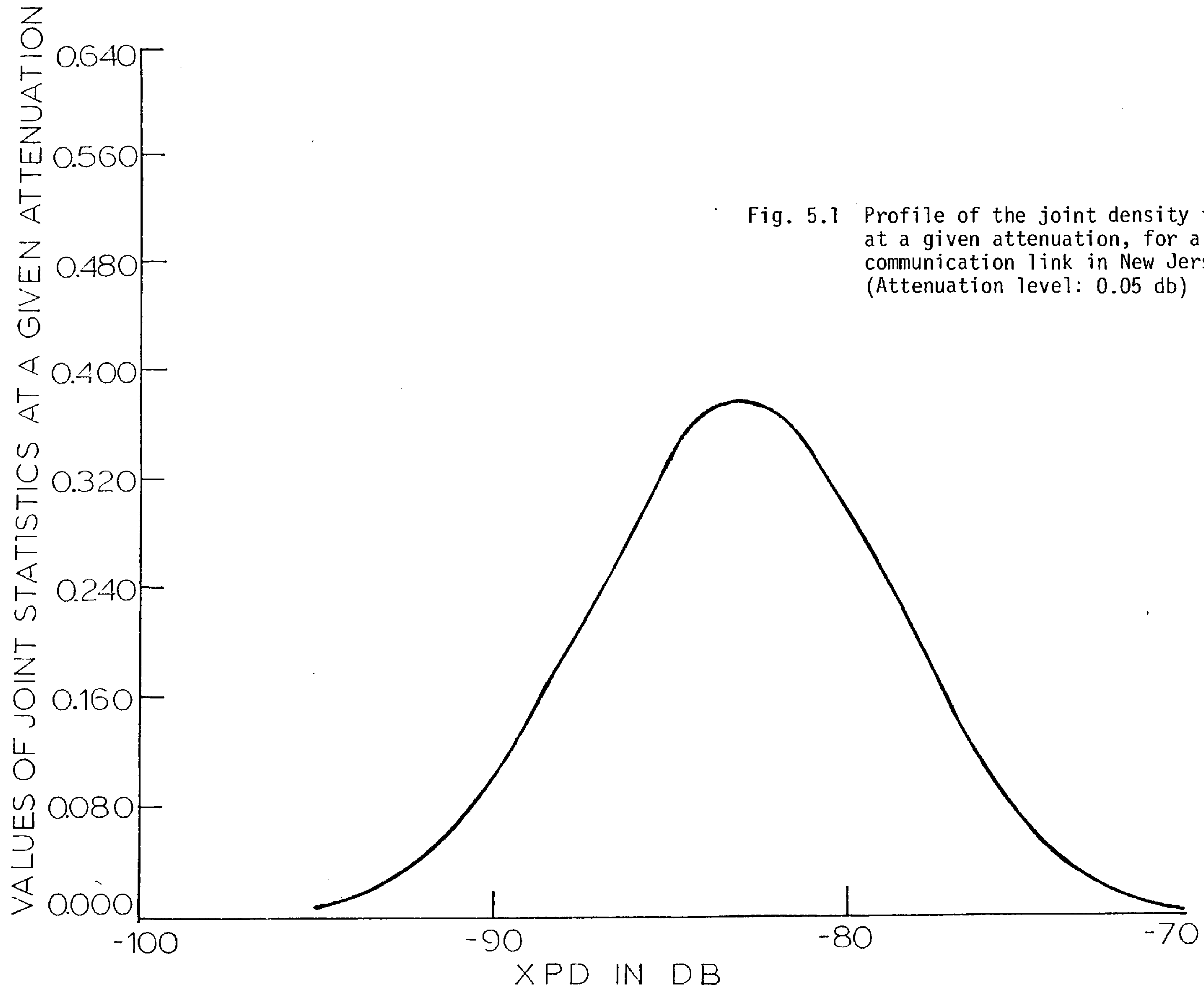

Fig. 5.1 Profile of the joint density function at a given attenuation, for a communication link in New Jersey (Attenuation level: 0.05 db)

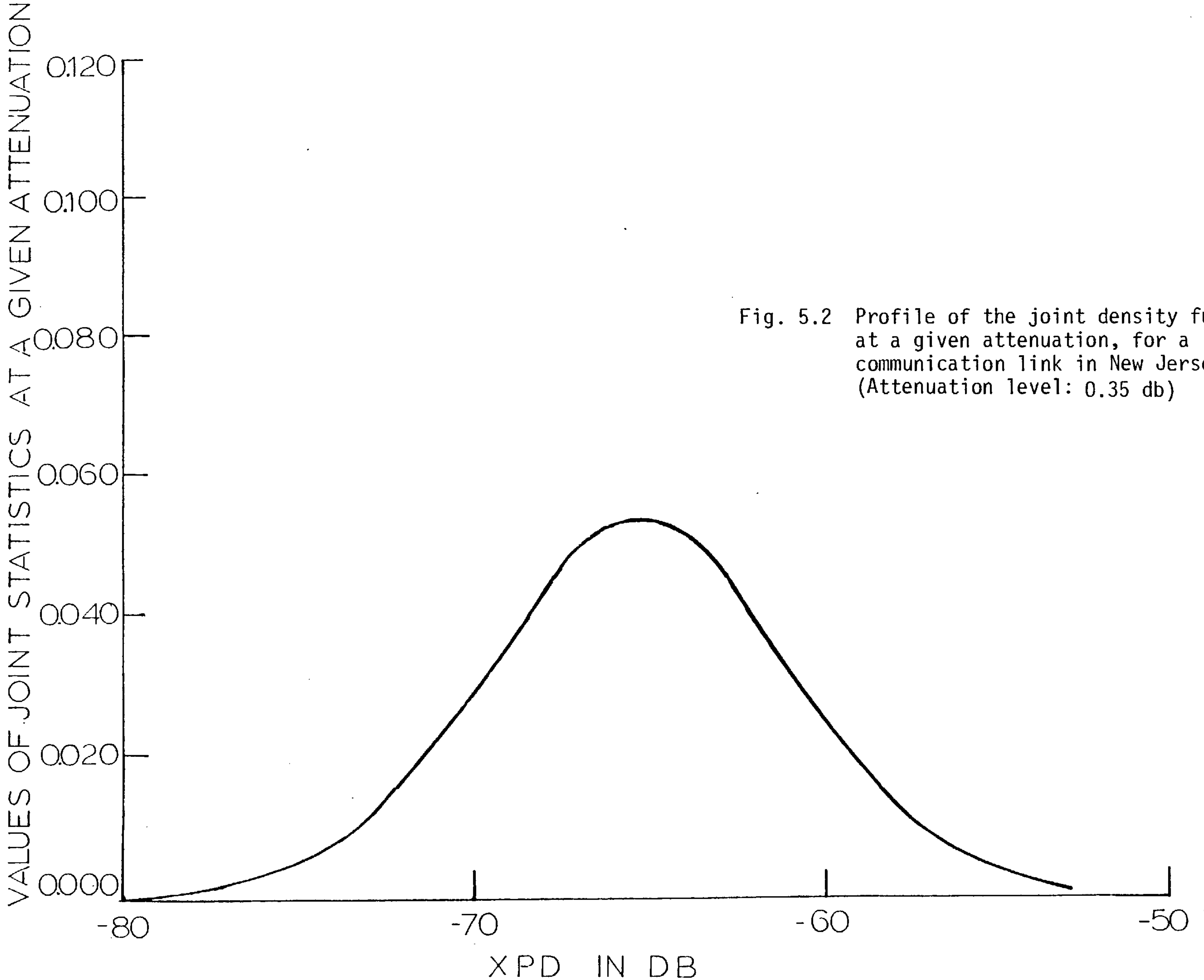

Fig. 5.2 Profile of the joint density function at a given attenuation, for a communication link in New Jersey (Attenuation level: 0.35 db)

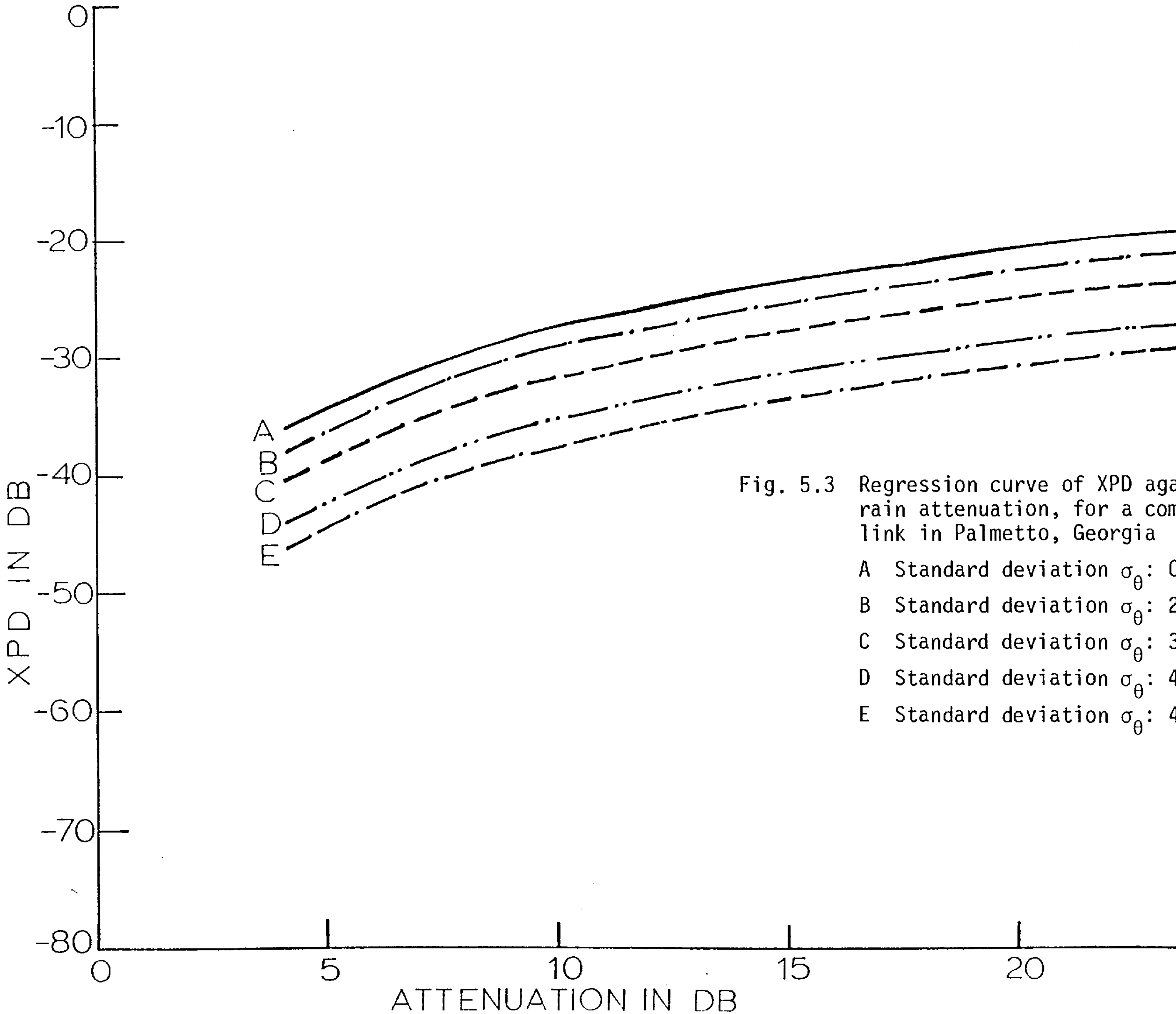

Fig. 5.3 Regression curve of XPD against copolar rain attenuation, for a communication link in Palmetto, Georgia

A Standard deviation σ_θ: 0^0

B Standard deviation σ_θ: 20^0

C Standard deviation σ_θ: 30^0

D Standard deviation σ_θ: 40^0

E Standard deviation σ_θ: 45^0

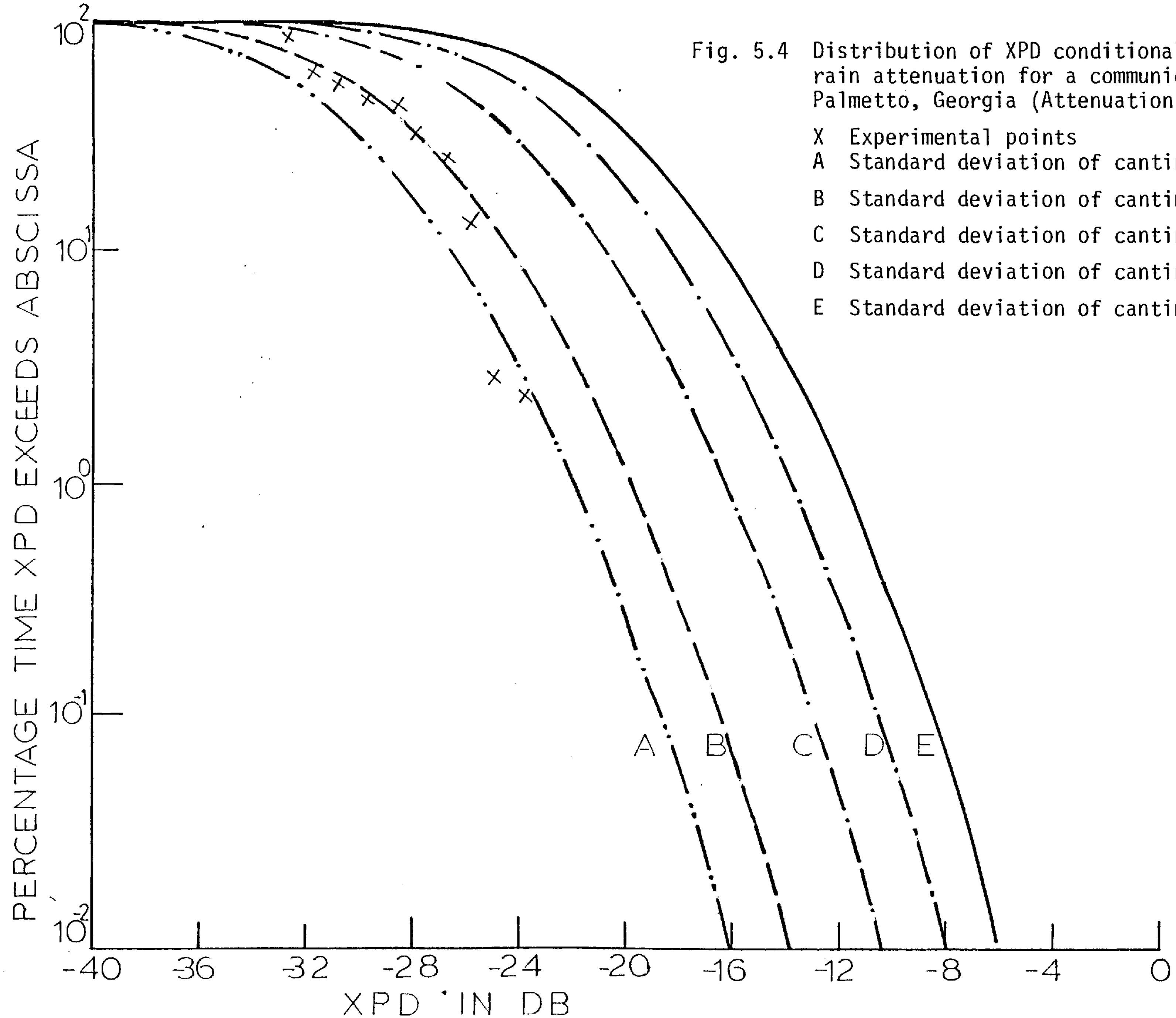

Fig. 5.4 Distribution of XPD conditional on copolar rain attenuation for a communication link in Palmetto, Georgia (Attenuation level: 20 db)

X Experimental points
A Standard deviation of canting angle σ_θ: 45^0
B Standard deviation of canting angle σ_θ: 40^0
C Standard deviation of canting angle σ_θ: 30^0
D Standard deviation of canting angle σ_θ: 20^0
E Standard deviation of canting angle σ_θ: 0^0

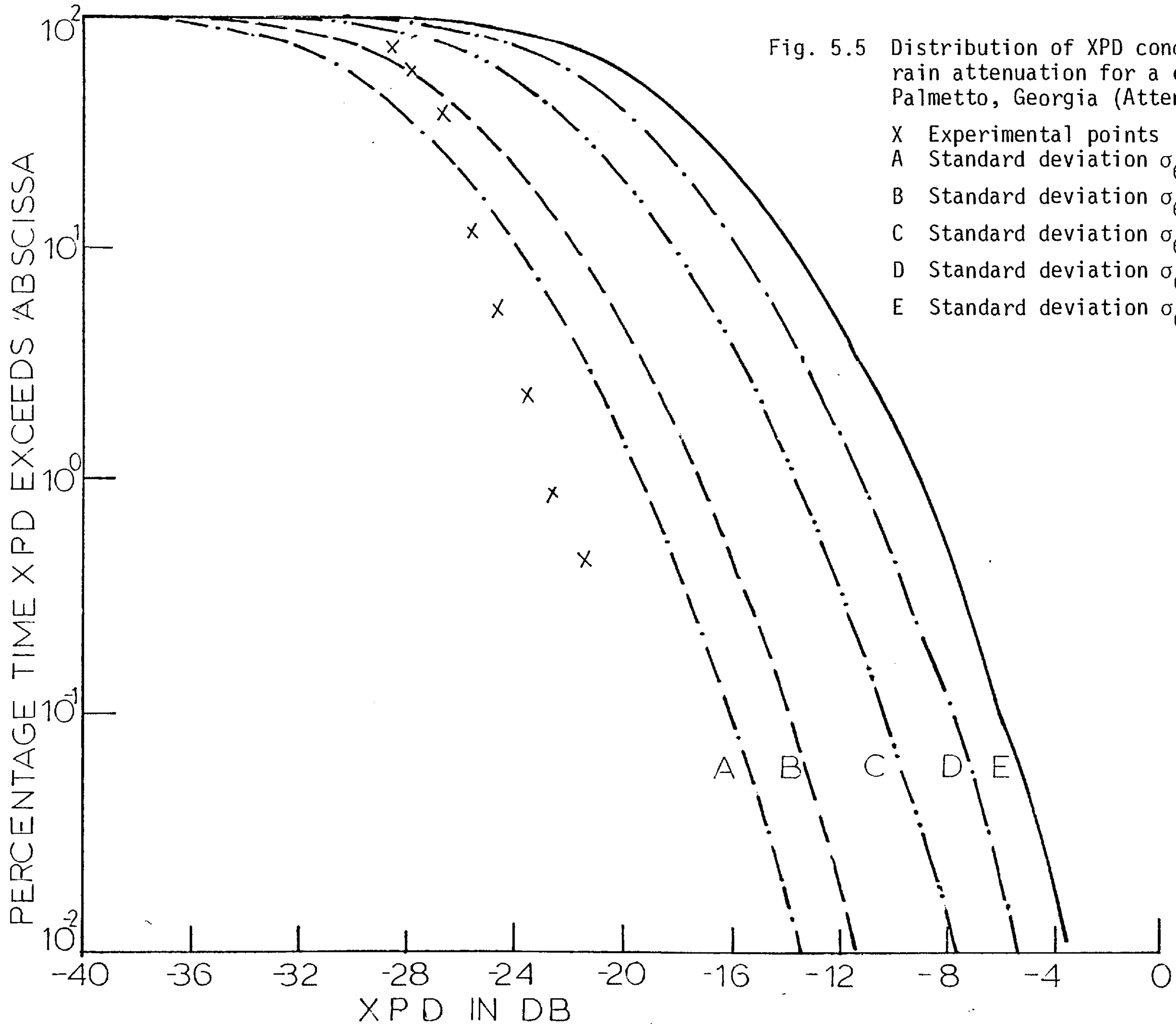

Fig. 5.5 Distribution of XPD conditional on a copolar rain attenuation for a communication link in Palmetto, Georgia (Attenuation level: 25 db)

X Experimental points
A Standard deviation σ_θ: 45^0
B Standard deviation σ_θ: 40^0
C Standard deviation σ_θ: 30^0
D Standard deviation σ_θ: 20^0
E Standard deviation σ_θ: 0^0

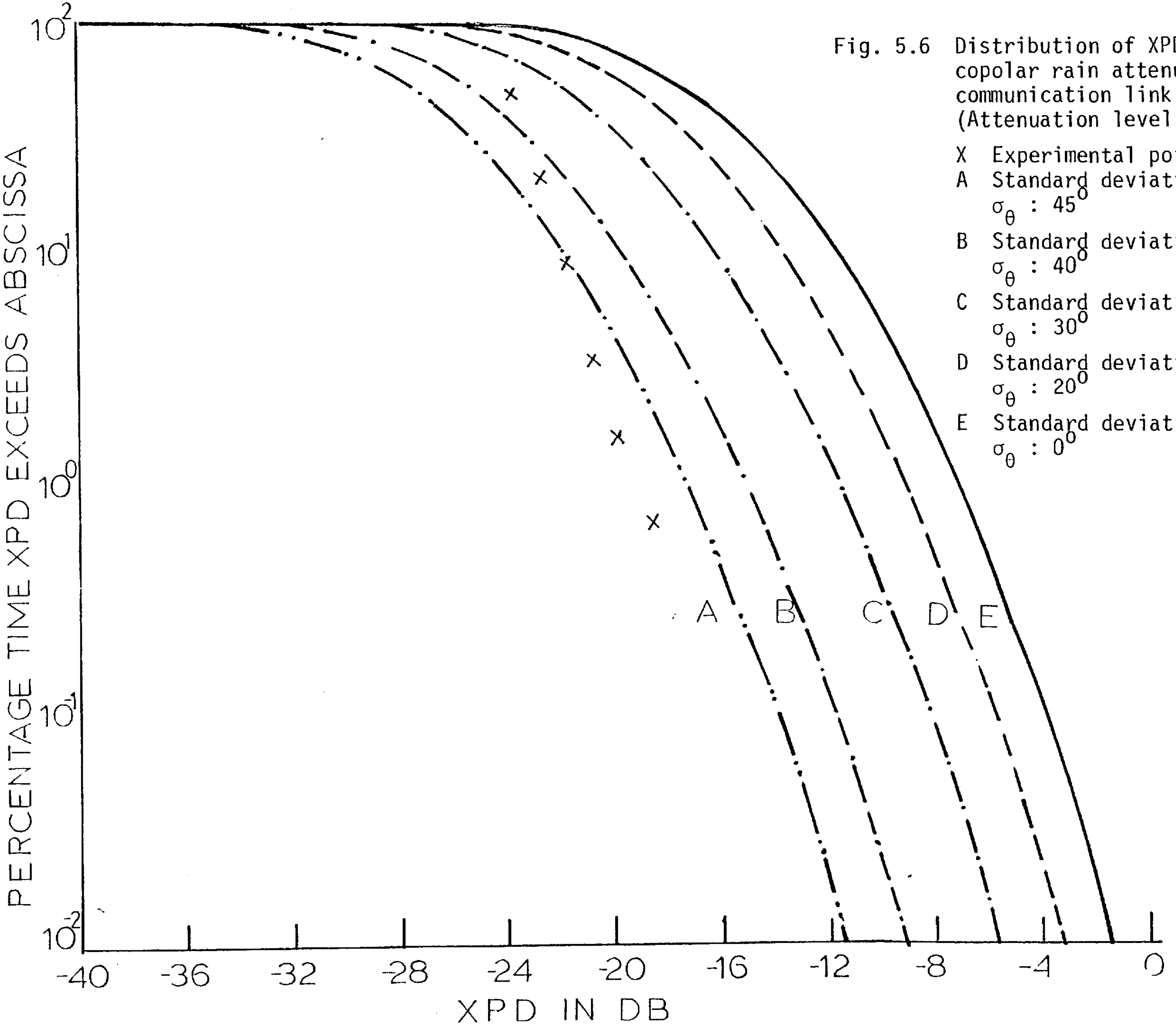

Fig. 5.6 Distribution of XPD conditional on a copolar rain attenuation for a communication link in Palmetto, Georgia (Attenuation level: 30 db)

X Experimental points
A Standard deviation of canting angle σ_θ : 45^0
B Standard deviation of canting angle σ_θ : 40^0
C Standard deviation of canting angle σ_θ : 30^0
D Standard deviation of canting angle σ_θ : 20^0
E Standard deviation of canting angle σ_θ : 0^0

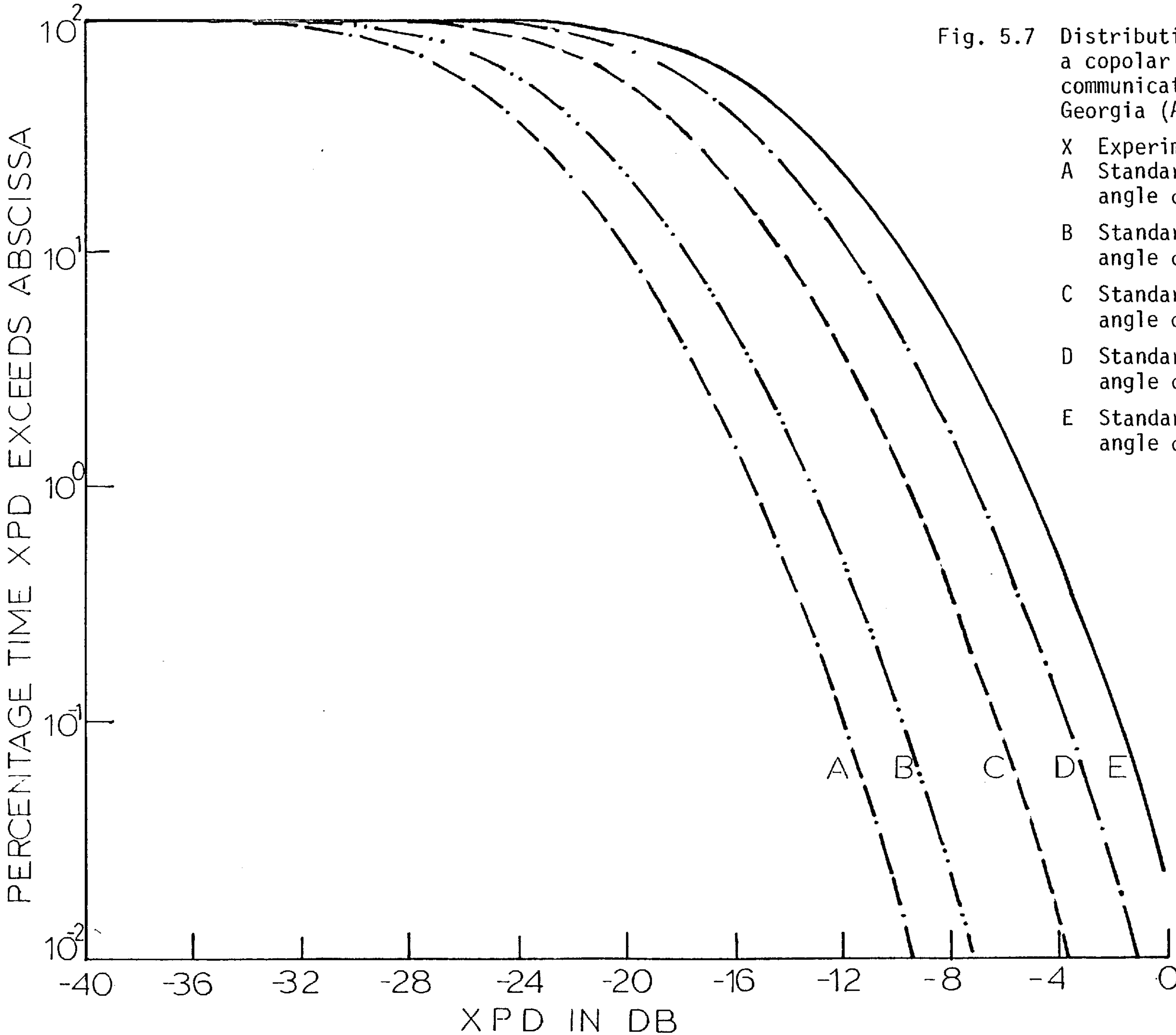

Fig. 5.7 Distribution of XPD conditional on a copolar rain attenuation for a communication link in Palmetto, Georgia (Attenuation level: 35 db)

X Experimental points

A Standard deviation of canting angle σ_θ: 45^0

B Standard deviation of canting angle σ_θ: 40^0

C Standard deviation of canting angle σ_θ: 30^0

D Standard deviation of canting angle σ_θ: 20^0

E Standard deviation of canting angle σ_θ: 0^0

TABLE 5.1

EXPERIMENTAL RESULTS FROM
PALMETTO, GEORGIA, USA

Fade Depth 20 db	
Cross-Polarization Discrimination (in db)	Excess Probability
- 22.75	1.5×10^{-2}
- 23.87	2.2×10^{-2}
- 25.00	2.62×10^{-2}
- 25.94	1.24×10^{-1}
- 26.89	2.40×10^{-1}
- 28.02	3.12×10^{-1}
- 28.77	4.14×10^{-1}
- 29.91	4.42×10^{-1}
- 31.04	5.04×10^{-1}
- 31.98	5.75×10^{-1}
- 32.92	8.16×10^{-1}
- 33.87	9.30×10^{-1}

Fade Depth 25 db	
Cross-Polarization Discrimination (in db)	Excess Probability
- 21.60	4.23×10^{-3}
- 22.74	8.16×10^{-3}
- 23.68	2.13×10^{-2}
- 24.81	5.04×10^{-2}
- 25.75	1.09×10^{-1}
- 26.89	3.55×10^{-1}
- 28.02	5.50×10^{-1}
- 28.77	6.85×10^{-1}

.... Continued

TABLE 5.1 (CONTINUED)

Fade Depth 30 db	
Cross-Polarization Discrimination (in db)	Excess Probability
- 18.58	6.01×10^{-3}
- 19.91	1.42×10^{-2}
- 20.85	3.12×10^{-2}
- 21.79	8.16×10^{-2}
- 22.74	1.93×10^{-1}
- 23.87	4.42×10^{-1}

Fade Depth 35 db	
Cross-Polarization Discrimination (in db)	Excess Probability
- 17.83	4.83×10^{-2}
- 18.96	2.98×10^{-1}

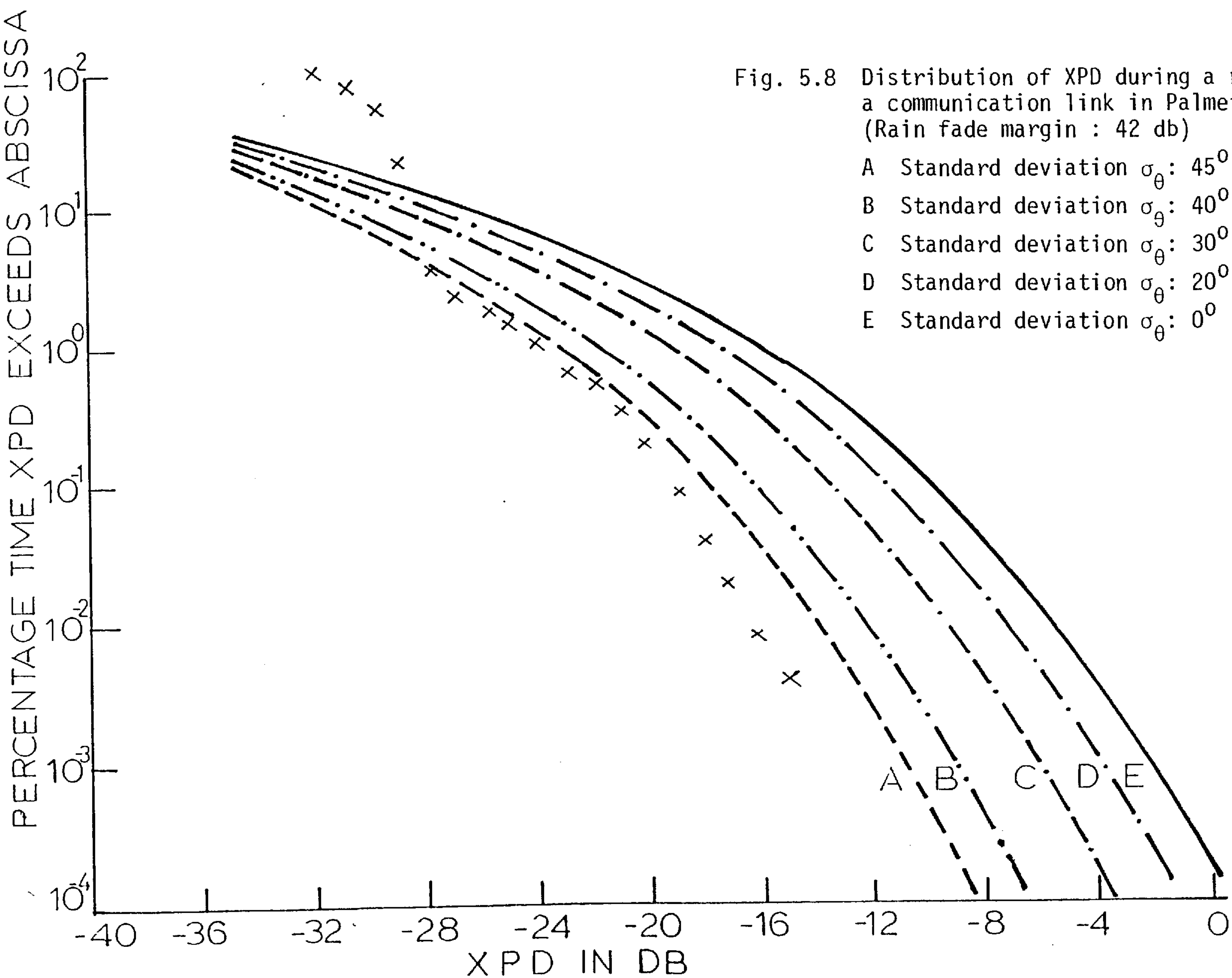

Fig. 5.8 Distribution of XPD during a rain fade for a communication link in Palmetto, Georgia (Rain fade margin : 42 db)

A Standard deviation σ_θ: 45^0

B Standard deviation σ_θ: 40^0

C Standard deviation σ_θ: 30^0

D Standard deviation σ_θ: 20^0

E Standard deviation σ_θ: 0^0

TABLE 5.2

EXPERIMENTAL RESULTS FROM
PALMETTO, GEORGIA, USA

Fade Depth $\leq$ 42 db	
Cross-Polarization Discrimination (in db)	Excess Probability
- 15.21	3.5×10^{-5}
- 16.27	7.44×10^{-5}
- 17.33	1.75×10^{-4}
- 18.18	3.61×10^{-4}
- 19.03	7.81×10^{-4}
- 20.30	1.74×10^{-3}
- 21.14	3.08×10^{-3}
- 22.00	4.82×10^{-3}
- 23.00	5.85×10^{-3}
- 24.11	1.78×10^{-3}
- 25.11	1.34×10^{-2}
- 25.81	1.62×10^{-2}
- 27.08	2.16×10^{-2}
- 27.92	3.33×10^{-2}
- 28.98	2.06×10^{-1}
- 29.83	4.98×10^{-1}
- 30.89	7.44×10^{-1}
- 32.16	9.17×10^{-1}

.... Continued

TABLE 5.2 (CONTINUED)

Fade Depth $\leq$ 35 db	
Cross-Polarization Discrimination (in db)	Excess Probability
- 18.39	5.85×10^{-5}
- 19.24	4.98×10^{-4}
- 20.30	1.45×10^{-3}
- 21.14	2.23×10^{-3}
- 22.00	4.24×10^{-3}
- 23.00	5.85×10^{-3}
- 24.11	9.78×10^{-3}
- 25.11	1.34×10^{-2}
- 25.81	1.62×10^{-2}
- 27.08	2.16×10^{-2}
- 27.92	3.33×10^{-2}
- 28.98	2.06×10^{-1}
- 29.83	4.98×10^{-1}
- 30.89	7.44×10^{-1}
- 32.16	9.17×10^{-1}

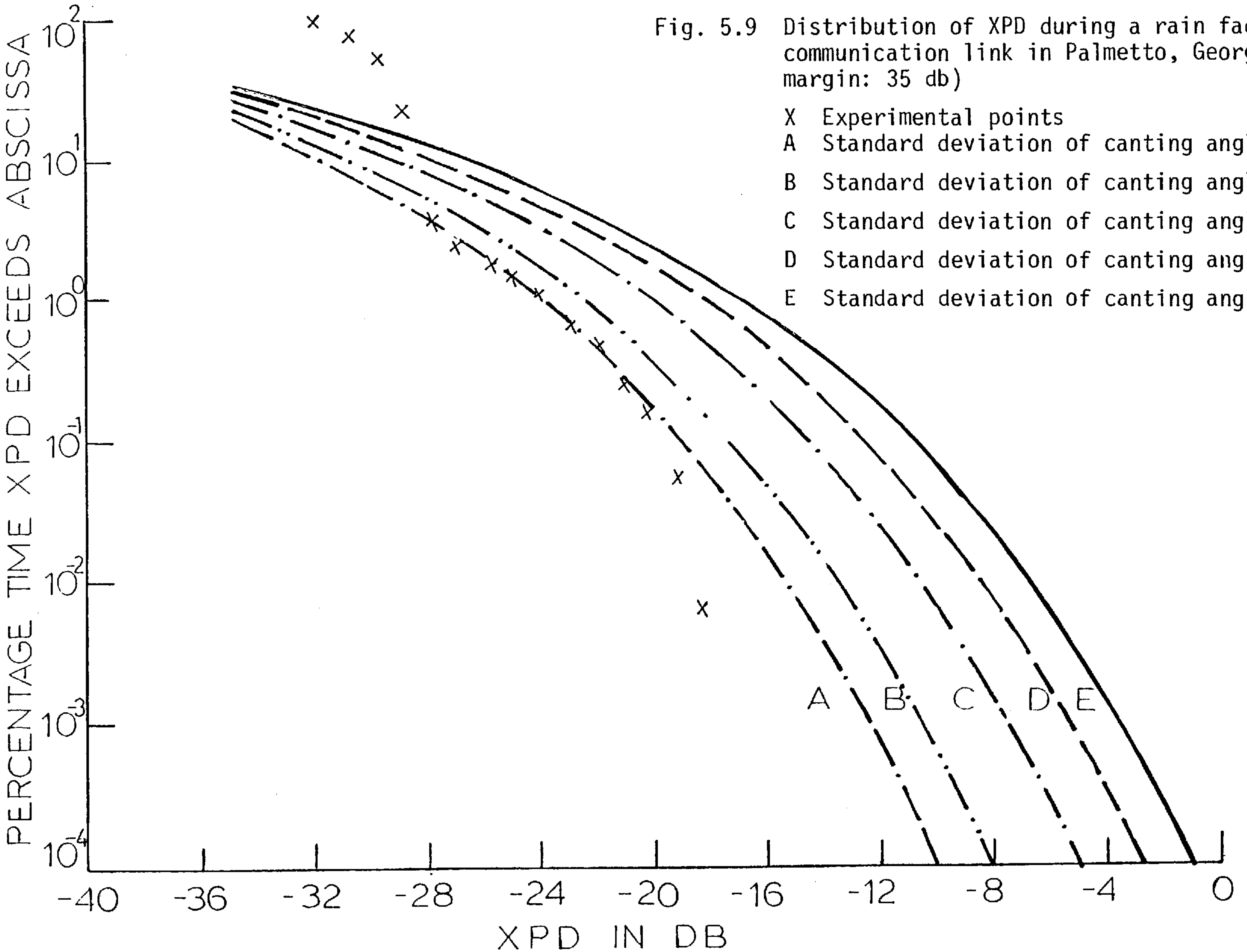

Fig. 5.9 Distribution of XPD during a rain fade for a communication link in Palmetto, Georgia (Rain fade margin: 35 db)

X Experimental points
A Standard deviation of canting angle σ_{θ}: 45^{0}
B Standard deviation of canting angle σ_{θ}: 40^{0}
C Standard deviation of canting angle σ_{θ}: 30^{0}
D Standard deviation of canting angle σ_{θ}: 20^{0}
E Standard deviation of canting angle σ_{θ}: 0^{0}

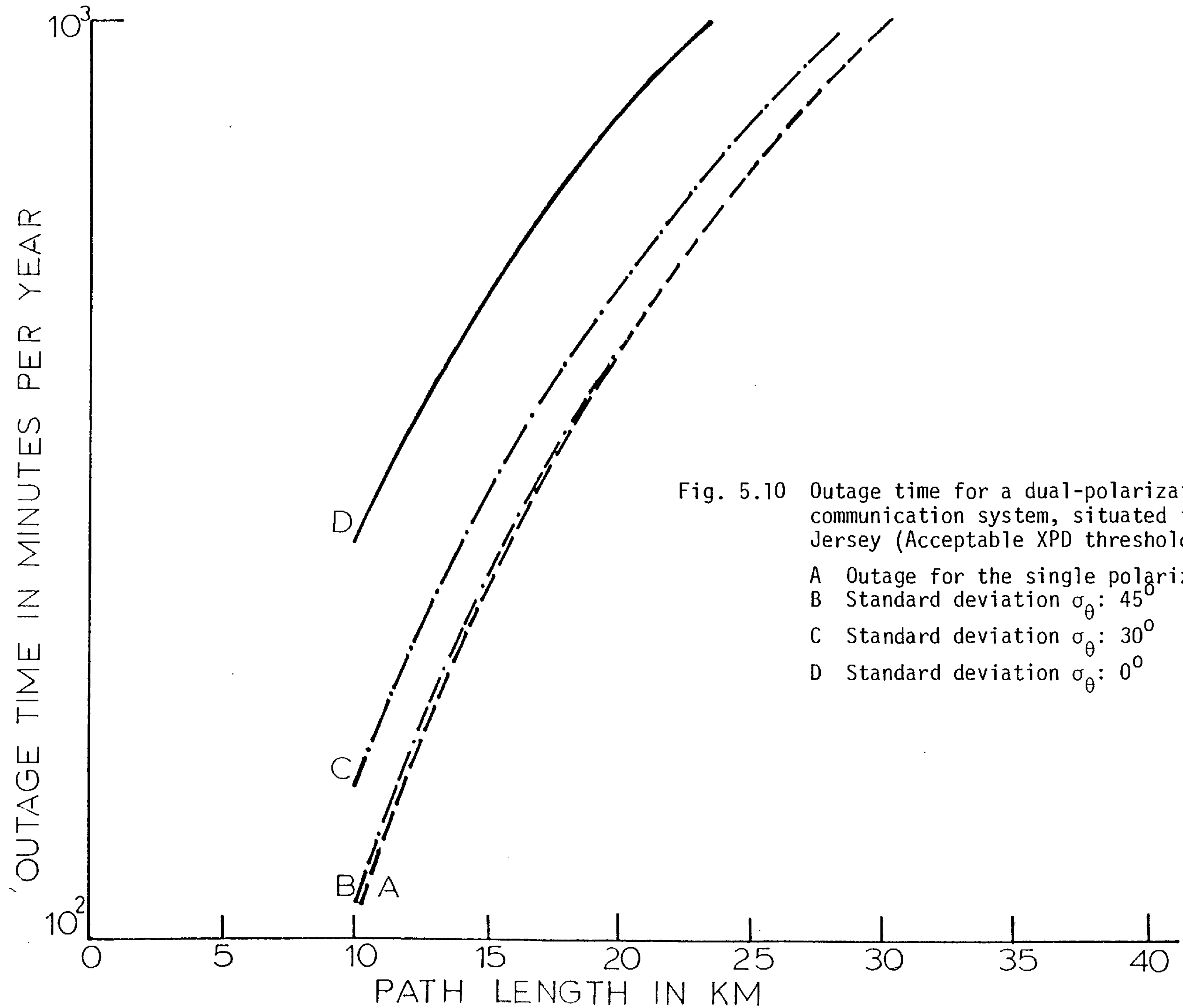

Fig. 5.10 Outage time for a dual-polarization communication system, situated in New Jersey (Acceptable XPD threshold: - 20 db)

A Outage for the single polarization system
B Standard deviation σ_θ: 45^o
C Standard deviation σ_θ: 30^o
D Standard deviation σ_θ: 0^o

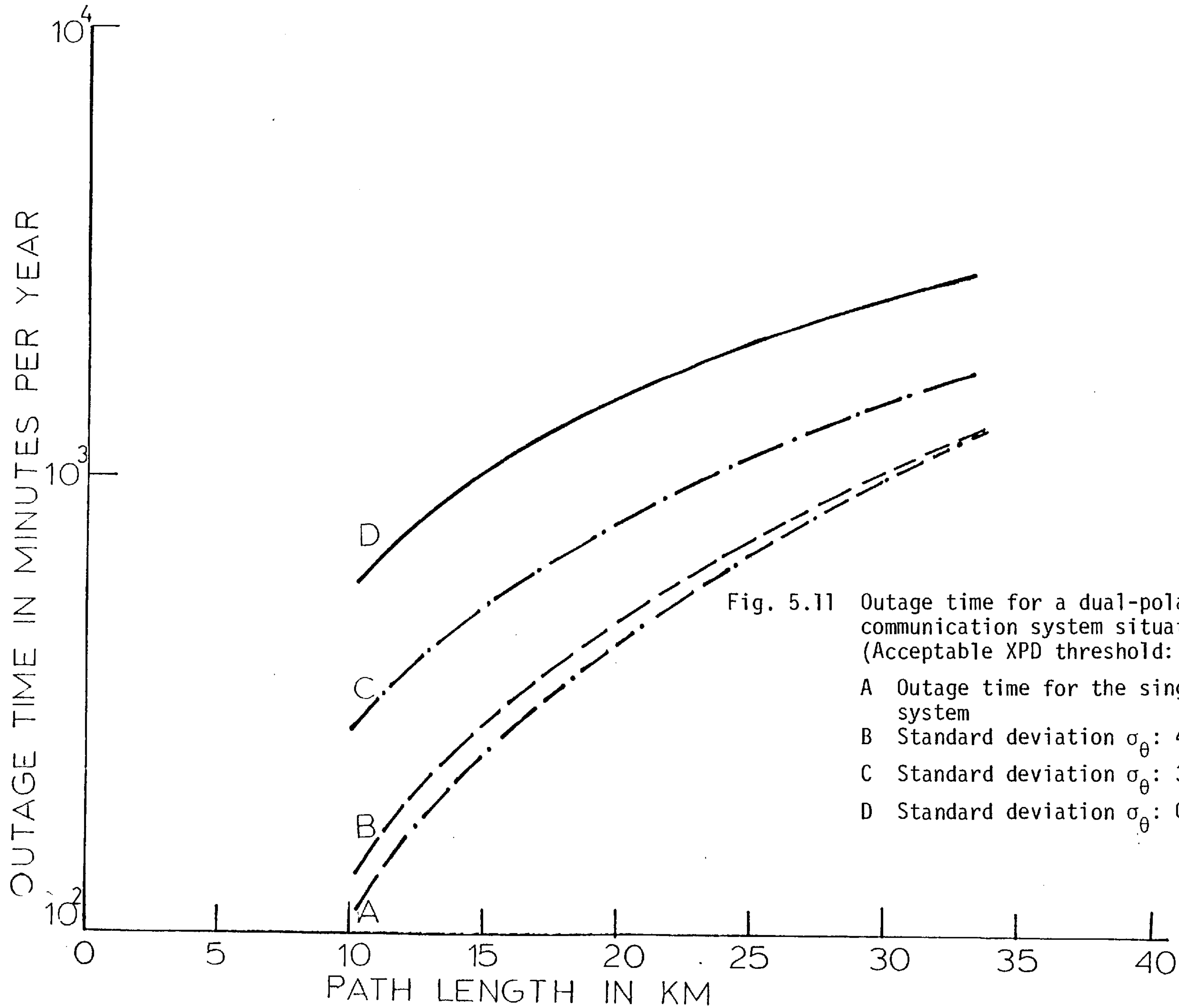

Fig. 5.11 Outage time for a dual-polarization communication system situated in New Jersey (Acceptable XPD threshold: - 25 db)

A Outage time for the single-polarization system

B Standard deviation σ_θ: 45^o

C Standard deviation σ_θ: 30^o

D Standard deviation σ_θ: 0^o

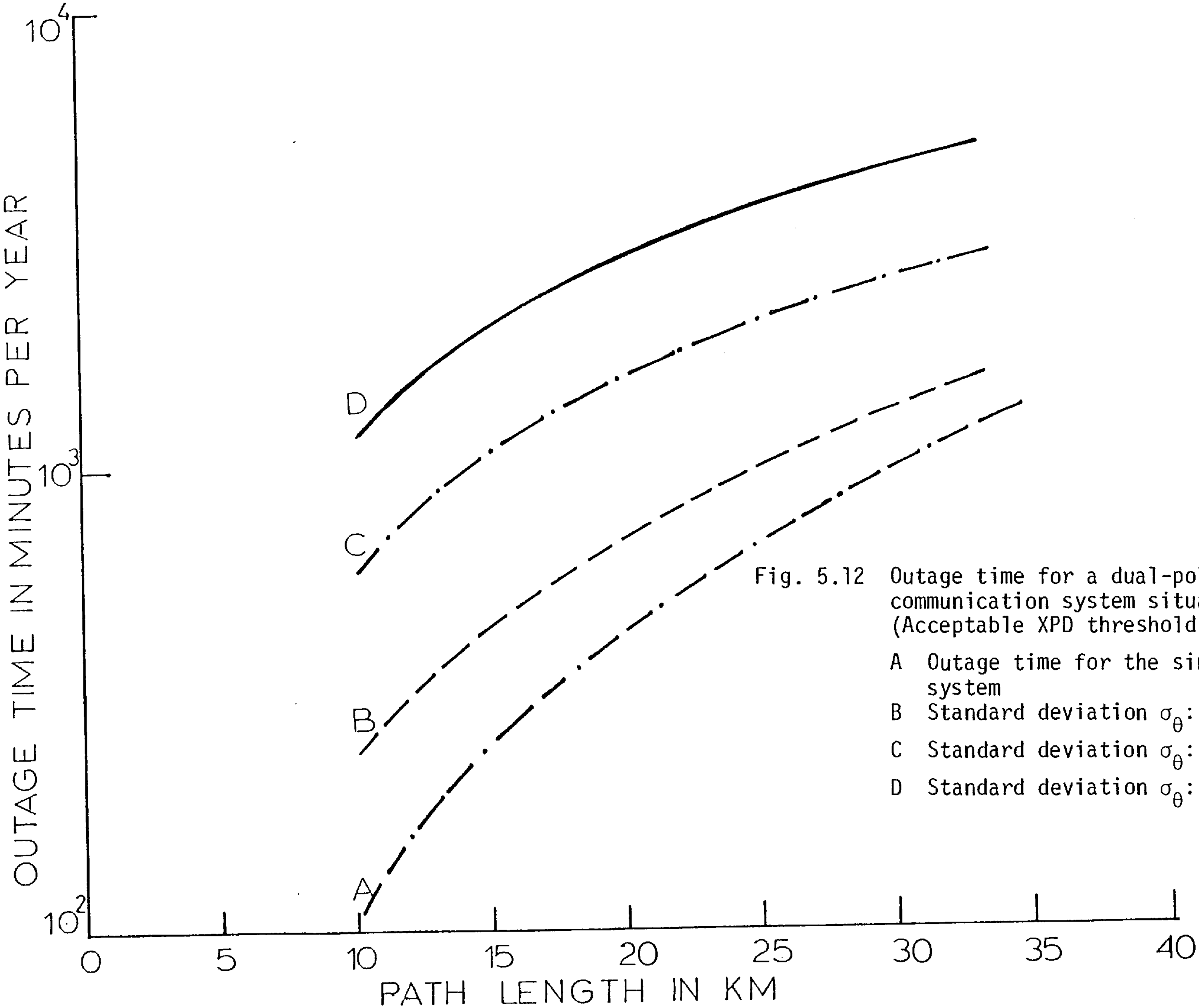

Fig. 5.12 Outage time for a dual-polarization communication system situated in New Jersey (Acceptable XPD threshold: - 30 db)

A Outage time for the single polarization system
B Standard deviation σ_θ: 45^0
C Standard deviation σ_θ: 30^0
D Standard deviation σ_θ: 0^0

5.4.3 Numerical Results for Southern England

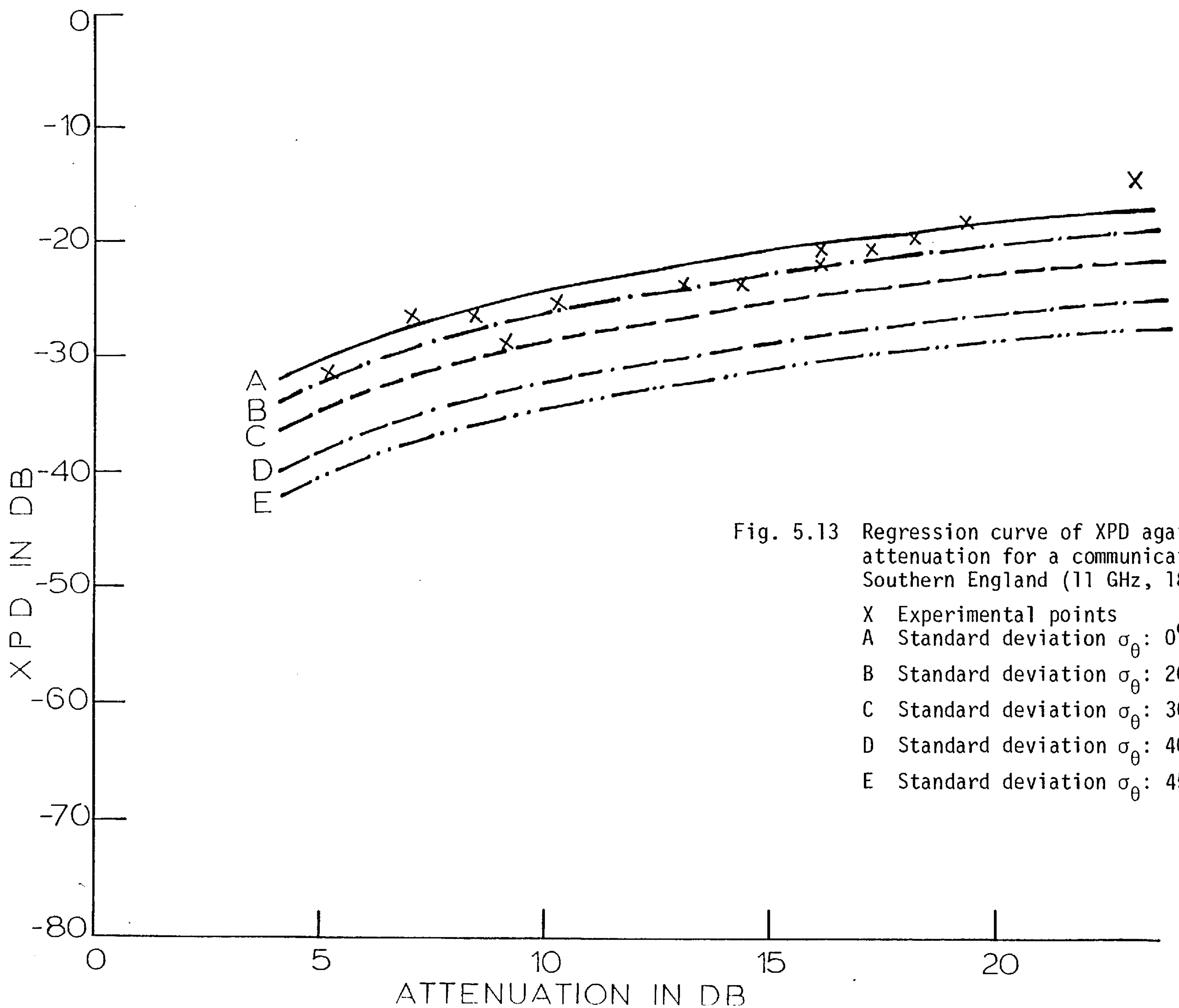

Fig. 5.13 Regression curve of XPD against copolar attenuation for a communication link in Southern England (11 GHz, 18 km)

X Experimental points
A Standard deviation σ_θ: 0^o
B Standard deviation σ_θ: 20^o
C Standard deviation σ_θ: 30^o
D Standard deviation σ_θ: 40^o
E Standard deviation σ_θ: 45^o

TABLE 5.3

EXPERIMENTAL RESULTS FROM SOUTHERN ENGLAND

Cross-Polarization Discrimination (in db)	Attenuation (in db)
- 14.87	23.02
- 18.59	19.30
- 19.98	18.14
- 20.91	17.21
- 20.91	16.05
- 22.30	16.05
- 24.16	14.28
- 24.16	13.02
- 26.02	10.23
- 29.28	9.07
- 26.95	8.37
- 26.95	6.98
- 32.06	5.12
- 27.88	3.95
- 29.28	3.02
- 27.88	3.02
- 34.39	2.09

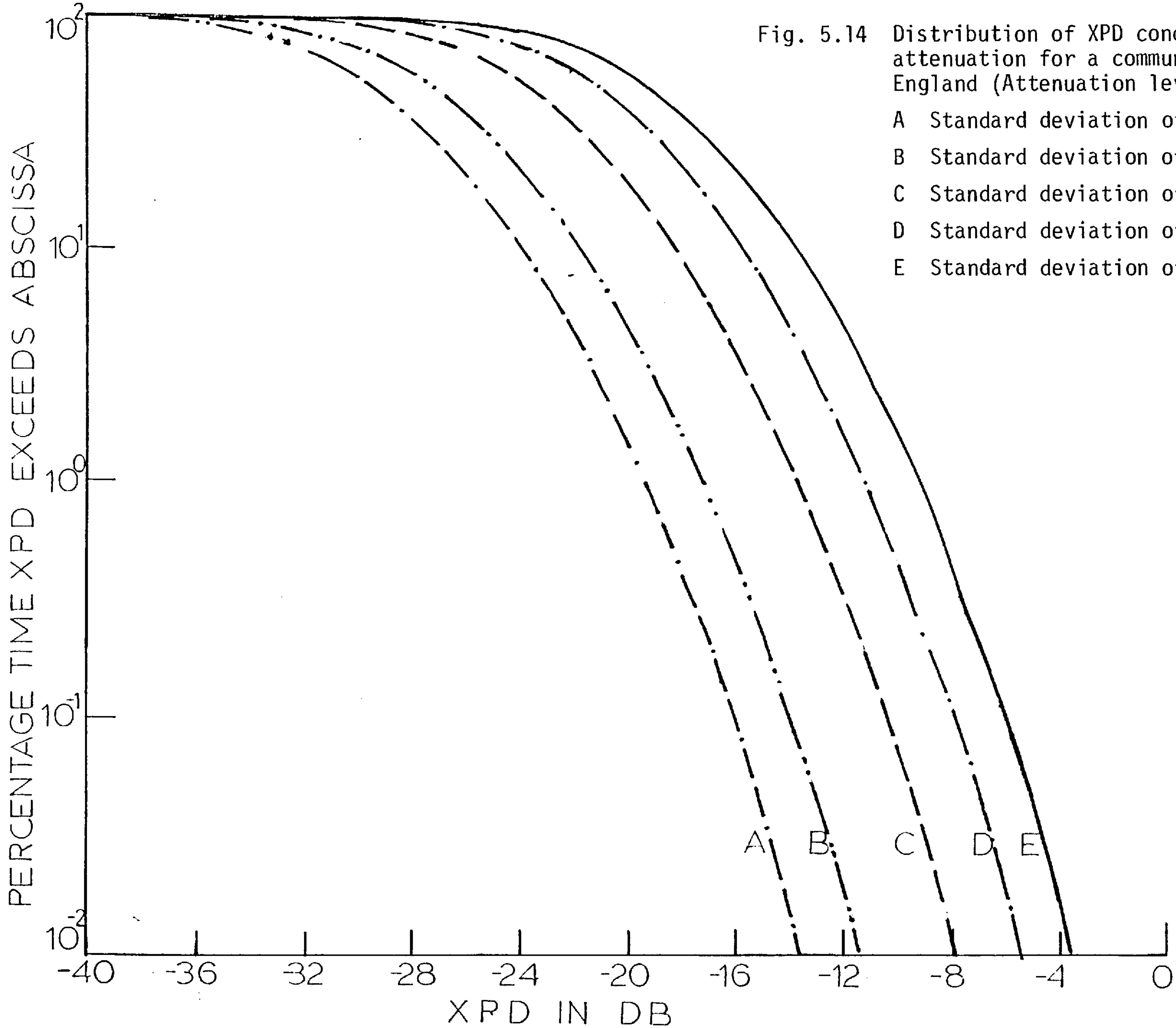

Fig. 5.14 Distribution of XPD conditional on copolar rain attenuation for a communication link in Southern England (Attenuation level: 20 db)

A Standard deviation of canting angle σ_θ: 45^0

B Standard deviation of canting angle σ_θ: 40^0

C Standard deviation of canting angle σ_θ: 30^0

D Standard deviation of canting angle σ_θ: 20^0

E Standard deviation of canting angle σ_θ: 0^0

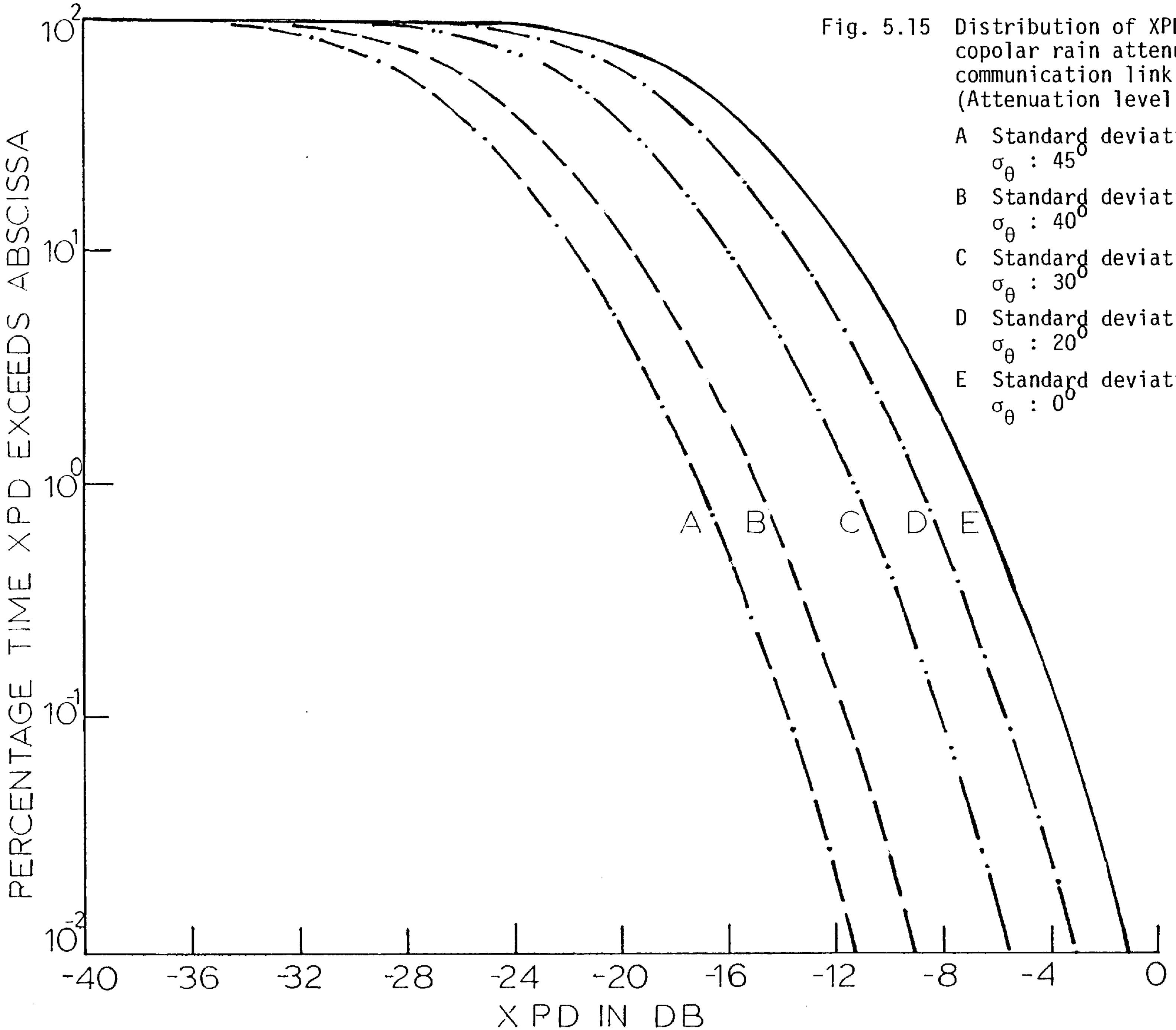

Fig. 5.15 Distribution of XPD conditional on a copolar rain attenuation for a communication link in Southern England (Attenuation level: 25 db)

A Standard deviation of canting angle σ_θ : 45^0

B Standard deviation of canting angle σ_θ : 40^0

C Standard deviation of canting angle σ_θ : 30^0

D Standard deviation of canting angle σ_θ : 20^0

E Standard deviation of canting angle σ_θ : 0^0

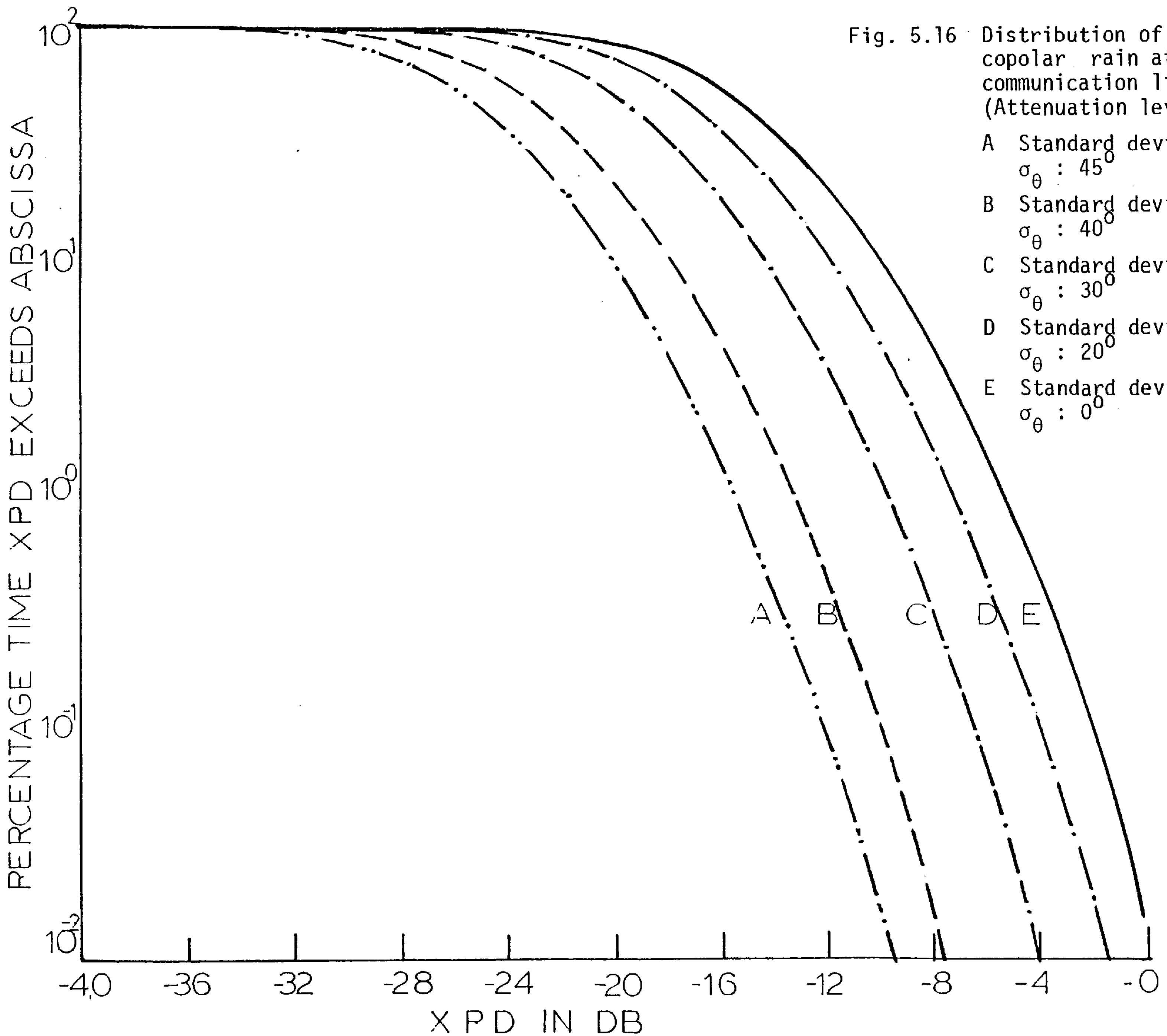

Fig. 5.16 Distribution of XPD conditional on a copolar rain attenuation for a communication link in Southern England (Attenuation level: 30 db)

A Standard deviation of canting angle σ_{θ} : 45^{0}

B Standard deviation of canting angle σ_{θ} : 40^{0}

C Standard deviation of canting angle σ_{θ} : 30^{0}

D Standard deviation of canting angle σ_{θ} : 20^{0}

E Standard deviation of canting angle σ_{θ} : 0^{0}

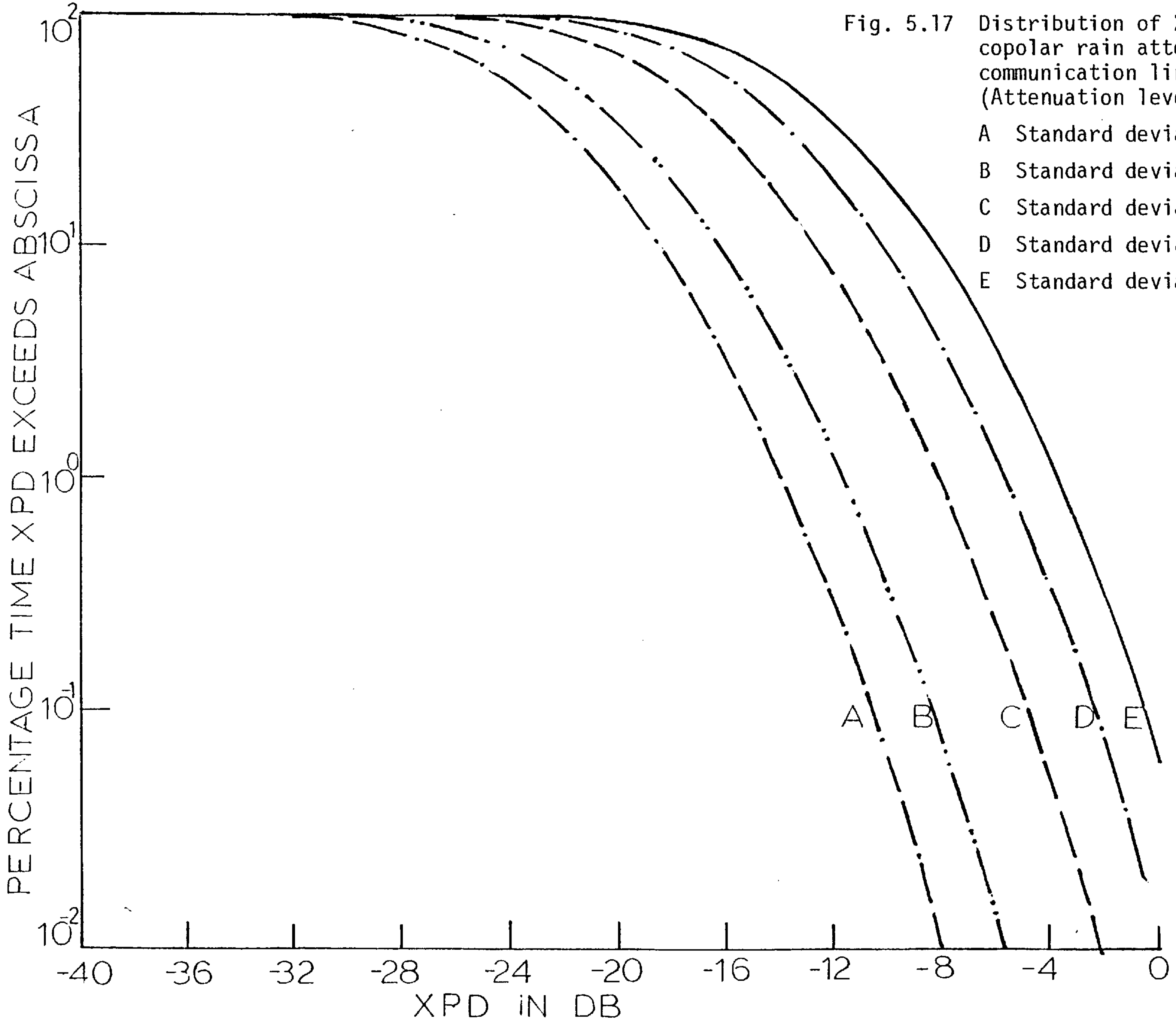

Fig. 5.17 Distribution of XPD conditional on a copolar rain attenuation for a communication link in Southern England (Attenuation level: 35 db)

A Standard deviation σ_θ: 45^o

B Standard deviation σ_θ: 40^o

C Standard deviation σ_θ: 30^o

D Standard deviation σ_θ: 20^o

E Standard deviation σ_θ: 0^o

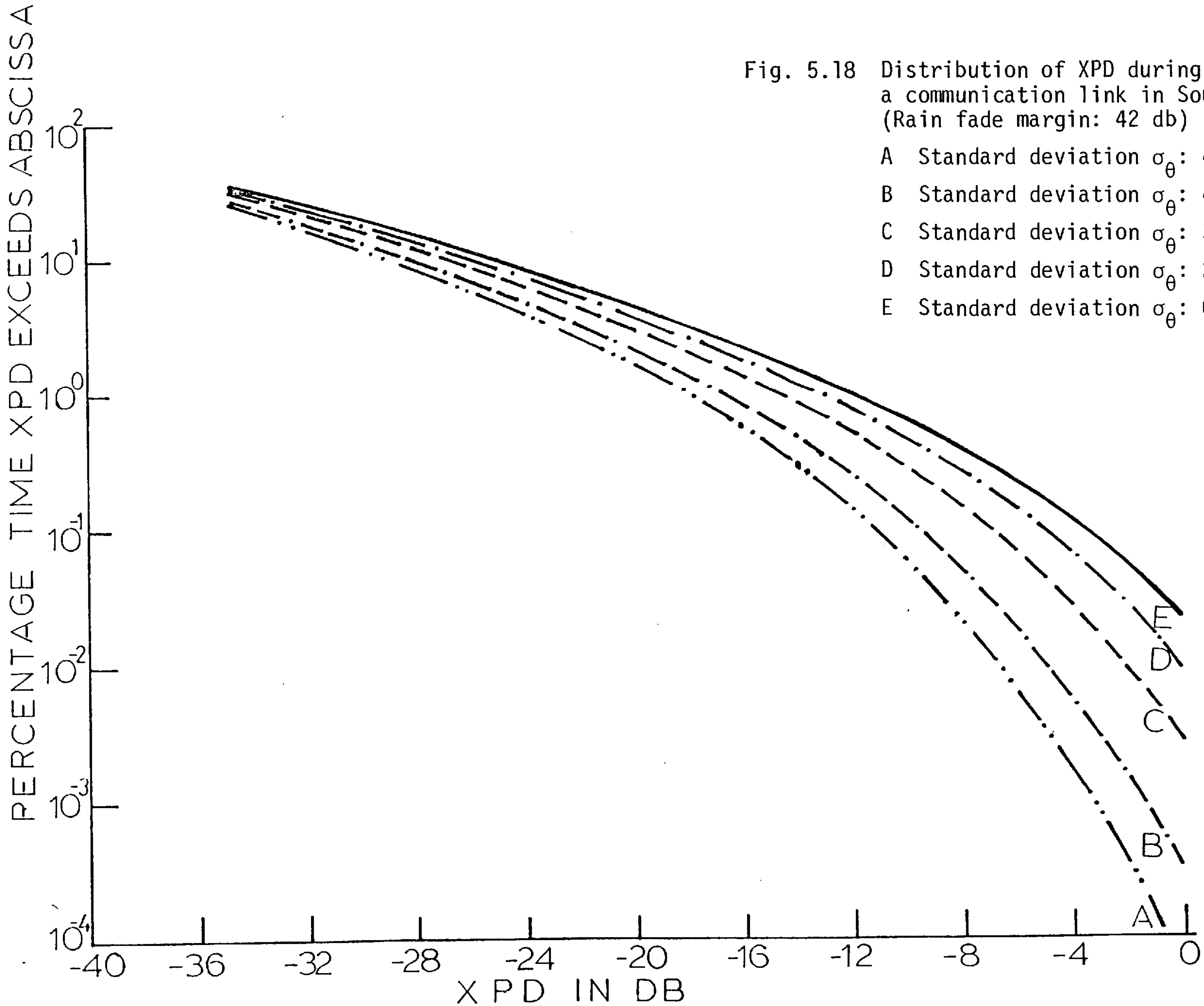

Fig. 5.18 Distribution of XPD during a rain fade for a communication link in Southern England (Rain fade margin: 42 db)

A Standard deviation σ_θ: 45^0

B Standard deviation σ_θ: 40^0

C Standard deviation σ_θ: 30^0

D Standard deviation σ_θ: 20^0

E Standard deviation σ_θ: 0^0

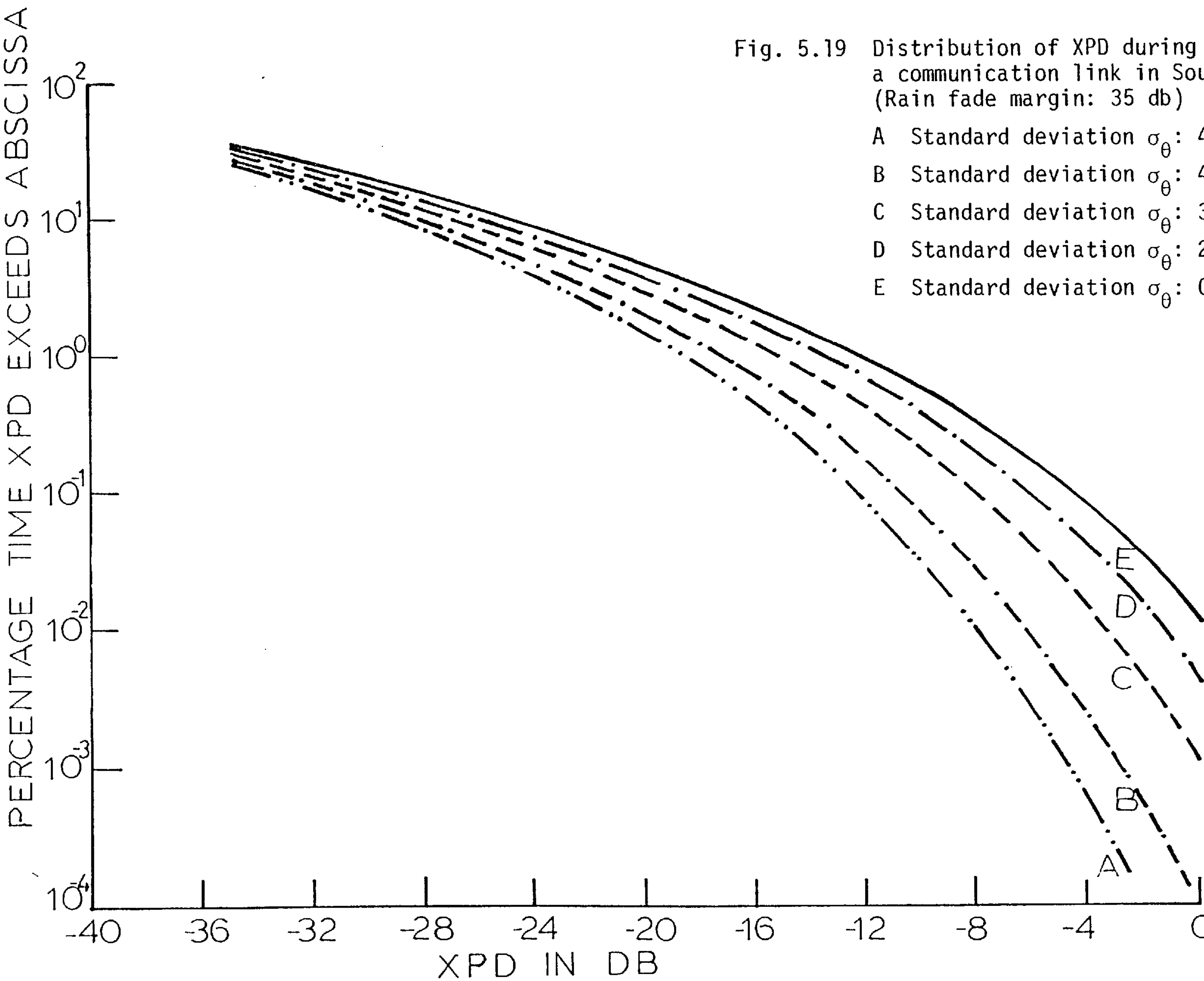

Fig. 5.19 Distribution of XPD during a rain fade for a communication link in Southern England (Rain fade margin: 35 db)

A Standard deviation σ_θ: 45^0

B Standard deviation σ_θ: 40^0

C Standard deviation σ_θ: 30^0

D Standard deviation σ_θ: 20^0

E Standard deviation σ_θ: 0^0

5.4.4 Concluding Remarks

A theoretical formula has been derived in this chapter for the joint statistics of XPD and rain attenuation for a microwave link, using Jacobian transformations (Papoulis, 1965) and assuming a log-normal and normal form for the individual rain attenuation and XPD distribution respectively.

This formula is then applied to the prediction of the distribution of XPD conditional on the co-polar rain attenuation and also the distribution of XPD during a rain fade. Experimental results from Palmetto, Georgia (Barnett, 1972) are compared with theoretical curves and the agreement has been found to be fairly good, as in the case also of scatter-grams taken in Southern England which are compared with regression curves of XPD in terms of the co-polar rain attenuation.

Finally, a new formula for the total outage time of a dual-polarization communication system is derived as an extension of a previous one, proposed by Lin (1975), which is appropriate for single-polarization systems. In the newly proposed formula, the interference caused by the orthogonal channel is also taken into account.

CHAPTER 6

SUMMARY AND CONCLUSIONS

In this chapter, the work reported in the thesis is summarised and the conclusions which can be drawn from the results are described in detail. Also, some suggestions are made relating to further research.

6.1 General Summary

Although recent studies of polarization effects have been directed towards providing long-term distribution functions for predicting the occurrence of cross-polarised signals, propagating through rain, there are many aspects that have not yet been investigated. The aim of the work reported in this thesis was to propose a theoretical prediction model of general applicability for the long-term statistics of cross-polarization discrimination (XPD) of a microwave communication system, and to compare it with experimental results.

General expressions and aspects of radio wave propagation through rain, which were used for the development of the prediction model, are described in Chapter 2. An analysis of long-term statistics of XPD for a spatially uniform rain medium (or equivalently inside a uniform rain cell) is given in Chapter 3. In Chapter 4, the same analysis for the more general case of a non-uniform medium is studied. Finally, in Chapter 5, an analysis of the joint statistics of XPD and rain attenuation is given, and the applications of this study in the prediction of the performance of radio links.

6.2 Summary of the Results

In Chapter 3, a Gaussian model for the long-term distribution of XPD in db, has been derived. This model is based upon the theoretically calculated log of a Rayleigh distribution for the short-term statistics of XPD in db and the observed log normality of the point rainfall rate distribution.* An approximate value of the short-term average of the XPD (or in other words, at a constant rainfall rate) has been used as a first estimation, in our stochastic calculations. This value is a function of the drop-size distribution, polarization, frequency, length of path, rainfall rate and canting angle distribution, and it has been proposed by many authors so far, such as Oguchi (1977), Nowland et al (1977), etc. For a specific link (frequency, polarization, length) the main uncertainty for the evaluation of this short-term average of XPD as a function of rainfall rate, lies in the prediction of the canting angle distribution model and secondly, the drop size distribution. Accepting, for the latter, the well known Laws-Parsons distribution and for the canting angle a Gaussian model, with mean value $m_\theta \cong 10^o$, then upper and lower bounds of this $\langle XPD \rangle_s$ for each rainfall rate, can be found by taking an equiorientated model with standard deviation of θ, $\sigma_\theta = 0^o$, and another one with $\sigma_\theta \cong 40^o - 45^o$, respectively. In the same way, upper and lower bounds on the long-term excess probability of XPD and outage time of a system due to co-channel interference can be found, corresponding to these values of the σ_θ. Direct comparison with experimental results from a specific link in Ipswich, Southern England shows that the most preferred model in this case, is rather the equiorientated one (Fig. 3.15).

On the other hand, a more general model for the long-term statistics of XPD, has been constructed in Chapter 4, taking into account the spatial non-uniformity of rainfall rate. A normal model has again been derived but with different statistical parameters. A direct, comparison of the two models (the uniform and non-uniform one) reveals that these are almost identical for path lengths up to 4 km.

* It must be noted here that the lognormal model for the point rainfall statistics is not too reliable in the UK.

In both the models the linear incident 45^{o} polarization has been identified as the one suffering most depolarization.

Finally, taking into account the log normal model for long-term rain attenuation statistics as has been proposed by Lin (1975), the joint statistics of XPD and attenuation is studied in Chapter 5. A theoretical formula is derived for this joint density function and this is then applied in several practical situations. These are the prediction of the mean value of XPD or its distribution conditional on a copolar rain attenuation, the prediction of the distribution of XPD conditional on a rain fade and the estimation of the outage time of a dual-polarization system. These theoretical results are compared with experimental ones from specific links in Palmetto, Georgia and Southern England. These comparisons show that the most preferred model of canting angle for the link in Palmetto is that with $\sigma_\theta = 40^{o} - 45^{o}$, but for the link in Southern England, it is the equiorientated one ($\sigma_\theta = 0^{o}$).*

As a general conclusion, it may be claimed thatmany aspects of any significance concerning rain depolarization statistics have been analysed, and practical applications relevant to the design of microwave communication systems have been made.** The model which has been constructed is based upon the observed log normality of point rainfall rate but takes into account the short-term statistical behaviour of XPD and the observed spatial non-uniformity of rain medium. The main advantage of this model is the resulting simple form for the long-term statistics of XPD, thus producing another simple model for the prediction of the joint statistics of XPD and attenuation.

6.3 Suggestions for Future Research

Although the work reported in this thesis has provided some valuable new information relating to the prediction of the long-term

* See page 217

** But in order to have a universal acceptance for the method which is analysed in the thesis, real long term data are needed.

distribution of XPD during rain, much remains to be done. In this concluding section of the thesis, several additional areas of investigation are suggested and briefly discussed.

First, for this particular model, a more detailed description of the canting angle distribution, and its relation to several meteorological factors (direction and velocity of wind, etc.) is needed. This distribution, as has been shown in the thesis, is of great importance in the prediction of the long-term statistics of XPD for a communication link. With the information presently available on this subject, this theoretical model can only predict upper and lower bounds of the XPD distribution. This work will be very difficult involving the collection of data on a long-term basis from all over the world.

Another important problem lies in the uncertainty of the available information concerning the spatial correlation ψ_R for the rain model. At some geographic locations, the squall lines of heavy rain may have a predominant orientation related to the predominant orientation of weather fronts. This means the spatial correlation ψ_R may depend not only on the spacing but also on the orientation. However, the information presently available is not sufficient to yield a quantitative description of such an anisotropic correlation. Therefore, we use the isotropic correlation coefficient (4.2.12) throughout our theoretical calculations.

Further the empirical formula (4.2.1) for the dependence of path rain probability on path length L is obtained from the rain gauge network data in Florida. The test of the applicability of this empirical formula to other locations and the improvement of this approximation will require further multiple rain gauge experiments at other locations.

The XPD prediction technique presented here has used a specific model for the statistics of rain, namely, that proposed by Lin (1975). Other authors have proposed different rain models which may be more appropriate to other parts of the world (e.g. Moritta and Higuti, 1974; Harden, Norbury and White, 1974). A formulation of the same problem (prediction of the long-term statistics of XPD) based upon these models, is also needed. The statistics of rain, as has been explained previously, mainly influence the long-term statistical behaviour of the short-term average of XPD, which has been found theoretically, in this thesis, to be the log of a Rayleigh variable. The difficulty with the analysis using other rain models, is that we cannot immediately find a simple analytic form for the long-term distribution of the short-term average XPD. On the other hand, Nakagami has claimed that if a Rayleigh variable has a fluctuating mean value then, under certain conditions, the overall distribution of this variable becomes successively a log normal one. But, so far, this conjecture has not been theoretically proved, unless the mean value itself obeys a log normal law. It is of vital importance that this problem be solved because if this conjecture is true for our case, then it is true for all the rain models. The overall distribution of XPD will be normal, which would be a physically reasonable result. In our opinion, advanced numerical techniques may well be needed for the investigation of this important problem.

This XPD prediction method is also more appropriate for terrestrial links, because for earth-space paths the uncertainty in the estimation of the length of path through the rain medium, arises. This length is, of course, a function of elevation angle and the rainfall rate, because rains with low rainfall rate are very extensive in the horizontal direction; on the other hand, thunderstorms have the form of a narrow localised vertical column. Nowland et al (1977) considering data from Canada and the northern USA, have proposed a formula to predict the effective rain path length as a function of elevation angle and point rainfall rate (see Chapter 2). But their formula is completely empirical and, so far, has not yet won universal acceptance. Hence, further work is needed on this line.

Finally, an extension of this work must be attempted in the case when snow or ice particles are present in the medium of propagation, as it is well known that such precipitation particles are an important factor for the depolarization of microwave signals. But in order to attempt such an analysis, information on the shape, distribution size, canting angle distribution of falling snow particles, and the long-term distribution of the fluctuating snowfall rate will be needed.

APPENDIX A

THEORETICAL RELATIONSHIPS BETWEEN THE PARAMETERS OF A LOG-NORMAL VARIABLE

If a random variable X follows a log-normal distribution, then the following relationships are valid between the X_m (median value), S_X (standard deviation of ln X), $\langle X \rangle$ (mean value) and $\mathrm{var}\left[X\right]$ (Aitchison and Brown, 1965):-

$$\left.\begin{aligned} X_m &= \langle X \rangle \exp(-\, S_X^2/2) \\ S_X^2 &= \ln\left[1 + (\mathrm{var}\left[X\right]/\langle X \rangle)^2\right] \end{aligned}\right\} \qquad \text{(A-1)}$$

As a direct consequence, we apply these formulas to the log-normal variables $\overline{R}$ (space-averaged rainfall rate), R_j (point rainfall rate) and Ω (short-term mean square value of the complex cross-polarization factor). Hence, we have:-

$$\left.\begin{aligned} \overline{R}_m &= \langle \overline{R} \rangle \exp(-\, S_{\overline{R}}^2/2) \\ R_m &= \langle R_j \rangle \exp(-\, S_R^2/2) \\ \Omega_m &= \langle \Omega \rangle \exp(-\, S_\Omega^2/2) \end{aligned}\right\} \qquad \text{(A-2)}$$

and:-

$$\left.\begin{aligned}
S^2_{\bar{R}} &= \ln\left[1 + \left(\mathrm{var}\left[\bar{R}\right]/\langle\bar{R}\rangle\right)^2\right] \\
S^2_{R} &= \ln\left[1 + \left(\mathrm{var}\left[R_j\right]/\langle R_j\rangle\right)^2\right] \\
S^2_{\Omega} &= \ln\left[1 + \left(\mathrm{var}\left[\Omega\right]/\langle\Omega\rangle\right)^2\right]
\end{aligned}\right\} \qquad \text{(A-3)}$$

On the other hand, if a random variable Y is identically zero during non-raining time and has a log-normal distribution during rain, then the following relationships between its unconditional and conditional parameters apply (Lin, 1975):-

$$\left.\begin{aligned}
\langle Y\rangle_u &= \langle Y\rangle \, P_o(0) \\
S^2_Y &= \ln\left\{P_o(0)\left[1 + \left(\frac{\mathrm{var}_u\left[Y\right]}{\langle Y\rangle_u}\right)^2\right]\right\}
\end{aligned}\right\} \qquad \text{(A-4)}$$

or:-

$$\left.\begin{aligned}
\langle Y\rangle_u &= \langle Y\rangle \, P_o(L) \\
S^2_Y &= \ln\left\{P_o(L)\left[1 + \left(\frac{\mathrm{var}_u\left[Y\right]}{\langle Y\rangle_u}\right)^2\right]\right\}
\end{aligned}\right\} \qquad \text{(A-5)}$$

The formulas (A-4) are valid when the random variable Y refers to a specific point on the radio path (such as the point rainfall rate R_j, where the appropriate rain probability is the point one, $P_o(0)$ and the formulas (A-5) are valid, when the variable Y refers to the total path (such as the space-averaged rainfall rate $\overline{R}$ or the mean square value Ω of the complex cross-polarization factor, where the appropriate rain probability is the $P_o(L)$). Application of these results to the random variables R_j, $\overline{R}$, Ω gives:-

$$\left.\begin{aligned} \langle R_j \rangle_u &= \langle R_j \rangle \, P_o(0) \\ \langle \overline{R} \rangle_u &= \langle \overline{R} \rangle \, P_o(L) \\ \langle \Omega \rangle_u &= \langle \Omega \rangle \, P_o(L) \end{aligned}\right\} \tag{A-6}$$

and:-

$$\left.\begin{aligned} S_R^2 &= \ln \left\{ P_o(0) \left[1 + \left(\frac{\mathrm{var}_u \left[R_j \right]}{\langle R_j \rangle_u} \right)^2 \right] \right\} \\ S_{\overline{R}}^2 &= \ln \left\{ P_o(L) \left[1 + \left(\frac{\mathrm{var}_u \left[\overline{R} \right]}{\langle \overline{R} \rangle_u} \right)^2 \right] \right\} \\ S_\Omega^2 &= \ln \left\{ P_o(L) \left[1 + \left(\frac{\mathrm{var}_u \left[\Omega \right]}{\langle \Omega \rangle_u} \right)^2 \right] \right\} \end{aligned}\right\} \tag{A-7}$$

APPENDIX B

THE m-DISTRIBUTION

B.1 Brief Description of the Distribution

This distribution was first derived by Nakagami in 1954 from his large-scale experiments on rapid fading in h.f. long distance propagation (Nakagami, 1960). The theoretical derivation of the m-distribution is briefly the following.

Regardless of the modes of propagation, i.e. whether ionospheric or tropospheric, it is reasonably supposed that the signal amplitude at an observing point is composed of some component signals $A_i\, e^{j\phi_i}$ ($i = 1, 2, \ldots .\, n$) which have travelled on different paths and whose amplitudes and phases vary according to certain statistical laws. So, the amplitude is the sum of independent random phasors ($\sum_{i=1}^{n} A_i\, e^{j\phi_i}$) subject only to the condition that the X and Y components ($X = \sum_{i=1}^{n} A_i \cos \phi_i$), ($Y = \sum_{i=1}^{n} A_i \sin \phi_i$) of the sum are normal (use of Central Limit Theorem). After a very complicated computation, the following formula for the distribution density of amplitude $R = \left| \sum_{i=1}^{n} A_i\, e^{j\phi_i} \right|$ is derived:-

$$p_R(r) = \frac{r_e^{-D}}{\sqrt{S_1 S_2}} \sum_{k=0}^{\infty} (-1)^k \, \varepsilon_k I_k(P) I_{2k}(\sqrt{Q^2 + \overline{r}^2}) \cos \left[2k \arctan(\overline{r}/Q)\right] \quad \text{(B-1)}$$

where $I_k(\ )$ is the modified Bessel function of order k, S_1 and S_2 are the variances of the variables X and Y respectively. The symbols D, P, Q, $\overline{r}$ are defined by Nakagami as:-

$$
\left.
\begin{aligned}
D &= \frac{\langle X\rangle^2}{2S_1} + \frac{\langle Y\rangle^2 + r^2}{2S_2} + \frac{S_2 - S_1}{4S_1 S_2}\, r^2 \\[2ex]
P &= \frac{S_2 - S_1}{4S_1 S_2}\, r^2 \\[2ex]
Q &= \frac{\langle X\rangle\, r}{S_1} \\[2ex]
\overline{r} &= \frac{\langle Y\rangle\, r}{S_2}
\end{aligned}
\right\} \qquad \text{(B-2)}
$$

This lengthy formula is not used in practical engineering applications. Nakagami defines the distribution by means of the parameters m and Ω (as $M(R, m, \Omega)$) where:-

$$
\left.
\begin{aligned}
m &= \frac{\langle R^2\rangle^2}{\langle (R^2 - \langle R^2\rangle)^2 \rangle} \geq \frac{1}{2} \quad \text{always and,} \\[2ex]
\Omega &= \langle R^2\rangle = \langle X\rangle + \langle Y\rangle + S_1 + S_2 \\[2ex]
p_R(r) &= M(r, m, \Omega) = \frac{2m^m\, r^{2m-1}}{\Gamma(m)\, \Omega^m}\, e^{-(m/\Omega)\, r^2}
\end{aligned}
\right\} \qquad \text{(B-3)}
$$

This formula defining the "m-distribution" includes both the Rayleigh distribution and the one-sided Gaussian distribution as special cases for m = 1 and m = 1/2, respectively.

B.2 Relationship Between the Mean Value and the Mean Square Value of an m-Distributed Variable

By definition, we have:-

$$\langle R\rangle = \int_{-\infty}^{\infty} rp_R(r)\ dr = \int_0^{\infty} \left[r2m^m\ r^{2m-1}/\left(\Gamma(m)\ \Omega^m\right)\right] \exp\left(-\ (m/\Omega)\ r^2\right) dr =$$

$$= \left[2m^m/\left(\Gamma(m)\ \Omega^m\right)\right] \int_0^{\infty} r^{2m} \exp\left(-\ (m/\Omega)\ r^2\right) dr \tag{B-4}$$

The integral:-

$$I = \int_0^{\infty} r^{2m} \exp\left(-\ (m/\Omega)\ r^2\right) dr$$

can be evaluated from Abramowitz and Stegun (1965) and its value is:-

$$I = \Omega^{m+\frac{1}{2}}\ \Gamma\left(m + \frac{1}{2}\right) / \left(2m^{m+\frac{1}{2}}\right) \tag{B-5}$$

Then:-

$$\langle R\rangle = \left[\Gamma\left(m + \frac{1}{2}\right) / \left(\Gamma(m)\ m^{\frac{1}{2}}\right)\right] \sqrt{\Omega} \tag{B-6}$$

where $\Gamma(\ )$ is the gamma function. This formula has been used in Chapter 3.

B.3 Effects of the Parameter Variations on the m-Distribution

In this section, we present Nakagami's conjecture for the final distribution of a general m-variable when its parameters fluctuate. These effects are of considerable importance in the estimation of the distribution over a long-term where the parameters can no longer be considered as constants.

If we start with an m-distributed variable R, then its probability density function is given by (B-3) and defining T, T_o as db intensities of R and $\sqrt{\Omega}$ above unit intensity, we have that:-

$$p_T(\tau) = \frac{2m^m}{M\Gamma(m)} \exp\left[m\left\{\frac{2(\tau - \tau_o)}{M} - e^{2(\tau - \tau_o)/M}\right\}\right] \equiv M_T(\tau, m, \tau_o) \qquad \text{(B-7)}$$

M = ln 10

Now let $p(\tau_o, m)$ be the joint distribution function of the parameters T_o and m, then the distribution of T can be written as:-

$$p_T(\tau) = \int_{\frac{1}{2}}^{\infty} dm \int_{-\infty}^{\infty} M_T(\tau, m, \tau_o)\, p(\tau_o, m)\, d\tau_o \qquad \text{(B-8)}$$

Nakagami's observations and some calculations seem to support strongly that:-

$$\left.\begin{aligned} p(\tau_o, m) &= p_{T_o}(\tau_o)\, p(m) \\ p(1/m) &= \frac{1}{\sqrt{2\pi}\, A}\, e^{-(1/2A^2)\{(1/m - 1/m_o)\}^2} \\ p_{T_o}(\tau_o) &= \frac{1}{\sqrt{2\pi}\,\sigma_o}\, e^{-(1/2\sigma_o^2)\{(\tau_o - \overline{\tau}_o)\}^2} \end{aligned}\right\} \qquad \text{(B-9)}$$

These relations, with the exception of the last, are not yet established. Therefore, only the effect of T_o will be considered. This is also the case for the rain depolarization problem, because the distribution of the amplitude of complex polarization factor C_R is a Rayleigh variable (m = 1), with its mean value fluctuating in a long-term period with a log-normal law.

After some calculations, we get a final expression:-

$$p_T(\tau) \cong C\, M_T(\tau, m, \overline{\tau}_0)\; S(\tau, m, \overline{\tau}_0) \tag{B-10}$$

where:-

$$S(\tau, m, \overline{\tau}_0) = \frac{M}{\sqrt{M^2 + 4\sigma_0^2\, m\, Q_1}} \exp\left\{\frac{2\sigma_0^2\, m^2\, (1 - Q_1)^2}{M^2 + 4\sigma_0^2\, m\, Q_1}\right\} \tag{B-11}$$

$Q_1 = e^{(2/M)\,(\tau - \overline{\tau}_0)}$, C = normalizing factor nearly equal to 1.

Numerical calculations (Nakagami, Tanaka and Kanehisa, 1957) clearly indicate the remarkable tendency that, with the increase in fluctuations of T_0 or Ω, $p_T(\tau)$ gradually approaches a normal type of distribution. For example, even in the extreme case of m equal to 1/2, $p_T(\tau)$ may be taken as normal form for larger values of σ_0 than 10 db, and the same will hold for the Rayleigh distribution for values of σ_0 beyond 7 db. As mentioned in Section 3.3, we have calculated the integral (B-8) for m = 1, by using numerical techniques. A comparison of the two methods is shown in Figs. B-1, B-2, B-3 for different parameters $\overline{\tau}_0 = 0$ and σ_0 = 5, 6, 7 db. It is clear that with the numerical integration, the tendency to the normal distribution is more rapid than using Nakagami's formulas.

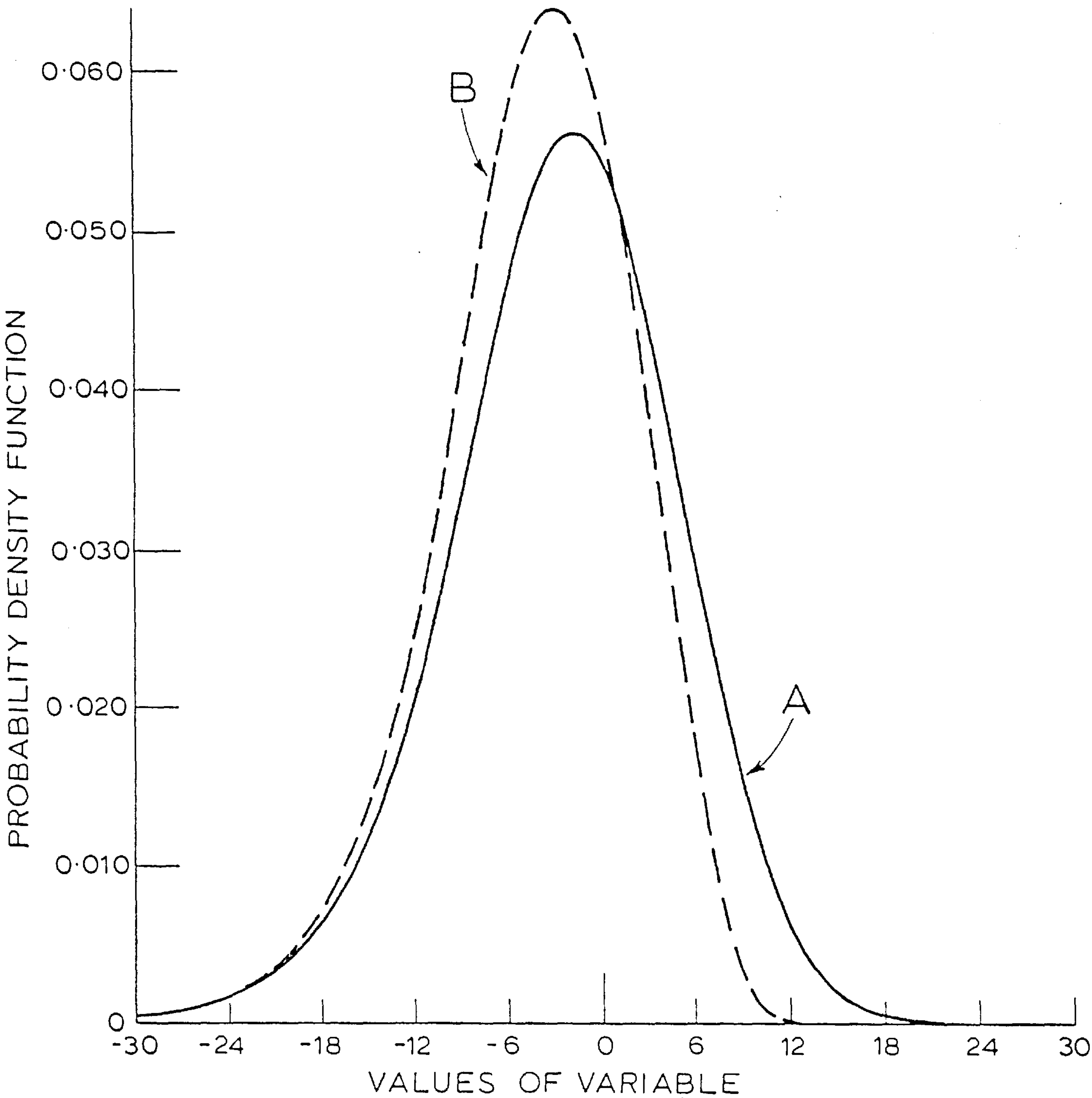

Fig. B.1 Lognormal approximation of a Rayleigh variable with its short-term mean value fluctuating.
Parameters of the short-term:
Expectation value 0; Standard deviation 5

A Numerical method
B Nakagami's method

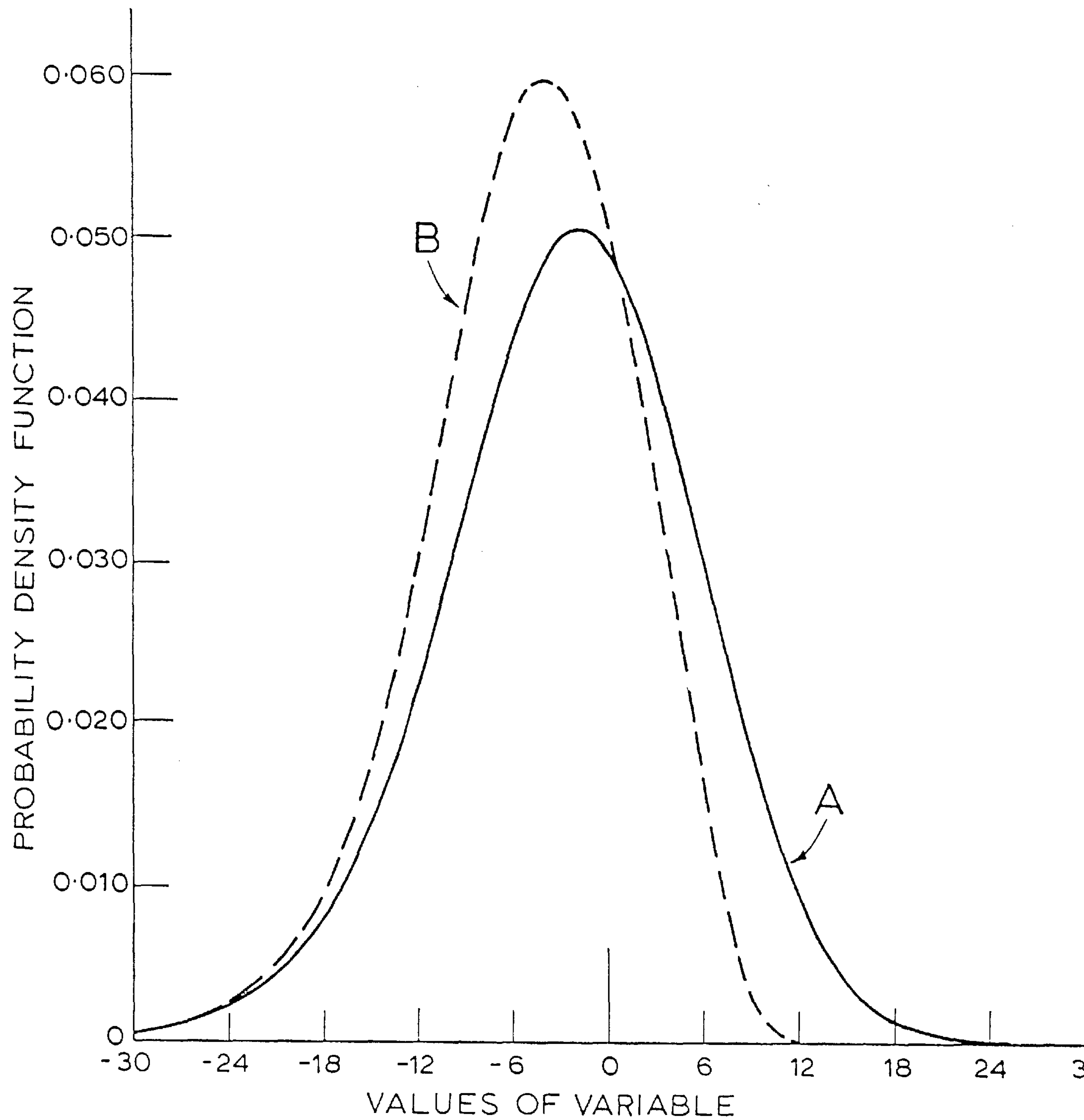

Fig. B.2 Lognormal approximation of a Rayleigh variable with its short-term mean value fluctuating. Parameters of the short-term: Expectation value 0; Standard deviation 6

A Numerical method
B Nakagami's method

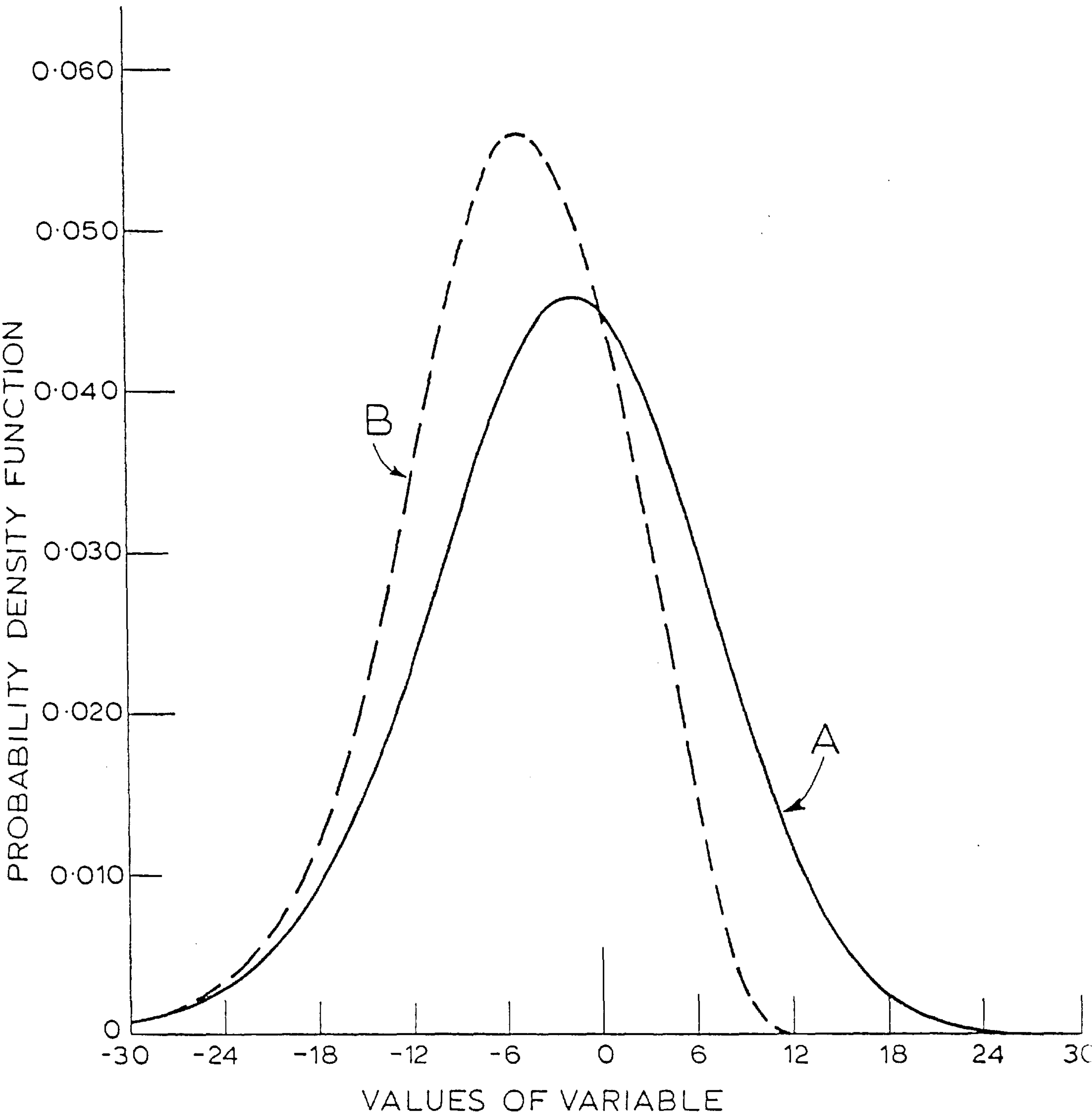

Fig. B.3 Lognormal approximation of a Rayleigh variable with its short-term mean value fluctuating. Parameters of the short-term: Expectation value 0; Standard deviation 7

A Numerical method
B Nakagami's method

APPENDIX C

RAYLEIGH AND RICE-NAKAGAMI PHASORS

C.1 Brief Description of Random Phasors

A signal of almost any kind can be represented by the real or imaginary part of:-

$$\vec{S}(t) = \vec{A}(t) \exp \{i\left[\omega(t)\ t + \Phi_0(t)\right]\} \tag{C-1}$$

where the amplitude $\vec{A}$, frequency ω and phase Φ_0 can be functions of time. The vector notation indicates that $\vec{S}$ can be a space vector, as in the case of the electric or magnetic field of a radio wave. However, if we limit ourselves to the scalar component of such a space vector, we can write (C-1) as a phasor:-

$$S = Ae^{i\Phi} \tag{C-2}$$

where A is the amplitude and $\Phi = \omega t + \Phi_0$ is the phase of the signal at time t. Both A and Φ can be random - in the case of noise evidently always, and in the case of a message because the exact nature of the message is unknown (or else there would be no point in transmitting it). The phase of a phasor $Ae^{i\Phi}$ is very often uniformly distributed between 0 and 2π:-

$$p_\Phi(\varphi) = \frac{1}{2\pi}\ (0 \leq \varphi \leq 2\pi) \tag{C-3}$$

A phasor with uniformly distributed phase, is very common in practical applications and deserves a shorter name: we shall call it a "UDP phasor" (Beckmann, 1967).

C.2 Rayleigh Phasors

Consider the sum:-

$$S = Re^{i\theta} = \sum_{j=1}^{n} A_j \, e^{i\Phi j} \tag{C-4}$$

where the terms are independent UDP phasors and the A_j are all distributed identically. It can easily be verified that the resulting phase distribution is again uniform. We wish now to find the amplitude distribution $p_R(r)$. Resolving S into its real and imaginary parts, we have:-

$$\left.\begin{aligned} X &= \text{Re } S = R \cos\theta = \sum_{j=1}^{n} A_j \cos\Phi_j = \sum_{j=1}^{n} X_j \\ Y &= \text{Im } S = R \sin\theta = \sum_{j=1}^{n} A_j \sin\Phi_j = \sum_{j=1}^{n} Y_j \end{aligned}\right\} \tag{C-5}$$

If n is large, then using Central Limit Theorem (Papoulis, 1965) (the A_j being all identically distributed), both X and Y will be distributed normally with mean values:-

$$\langle X \rangle = \sum_{j=1}^{n} \langle A_j \cos\Phi_j \rangle \,, \; \langle Y \rangle = \sum_{j=1}^{n} \langle A_j \sin\Phi_j \rangle \tag{C-6}$$

In particular, if A_j are not correlated with the Φ_j, then:-

$$\langle X \rangle = \sum_j \langle A_j \rangle \langle \cos\Phi_j \rangle = \sum_j \langle A_j \rangle \frac{1}{2\pi} \int_C^{C+2\pi} \cos\varphi_j \, d\varphi_j = 0 \tag{C-7}$$

and similarly:-

$$\langle Y \rangle = \sum_{j=1}^{n} \langle A_j \rangle \langle \sin \Phi_j \rangle = 0 \qquad \text{(C-8)}$$

The variances of X and Y are (since $\langle X \rangle = \langle Y \rangle = 0$):-

$$\mathrm{var}\left[X\right] = \langle X^2 \rangle = \sum_{j=1}^{n} \langle A_j^2 \rangle \langle \cos^2 \Phi_j \rangle = \frac{1}{2} n \langle A_j^2 \rangle \qquad \text{(C-9)}$$

$$\mathrm{var}\left[Y\right] = \langle Y^2 \rangle = \sum_{j=1}^{n} \langle A_j^2 \rangle \langle \sin^2 \Phi_j \rangle = \frac{1}{2} n \langle A_j^2 \rangle \qquad \text{(C-10)}$$

Setting:-

$$\frac{1}{2} n \langle A_j^2 \rangle = \sigma^2 \qquad \text{(C-11)}$$

we find the distributions of X and Y as:-

$$p_X(x) = \frac{1}{\sqrt{2\pi}\,\sigma} e^{-x^2/2\sigma^2} \quad , \quad p_Y(y) = \frac{1}{\sigma\sqrt{2\pi}} e^{-y^2/2\sigma^2} \qquad \text{(C-12)}$$

Next, we check whether X and Y are correlated:-

$$\langle XY \rangle = \sum_{j=1}^{n} \sum_{k=1}^{n} \langle A_j A_k \rangle \langle \cos \Phi_j \sin \Phi_k \rangle = 0 \qquad \text{(C-13)}$$

since $\langle \cos \Phi_j \sin \Phi_k \rangle = 0$ for all j and k. Thus X and Y are uncorrelated, which in the case of the normal distribution implies that they are independent. Hence, from (C-12) their two-dimensional distribution is:-

$$p_{XY}(x, y) = \frac{1}{2\pi\ \sigma^2}\ e^{-\ (x^2 + y^2)/2\sigma^2} \qquad \text{(C-14)}$$

Transforming back to polar coordinates, we obtain:-

$$p_{R\theta}(r, \partial) = \frac{r}{2\pi\ \sigma^2}\ e^{-\ r^2/2\sigma^2} \qquad (0 \leq \partial \leq 2\pi\ ,\ 0 \leq r < \infty) \qquad \text{(C-15)}$$

where σ^2 is by (C-9), (C-10) the variance of X and Y, which may easily be expressed in terms of the mean-square value of R:-

$$<R^2> = <X^2> + <Y^2> = 2\sigma^2 \qquad \text{(C-15)}$$

Setting $<R^2> = 2\sigma^2 = \Omega$, we, therefore, obtain:-

$$p_{R\theta}(r, \partial) = \frac{r}{\pi\Omega}\ e^{-\ r^2/\Omega} \qquad \text{(C-16)}$$

The distribution of ∂ is, as expected, uniform:-

$$p_{\theta}(\partial) = \int_0^{\infty} p_{R\theta}(r, \partial)\ dr = \frac{1}{\pi\Omega}\int_0^{\infty} re^{-\ r^2/\Omega}\ dr = \frac{1}{2\pi} \quad (0 < \partial < 2\pi) \qquad \text{(C-17)}$$

and the required distribution of R is:-

$$p_R(r) = \int_0^{2\pi} \frac{r}{\pi\Omega}\ e^{-r^2/\Omega}\ d\partial = \frac{2r}{\Omega}\ e^{-\ r^2/\Omega} \qquad (r \geq 0) \qquad \text{(C-18)}$$

i.e. the Rayleigh distribution. The parameter Ω is its mean-square value, and by (C-15) and (C-11), it is given by:-

$$\Omega = n \langle A_j^2 \rangle \tag{C-19}$$

Looking over this derivation from (C-12) onward, we see that the Rayleigh distribution is the solution of a more general problem than the one we originally set out to investigate - the distribution of R when all A_j are distributed identically and the Φ_j are all uniform over a basic phase cycle. It follows from (C-12) that the Rayleigh distribution will be obtained for any quantity R given by:-

$$R^2 = X^2 + Y^2 \tag{C-20}$$

if X and Y are independent and both normal with the same variance and zero mean. Conversely, it is evident that any Rayleigh-distributed quantity may always be decomposed into two components X and Y as in (C-20), where both X and Y are normal with zero mean and the same variance.

Thus, (C-12) may be obtained from (C-4) under more general conditions. Although the terms in (C-4) must be UDP phasors, since otherwise the conditions of zero mean and equal variances for X and Y could not be satisfied (except by artificially constructed exceptions), we need not require that the A_j be distributed identically: it is enough that their distributions be such that the Central Limit Theorem is satisfied for X and Y. Referring to Beckmann (1967), we find that in practice this means:-

$$\left.\begin{array}{ll} (1) & n \text{ must be large} \\ (2) & \langle A_j^2 \rangle \ll \sum_{j=1}^{n} \langle A_j^2 \rangle \text{ for all } j \end{array}\right\} \tag{C-21}$$

i.e. in the sum there must be no predominant term, which by its large mean-square value would violate (C-21).

A phasor with the distribution (C-16), i.e. with the amplitude distribution (C-18) and the phase distribution (C-17) will be called a Rayleigh phasor. It follows that a Rayleigh phasor is always a UDP phasor.

Finally, a direct corollary of all the above theory is that the sum of any (not necessarily identical) Rayleigh phasors is itself a Rayleigh phasor. This important conclusion is used in Chapters 3 and 4.

C.3 Constant Plus Rayleigh Phasors

Consider the sum:-

$$Re^{i\theta} = C + \sum_{j=1}^{n} A_j \, e^{i\Phi j} \tag{C-22}$$

where C is a real constant and the second term adds up to a Rayleigh phasor.

Let the Rayleigh phasor equal $\rho e^{i\Phi}$. Its X and Y components are (from the preceding section) both normal with zero mean and variance $\Omega/2$, where $\Omega = \langle\rho^2\rangle$. Therefore, the X component of (C-22) is given by the sum of C and the X component of ρ (i.e. $\rho \cos \Phi$) and is thus distributed normally with mean C and variance $\Omega/2$. The Y component of (C-22) is equal to the Y component of the Rayleigh phasor ($\rho \sin \Phi$). Hence:-

$$p_{XY}(x, y) = \frac{1}{\Omega\pi} \exp\left[- \frac{(x - C)^2}{\Omega} - \frac{y^2}{\Omega}\right] \tag{C-23}$$

and transforming to polar coordinates as in the preceding section, we now have:-

$$p_{R\theta}(r, \partial) = \frac{r}{\pi\Omega} \exp\left[- \frac{(r \cos \partial - C)^2}{\Omega} - \frac{r^2 \sin^2 \partial}{\Omega}\right] \tag{C-24}$$

$$(r \geq 0,\ 0 \leq \partial \leq 2\pi)$$

or, after elementary manipulations:-

$$p_{R\theta}(r, \partial) = \frac{r}{\pi\Omega} e^{-(r^2 + C^2)/\Omega} e^{2rC \cos \partial/\Omega} \quad (r \geq 0,\ 0 \leq \partial \leq 2\pi) \tag{C-25}$$

Therefore, the required distribution of R is:-

$$p_R(r) = \int_0^{2\pi} p_{R\theta}(r, \partial)\, d\partial = \frac{r}{\pi\Omega} e^{-(r^2 + C^2)/\Omega} \int_0^{2\pi} e^{(2rC/\Omega) \cos \partial}\, d\partial \tag{C-26}$$

The integral can be expressed by means of a Bessel function:-

$$\frac{1}{2\pi} \int_0^{2\pi} e^{x \cos \partial}\, d\partial = I_o(x) = J_o(ix) \tag{C-27}$$

where $I_o(x)$ is the modified Bessel function of order zero. Using (C-27), we finally find from (C-26):-

$$p_R(r) = \frac{2r}{\Omega} e^{-(r^2 + C^2)/\Omega} I_o\left(\frac{2rC}{\Omega}\right), \quad (r \geq 0) \tag{C-28}$$

This is known as the "Rice-Nakagami distribution" (Beckmann, 1967). The phase distribution of (C-22) is no longer uniform. After a straightforward, though cumbersome, integration of (C-25), we find:-

$$p_\theta(\partial) = \int_0^\infty p_{R\theta}(r, \partial)\, dr = \frac{1}{2\pi} e^{-C^2/\Omega} \left[1 + G \sqrt{\pi}\, e^{G^2} (1 + \text{erf } G)\right] \tag{C-29}$$

where:-

$$G = \frac{C \cos \partial}{\sqrt{\Omega}} \qquad (0 \leq \partial \leq 2\pi) \tag{C-30}$$

APPENDIX D

EVALUATION OF THE FACTOR H(L)

The integral:-

$$H(L) = \int_0^L \int_0^L \frac{G\,dz\,dz'}{\left[G^2 + (z - z')^2\right]^{1/2}}$$

which is encountered in formula (4.2.16), is calculated as follows. We put:-

$$x = z - z' \tag{D-1}$$

as a new variable and the result is:-

$$H(L) = \int_0^L G\,dz' \int_{-z'}^{L - z'} \frac{dx}{\left[G^2 + x^2\right]^{1/2}} \tag{D-2}$$

The single integral:-

$$I(L) = \int_{-z'}^{L - z'} \frac{dx}{\left[G^2 + x^2\right]^{1/2}} \tag{D-3}$$

can be evaluated from Abramovitz and Stegun (1965) as:-

$$I(L) = \sinh^{-1}\left[(L - z')/G\right] - \sinh^{-1}\left[- z'/G\right] \tag{D-4}$$

so the integral (D-2) can now be written:-

$$H(L) = \int_0^L G \sinh^{-1}\left(\frac{L - z'}{G}\right) dz' - \int_0^L G \sinh^{-1}\left[- z'/G\right] dz' \qquad \text{(D-5)}$$

The two partial integrations which are indicated in expression (D-5) can be taken again from Abramovitz and Stegun (1975) and the final result is:-

$$H(L) = 2G^2 \left[\frac{L}{G}\left[\frac{\sinh^{-1}(L/G) - \sinh^{-1}(- L/G)}{2}\right] - \sqrt{1 + \frac{L^2}{G^2}} + 1\right] \qquad \text{(D-6)}$$

APPENDIX E

EVALUATION OF THE DOUBLE INTEGRAL (5.3.15) or (5.3.27)

The integral:-

$$I(x,\ y) \equiv \int_0^y \int_x^\infty p_{X_1 X_2}(x_1,\ x_2)\ dx_1\ dx_2 \tag{E-1}$$

can be calculated, substituting the joint density function from formula (5.2.15), as:-

$$I(x,\ y) = \int_0^y \frac{1}{2\pi\ \sigma_1\sigma_3\ \sqrt{1 - r^2}\ x_2}\ \exp\left(\left(-\ \frac{1}{2(1 - r^2)}\right)\left[\frac{(\ln\ x_2\ -\ \langle X_3\rangle)^2}{\sigma_3^2}\right]\right)\ \cdot$$

$$\cdot \left[\int_x^\infty \exp\left(\left(-\ \frac{1}{2(1-r^2)}\right)\left[\frac{(x_1\ -\ \langle X_1\rangle)^2}{\sigma_1^2} - \frac{2r(x_1\ -\ \langle X_1\rangle)(\ln\ x_2\ -\ \langle X_3\rangle)}{\sigma_1\ \sigma_3}\right]\right) dx_1\right] dx_2 \tag{E-2}$$

We treat separately the integral:-

$$I_1(x) = \int_x^\infty \exp\left(\left(-\ \frac{1}{2(1-r^2)}\right)\left[\frac{(x_1\ -\ \langle X_1\rangle)^2}{\sigma_1^2} - \frac{2r(x_1\ -\ \langle X_1\rangle)(\ln\ x_2\ -\ \langle X_3\rangle)}{\sigma_1\ \sigma_3}\right]\right) dx_1 \tag{E-3}$$

Putting $z = x_1 - x$, we have that:-

$$I_1(x) = \int_0^{\infty} \exp\left(- \frac{z^2}{2(1 - r^2)\,\sigma_1^2} - 2z\left[\frac{(x - \langle X_1\rangle)}{2(1 - r^2)\,\sigma_1^2} - \frac{r(\ln x_2 - \langle X_3\rangle)}{2(1 - r^2)\,\sigma_1\sigma_3}\right] - \right.$$

$$\left. - \left[\frac{(x - \langle X_1\rangle)^2}{2(1 - r^2)\,\sigma_1^2} - \frac{2r(x - \langle X_1\rangle)\,(\ln x_2 - \langle X_3\rangle)}{2(1 - r^2)\,\sigma_1\,\sigma_3}\right]\right) dz \qquad \text{(E-4)}$$

The integral (E-4) can be calculated from Abramovitz and Stegun (1965) as a special error integral and the result is that:-

$$I_1(x) = \left(\frac{1}{2}\right) \sqrt{\pi/f_1}\, \exp\left[(f_2^2/f_1^2) - f_3\right] \operatorname{erfc}\,(f_2/\sqrt{f_1}) \qquad \text{(E-5)}$$

where the parameters f_1, f_2, f_3 are given by:-

$$\left.\begin{aligned}
f_1 &= \frac{1}{2(1 - r^2)\,\sigma_1^2} \\
f_2 &= \left[\frac{(x - \langle X_1\rangle)}{2(1 - r^2)\,\sigma_1^2} - \frac{r(\ln x_2 - \langle X_3\rangle)}{2(1 - r^2)\,\sigma_1\sigma_3}\right] \\
f_3 &= \left[\frac{(x - \langle X_1\rangle)^2}{2(1 - r^2)\,\sigma_1^2} - \frac{2r(x - \langle X_1\rangle)\,(\ln x_2 - \langle X_3\rangle)}{2(1 - r^2)\,\sigma_1\,\sigma_3}\right]
\end{aligned}\right\} \qquad \text{(E-6)}$$

Substituting relations (E-5), (E-6) into the double integral (E-2), we have:-

$$I(x, y) = \int_0^y \frac{1}{2\sqrt{2\pi}\,\sigma_3\, x_2} \exp\left\{-\frac{(\ln x_2 - \langle X_3\rangle)^2}{2\sigma_3^2}\right\} .$$

$$. \operatorname{erfc}\left\{\frac{(x - \langle X_1\rangle)}{\sqrt{2}\sqrt{1 - r^2}\,\sigma_1} - \frac{r(\ln x_2 - \langle X_3\rangle)}{\sqrt{2}\sqrt{1 - r^2}\,\sigma_3}\right\} dx_2 \qquad \text{(E-7)}$$

If we now put $Y = -\ln x_2$, then the integral (E-7) becomes:-

$$I(x, y) = \int_{-\ln y}^{\infty} e^{-Y} f(Y)\, dY \qquad \text{(E-8)}$$

with:-

$$f(Y) = \frac{1}{2\sqrt{2\pi}\,\sigma_3} \exp\left\{-\frac{(Y + \langle X_3\rangle)^2}{2\sigma_3^2} + Y\right\} .$$

$$. \operatorname{erfc}\left[\frac{(x - \langle X_1\rangle)}{\sqrt{2}\sqrt{1 - r^2}\,\sigma_1} + \frac{r(Y + \langle X_3\rangle)}{\sqrt{2}\sqrt{1 - r^2}\,\sigma_3}\right] \qquad \text{(E-9)}$$

The integral (E-8) can be evaluated numerically using Gauss-Laguerre polynomials. This procedure estimates the value of an integral of the form:-

$$I_2 = \int_{\alpha}^{\infty} e^{-Y} f(Y)\, dY \qquad \text{(E-10)}$$

This integral is approximated by the formula:-

$$I_2 = \sum_{k=1}^{n} A_k f(Y_k) \qquad \text{(E-11)}$$

where A_k are the weights and Y_k the pivots. The pivots are the zeros of the Laguerre polynomials. This quadrature formula is exact if the function $f(Y)$ is a polynomial of degree not exceeding $2n - 1$, where n is the number of pivots used. In the estimation of our integral, we use 48 pivots.

APPENDIX F

DESCRIPTION OF COMPUTER PROGRAM

In this appendix, a description of the computer programs which are used in the thesis, is given. The first program evaluates the density distribution function and its best-fit normal approximation for the long-term rain cross-polarization statistics (Figs. 3.3, 3.4, 3.9, 3.10 and 4.3, 4.4, 4.15, 4.16). The second program calculates the cumulative distribution of the XPD for any microwave link (Figs. 3.5, 3.11, 4.5 to 4.11 and 4.17 to 4.23). The third program gives the outage time due to co-channel interference as a function of path length (Figs. 3.6 to 3.9, 3.12 to 3.14, 4.12 to 4.14 and 4.24 to 4.26). The fourth program evaluates the conditional distribution of XPD on a co-polar rain attenuation (Figs. 5.4 to 5.7 and 5.14 to 5.17), while the fifth gives the distribution of XPD under the condition of rain fade (Figs. 5.8, 5.9 and 5.18, 5.19). Finally, the sixth program calculates the total outage time for a dual-polarization communication system (Figs. 5.10 to 5.12).

LIST OF PROGRAMS

```
      PROGRAM JOHN (INPUT,OUTPUT,TAPE 62, TAPE 6 = OUTPUT)
C     THIS PROGRAM EVALUATES THE DENSITY DISTRIBUTION FUNCTION
      COMMON/GUC1/RM1,SR1
      DIMENSION AMEAN(11),DEVIAT(11),ERR(15,15),X(1Ø2),X1(1Ø2),
     1 X2(2Ø4),X3(2Ø4),X4(3Ø2),Y3(3Ø2),Y4(3Ø2),X5(7Ø),X6(21Ø),
     2 Y5(21Ø),A5Ø(4),B5Ø(4),C5Ø(6),A51(4),B51(4),C51(6)
      CALL START (2)
      CALL SCALEZ (1.)
      RM = Ø.64
      SR = 1.52
      P11 = 3.14159265
      THM = 1Ø. * P11/18Ø.
      STH = 4Ø. * P11/18Ø.
      AL = 1Ø.
      DO 8 I = 1, 4
      READ 9, B5Ø(I), A5Ø(I)
    9 FORMAT (F5.3, F4.2)
    8 CONTINUE
      DO 18 I = 1, 4
      READ 19, B51(I), A51(I)
   19 FORMAT (F5.3, F4.2)
   18 CONTINUE
      CALL EØ1AAF(A5Ø, B5Ø, C5Ø, 4, 6, 3, 22.)
      CALL EØ1AAF(A51, B51, C51, 4, 6, 3, 22.)
      C = C5Ø(6) * Ø.ØØØ1
      D = C51(6)
```

```
      AM = EXP(- 2. * STH * STH)
      AO = AM*AM*AL*AL*C*C*SIN(2. * THM) * SIN(2. * THM) /
     1 P11
      BO = 2. * D
      PO = Ø.Ø33
      DEN = (1. + AL * AL/21.5) * * Ø.Ø14
      PL = 1. - (1. - PO)/DEN
      G = 1.5
      ARG = AL/G
      ARG1 = 1./ARG
      IFAIL = Ø
      P = S11ABF(ARG, IFAIL)
      IFAIL = Ø
      P1 = S11ABF(- ARG, IFAIL)
      H = 2.*ARG1*ARG1*(ARG*(P-P1)/2. - SQRT(1. + ARG *
     1 ARG) + 1.)
      FAC = 1. + (EXP(SR * SR)/PO - 1.) * H
      SR1 = ALOG(PL * FAC)
      RM1 = RM*PO*EXP(SR*SR/2. - SR1/2.)/PL
      X4(1) = 1Ø.*ALOG1Ø(AO) + 1Ø.*BO*ALOG1Ø(RM1) - 3.
      DO 8ØØ I = 1,3ØØ
      A5 = X4(I)
      CALL DISTR3(AO, BO, A5, DIS)
      Y4(I) = DIS
8ØØ   X4(I + 1) = X4(I) + Ø.ØØ7
      AMAX = 1.Ø E-99
      DO 8Ø1 I = 1,3ØØ
      T1 = Y4(I)
```

```
      IF(T1 . GE . AMAX) GO TO 8Ø3
      GO TO 8Ø1
8Ø3   AMAX = T1
      L1 = I
      A2 = X4(L1)
      B2 = Ø.399/T1
8Ø1   CONTINUE
      WRITE (6,45Ø) A2, B2
45Ø   FORMAT(1H,5ØX,6HMEAN =, E16.7,4X,13HSTAND.DEV. =,E
     1 16.7)
      X(1) = - 11Ø.
      DO 1Ø5 I = 1,1ØØ
      A3 = X(I)
      CALL DISTR3(A0, B0, A3, DIS)
      CALL GAUSS(A2, B2, A3, GAS)
      X1(I) = DIS
      X2(I) = GAS
1Ø5   X(I + 1) = X(I) + 1.
      DO 1Ø6 I = 1,1ØØ
1Ø6   X3(I) = X(I)
      CALL LINAX (1.2, 1.2, 1, 1.58, 11, - 11Ø., 1Ø., 5, 1, 1, - 1, 1)
      CALL LINAX (1.2, 1,2, 2, Ø.9, 15, Ø., Ø.ØØ2, 1, 2, 2, 3, 1)
      CALL POINTS (X3, X2, 1ØØ)
      CALL POINTS (X3, X1, 1ØØ)
      CALL ENPLOT
      STOP
      END
```

```
      PROGRAM JOHN (INPUT,OUTPUT,TAPE 62,TAPE 6 = OUTPUT)
C     THIS PROGRAM EVALUATES THE CUMULATIVE DISTRIBU
     1TION FOR XPD
      COMMON/GUC1/RM1,SR1
      DIMENSION AMEAN(11),DEVIAT(11),ERR(15, 15),X(1Ø2),X1
     1(1Ø2),X2(2Ø4),X3(2Ø4),X4(3Ø2),Y4(3Ø2),X5(7Ø),X6(21Ø),
     2Y5(21Ø),A5Ø(4),B5Ø(4),C5Ø(6),A51(4),B51(4),C51(6)
      CALL START (2)
      CALL SCALEZ (1.)
      RM = Ø.64
      SR = 1.52
      AL = 4
      P11 = 3.14159265
      THM = 1Ø. * P11/18Ø
      STH = 4Ø. * P11/18Ø
      DO 8 I = 1,4
      READ 9, B5Ø(I), A5Ø(I)
    9 FORMAT (F5.3, F4.2)
    8 CONTINUE
      DO 18 I = 1,4
      READ 19, B51(I), A51(I)
   19 FORMAT (F5.3, F4.2)
   18 CONTINUE
      CALL EØ1AAF (A5Ø, B5Ø, C5Ø, 4, 6, 3, 22.)
      CALL EØ1AAF (A51, B51, C51, 4, 6, 3, 22.)
      C = C5Ø(6). * Ø.ØØØ1
      D = C51(6)
      AM = EXP (- 2. * STH * STH)
```

```
      AO = AM*AM*AL*AL*C*C*SIN(2. * THM)*SIN(2. * THM)/P11
      BO = 2. * D
      PO = Ø.Ø33
      DEN = (1. + AL * AL/21.5) * * Ø.Ø14
      PL = 1. - (1. - PO)/DEN
      G = 1.5
      ARG = AL/G
      ARG1 = 1./ARG
      IFAIL = Ø
      P = S11ABF(ARG, IFAIL)
      IFAIL = Ø
      P1 = S11ABF(- ARG, IFAIL)
      H = 2.*ARG1*ARG1*(ARG*(P-P1)/2. - SQRT(1. + ARG *
     1 ARG) + 1.)
      FAC = 1. + (EXP(SR * SR)/PO - 1.) * H
      SR1 = ALOG(PL * FAC)
      RM1 = RM * PO * EXP(SR * SR/2. - SR1/2.)/PL
      X4(1) = 1Ø.*ALOG1Ø(AO)+1Ø.*BO*ALOG1Ø(RM) - 3.
      DO 8ØØ I = 1,3ØØ
      A5 = X4(I)
      CALL DISTR3(RM, SR, AO, BO, A5, DIS)
      Y4(I) = DIS
8ØØ   X4(I + 1) = X4(I) + Ø.ØØ7
      AMAX = 1.Ø E-99
      DO 8Ø1 I = 1,3ØØ
      T1 = Y4(I)
      IF (T1 . GE . AMAX) GO TO 8Ø3
      GO TO 8Ø1
```

```
803   AMAX = T1
      L1 = I
      A2 = X4(L1)
      B2 = Ø.399/T1
8Ø1   CONTINUE
      WRITE (6, 45Ø) A2, B2
45Ø   FORMAT (1H,5ØX,6HMEAN=,E16.7,4X,13HSTAND.DEV.=
     1,E16.7)
      X5(1) = - 4Ø.
      DO 2ØØ I = 1,7Ø
      PRM = (X5(I) - A2)/B2
      IFAIL = Ø
      P2 = S15ACF (PRM, IFAIL)
      Y5(I) = P2 * 3.3
2ØØ   X5(I + 1) = X5(I) + Ø.3
      DO 2Ø1 I = 1,7Ø
2Ø1   X6(I) = X5(I)
      CALL LOGAX(1.2, 1.2, 2, 7., 2, - 3, 2, 2, 1)
      CALL LINAX(1.2, 1.2, 1, 3.2, 5, - 45., 5., 5, 1, 1, - 1, 1)
      CALL POINTS(X6, Y5, 7Ø)
      X4(1) = 1Ø.*ALOG1Ø(A0) + 1Ø.*BO*ALOG1Ø(RM1) - 3.
      DO 7ØØ I = 1,3ØØ
      A5 = X4(I)
      CALL DISTR2(AO, BO, A5, DIS)
      Y4(I) = DIS
7ØØ   X4(I + 1) = X4(I) + Ø.ØØ7
      AMAX = 1.Ø E-99
      DO 7Ø1 I = 1,3ØØ
```

```
      T1 = Y4(I)
      IF (T1 . GE . AMAX) GO TO 7Ø3
      GO TO 7Ø1
7Ø3   AMAX = T1
      L1 = I
      A21 = X4(L1)
      B21 = Ø.399/T1
7Ø1   CONTINUE
      WRITE (6,75Ø) A21, B21
75Ø   FORMAT(1H,50X,6HMEAN = ,E16.7,4X,13HSTAND.DEV. =
     1,E16.7)
      DO 3ØØ I = 1,7Ø
      PRM = (X5(I) - A21)/B21
      IFAIL = Ø
      P3 = S15ACF(PRM, IFAIL)
      Y5(I) = P3 * 1ØØ. * PL
3ØØ   X5(I + 1) = X5(I) + Ø.3
      DO 3Ø1 I = 1,7Ø
3Ø1   X6(I) = X5(I)
      CALL POINTS (X6, Y5, 7Ø)
      CALL ENPLOT
      STOP
      END
```

```
      PROGRAM JOHN (INPUT,OUTPUT,TAPE 62,TAPE 6 = OUTPUT)
C     THIS PROGRAM EVALUATES THE OUTAGE TIME DUE TO
     1CHANNEL INTERFERENCE
      COMMON/GUC1/RM1, SR1
      DIMENSION R(4Ø),X(4Ø),Y5(4Ø),X6(4Ø),X4(3Ø2),Y4(3Ø2)
     1,XP(4Ø),YP(4Ø),A5Ø(4),B5Ø(4),C5Ø(6),A51(4),B51(4),C51(6)
      CALL START (2)
      CALL SCALEZ (1.)
      RM = 1.52
      SR = 1.38
      P11 = 3.14159265
      THM = 1Ø. * P11/18Ø
      STH = 4Ø. * P11/18Ø
      DO 8 I = 1,4
      READ 9, B5Ø(I), A5Ø(I)
    9 FORMAT (F5.3, F4.2)
    8 CONTINUE
      DO 18 I = 1,4
      READ 19, B51(I), A51(I)
   19 FORMAT (F5.3, F4.2)
   18 CONTINUE
      CALL EØ1AAF (A5Ø, B5Ø, C5Ø, 4, 6, 3, 3Ø.)
      CALL EØ1AAF (A51, B51, C51, 4, 6, 3, 3Ø.)
      C = C5Ø(6) * Ø.ØØØ1
      D = C51(6)
      PO = Ø.Ø26
      G = 1.5
      AM = EXP (- 2. * STH * STH)
```

```
      X(1) = 1.
      DO 5 I = 1,3Ø
      AL = X(I)
      AO = AM*AM*AL*AL*C*C*SIN(2. * THM)*SIN(2. * THM)/P11
      BO = 2. * D
      DEN = (1. + AL * AL/21.5) * * Ø.Ø14
      PL = 1. - (1. - PO)/DEN
      ARG = AL/G
      ARG1 = 1./ARG
      IFAIL = Ø
      P = S11ABF(ARG, IFAIL)
      IFAIL = Ø
      P1 = S11ABF(- ARG, IFAIL)
      H = 2.*ARG1*ARG1*(ARG*(P-P1)/2.-SQRT(1.+ARG*ARG)+1.)
      FAC = 1. + (EXP(SR * SR)/PO - 1.) * H
      SR1 = ALOG(PL * FAC)
      RM1 = RM * PO * EXP(SR * SR/2. - SR1/2.)/PL
      HINT = 1Ø. * ALOG1Ø(AO) + 1Ø. * BO * ALOG1Ø(RM1)
      X4(1) = HINT - 3.
      DO 8ØØ J = 1,3ØØ
      A5 = X4(J)
      CALL DISTR2(AO, BO, A5, DIS)
      Y4(J) = DIS
8ØØ   X4(J + 1) = X4(J) + Ø.8
      AMAX = 1.Ø E-99
      DO 8Ø1 L = 1,3ØØ
      T1 = Y4(L)
      IF (T1 . GE . AMAX) GO TO 8Ø3
```

```
      GO TO 8Ø1
803   AMAX = T1
      L1 = L
      A2 = X4(L1)
      B2 = Ø.399/T1
8Ø1   CONTINUE
      WRITE(6,45Ø) A2, B2
45Ø   FORMAT(1H,5ØX,6HMEAN =,E16.7,4X,13HSTAND.DEV. = ,
     1E16.7)
      ALEV = - 2Ø.
      PRM = (ALEV - A2)/B2
      IFAIL = Ø
      P2 = S15ACF(PRM, IFAIL)
      Y5(I) = P2 * 876Ø. * 6Ø. * PL
      X(I + 1) = X(I) + Ø.3
5     CONTINUE
      DO6 I = 1,3Ø
6     X6(I) = X(I)
      CALL LOGAX(1.2, 1.2, 2, 6.5, 4, 0, 2, 2, 1)
      CALL LINAX(1.2, 1.2, 1, 1.5, 10, 0., 1., 1, 1, 1, - 1, 1)
      DO 1ØØ5 I = 1,3Ø
      CALL LØCATE(X6(I), Y5(I), XP(I), YP(I), N5)
1ØØ5  CONTINUE
      CALL ARKIST(XP, YP, 1, 3Ø, 1Ø, 1., 1., Ø., Ø., 2, 1)
      WRITE (6,551)
551   FORMAT(1H, 5ØX, 1HC)
      THM = THM + P11/4.
      DO 15 I = 1,3Ø
```

```
      AL1 = X(I)
      A0 = AM*AM*AL*AL*C*C*SIN(2. * THM)*SIN(2. *THM)/P11
      B0 = 2. * D
      DEN = (1. + AL1 * AL1/21.5) * * Ø.Ø14
      PL = 1. - (1. - P0)/DEN
      ARG = AL1/G
      ARG1 = 1./ARG
      IFAIL = Ø
      P = S11ABF(ARG, IFAIL)
      IFAIL = Ø
      P1 = S11ABF(- ARG, IFAIL)
      H = 2.*ARG1*ARG1*(ARG*(P-P1 )/2.-SQRT(1.+ARG*ARG)+1.)
      FAC = 1. + (EXP(SR * SR)/P0 - 1.) * H
      SR1 = ALOG(PL * FAC)
      RM1 = RM * P0 * EXP(SR * SR/2. - SR1/2.)/PL
      HINT = 1Ø. * ALOG1Ø(A0) + 1Ø. * B0 * ALOG1Ø(RM1)
      X4(1) = HINT - 3.
      DO 9ØØ J = 1,3ØØ
      A5 = X4(J)
      CALL DISTR2(A0, B0, A5, DIS)
      Y4(J) = DIS
9ØØ   X4(J + 1) = X4(J) + Ø.Ø3
      AMAX = 1.Ø E-99
      DO 9Ø1 L = 1,3ØØ
      T1 = Y4(L)
      IF(T1 . GE . AMAX) GO TO 9Ø3
      GO TO 9Ø1
9Ø3   AMAX = T1
```

```
      L1 = L
      A2 = X4(L1)
      B2 = Ø.399/T1
901   CONTINUE
      WRITE(6,55Ø) A2, B2
55Ø   FORMAT(1H,5ØX,6HMEAN = ,E16.7,4X,13HSTAND.DEV. = ,
     1E16.7)
      PRM = (ALEV - A2)/B2
      IFAIL = Ø
      P3 = S15ACF(PRM, IFAIL)
      Y5(I) = P3 * 876Ø. * 6Ø. * PL
15    CONTINUE
      DO 1ØØ6 I = 1,3Ø
      CALL LOCATE(X6(I), Y5(I), XP(I), YP(I), N5)
1ØØ6  CONTINUE
      CALL ARKIST(XP, YP, 1, 3Ø, 1Ø, 1., 1., Ø., 2, 1)
      CALL ENPLOT
      STOP
      END
```

```
      PROGRAM JOHN(INPUT,OUTPUT,TAPE 62,TAPE 6 = OUTPUT)
C     THIS PROGRAM EVALUATES THE CONDITIONAL DISTRIBUTION
     1OF XPD AT A COPOLAR RAIN ATTENUATION
      COMMON/GUC1/RM1, SR1
      DIMENSION X4(3Ø2),Y4(3Ø2),X5(41),Y6(41),X6(41),A5Ø(4),B
     15Ø(4),C5Ø(6),A51(4),B51(4),C51(6),A52(4),B52(4),C52(6),A53
     2(4),C53(6),A54(4),B54(4),C54(6),A55(4),B55(4),C55(6),X(12),
     3Y(12),XP(12),YP(12),Y5(4Ø,5),Y7(4Ø),Y8(4Ø),Y9(4Ø),Y1Ø(4Ø),
     4SER(5)
      CALL START (2)
      CALL SCALEZ (1.)
      DO 8 I = 1,4
      READ 9, B5Ø(I), A5Ø(I)
    9 FORMAT (F5.3, F4.2)
    8 CONTINUE
      DO 18 I = 1,4
      READ 19, B51(I), A51(I)
   19 FORMAT (F5.3, F4.2)
   18 CONTINUE
      CALL EØ1AAF(A5Ø, B5Ø, C5Ø, 4, 6, 3, 11.)
      CALL EØ1AAF(A51, B51, C51, 4, 6, 3, 11.)
      C = C5Ø(6) * Ø.ØØØ1
      D = C51(6)
      DO 28 I = 1,4
      READ 29, B52(I), A52(I)
   29 FORMAT (F5.3, F4.2)
   28 CONTINUE
      CALL EØ1AAF(A52, B52, C52, 4, 6, 3, 11.)
```

```
      AX = C52(6) * Ø.Ø1
      DO 38 I = 1,4
      READ 39, B53(I), A53(I)
39    FORMAT (F5.3, F4.2)
38    CONTINUE
      CALL EØ1AAF(A53, B53, C53, 4, 6, 3, 11.)
      AY = C53(6) * Ø.Ø1
      DO 48 I = 1,4
      READ 49, B54(I), A54(I)
49    FORMAT (F5.3, F4.2)
48    CONTINUE
      CALL EØ1AAF(A54, B54, C54, 4, 6, 3, 11.)
      BX = C54(6)
      DO 58 I = 1,4
      READ 59, B55(I), A55(I)
59    FORMAT (F5.3, F4.2)
58    CONTINUE
      CALL EØ1AAF(A55, B55, C55, 4, 6, 3, 11.)
      BY = C55(6)
      PO = Ø.Ø33
      G = 1.5
      AL = 11.
      RM = Ø.64
      SR = 1.52
      PI1 = 3.14159265
      DEN = (1. + AL * AL/21.5) ** Ø.Ø14
      PL = 1. - (1. - PO)/DEN
      ARG = AL/G
```

```
      ARG1 = 1./ARG
      IFAIL = Ø
      P = S11ABF(ARG, IFAIL)
      IFAIL = Ø
      P1 = S11ABF(- ARG, IFAIL)
      H = 2.*ARG1*ARG1*(ARG*(P-P1)/2.-SQRT(1.+ARG*ARG)+1.)
      H1 = 2.*ARG1*ARG1*(ARG*ALOG(ARG+SQRT(1.+ARG*ARG))
     1-SQRT(1.+ARG*ARG)+1.)
      FAC = 1. + (EXP(SR * SR)/PO - 1.) * H
      SR1 = ALOG(PL * FAC)
      RM1 = RM * PO * EXP(SR * SR/2. - SR1/2.)/PL
      A1 = AX + AY
      B1 = AX - AY
      A2 = AX * BX + AY * BY
      B2 = AX * BX - AY * BY
      THM = 1Ø. * P11/18Ø
      DO 8Ø7 K = 1,5
      READ 8Ø8, SER(K)
8Ø8   FORMAT (F4.2)
      STH = SER(K) * P11/18Ø.
      AM = EXP(- 2. * STH * STH)
      AO = AM*AM*AL*AL*C*C*SIN(2.*THM)*SIN(2.*THM)/P11
      BO = 2. * D
      A = (A1 + AM * B1 * COS(2. * THM))/2.
      B = (A2 + AM * B2 * COS(2. * THM))/2./A
      HINT = 1Ø. * ALOG1Ø(AO) + 1Ø. * BO * ALOG1Ø(RM1)
      X4(1) = HINT - 3.
      DO 8ØØ J = 1,3ØØ
      A5 = X4(J)
```

```
      CALL DISTR2 (A0, B0, A5, DIS)
      Y4(J) = DIS
800   X4(J + 1) = X4(J) + Ø.Ø8
      AMAX = 1.Ø E-99
      DO 8Ø1 L = 1,3ØØ
      T1 = Y4(L)
      IF (T1 . GE . AMAX) GO TO 8Ø3
      GO TO 8Ø1
8Ø3   AMAX = T1
      L1 = L
      A21 = X4(L1)
      B21 = Ø.399/T1
8Ø1   CONTINUE
      WRITE (6,45Ø) A21, B21
45Ø   FORMAT(1H,5ØX,6HMEAN = ,E16.7 ,4X,13HSTAND.DEV. =
     1 ,E16.7)
      BM = A * RM * * B
      SB = B * SR
      FAC1 = 1. + (EXP(SB * SB)/P0 - 1.) * H1
      SA = ALOG(PL * FAC1)
      AMM = BM * AL * P0 * EXP(SB * SB/2. - SA/2.)/PL
      S3 = SQRT(SA)
      X3 = ALOG(AMM)
      WRITE (6,451) X3, S3
451   FORMAT(1H,5ØX,6HMEAN = ,E16.7,4X,13HSTAND.DEV. = ,
     1 E16.7)
      WRITE (6,4ØØ)
400   FORMAT (1H, 5ØX, 1HC)
      ATT = 16.
```

```
      AM1 = 2Ø. * Ø.4342944819
      AR = SQRT(1. - AM1 * AM1/4./B21/B21)
      ARG2 = A21 + AR * B21 *(ALOG(ATT) - X3)/S3
      ST = B21 * SQRT(1. - AR * AR)
      X5(1) = - 4Ø.
      DO 2ØØ I = 1, 4Ø
      PRM = (X5(I) - ARG2)/ST
      IFAIL = Ø
      P4 = S15ACF(PRM, IFAIL)
      Y5(I, K) = P4 * 1ØØ.
2ØØ   X5 (I + 1) = X5(I) + 1.
8Ø7   CONTINUE
      DO 2Ø1 I = 1,4Ø
2Ø1   X6(I) = X5(I)
      CALL LOGAX(1.2, 1.2, 2, 3.5, 4, - 2, 2, 2, 1)
      CALL LINAX(1.2, 1.2, 1, 1.6, 1Ø, - 4Ø., 4., 1, 1, 1, - 1, 1)
      DO 812 I = 1,4Ø
      Y6(I) = Y5(I, 1)
      Y7(I) = Y5(I, 2)
      Y8(I) = Y5(I, 3)
      Y9(I) = Y5(I, 4)
      Y1Ø(I) = Y5(I, 5)
812   CONTINUE
      CALL POINTS (X6, Y6, 4Ø)
      CALL POINTS (X6, Y7, 4Ø)
      CALL POINTS (X6, Y8, 4Ø)
      CALL POINTS (X6, Y9, 4Ø)
      CALL POINTS (X6, Y1Ø, 4Ø)
      CALL ENPLOT
      STOP
      END
```

```
      PROGRAM JOHN (INPUT,OUTPUT,TAPE 62,TAPE 6 = OUTPUT)
C     THIS PROGRAM EVALUATES THE DISTRIBUTION OF XPD
     1UNDER THE CONDITION OF A RAIN FADE
      COMMON/GUC1/RM1, SR1
      COMMON/GUC2/P11, A21, B21, X3, S3, AR, ALEV
      EXTERNAL FUN16
      DIMENSION X(4Ø),Y7(4Ø),Y6(4Ø),X6(4Ø),X4(3Ø2),Y4(3Ø2)
     1A5Ø(4),B5Ø(4),C5Ø(6),A51(4),B51(4),C51(6),A52(4),B52
     2(4),C52(6),A53(4),B53(4),C53(6),A54(4),B54(4),C54(6),A55
     3(4),B55(4),C55(6),X1(18),Y1(18),XP(18),YP(18),Y5(4Ø,5),
     4Y8(4Ø),Y9(4Ø),Y1Ø(4Ø),Y11(4Ø),SER(5)
      CALL START (2)
      CALL SCALEZ (1.)
      DO 8 I = 1,4
      READ 9, B5Ø(I), A5Ø(I)
    9 FORMAT (F5.3, F4.2)
    8 CONTINUE
      DO 18 I = 1,4
      READ 19, B51(I), A51(I)
   19 FORMAT (F5.3, F4.2)
   18 CONTINUE
      CALL EØ1AAF(A5Ø, B5Ø, C5Ø, 4, 6, 3, 11.)
      CALL EØ1AAF(A51, B51, C51, 4, 6, 3, 11.)
      C = C5Ø(6) * Ø.ØØØ1
      D = C51(6)
      DO 28 I = 1,4
      READ 29, B52(I), A52(I)
   29 FORMAT (F5.3, F4.2)
   28 CONTINUE
```

```
      CALL EØ1AAF(A52, B52, C52, 4, 6, 3, 11.)
      AX = C52(6) * Ø.Ø1
      DO 38 I = 1,4
      READ 39, B53(I), A53(I)
39    FORMAT (F5.3, F4.2)
38    CONTINUE
      CALL EØ1AAF(A53, B53, C53, 4, 6, 3, 11.)
      AY = C53(6) * Ø.Ø1
      DO 48 I = 1,4
      READ 49, B54(I), A54(I)
49    FORMAT (F5.3, F4.2)
48    CONTINUE
      CALL EØ1AAF(A54, B54, C54, 4, 6, 3, 11.)
      BX = C54(6)
      DO 58 I = 1,4
      READ 59, B55(I), A55(I)
59    FORMAT (F5.3, F4.2)
58    CONTINUE
      CALL EØ1AAF(A55, B55, C55, 4, 6, 3, 11.)
      BY = C55(6)
      RM = Ø.64
      SR = 1.52
      P11 = 3.14159265
      AL = 11.
      PO = Ø.Ø33
      G = 1.5
      A1 = AX + AY
      B1 = AX - AY
      A2 = AX * BX + AY * BY
```

```
      B2 = AX * BX - AY * BY
      DEN = (1. + AL * AL/21.5) * * Ø.Ø14
      PL = 1. - (1. - P0)/DEN
      ARG = AL/G
      ARG1 = 1./ARG
      IFAIL = Ø
      P = S11ABF(ARG, IFAIL)
      IFAIL = Ø
      P1 = S11ABF(- ARG, IFAIL)
      H = 2.*ARG1*ARG1*(ARG*(P-P1)/2.-SQRT(1.+ARG*ARG)
     1+1.)
      FAC = 1. + (EXP(SR * SR)/P0 - 1.) * H
      SR1 = ALOG(PL * FAC)
      RM1 = RM * P0 * EXP(SR * SR/2. - SR1/2.)/PL
      H1 = 2.*ARG1*ARG1*(ARG*ALOG(ARG+SQRT(1.+ARG
     1*ARG)) - SQRT(1.+ARG*ARG)+1.)
      THM = 1Ø. * P11/18Ø
      DO 8Ø8 K = 1,5
      READ 8Ø9, SER(K)
8Ø9   FORMAT (F4.2)
      STH = SER(K) * P11/18Ø
      AM = EXP(- 2. * STH * STH)
      A0 = AM*AM*AL*AL*C*C*SIN(2.*THM)*SIN(2.*THM)/P11
      B0 = 2. * D
      A = (A1 + AM * B1 * COS(2. * THM))/2.
      B = (A2 + AM * B2 * COS(2. * THM))/2./A
      HINT = 1Ø. * ALOG1Ø(A0) + 1Ø. * ALOG1Ø(RM1)
      X4(1) = HINT - 3.
      DO 8ØØ J = 1,3ØØ
```

```
          A5 = X4(J)
          CALL DISTR2 (A0, B0, A5, DIS)
          Y4(J) = DIS
  8ØØ     X4(J + 1) = X4(J) + Ø.Ø8
          AMAX = 1.Ø E-99
          DO 8Ø1 L = 1,3ØØ
          T1 = Y4(L)
          IF (T1 . GE . AMAX) GO TO 8Ø3
          GO TO 8Ø1
  8Ø3     AMAX = T1
          L1 = L
          A21 = X4(L1)
          B21 = Ø.399/T1
  8Ø1     CONTINUE
          WRITE (6,45Ø) A21, B21
  45Ø     FORMAT (1H,5ØX,6HMEAN = ,E16.7,4X,13HSTAND.DEV
         1. = ,E16.7)
          BM = A * RM * * B
          SB = B * SR
          FAC1 = 1. + (EXP(SB * SB)/PO - 1.) * H1
          SA = ALOG(PL * FAC1)
          AMM = BM * AL * PO * EXP(SB * SB/2. - SA/2.)/PL
          S3 = SQRT(SA)
          X3 = ALOG(AMM)
          WRITE (6,451) X3, S3
  451     FORMAT (1H,5ØX,6HMEAN = ,E16.7,4X,13HSTAND.DEV = ,
         1E16.7)
          WRITE (6,555)
  555     FORMAT (1H, 5ØX, 1HC)
```

```
      AM1 = 2Ø. * Ø.4352944819
      AR = SQRT(1. - AM1 * AM1/4./B21/B21)
      FØ = 31.
      ALHT = - ALOG(FO)
      ALEV = - 45.
      CALL DØ1AEF(ALHT, FUN16, 48, ANS1)
      X(1) = - 35.
      DO 2ØØ I = 1,4Ø
      ALEV = X(I)
      CALL DØ1AEF(ALHT, FUN16, 48, ANS)
      P5 = ANS/ANS1
      Y5(I, K) = P5 * 1ØØ
      X(I + 1) = X(I) + 1.
2ØØ   CONTINUE
8Ø8   CONTINUE
      DO 2Ø1 I = 1,4Ø
2Ø1   X6(I) = X(I)
      DO 812 I = 1,4Ø
      Y7(I) = Y5(I, 1)
      Y8(I) = Y5(I, 2)
      Y9(I) = Y5(I, 3)
      Y1Ø(I) = Y5(I, 4)
      Y11(I) = Y5(I, 5)
812   CONTINUE
      CALL LOGAX(1.2, 1.2, 2, 2., 6, - 4, 2, 2, 1)
      CALL LINAX(1.2, 1.2, 1, 1.6, 1Ø, - 4Ø., 4., 1, 1, 1, - 1, 1)
      CALL POINTS (X6, Y7, 4Ø)
      CALL POINTS (X6, Y8, 4Ø)
      CALL POINTS (X6, Y9, 4Ø)
```

```
CALL POINTS (X6, Y1Ø, 4Ø)
CALL POINTS (X6, Y11, 4Ø)
CALL ENPLOT
STOP
END
```

```
      PROGRAM JOHN (INPUT,OUTPUT,TAPE 62,TAPE 6 = OUTPUT)
C     THIS PROGRAM EVALUATES THE TOTAL OUTAGE TIME
     1OF A DUAL-POLARIZATION COMMUNICATION SYSTEM
      COMMON/GUC1/RM1, SR1
      COMMON/GUC2/P11, A21, B21, X3, S3, AR, ALEV
      EXTERNAL FUN16
      DIMENSION X(4Ø),Y7(4Ø),Y6(4Ø),X6(4Ø),X4(3Ø2),Y4(3Ø2),
     1A5Ø(4),B5Ø(4),C5Ø(6),A51(4),B51(4),C51(6),A52(4),B52
     2(4),C52(6),A53(4),B53(4),C53(6),A54(4),B54(4),C54(6),
     3A55(4),B55(4),C55(6),Y8(4Ø),Y9(4Ø),Y5(4Ø,3),AR1(3)
      CALL START (2)
      CALL SCALEZ (1.)
      RM = 1.52
      SR = 1.38
      P11 = 3.14159265
      THM = 1Ø. * P11/18Ø
      DO 8 I = 1,4
      READ 9, B5Ø(I), A5Ø(I)
    9 FORMAT (F5.3, F4.2)
    8 CONTINUE
      DO 18 I = 1,4
      READ 19, B51(I), A51(I)
   19 FORMAT (F5.3, F4.2)
   18 CONTINUE
      CALL EØ1AAF (A5Ø, B5Ø, C5Ø, 4, 6, 3, 18.)
      CALL EØ1AAF (A51, B51, C51, 4, 6, 3, 18.)
      C = C5Ø(6) * Ø.ØØØ1
      D = C51(6)
      DO 28 I = 1,4
```

```
      READ 29, B52(I), A52(I)
29    FORMAT (F5.3, F4.2)
28    CONTINUE
      CALL EØ1AAF (A52, B52, C52, 4, 6, 3, 18.)
      AX = C52(6) * Ø.Ø1
      DO 38 I = 1,4
      READ 39, B53(I), A53(I)
39    FORMAT (F5.3, F4.2)
38    CONTINUE
      CALL EØ1AAF (A53, B53, C53, 4, 6, 3, 18.)
      AY = C53(6) * Ø.Ø1
      DO 48 I = 1,4
      READ 49, B54(I), A54(I)
49    FORMAT (F5.3, F4.2)
48    CONTINUE
      CALL EØ1AAF (A54, B54, C54, 4, 6, 3, 18.)
      BX = C54(6)
      DO 58 I = 1,4
      READ 59, B55(I), A55(I)
59    FORMAT (F5.3, F4.2)
58    CONTINUE
      CALL EØ1AAF (A55, B55, C55, 4, 6, 3, 18.)
      BY = C55(6)
      PO = Ø.Ø26
      G = 1.5
      A1 = AX + AY
      B1 = AX - AY
      A2 = AX * BX + AY * BY
      B2 = AX * BX - AY * BY
```

```
      DO 266 K = 1,3
      READ 26Ø, AR1(K)
26Ø   FORMAT (F4.2)
      STH = AR1(K) * P11/18Ø.
      AM = EXP(- 2. * STH * STH)
      X(1) = 1Ø.
      DO 5 I = 1,3Ø
      AL = X(I)
      AO = AM*AM*AL*AL*C*C*SIN(2.*THM)*SIN(2.*THM)
     1/P11
      BO = 2. * D
      DEN = (1. + AL * AL/21.5) * * Ø.Ø14
      PL = 1. - (1. - PO)/DEN
      ARG = AL/G
      ARG1 = 1./ARG
      IFAIL = Ø
      P = S11ABF(ARG, IFAIL)
      IFAIL = Ø
      P1 = S11ABF(- ARG, IFAIL)
      H = 2.*ARG1*ARG1*(ARG*(P-P1)/2.-SQRT(1.+ARG*ARG)+1.)
      FAC = 1. + (EXP(SR * SR)/PO - 1.) * H
      SR1 = ALOG(PL * FAC)
      RM1 = RM * PO * EXP(SR * SR/2. - SR1/2.)/PL
      H1 = 2.*ARG1*ARG1*(ARG*ALOG(ARG+SQRT(1.+ARG
     1*ARG)) - SQRT(1.+ARG*ARG) + 1.)
      A = (A1 + AM * B1 * COS(2. *THM))/2.
      B = (A2 + AM * B2 * COS(2. * THM))/2./A
      HINT = 1Ø. *  ALOG1Ø(AO) + 1Ø. * ALOG1Ø(RM1)
      X4(1) = HINT - 3.
```

```
      DO 8ØØ J = 1,3ØØ
      A5 = X4(J)
      CALL DISTR2 (AO, BO, A5, DIS)
      Y4(J) = DIS
8ØØ   X4(J + 1) = X4(J) + Ø.Ø8
      AMAX = 1.Ø E-99
      DO 8Ø1 L = 1,3ØØ
      T1 = Y4(L)
      IF (T1 . GE . AMAX) GO TO 8Ø3
      GO TO 8Ø1
8Ø3   AMAX = T1
      L1 = L
      A21 = X4(L1)
      B21 = Ø.399/T1
8Ø1   CONTINUE
      WRITE (6,45Ø) A21, B21
45Ø   FORMAT (1H,5ØX,6HMEAN = ,E16.7,4X,13HSTAND.DEV
     1. = ,E16.7)
      BM = A * RM * * B
      SB = B * SR
      FAC1 = 1. + (EXP(SB * SB)/PO - 1.) * H1
      SA = ALOG(PL * FAC1)
      AMM = BM * AL * PO * EXP(SB * SB/2. - SA/2.)/PL
      S3 = SQRT(SA)
      X3 = ALOG(AMM)
      WRITE (6,451) X3, S3
451   FORMAT (1H,5ØX,6HMEAN = , E16.7,4X,13HSTAND.DEV. = E16.7)
      WRITE (6,454)
454   FORMAT (1H, 5ØX, 1HC)
```

```
      ALEV = - 30.
      FL = 4Ø.
      FO = FL - 2Ø. * ALOG1Ø(AL/4.) - 4.
      ALHT = - ALOG(FO)
      AM1 = 2Ø. * Ø.4342944819
      AR = SQRT(1. - AM1 * AM1/4./B21/B21)
      CALL DØ1AEF(ALHT, FUN16, 48, ANS)
      IFAIL = Ø
      PRM = (ALOG(FO) - X3)/SQRT(2.)/S3
      P2 = S15ADF(PRM, IFAIL)
      P3 = P2/2.
      P5 = ANS
      P6 = P5 + P3
      Y5(I, K) = P6 * 876Ø. * 6Ø. * PL
      Y6(I) = P3 * 876Ø. * 6Ø. * PL
      X(I + 1) = X(I) + Ø.8
    5 CONTINUE
  266 CONTINUE
      DO 6 I = 1,3Ø
    6 X6(I) = X(I)
      CALL LOGAX(1.2, 1.2, 2, 6.8, 2, 2, 2, 2, 1)
      CALL LINAX(1.2, 1.2, 1, 2., 9, Ø., 5., 1, 1, 1, - 1, 1)
      DO 262 I = 1,3Ø
      Y7(I) = Y5(I, 1)
      Y8(I) = Y5(I, 2)
      Y9(I) = Y5(I, 3)
  262 CONTINUE
      CALL POINTS (X6, Y6, 3Ø)
      CALL POINTS (X6, Y7, 3Ø)
```

```
CALL POINTS (X6, Y8, 3Ø)
CALL POINTS (X6, Y9, 3Ø)
CALL ENPLOT
STOP
END
```

```
SUBROUTINE GAUSS (A2, B2, A, GAS)
P11 = 3.14159265
ARG = (A - A2) * (A - A2)/(2. * B2 * B2)
GAS = 1./(SQRT(2. * P11) * B2) * EXP(- ARG)
RETURN
END
SUBROUTINE DISTR3 (A0, B0, A, DIS)
EXTERNAL FUN15
COMMON/GUC/ASM, AST
COMMON/GUC1/RM1, SR1
P11 = 3.14159265
WM = A0 * RM1 * * B0
SW = B0 * SQRT(SR1)
AM = Ø.4342944819
AM1 = 2Ø. * AM
T0 = 1Ø. * AM * ALOG(WM)
S0 = SW * 1Ø. * AM
AS1 = 1./(2. * S0 * S0)
AS0 = 1./(SQRT(P11 * 2.) * S0)
ASM = 2. * SQRT(2.) * S0/AM1
AT1 = A - T0
AST = SQRT(2.) * AT1/S0
CALL DØ1AFF (FUN15, 48, ANS)
DIS = AS0 * EXP(- AS1 * AT1 * AT1) * ASM * ANS
RETURN
END
FUNCTION FUN15(X)
COMMON/GUC/ASM, AST
FUN = EXP((ASM + AST) * X - EXP(ASM * X))
```

```
FUN15 = FUN
RETURN
END
SUBROUTINE DISTR2 (AO, BO, A, DIS)
EXTERNAL FUN15
COMMON/GUC/ASM, AST
COMMON/GUC1/RM1, SR1
P11 = 3.14159265
WM = AO * RM1 * * BO
SW = BO * SQRT(SR1)
AM = Ø.4342944819
AM1 = 2Ø. * AM
TO = 1Ø. * AM * ALOG(WM)
SO = SW * 1Ø. * AM
AS1 = 1./(2. * SO * SO)
ASO = 1./(SQRT(P11 * 2.) * SO)
ASM = 2. * SQRT(2.) * SO/AM1
AT1 = A - TO
AST = SQRT(2.) * AT1/SO
CALL DØ1AFF (FUN15, 48, ANS)
DIS = ASO * EXP(- AS1 * AT1 * AT1) * ASM * ANS
RETURN
END
SUBROUTINE DISTR3 (RM, SR, AO, BO, A, DIS)
EXTERNAL FUN15
COMMON/GUC/ASM, AST
P11 = 3.14159265
WM = AO * RM * * BO
SW = BO * SR
```

```
AM = Ø.4342944819
AM1 = 2Ø. * AM
TO = 1Ø. * AM * ALOG(WM)
SO = SW * 1Ø. * AM
AS1 = 1./(2. * SO * SO)
ASO = 1./(SQRT(P11 * 2.) * SO)
ASM = 2. * SQRT(2.) * SO/AM1
AT1 = A - TO
AST = SQRT(2.) * AT1/SO
CALL DØ1AFF (FUN15, 48, ANS)
DIS = ASO * EXP(- AS1 * AT1 * AT1) * ASM * ANS
RETURN
END
FUNDTION FUN16(X)
COMMON/GUC2/P11, A21, B21, X3, S3, AR, ALEV
EXTERNAL S15ADF
ST = 1./2./SQRT(2. * P11)/S3
ARG = (X + X3) * (X + X3)/2./S3/S3
A1 = (ALEV - A21)/SQRT(2.)/SQRT(1. - AR * AR)/B21
B1 = AR * (X + X3)/SQRT(2.)/SQRT(1. - AR * AR)/S3
A = A1 + B1
IFAIL = Ø
P = S15ADF(A, IFAIL)
FUN16 = ST * P * EXP(- ARG + X)
RETURN
END
```

REFERENCES

ABRAMOWITZ, M. and STEGUN, A. I. (1965)
"Handbook of Mathematical Functions".
Dover Publications, New York.

AITCHISON, J. and BROWN, J. A. C. (1957)
"The Lognormal Distribution".
Cambridge University Press, London.

ATTISANI, A., CAPSONI, C. and PARABONI, A. (1974)
"Effects of Non-Spherical Hydrometeors on the EM Propagation Through Atmospheric Precipitation".
J. Rech. Atmos., Vol. 8, p. 137.

BARNETT, W. T. (1972)
"Some Experimental Results on 18 GHz Propagation".
Conference Record of the National Telecommunications Conference, IEEE Publication, 72 CHO 601-5-NTC, p. 10E-1.

BEARD, K. and PRUPPACHER, H. (1969)
"A Determination of the Terminal Velocity and Drag of Small Water Drops by Means of a Wind Tunnel".
J. Atmos. Sci., Vol. 26, p. 1066.

BECKMANN, P. (1967)
"Probability in Communication Engineering".
Harcourt, Brace and World, New York.

BECKMANN, P. (1968)
"Depolarization of Electromagnetic Waves".
The Golem Press, Boulder, Colorado.

BODTMANN, W. F. and RUTHROFF, C. L. (1974)
"Rain Attenuation on Short Radio Paths: Theory, Experiment and Design".
Bell Syst. Tech. J., Vol. 53(7), p. 1329.

BOSTIAN, C. W. (1973)
"Millimeter Wave Rain Depolarization: Some Recent 17.65 GHz Measurements".
G-AP International Symposium Digest, p. 289.

BRUSSAARD, G. (1976)
"A Meteorological Model for Rain Induced Cross-Polarization".
IEEE Trans. Antennas and Propagation, Vol. AP-24, p. 5.

CHU, T. S. (1974)
"Rain-Induced Cross-Polarization at Centimeter and Millimeter Wavelengths".
Bell Syst. Tech. J., Vol. 53, p. 1557.

CLENSHAW, C. W. (1962)
"Mathematical Tables".
Vol. 5, NPL HMSO.

COLE, et al (1969)
"Precipitation and Clouds, a Revision of Chapter 5, Handbook of Geophysics and Space Environments".
AFCRL-69-0487, Air Force Surveys in Geophysics, US Air Force Cambridge Research Laboratories, Bedford, Massachusetts.

CONWAY, H. M., MAY, S. L. and ARMSTRONG, E. (1963)
"The Weather Handbook".
Atlanta: Conway Publications.

DRUFUCA, G. and ZAWADZKI, I. I. (1973)
"Statistics of Rain Gauge Records".
Inter-Union Commission on Radio Meteorology (IUCRM), Colloquium on The Fine Scale Structure of Precipitation and EM Propagation, Nice, France.

EVANS, B. G. and TROUGHTON, J. (1973a)
"Calculation of Cross-Polarization due to Precipitation".
Conference on the Propagation of Radiowaves at Frequencies Above 10 GHz. IEE Publication No. 98, p. 162, London.

EVANS, B. G. and TROUGHTON, J. (1973b)
"Linear and Circular Cross-Polarization Statistics".
Conference on the Propagation of Radiowaves at Frequencies Above 10 GHz. IEE Publication No. 98, p. 172, London.

FOX, L. and PARKER, I. B. (1968)
"Chebyshev Polynomials in Numerical Analysis".
Oxford University Press.

FREENY, A. E. and GABBE, J. D. (1969)
"A Statistical Description of Intense Rainfall".
Bell Syst. Tech. J., Vol. 48(6), p. 1789.

FRÖBERG, C. E. (1965)
"Introduction to Numerical Analysis".
Addison-Wesley.

FUNAKAWA, K. and KATO, J. (1962)
"Experimental Studies of Propagational Characteristics of 8.6 mm Wave on the 24 km Path".
J. Radio Res. Lab. (Japan), Vol. 9 (45), p. 351.

GRUNOW, J. (1961)
"Investigations on the Structure of Precipitation".
Final Report to the US Department of the Army, European Research Office, Hohenpeissenberg Meteorological Observatory, Oberbayern, Germany.

GUMBEL, E. J. (1954)
"Statistical Theory of Extreme Values and Some Practical Applications".
National Bureau of Standards, Applied Mathematics Series No. 33.

GUMBEL, E. J. (1958)
"Statistics of Extremes".
New York: Columbia University Press.

HALD, A. (1952)
"Statistical Theory with Engineering Applications".
New York: John Wiley & Sons Inc.

HARDEN, B. N., NORBURY, J. R. and WHITE, W. J. K. (1974)
"Model of Intense Convective Raincells for Estimating Attenuation on Terrestrial Millimetric Radio Links".
Electron. Lett., Vol. 10, p. 483.

HARDEN, B. N., NORBURY, J. R. and WHITE, W. J. K. (1978)
"Attenuation/Rain-Rate Relationships on Terrestrial Microwave Links in the Frequency Range 10 - 40 GHz".
Electron. Lett., Vol. 14(5), p. 154.

HOGLER, J. L., BOSTIAN, C. W., STUTZMAN, W. L. and WILEY, P. (1975)
"Statistical Variations in Forward Propagation Rain Depolarization due to Drop Size Fluctuations".
IEEE Trans. Antennas and Propagation, Vol. AP-23, p. 444.

JONES, D. M. A. (1959)
"The Shape of Raindrops".
J. Meteor., Vol. 16, p. 504.

JONES, D. M. A. and SIMS, A. L. (1971)
"Climatology of Instantaneous Precipitation Rates".
Illinois State Water Survey at the University of Illinois, Urbana, Illinois, Project No. 8624, Final Report.

JOSS, J., THAMS, J. C. and WALDVOGEL, A. (1968)
"The Variation of Raindrop Size Distributions at Locarno".
Proc. International Conference on Cloud Physics, Toronto, Canada, p. 369.

KERR, D. E. (1964)
"Propagation of Short Radio Waves".
Lexington, Mass.: Boston Tech.

LAWS, J. O. and PARSONS, D. A. (1943)
"The Relation of Raindrop Size to Intensity".
Trans. Amer. Geophys. Union, Vol. 24(II), p. 452.

LIN, S. H. (1973)
"Statistical Behaviour of Rain Attenuation".
Bell Syst. Tech. J., Vol. 52(4), p. 557.

LIN, S. H. (1975)
"A Method for Calculating Rain Attenuation Distribution on Microwave Paths".
Bell Syst. Tech. J., Vol. 54(6), p. 1051.

LIN, S. H. (1976)
"Rain-Rate Distributions and Extreme-Value Statistics".
Bell Syst. Tech. J., Vol. 55(8), p. 1111.

LIN, S. H. (1978)
"More on Rain Rate Distributions and Extreme Value Statistics".
Bell Syst. Tech. J., Vol. 57(5), p. 1545.

MAGNUS, W. and OBERHETTINGER, F. (1954)
"Formulas and Theorems for the Functions of Mathematical Physics".
New York: Chelsea.

MAGONO, C. (1954)
"On the Shape of Waterdrops Falling in Stagnant Air".
J. Meteor., Vol. 11, p. 77.

MARSHALL, J. S. and PALMER, W. McK. (1948)
"The Distribution of Raindrops with Size".
J. Meteor., Vol. 5, p. 165.

McCORMICK, G. C. (1975)
"Propagation Through a Precipitation Medium: Theory and Measurement".
IEEE Trans. Antennas and Propagation, Vol. AP-23, p. 266.

MEDHURST, R. G. (1965)
"Rainfall Attenuation of Centimeter Waves: Comparison of Theory and Measurement".
IEEE Trans. Antennas and Propagation, Vol. AP-13, p. 550.

MIE, G. (1908)
"Beitrüge zur Optik Trüber Medien, speziell kolloidater Metallosungen".
Ann. der Phys., Vol. 25, p. 377.

MORITTA, K. and HIGUTI, I. (1971)
"Statistical Studies on Electromagnetic Wave Attenuation due to Rain".
Review of the Elec. Commun. Labs. (Japan), Vol. 19(7-8), p. 798.

MORRISON, J. A., CROSS, M. J. and CHU, T. S. (1973)
"Rain-Induced Differential Attenuation and Differential Phase Shift at Microwave Frequencies".
Bell Syst. Tech. J., Vol. 52(4), p. 599.

MORRISON, J. A. and CROSS, M. J. (1974)
"Scattering of a Plane Electromagnetic Wave by Axisymmetric Raindrops".
Bell Syst. Tech. J., Vol. 53(6), p. 955.

MUELLER, E. A. and SIMS, A. L. (1966)
"Investigation on the Quantitative Determination of Point and Areal Precipitation by Radar Echo Measurement".
Technical Report ECOM-00032-F, Illinois State Water Survey at the University of Illinois, Urbana, Illinois.

MULLIN, C. R. et al (1965)
"A Numerical Technique for the Determination of Scattering Cross Sections of Infinite Cylinders of Arbitrary Geometrical Cross Section".
IEEE Trans. Antennas and Propagation, Vol. AP-13(1), p. 141.

NAKAGAMI, M., TANAKA, K. and KANEHISA, M. (1957)
Memo.
Facu. of Eng., Kobe University, No. 4, 78.

NAKAGAMI, M. (1960)
"The m-Distribution - a General Formula of Intensity Distribution of Rapid Fading".
In Statistical Methods on Radio Wave Propagation, Edited by W. C. Hoffman, p. 3, Pergamon, New York.

NORBURY, J. R. and WHITE, W. J. K. (1973)
"Point Rainfall Rate Measurements at Slough, UK".
Conference on the Propagation of Radiowaves at Frequencies Above 10 GHz, IEE Publication No. 98, p. 190, London.

NORTON, K. A. and VOGLER, L. E. (1955)
"The Probability Distribution of the Amplitude of a Constant Vector Plus a Rayleigh-Distributed Vector".
Proc. IRE, Vol. 43(10), p. 1354.

NOWLAND, W. L., OLSEN, R. L. and SHKAROFSKY, I. P. (1977)
"Theoretical Relationship Between Rain Depolarization and Attenuation".
Electron. Lett., Vol. 13, p. 676.

OGUCHI, T. (1960)
"Attenuation of Electromagnetic Waves due to Rain with Distorted Raindrops".
J. Radio Res. Labs. (Japan), Vol. 7(33), p. 467.

OGUCHI, T. (1962)
"Statistical Fluctuation of Amplitude and Phase of Radio Signals Passing Through the Rain".
J. Radio Res. Labs. (Japan), Vol. 9(41), p. 51.

OGUCHI, T. (1964)
"Attenuation of Electromagnetic Waves due to Rain with Distorted Raindrops (II)".
J. Radio Res. Labs. (Japan), Vol. 11, p. 19.

OGUCHI, T. (1973)
"Attenuation and Phase Rotation of Radio Waves due to Rain: Calculations at 19.3 and 34.8 GHz".
Radio Sci., Vol. 8, p. 31.

OGUCHI, T. and HOSOYA, Y. (1974)
"Scattering Properties of Oblate Raindrops and Cross Polarization of Radio Waves due to Rain (Part II): Calculations at Microwave and Millimeter Wave Regions".
J. Radio Res. Labs. (Japan), Vol. 21(105), p. 191.

OGUCHI, T. (1977)
"Scattering Properties of Pruppacher-and-Pitter Form Raindrops and Cross Polarization due to Rain: Calculations at 11, 13, 19.3 and 34.8 GHz".
Radio Sci., Vol. 12, p. 41.

OLSEN, R. L., ROGERS, D. V. and HODGE, D. B. (1978)
"The aR^b Relation in the Calculation of Rain Attenuation".
IEEE Trans. Antennas and Propagation, Vol. AP-26, p. 318.

ÖSTBERG, K. (1976)
"Effect of Drop Canting-Angle Distribution on Depolarization of Microwaves in Rain".
FOA Rep. 10(2), National Defence Research Institute, Stockholm, Sweden.

PAPOULIS, A. (1965)
"Probability, Random Variables and Stochastic Processes".
McGraw-Hill: New York.

PRUPPACHER, H. R. and BEARD, K. (1970)
"A Wind Tunnel Investigation of the Internal Circulation and Shape of Water Drops Falling at Terminal Velocity in Air".
Quart. J. Roy. Meteor. Soc., Vol. 96, p. 247.

PRUPPACHER, H. R. and PITTER, R. L. (1971)
"A Semi-Empirical Determination of the Shape of Cloud and Raindrops".
J. Atmos. Sci., Vol. 28, p. 86.

RALSTON, A. (1965)
"A First Course in Numerical Analysis".
McGraw-Hill.

RAY, P. S. (1972)
"Broadband Complex Refractive Indices of Ice and Water".
J. Appl. Opt., Vol. 11, p. 1836.

RUTHROFF, C. L. (1970)
"Rain Attenuation and Radio Path Design".
Bell Syst. Tech. J., Vol. 49(1), p. 121.

RYDE, J. W. (1941)
"Echo Intensity and Attenuation due to Clouds, Rain, Hail, Sand and Dust Storms at Centimetre Wavelengths".
Rept. 7831, General Electric Co. Research Labs., Wembley, England.

RYDE, J. W. and RYDE, D. (1944)
"Attenuation of Centimetre Waves by Rain, Hail and Clouds".
Rept. 8516, General Electric Co. Research Labs., Wembley, England.

RYDE, J. W. and RYDE, D. (1945)
"Attenuation of Centimetre and Millimetre Wave by Rain, Hail, Fogs and Clouds".
Rept. 8670, General Electric Co. Research Labs., Wembley, England.

SAUNDERS, M. J. (1971)
"Cross-Polarization at 18 and 30 GHz due to Rain".
IEEE Trans. Antennas and Propagation, Vol. AP-19(2), p. 273.

SCHÖNFELDER, J. L. (1976)
"The Production of Special Function Routines for a Multi-Machine Library".
Software Practice and Experience, Vol. 6(1).

SEAMON, L. H. and BARTLETT, G. S. (1956)
"Climatological Extremes".
Weaterwise, Vol. 9, p. 194.

SEMPLAK, R. A. and TURRIN, R. H. (1969)
"Some Measurements of Attenuation by Rainfall at 18.5 GHz".
Bell Syst. Tech. J., Vol. 48(6), p. 1767.

SETZER, D. E. (1970)
"Computed Transmission Through Rain at Microwave and Visible Frequencies".
Bell Syst. Tech. J., Vol. 49(8), p. 1873.

SHKAROFSKY, I. P. (1977)
"Depolarization due to Precipitation in Satellite Communications".
RCA Rev., Vol. 38, p. 257.

SIMS, A. L. and JONES, D. M. A. (1973)
"Climatology of Instantaneous Precipitation Rates".
Illinois State Water Survey at the University of Illinois, Urbana, Illinois, Project No. 8624.

SLATER, J. C. and FRANK, N. H. (1933)
"Introduction to Theoretical Physics".
New York: McGraw-Hill.

STRATTON, J. A. (1941)
"Electromagnetic Theory".
New York: McGraw-Hill.

THOMAS, D. T. (1971)
"Cross-Polarization Distortion in Microwave Radio Transmission due to Rain".
Radio Sci., Vol. 6(10), p. 833.

TURNER, D. J. W. and TATTERSALL, R. L. O. (1977)
"Analysis of Fading due to Rain, Snow and Multipath Propagation for 11 GHz Radio Links Variously Located in England".
Electron. Lett., Vol. 13(20), p. 619.

UZUNOGLU, N. K., EVANS, B. G. and HOLT, A. R. (1977)
"Scattering of Electromagnetic Radiation by Precipitation Particles and Propagation Characteristics of Terrestrial and Space Communication Systems".
Proc. IEE, Vol. 124(5), p. 417.

VAN DE HULST, H. C. (1957)
"Light Scattering by Small Particles".
Wiley & Sons, New York.

WATSON, P. A. and ARBABI, M. (1973)
"Rain Cross-Polarization at Microwave Frequencies".
Proc. IEE, Vol. 120(4), p. 413.

WATSON, P. A. and ARBABI, M. (1975)
"Semi-Empirical Law Relating Cross-Polarization Discrimination to Fade Depth for Rainfall".
Electron. Lett., Vol. 11(2), p. 42.